REGULATION OF ANATOMICAL PLASTICITY AT NEUROMUSCULAR JUNCTIONS

Inauguraldissertation

zur

Erlangung der Würde eines Doktors der Philosophie

vorgelegt der

Philosophisch-Naturwissenschaftlichen Fakultät

der Universität Basel

von

Alexandre Ferrão Santos

aus Huambo, Angola

Basel, 2006

Friedrich Miescher Institute

Genehmigt von der Philosophisch-
Naturwissenschaftlichen Fakultät auf
Antrag von

Prof. Denis Monard
Dr. Pico Caroni
Prof. Silvia Arber

Basel, den 20.12.2005

_____
Dekan
Prof. Hans-Jakob Wirz

Acknowledgments

I would like to take this opportunity to thank Pico Caroni for having invited me to participate in the excellent scientific work of his lab and enjoy such an outstanding technical and scientific environment. Thank you Pico not only for introducing me into a top scientific research, and for the attentive PhD mentoring, but also and not least for the personal support you provided. I have appreciated our excellent scientific and non-scientific discussions, and am very grateful for the constant input you provided. I would also like to thank you for giving me the opportunity to attend a variety of meetings such as the Neuroscience or the Ascona meetings which have been essential to broaden my scientific culture.

I would also like to warmly thank Silvia Arber for the excellent collaborations and technical contributions that she and her lab provided for many of the projects discussed in this dissertation. I would also like to mention people from her lab such as Simon Hippenmeyer, Markus Sigrist, and Rishard Salie for their contributions and help. Finally, I would also like to thank Silvia for accepting to participate in my thesis evaluation.

Many thanks to Denis Monard for taking the vorsitz in my thesis exam. But I would also like to thank him and his lab members for the technical help and exchange that they have provided throughout my thesis. I would like to thank in particular Sabrina Taieb, Maddalena Lino and Xiaobiao Li for their help.

I am also indebted to Markus Rüegg and Shao Lin for providing me with reagents and technical advice to carry out the siRNA experiments.

Thanks are also due to Reto Portmann, Anne Ulvestad and Daniel Hess for their dedicated and expert contribution to the proteomics analysis.

I would also like to acknowledge the help and advice provided by Jean-François Spetz and the whole animal facility team, not only by making possible to work with transgenic animals but also for discussions on surgical operations and treatments.

I also owe a great debt to the Caroni lab members. They have not only become good friends of mine but have also immensely contributed by providing technical advice and help. I would like to thank not only San Pun, and Smita Saxena with whom I collaborated in several research projects, but also Nadine Gogolla and Ivan Galimberti for their help, friendship and good times. I am also grateful to Corinna Schneider and Lan Xu for their help and contribution, and I would like to mention Tamara Golub, which became a great friend of mine.

I would also like to mention in general the people of the FMI for the breadth of their knowledge and availability for help and tips, and for making of the FMI such a nice working environment.

I would finally like to express my gratitude to my family, to which I own everything, but also for their encouragements and helpful discussions on the thesis. Many thanks to Ivone Ferrão, Lúcio and Susana Santos, and Piedad Calderon for your help and kindness.

Last but not least, I would like to thank my beloved partner Joëlle Attas for her unflinching and demanding support throughout the thesis.

Contents in brief

Table of Contents

Abbreviations

AChE	Acetylcholine Esterase
AChRs	Acetylcholine Receptors
α-DG	α-dystroglycan
Bot A	Botulinum toxin A
BTX	α-Bungarotoxin
CNS	Central Nervous System
DeSyn	Delayed Synapsing
DTX	Diphteria toxin
EM	Electron Micrograph
ECM	Extracellular Matrix
FaSyn	Fast Synapting
GPI	glycosylphosphatidylinositol
LGC	Lateral Gastrocnemius
MGC	Medial Gastrocnemius
MMP	Matrix Metalloproteases
MN	Motoneuron
Mnd	motor neuron disease
MuSK	muscle skeletal receptor tyrosine kinase
NF	neurofilament
NMJ	Neuromuscular Junction
pmn	progressive motor neuropathy
SFK	Src Family of Kinases
SMA	spinal muscular atrophy
SOD1	Superoxide Dismutase
RF	Rectus Femoris
TA	Tibialis Anterior
tPA	tissue Plasminogen Activator
tSC	terminal Schwann cell
WFA	Wisteria floribunda agglutinin

Chapter 1 - Summary

The focus of this thesis has been the study of the cellular mechanisms regulating the neuromuscular junction organization in development, mature and disease state.

As communication bridges between nervous cells, synapses are a key component of the nervous system, and thought to mediate important aspects of its function. The neuromuscular junction (NMJ) is an attractive synapse model, because of its ease of access for experimental purposes.

The work described in this thesis yielded three major insights:

1 – In development, we have shown that synaptogenesis follows two different pathways in two newly identified muscle types. In FaSyn muscles synaptogenesis is rapid, whereas in DeSyn muscles formation of mature looking NMJs is delayed until birth. These two pathways of synapse maturation are regulated by muscle type and independent of nerve (chapter 10).

2 – In mature NMJs, we have shown that local axon growth is tightly regulated by its postsynaptic partner in a process coupled to the state of postsynaptic receptor complex assembly (chapter 11).

3 – In a mouse model of Amyotrophic Lateral Sclerosis, we have shown that the disease process affects the motoneuron axon in a stereotyped manner, and that different types of motoneurons show selective vulnerability to the pathogenesis process (chapter 12).

Chapter 2 - Introduction

The nervous system is one of the most impressive achievements of evolution. It enables the organism to produce rapid and flexible adaptive behavior to changing environmental conditions. To allow this, the nervous system has to sample information from the environment and produce appropriate motor and physiological responses. It must also be able to compare present conditions to previous experiences and to develop deductive and decision making capacities.

In order to process information, the nervous system is organized into multiple sets of interconnected neurons, capable of exchanging and integrating stimuli. Because of this network organization, synapses, the points of contact and information exchange between neurons, are crucial elements in the function of the nervous system.

Synapses are not only important in determining the connectivity between neurons, but their molecular organization will also determine whether the target neuron will be excited or suppressed by the synapse activation. Changes in synapse numbers or behavior alter profoundly the activity pattern of the network. Critical periods, phases of development in which the mature pattern of activity of the network is being established, are characterized by activity dependent production and destruction of large numbers of synapses. Conversely, the end of critical periods is marked by a drop in synaptogenesis and synapse removal, and results in much more stable behavior of the network.

Synapse formation and removal is observed not only during development or during critical periods, but is also a feature of a normal mature nervous system network. Synapse recycling has been observed in hippocampal slice cultures, and *in vivo*, in the adult cortex (de Paola et al., 2003, Trachtenberg JT et al., 2002). In a mature network, although the majority of synapses remain stable for months, a significant fraction of synapses form and disappear within days. Such a pool of labile synapses might provide the substrate that enables the encoding of new information within the network or mediates long-term changes of behavior.

Although remodeling of synapses is too slow to account for rapid changes in nervous system function, anatomical synaptic rearrangements could provide a mechanism to enforce long-term nervous system plasticity. Production of spines has been observed during events of synaptic plasticity (Engert F., Bonhoeffer T., 1999). Conversely, long-term changes in nervous system behavior (for instance in the motor cortex following amputation or fingers immobilization) have been shown to lead to changes in network connectivity.

A possible role of anatomical plasticity in the plasticity of the nervous system might be to determine the potential range of functional coupling between pairs of pre- and postsynaptic cells. This might involve variations in relative synapse numbers, as well as on the relative positions of synapses within dendritic trees.

Because of the role of synapses in shaping the behavior of the network, it is essential to understand the principles guiding the formation, maintenance and removal of synapses. The study of such principles is the underlying theme of this work.

Chapter 3 - Overview

The thesis is organized into five introductory chapters, three results and one discussion chapter :

Chapter 4 discusses the rationale of using the NMJ as a model synapse, whereas chapters 5 and 6 introduce the anatomical and molecular organization of the NMJ, and its evolution during development.

Chapter 7 discusses the impact of activity in the organization of the mature NMJ, and the role of lipid rafts and cholesterol in the organization of the postsynaptic apparatus.

Chapter 8 introduces the reader to Amyotrophic Lateral Sclerosis (ALS) and its mouse model.

Chapter 9 presents the aims of this thesis.

Results of the thesis are presented in chapters 10 to 12 and annex 1. The discussion of the main findings is made in chapter 13.

Chapter 4 - The NMJ as a model synapse

The work described in this thesis has used the neuromuscular junction (NMJ) as a model synapse. The NMJ, the synapse connecting the motor neuron (MN) to a skeletal muscle fiber, has significant experimental advantages over central nervous system (CNS) synapses, which render it an attractive subject of study :

1) The NMJ is a large synaptic structure (~30μm), which facilitates study of its morphology and behavior in various experimental conditions

2) The NMJ has a simple organization: The NMJs are well separated, with one synapse per muscle fiber, which allows monitoring of single synapses. The NMJ is organized as a relatively flat superposition of a postsynaptic muscle fiber endplate, the nerve terminal, and the terminal Schwann cell, facilitating the study of each partner of the synapse.

3) The NMJ is accessible: The easy access offered by the NMJs allows various types of surgical and pharmacological interventions in specific target synapses.

4) The availability of tools such as α-bungarotoxin and membrane tagged GFP positive neurons enables fine morphological studies and monitoring of the synapse.

Advantages in the study of the NMJ also entail disadvantages, mainly concerning how much of what is found in its context can be extended to CNS synapses. The NMJ is in the peripheral nervous system and is not part of a neuron-neuron network. More profoundly, it has been sometimes difficult to ascertain the function in the CNS of molecules such as agrin or MuSK which have been shown to play essential roles in NMJ organization. Moreover, whereas synapses in the CNS show a large diversity in their behavior and characteristics, NMJs have traditionally been assumed to be a single uniform type of synapse.

Despite these caveats NMJs, just as CNS synapses, undergo periods of synaptic competition and pruning, and display a sensitivity to activity patterns during development and in the adult. These features turn the NMJ into an attractive model system to study principles of synapse creation, maintenance and removal.

Chapter 5 - NMJ organization

5.1 Cellular organization

The NMJ is formed by the apposition of the nerve and the muscle membranes, separated by the synaptic cleft, an extracellular space containing synapse-specific extracellular matrix (ECM), the synaptic basal lamina.

Electron microscopy (EM) pictures show that the muscle membrane forms deep folds under the nerve, enriched in acetylcholine receptors (AChRs) at their edges. At mature NMJs, AChRs are distributed in grooves that match tightly the axon arborization.

GFP labeling of terminal Schwann cells (tSCs) and EM analysis also show that at the NMJ axons are associated with 2 to 4 tSCs, whose processes are tightly associated with each axon branch at the synapse, and isolate the nerve from the extrasynaptic space. At mature NMJs, tSCs do not extend onto ECM facing muscle, but remain instead exclusively associated with presynaptic nerve.

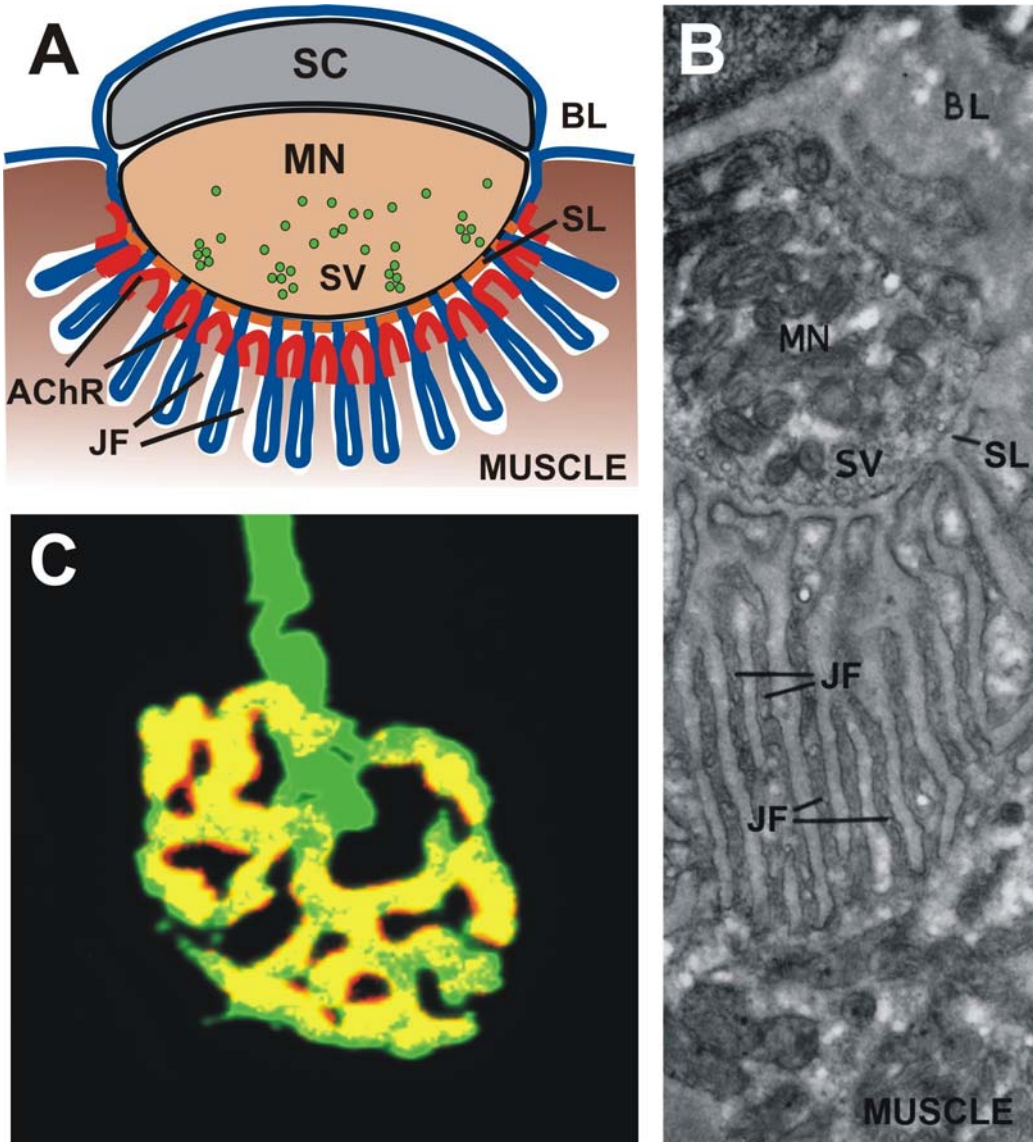

Figure 1 : A – Scheme of a NMJ illustrating the apposition of the Schwann Cell (SC) and the motoneuron (MN) on a muscle groove. The muscle membrane is folded into junction folds (JF) enriched in AChRs near the MN. The tSC and the MN are surrounded by a basal lamina (BL) which is becomes a specialized synaptic lamina (SL) between the synaptic vesicle (SV) release sites and the facing AChRs.

B – EM of a human NMJ (modified from de Harven and Coërs 1959, with permission)

C – photography of a GFP labeled MN (green) and α-bungarotoxin labeled AChRs (red)

5.2 Molecular organization

The tight association and signaling between the MN axon and the muscle fiber is mediated by a complex molecular organization spanning from the cytoskeletal network

of the axon through its membrane into the basal lamina until the muscle fiber membrane and underlying cytoskeletal cortex.

In the muscle fiber, a dense network of F-actin is required to anchor the components of the postsynaptic apparatus. Proteins such as utrophin and dystrophin connect the actin cytoskeleton to rapsyn and dystroglycan, elements of the postsynaptic apparatus.

The postsynaptic apparatus itself is formed by the close association of protein complexes containing among others rapsyn, MuSK (muscle skeletal receptor tyrosine kinase), AChRs, and dystroglycan. These complexes are a scaffold of proteins forming a microcluster, the smallest unit of AChRs at the membrane. The microclusters can cluster into larger aggregates to form mature postsynaptic specializations.

The microclusters are called protein scaffolds because removal of any of their key components (MuSK, AChRs, rapsyn) results in dispersal of the microcluster. Furthermore, they are produced in the Golgi and shipped to the membrane together as a unit.

The microcluster is not only anchored to the cortical cytoskeleton, but also connected to the extracellular matrix. Laminin and agrin are key components of the ECM at the NMJ. They are part of an interconnected network which binds postsynaptically to dystroglycan and integrins. By producing a mesh that connects postsynaptic and presynaptic membrane complexes, the synaptic ECM ensures a very thigh apposition of the nerve to the muscle.

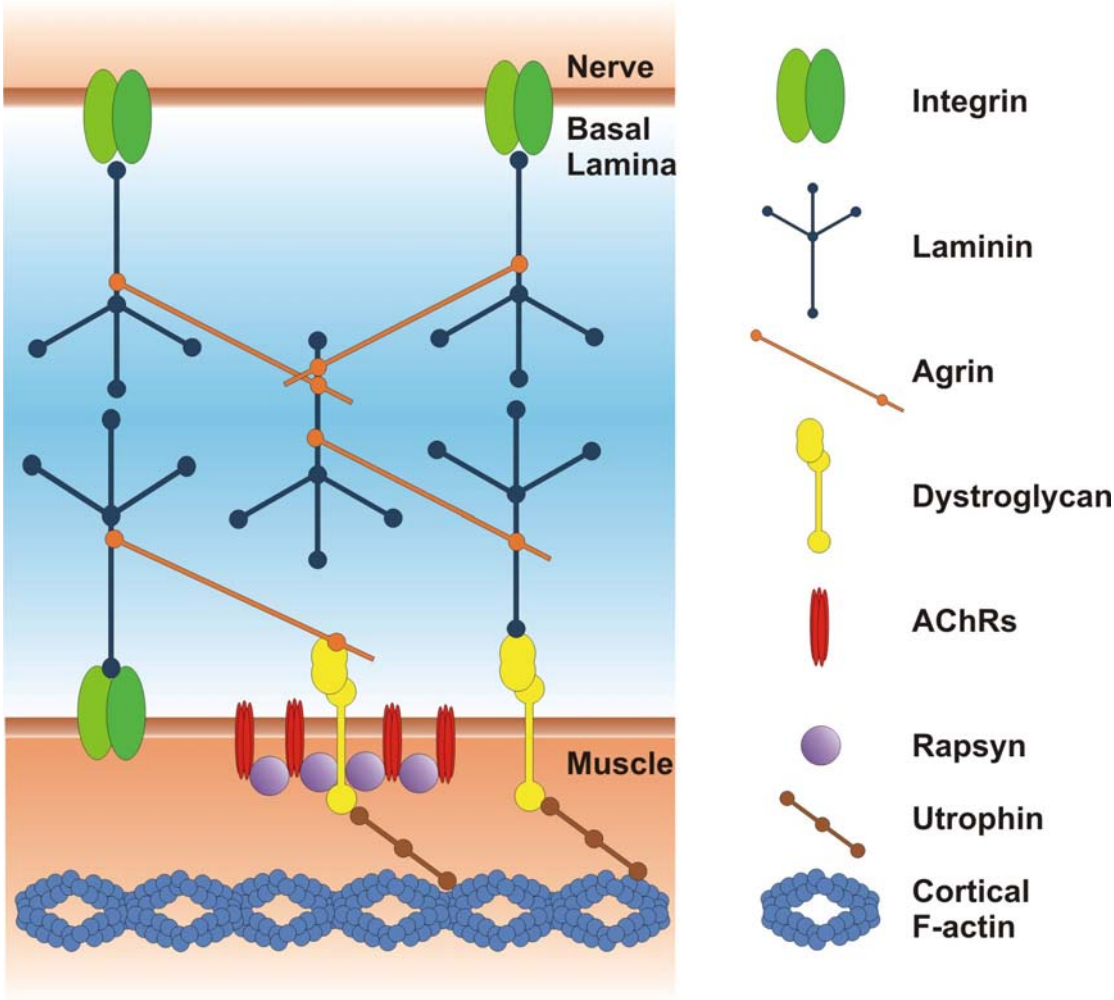

Figure 2 : Molecular organization of the NMJ

Chapter 6 - NMJ development

Because of its experimental advantages, studies of the mechanisms of synaptogenesis at the NMJ have been very detailed (Sanes and Lichtman, 1999). Early studies by McMahan and colleagues have shown that the ECM in the synaptic cleft contains the signal sufficient to instruct re-formation of the synapse after denervation (Sanes 1978, Burden 1979). This signal was subsequently purified from the electric organ of the *Torpedo californica*, and named agrin.

The fact that agrin is secreted by the nerve and is able to induce AChR clustering and postsynaptic differentiation led McMahan to formulate the "agrin hypothesis", that postulates that the nerve directs the assembly of the postsynaptic apparatus in vivo through secretion of agrin.

Subsequent studies have supported the agrin hypothesis. First, agrin-deficient mice die soon after birth because of respiratory insufficiency (Gautam et al., 1996), and analysis of their muscles shows an absence of functional postsynaptic structures. Second, recombinant expression of agrin in non-synaptic regions of innervated muscles is sufficient to induce the formation of fully functional, mature postsynaptic apparatus *in vivo* and activates synapse-specific transcription (Jones et al., 1997; Bezakova et al., 2001).

The synaptogenic activity of agrin was later suggested to be mediated via MuSK (a transmembrane receptor tyrosine kinase). In myotubes, application of agrin leads to rapid MuSK activation (Glass et al., 1996). $MuSK^{-/-}$ myotubes do not respond to agrin, but their ability aggregate AChRs in response to agrin is restored by expression of MuSK (Herbst et al., 2002). MuSK-deficient mice lack any postsynaptic specializations at the nerve-muscle contact and die perinatally, like agrin-deficient mice (DeChiara et al. 1996).

Rapsyn is another essential mediator of postsynaptic differentiation downstream of MuSK. Rapsyn is a cytoplasmic protein tightly associated with AChRs. Rapsyn is

trafficked to the membrane in association with AChRs, co-distributes with AChRs in mature NMJs, and is present at a 1:1 stoichiometry with AChRs in the electric organ (LaRochelle and Froehner, 1986; Noakes *et al*., 1993). No AChR clusters form on muscles of rapsyn-null mice, and myotubes isolated from these mutants are unresponsive to agrin (Gautam et al., 1995). Furthermore, while recombinant expression of AChRs in non-muscle cells leads to a dispersed distribution of clusters at the membrane, co-expression of AChRs with rapsyn results in the formation of AChR-rapsyn co-clusters (Froehner et al., 1990; Phillips et al., 1991).

Accumulating results from these studies have established the agrin hypothesis as a useful framework to model the principles leading to synapse formation. However, new studies on early events of synaptogenesis have led to a reappraisal of the agrin hypothesis. First, AChR clusters do form and persist in a broad, central band of muscles lacking MN axons or agrin (Harris 1981; Yang et al., 2000). Second, these postsynaptic clusters are pre-patterned in the absence of agrin, or even nerve, but still require MuSK (Lin et al., 2001; Yang *et al*., 2001). Third, AChR clusters disperse more readily in muscles innervated by agrin-deficient nerves than in aneural muscles (San et al., 2003).

These results suggest that whereas in fact postsynaptic differentiation is autonomously initiated in a pre-patterned central zone, the nerve uses agrin to stabilize AChR clusters which it contacts, and a separate signal to disperse clusters that have not been induced or stabilized by agrin. This second signal has often been suggested to be neurotransmitter release (Misgeld T. et al., 2005).

During development, axons of MNs reach hind limb muscles, branch and innervate muscle fibers. Initially, each muscle fiber is innervated by several MNs. Gradually MNs will retract from synapses until, by the second week after birth, a single axon innervates each muscle fiber.
While at birth AChR clusters cover uniformly the NMJ, by the third week they have become organized into the characteristic groove pattern.

Chapter 7 - Mature NMJ

During the adult lifetime, the NMJ is a remarkably stable structure. The NMJ has multiple redundant mechanisms that produce a large safety factor and allow reliable activation upon nerve stimulation and that preserve normal function even when experimental manipulations alter different physiological parameters of the synapse (such as quantal content, pool trafficking, etc).

At the anatomical level, studies monitoring NMJs over months have shown very little change in the pre and postsynaptic structures (Gan et al., 2003).

Despite this apparent robust stability, the organization of the NMJ is the result of a continuous feedback regulation between the nerve and the muscle fiber. This is well illustrated by the profound effect that changes in the activity pattern of the NMJ have on synapse organization.

7.1 Role of activity

The importance of activity in the organization of the NMJ can be shown by local injection of botulinum toxin A (BotA). BotA is an enzyme that selectively cleaves SNAP-25, preventing vesicle fusion to the membrane and blocking calcium dependent neurotransmitter release (Blasi et al., 1993).

Application of BotA results in long term (several weeks) paralysis of the muscle, and induces anatomical rearrangements of the NMJ. One week after paralysis nerve sprouts grow from the axonal endplate along the muscle fiber.

The terminal Schwann cells also react to chronic paralysis by extending processes along the muscle fiber and migrating away from the original endplate. Because axons in muscle are always associated with tSC processes, and Thompson's work has shown that in partially denervated muscle axons prefer to grow along tSC processes (Son et al., 1995), it is likely that tSCs play an important role in the regulation of paralysis induced anatomical plasticity.

7.2 Role of Cholesterol and Rafts

The manner in which the microclusters associate with each other probably determines the stability and organization of the postsynaptic endplate. Many of the proteins

present at the postsynaptic cluster (AChR, rapsyn, Src family kinases) have been shown to be associated with lipid rafts (Bruses et al*.,* 2001; Marchand et al., 2002), and their distribution and function is thus expected to be dependent on lipid raft regulation.

Lipid rafts are mobile microdomains of many biological membranes including the plasma membrane, characterized by a dynamic assembly of a cholesterol and sphingolipids-rich platform accumulating or excluding certain types of proteins. Lipid rafts accumulate glycosylphosphatidylinositol (GPI) anchored proteins or doubly acetylated proteins such as Src family kinases (SFK) (Brown and London, 1998; Simons and Toomre, 2000).

Lipid rafts microdomains can coalesce into larger functional domains and can locally modify the plasma membrane environment, changing the conditions regulating phosphorylation by local kinases and phosphatases.

In this way lipid rafts are thought to create signalling platforms in which conditions for signal activation and regulation are modified.

Several lines of evidence suggest that lipid rafts may play and important role in the regulation of synapse assembly and maintenance. Depletion of cholesterol causes removal of surface AMPA receptors and of hippocampal neuron synapses (Hering et al. 2003). In ciliary neurons, lipid rafts are required to maintain AChRs in synapse-associated clusters (Bruses et al. 2001). Also, cholesterol is required at the NMJ to ensure correct AChR gating functions (Barrantes, 1993), and AChRs depend on lipid rafts for their trafficking toward the plasma membrane in transfected heterologous cells (Marchand et al., 2002).

Furthermore, Src and Fyn, two Src-family kinases (SFKs) associated with lipid rafts play an important role in synapse maturation. In cultured myotubes deficient for Src and Fyn, agrin or laminin induced clusters are unstable and rapidly disassemble upon removal of these factors (Marangi et al., 2002; Smith et al., 2001).

A further indication that lipid rafts play a role in synapse development is the observation that agrin treatment leads to lipid raft concentration (Khan et al., 2001). Agrin also leads to activation of SFKs (Mittaud et al., 2004).

A possible mechanism of postsynaptic stabilization by SFKs might involve regulation of the cortical cytoskeleton at the synapse. Cortactin is an effector of Src (Weed and Parsons, 2001), and its activation leads to increased F-actin polymerization (Weaver et al., 2001).

Chapter 8 - NMJ in disease

Amyotrophic lateral sclerosis (ALS) is a progressive neurodegenerative disease in which muscle weakness gradually develops leading to generalized paralysis and death. Although most cases of ALS are sporadic, 5% of total cases are familial (FALS). Among them, point mutations in the Cu, Zn superoxide dismutase SOD1(G93A) account for about 20% of the cases. Mechanisms enabling the mutant SOD1 to cause the disease seem to include pathogenic processes in the local environment of MNs (Lino et al., 2002; Clement et al., 2003), or mitochondrial accumulation of mutant SOD1 in affected MNs (Liu *et al*., 2004; Pasinelli et al., 2004). Early MN dysfunction includes mitochondrial pathology (Wong et al., 1995; Kong and Xu, 1998), axonal deficits such as the accumulation of neurofilaments and slowing of axonal transport (Collard *et al.*, 1995; Zhang et al., 1995; Williamson and Cleveland, 1999; Jablonka et al., 2004), and failure (Pinter et al.,1995) and loss of peripheral synapses (Frey et al., 2000; Fischer et al., 2004).

Transgenic mice overexpressing mutant SOD1 associated with human FALS (Rosen et al., 1993) develop a MN disease similar to human ALS, and provide excellent mouse models of motoneuron disease, because of the reproducibility of the phenotype among individuals of the same transgenic line (Gurney et al., 1994).

In a line of mice expressing SOD1(G93A) and exhibiting particularly high transgene expression levels, clinical symptoms of muscle weakness develop at about postnatal day 90 (P90), spinal MNs are lost after P100, and the mice die on average at P136 (Gurney et al., 1994; Chiu et al., 1995). Remarkably, these mice already exhibit extensive local muscle denervation at P50 (Frey et al., 2000a).

A similar pattern of early losses in the peripheral innervation has been reported in other models of motoneuron disease such as spinal muscular atrophy (SMA) (Frugier et al., 2002), progressive motor neuropathy (pmn) (Frey et al., 2000a), and motor neuron disease (Mnd) (Frey et al., 2000a), indicating that axonal "dying-back" (Raff et al., 2002) may be a key mechanism of early disease progression in many motoneuron diseases. Studies by Pinter and colleagues using a canine model of motoneuron disease have shown that progressive NMJ dysfunction is an early event in the disease process, suggesting that early dysfunctions lead to deficits in neuromuscular transmission, fol-

lowed by the progressive loss of subgroups of NMJs, leading to paralysis and death (Pinter et al., 1995; Pinter et al., 1997; Rich et al., 2002a; Rich et al., 2002b).

Thus, studies of peripheral motoneuron diseases suggest that dysfunctions affecting synaptic and axonal maintenance rather than motoneuron survival are the most relevant issues for disease progression, and that therapeutic targets addressing those dysfunctions are more likely to have a positive impact on disease progression (Lobsiger *et al*., 2005; Sagot et al., 1998; Sendtner et al., 1992).

Interestingly, synapses are lost in specific patterns during disease progression (Frey et al., 2000b). This reproducible selective vulnerability of certain NMJs in disease opens ways of studying the mechanisms facilitating or delaying disease progression.

Chapter 9 - Subject and aims of the study

The objective of the studies presented in this work have been to explore and uncover principles controlling the assembly, maintenance and loss of synapses, using the NMJ as a model system. Most of the studies focused on the relative roles of nerve, muscle and Schwann cells in synaptogenesis during development and synaptic plasticity in the adult.

The first study (chapter 10) analyzes mechanisms regulating synaptogenesis during development. It shows that the muscle fiber is a key player in directing synapse formation, and singles out two new classes of muscles (FaSyn and DeSyn), which undergo distinct pathways of synaptogenesis, and retain functionally different NMJs in the adult.

The second study (chapter 11) focuses on the regulation of anatomical plasticity at the adult NMJ in FaSyn and DeSyn muscles. It describes the relative roles of the muscle fiber and nerve in regulating anatomical plasticity, and addresses the impact of processes regulating assembly of postsynaptic clusters and of cell adhesion on synapse maintenance and plasticity.

The third study (chapter 12) shows how (unlike anatomical plasticity) synapse loss in motoneuron disease is determined by properties of presynaptic nerves.

A fourth study presented in Annex 1 expands on the role of lipid rafts on the postsynaptic apparatus and their impact on synaptic maintenance.

The sum of these results is further discussed in chapter 13.

Chapter 10 - An intrinsic distinction in neuromuscular junction assembly and maintenance in different skeletal muscles

Neuron Volume 34, Issue 3 , 25 April 2002, Pages 357-370

San Pun[1], Markus Sigrist[2], Alexandre Ferrão Santos[1], Markus A. Ruegg[3], Joshua R. Sanes[4], Thomas M. Jessell[5], Silvia Arber[1, 2] and Pico Caroni[1]

1 Friedrich Miescher Institute, Maulbeerstrasse 66, CH-4058, Basel, Switzerland

2 Department of Cell Biology, Biozentrum, Klingelbergstrasse 70, CN-4056, Basel, Switzerland

3 Department of Pharmacology, Biozentrum, Klingelbergstrasse 70, CN-4056, Basel, Switzerland

4 Department of Anatomy and Neurobiology, Washington University School of Medicine, 660 South Euclid Avenue, Saint Louis, MO 63110, USA

5 HHMI, Department of Molecular Biochemistry and Biophysics, Columbia University HHSC, 701 W 168th Street, New York, NY 10032, USA

10.1Summary

We analyzed the formation of neuromuscular junctions (NMJs) in individual muscles of the mouse embryo. Skeletal muscles can be assigned to one of two distinct classes of muscles, termed "Fast Synapsing" (FaSyn) and "Delayed Synapsing" (DeSyn) muscles, which differ significantly with respect to the initial focal clustering of postsynaptic AChRs, the timing of presynaptic maturation, and the maintenance of NMJs in young adult mice. Differences between classes were intrinsic to the muscles and manifested in the absence of innervation or agrin. Paralysis or denervation of young adult muscles resulted in disassembly of AChR clusters on DeSyn muscles, whereas those on FaSyn muscles were preserved. Our results show that postsynaptic differentiation

processes intrinsic to FaSyn and DeSyn muscles influence the formation of NMJs during development and their maintenance in the adult.

10.2Introduction

Synapses are the signaling interfaces between neurons. Their formation during development and modification in the mature organism are thought to involve reciprocal interactions between pre- and postsynaptic cell types. Although much is known about molecules associated with pre- and postsynaptic structures in the mature state, a clear understanding of the initial steps in synapse formation requires a more precise analysis of the individual contributions of pre- and postsynaptic partners to this process. Nerve-muscle synapses are well suited to studies of the relative roles of pre- and postsynaptic elements in the formation of synaptic connections because of the relative accessibility of presynaptic motor neurons (MN) and postsynaptic muscles (Sanes and Lichtman, 1999). In the mouse, the formation of the NMJ depends on the activation of a muscle-specific receptor tyrosine kinase (MuSK) (DeChiara et al. 1996; Glass et al. 1996 and Zhou et al. 1999) and the recruitment of a postsynaptic adaptor protein, rapsyn (Gautam et al. 1995 and Apel et al. 1997). Subsequent steps in synaptic differentiation appear to involve a series of bidirectional signaling interactions between nerve and muscle (Sanes and Lichtman, 2001).

The motor nerve has long been considered to exert a predominant role in organizing synaptogenesis at the developing neuromuscular junction. This view arose from in vitro studies in which motor nerves did not seek preexisting acetylcholine receptor (AChR) clusters as sites of synaptogenesis but, instead, induced new AChR clusters at sites of initial contact (Frank and Fischbach 1977 and Anderson and Cohen 1977). Subsequent studies in vivo indicated that incoming motor nerves secrete z-agrin (Gautam et al. 1996 and Burgess et al. 1999) to activate MuSK (DeChiara et al. 1996 and Glass et al. 1996) in myotubes, thereby promoting the clustering of AChRs. Moreover, activation of MuSK through overexpression of agrin in adult soleus muscle in-

duces the formation of a complex, aneural postsynaptic apparatus (Jones et al., 1997). These results demonstrated critical roles for agrin and MuSK in synaptogenesis and were generally interpreted as consistent with the earlier work in vitro (Sanes and Lichtman, 2001).

Recently, however, a new set of studies raised questions about whether agrin in particular or even motor nerves in general are necessary for the initial steps in postsynaptic differentiation. AChR clusters still form and persist in a broad, central synapse-like band in the absence of intramuscular motor nerves (Harris 1981 and Yang et al. 2000). In addition, postsynaptic clusters are prepatterned in a nerve- and agrin-independent, but MuSK-dependent, manner (Lin et al. 2001 and Yang et al. 2001). Moreover, these AChR clusters disperse more readily in muscles innervated by agrin-deficient nerves than in aneural muscles. These findings raise the possibility that postsynaptic differentiation is initiated nerve-independently in a prepatterned central zone and that the nerve then uses both agrin to stabilize AChR clusters it contacts and a separate signal to disperse clusters that have not been induced or stabilized by agrin.

One limitation of the genetic studies that have led to these models is that most of them have focused on a single muscle, the diaphragm (Gautam et al. 1995; Gautam et al. 1996; DeChiara et al. 1996; Burgess et al. 1999; Yang et al. 2000; Yang et al. 2001 and Lin et al. 2001). Although it seems reasonable to suppose that all NMJs develop in similar ways, in fact, it is well known that NMJs vary substantially in size and shape and that muscle fibers differ greatly in physiology, metabolism, and patterns of gene expression (Burke, 1994). We therefore wondered whether synaptogenesis proceeds in all muscles along the lines documented in diaphragm. To determine whether the steps in synapse formation and maturation exhibit muscle-type specific features, we carried out a detailed analysis of synaptogenesis and synaptic disassembly in identified limb muscles in wild-type mice, mice lacking MNs, mice mutant for agrin, and adult mice overexpressing agrin in MNs.

We found that developing and adult skeletal muscles can be subdivided into two distinct and previously unappreciated categories: Fast Synapsing (FaSyn) and Delayed Synapsing (DeSyn) muscles. These muscle classes exhibit intrinsically distinct features of focal AChR clustering and differ in the rates at which they aquire the characteristic organization of the mature NMJ. In particular, these two classes of muscles differ in: (1) the focal clustering of AChRs, (2) the alignment of the presynaptic nerve with focal AChR clusters, and (3) the alignment of Schwann cells (SCs) with the presynaptic nerve terminal. In FaSyn muscles, these three steps are achieved within less than 1 day of development, whereas in DeSyn muscles, the focal organization process involved a transition period of up to 5 days. In the absence of agrin, many NMJs on FaSyn muscles are apparently normal for the first 2–3 days, whereas those on DeSyn muscles do not form. While NMJs on FaSyn and DeSyn muscles exhibit a comparable anatomical organization in postnatal mice, treatments that challenge synaptic stability in young adult mice result in the selective disassembly of NMJs on DeSyn muscles, whereas those on FaSyn muscles are preserved. Between 3–9 months of age, NMJs on DeSyn muscles gradually become less sensitive to disassembly, suggesting that the consolidation of NMJs on DeSyn muscles is a protracted process in postanatal mice. Taken together, these findings provide evidence that intrinsic properties of FaSyn and DeSyn muscles play a prominent role in defining the progress of NMJ formation during the development of synapses and in their maintenance in the adult.

10.3Results

Two Patterns of Synaptogenesis in Hindlimb Muscles

To determine whether the process of synapse formation between MNs and skeletal muscle fibers differs among different muscles, we analyzed a large number of hindlimb muscles in mouse embryos. AChR clustering, a cardinal sign of postsynaptic differentiation, was detected with the specific ligand α-bungarotoxin (BTX). Initially, we noted that some muscles had bright, compact clusters of AChRs with little diffuse AChR signal, whereas other muscles in the same limb showed more weakly labeled,

less-compacted clusters, with appreciable diffuse AChR labeling (Figure 1A). Surprisingly, most muscles exhibited one of these two patterns that we call FaSyn and DeSyn for reasons detailed below. AChR clustering in muscle depends critically on the expression of the receptor tyrosine kinase MuSK and the adaptor protein rapsyn. However, the differences between FaSyn and DeSyn muscles in focal AChR clustering did not reflect differential expression levels of rapsyn (Figures 1B–E) or MuSK (data not shown), and the distribution of rapsyn in FaSyn and DeSyn muscles mirrored that of AChRs (Figures 1B–1E). We therefore undertook a systematic study, spanning the period from embryonic day (E)13.5, when motor axons in the mouse embryo start to invade individual cleaved muscle masses (Jones, 1979), to birth, by which time neuromuscular junctions (NMJs) have matured considerably (Sanes and Lichtman, 1999). Muscles were double-labeled with BTX and either antibody to GAP-43 (to label axons) or antibody to the S-100 protein (to label SCs).

Development of NMJs in the adductor, a FaSyn muscle, and the gracilis anterior, a DeSyn muscle, are compared in Figure 2. At E13.75, when the majority (not, vert, similar95%) of motor nerves are not yet associated with AChR clusters, muscles differed significantly in the appearance and intensity of nascent AChR clusters, which were already compact in the adductor (Figure 2A) but diffuse and weaker in the gracilis (Figure 2B). Between E14.5 and birth, AChR clusters on the adductor remained compact and became more intensely labeled, whereas AChR clusters on the gracilis remained poorly compacted between E14.5 and E16.5 (Figure 2). From E14.5, presynaptic nerves in FaSyn muscles were unbranched and confined to the AChR cluster region, and S-100+ SCs exhibited a compact configuration in close association with regions of AChR clusters (Figure 2). In contrast, between E14.5 and E16.5, terminal nerves in DeSyn muscles were branched and not aligned with AChR clusters (Figures 2D, 2F, and 2M), and SC cell bodies were not positioned over AChR clusters (Figures 2J, 2L, and 2M). From birth and up to adult, all muscles possessed NMJs of comparable appearance (Figures 2G, 2H, and 2M).

The distinct patterns of synaptogenesis in the adductor and gracilis were highly reproducible between different mouse embryos (see supplemental figure S1 online at http://www.neuron.org/cgi/content/full/34/3/357/DC1). To quantitate the differences between the adductor and gracilis, we compiled three "synapsing indices" for individual muscles. The compactness of AChR clusters, the alignment of presynaptic nerves with AChR clusters, and the alignment of SCs with AChR clusters were each scored on a scale of one (low) to five (high). Results are displayed in Figure 2M. In both muscles, focal clustering of AChRs preceded alignment of the nerve with the cluster, and alignment of the nerve preceded that of the SC. However, the rate at which these events occurred differed markedly between the muscles: the alignment process was substantially faster in adductor (1 day, from E13.75 to E15) than in gracilis (3 days, from E16.5 to birth) (Figure 2M).

Classification of Muscles as FaSyn or DeSyn

To ask how many patterns of synaptogenesis we could discern in the hindlimb, we applied the synapsing indices described above to a set of 37 muscles in hindlimbs of three mice at daily intervals from E13.75 to postnatal day (P)0 for individual muscles. Values from each of the three indices were summed (see Experimental Procedures), so the total score for each muscle ranged from 3–15. A detailed analysis of E13.5–E17.5 embryos revealed that most muscles could be assigned unequivocally to one of two distinct groups based on their synapse index values (Figure 3). Fast Synapsing muscles (FaSyn muscles) were defined as muscles with synapsing indices of 11–15. In these muscles, AChR clusters were intensely labeled and compact, and extrasynaptic AChR labeling was very low from E13.5 on (Figure 2 and Figure 3). Delayed Synapsing muscles (DeSyn muscles) were defined as muscles with synapsing indices between three and six. In these muscles, AChR clusters were weak and frequently fragmented, and there was extensive extrasynaptic AChR labeling up to E17 (Figure 2 and Figure 3). Using the same criteria, diaphragm and sternomastoid were classified as DeSyn muscles, and intercostals were classified as FaSyn muscles (not shown). A few

muscles exhibited "Intermediate Synapsing" (IntSyn) properties, with intermediate "synapsing index" values (seven to ten) between E14.5 and E16.5 (Figure 3G). These muscles exhibited DeSyn-type AChR cluster configurations but more frequent cluster-associated SCs, and they made the transition from immature to mature synapses earlier than in DeSyn muscles (Figure 3H; medial gastrocnemius [MGC]). A detailed analysis of the synapse organization process in FaSyn and DeSyn muscles revealed distinct differences in the rates at which alignment of AChR, nerve, and SC were achieved in the different muscles (Figure 2 and Figure 3). First, at any given time in development, the variability among the muscle fibers of a given muscle was low (Figure 2 and Figure 3). Second, the alignment process was substantially faster in FaSyn than in DeSyn muscles (Figure 2 and Figure 3). Linear regression analysis of the alignment rates yielded slopes of 11.5 (Adductor) and 14 (TA) for FaSyn muscles, 4.1 (LGC) and 4.2 (Gracilis) for DeSyn muscles, and 4.4 for MGC. Alignment rates in FaSyn and DeSyn muscles differed significantly ($p < 0.003$; Student's t test). Taken together, these findings provide evidence that with respect to several aspects of neuromuscular synaptogenesis, individual skeletal muscles can be subdivided into two main categories that exhibit distinct rates of NMJ formation.

The availablility of data from a large set of muscles provided an opportunity to test whether FaSyn- and DeSyn-type synaptogenesis may be related to rates of muscle maturation, physiological subtypes, or relative position in the embryo (Figure 3). First, we compared muscles of comparable fiber-type composition within the hindlimb. Two muscles with predominantly fast-fatiguable motor units, the lateral gastrocnemius (LGC) and the rectus femoris, exhibited different innervation patterns. The rectus femoris is a FaSyn muscle (the synapsing index at E16.5 is 13.8), whereas the LGC is a DeSyn muscle (the synapsing index at E16.5 is 3.5) (Figure 3). In addition, within any individual mixed-type muscle, FaSyn- and DeSyn-type innervation patterns were comparable among muscle fibers, further arguing against the possibility that these differences reflect the formation of functional subtypes of motor units. Second, no correlation was found between the proximodistal location of a muscle and the type

of innervation (Figure 3). But, there was a clear tendency for muscles of the same type to occur in groups (Figure 3), although individual muscles within such groups exhibited slightly different synapsing indices (e.g., three, five, and four for gracilis anterior, gracilis posterior, and semitendinosus ventral, respectively [E16.5]). Third, during this developmental period and up to birth, relative labeling intensities for myosin heavy chain isoforms were undistinguishable in FaSyn and DeSyn muscles (see supplemental figure S2 online at http://www.neuron.org/cgi/content/full/34/3/357/DC1), arguing against the possibility that they reflect differences in the rate of differentiation of individual muscles. Together, these findings suggest that the innervation pattern is a specific property of an entire muscle or the corresponding motor pool innervating the muscle.

Distinct Patterns of AChR Cluster Organization Reflect Muscle-Intrinsic Properties

To determine whether the different rates of AChR clustering reflect intrinsic properties of muscle or depend on motor innervation, we selectively eliminated MNs before their axons reached the target muscle (Yang et al., 2001). For the purpose of this study, it was essential that MNs to all muscles be eliminated at an early developmental stage. This requirement ruled out HB9−/− mice, where motor nerves are only absent in the diaphragm (Arber et al., 1999). Instead, we used a CRE-lox mediated system to activate a silent form of the diphtheria toxin A subunit gene (DTX) selectively in MNs (Figures 4A–4C). At E11.5, 2 days before invasion of cleaved muscle masses by motor nerves in the periphery, we detected a large (>90%) reduction in the number of MN cell bodies present in the ventral horn of the spinal cord in embryos positive for both alleles (Figures 4F and 4G), when compared to the control littermates where the silent DTX gene was present (Figures 4D and 4E).

Embryos lacking MNs were used to compare the pattern of AChR clusters in different muscles of the hindlimb. AChRs accumulated and clustered in central bands of forming muscles in the complete absence of motor axons in MN-free embryos, in agree-

ment with previous findings on diaphragm (Yang et al. 2001 and Lin et al. 2001). The level of AChR labeling intensity at E16.5 was reduced in all hindlimb muscles in the absence of motor axons, but pronounced differences in the intensity and patterning of these aneural clusters were still detected in different muscles. FaSyn muscles accumulated compact focal clusters, with low levels of AChR labeling along the rest of the muscle fiber surface (Figure 4J; see also Figure 2A), whereas DeSyn muscles exhibited weakly labeled and less-compacted clusters and a substantial level of extra-cluster AChR labeling (Figure 4K). These muscle-specific differences in AChR clustering in the absence of nerve corresponded consistently to FaSyn and DeSyn patterns during muscle innervation in wild-type mice (Figures 4H and 4I), suggesting that the distinct temporal patterns of neuromuscular synaptogenesis reflect properties intrinsic to individual developing muscles.

Differing Sensitivities of FaSyn and DeSyn Muscles to the Absence of agrin

In mouse embryos mutant for agrin, nerves invade muscles, but such embryos are severely impaired in AChR clustering (Gautam et al., 1996). We therefore considered the possibility that differences in agrin level or distribution might lead to DeSyn or FaSyn properties. To test this possibility, we analyzed agrin−/− embryos, which lack all forms of agrin (Lin et al., 2001). As shown in Figures 5A–5F, neuromuscular synaptogenesis remained distinct in FaSyn and DeSyn muscles, ruling out the possibility that differences in nerve and/or muscle agrin cause differential clustering of AChRs in FaSyn and DeSyn muscles.

Although muscles lacking motor nerves and agrin cluster AChRs in a muscle-type specific pattern, the presence of the nerve has a strong influence on the intensity of AChRs. We therefore extended our analysis of agrin mutant mice to determine whether FaSyn and DeSyn muscles differ in their sensitivity to agrin. For these studies, we used both the agrin−/− mutant described above and a hypomorphic mutant that lacks all nerve-derived z-agrin but retains low levels of m-agrin (z-agrin−/− mice;

Gautam et al., 1996; z-agrin designates the splicing forms of agrin that can activate MuSK, whereas m-agrin designates those that do not activate MuSK). Results from both alleles were the same and are presented together.

In agreement with published reports (Gautam et al., 1996), muscle fibers in several muscles, including the diaphragm (data not shown), were defective in AChR clustering in the absence of z-agrin from E14.5 on. In addition, we detected dramatic differences between FaSyn and DeSyn muscles. In the FaSyn muscles of z-agrin−/− mice, a majority of the AChR clusters were normal in size at E14.5 (Figure 5I; see Figure 5E for quantitative data in agrin−/− mice). At later developmental stages, AChR clusters failed to grow and then dispersed in the absence of agrin (Figures 5E and 5F). AChR clusters were partially associated with nerves (Figure 5F, agrin−/− mice) and tSCs (Figures 5A, 5F, 5I, and 5K). At nonnerve, non-tSC-associated AChR clusters, a marked decrease in AChR cluster labeling suggested that AChR loss and retraction of the presynaptic nerve and tSC after E15.5 are coincident.

Nevertheless, AChR labeling patterns in FaSyn muscle fibers that lost AChR clusters in the absence of agrin did not resemble those in DeSyn muscle fibers of wild-type mice. Specific differences included the maintenance of compact, although less intensely labeled, clusters and the absence of ectopic AChR labeling throughout the dispersal process. Analysis of DeSyn muscles of agrin−/− and z-agrin−/− mice revealed a very different pattern. In the absence of z-agrin, AChR clusters were undetectable at many muscle fibers of DeSyn-muscles by E14.5 (Figure 5J) and only very weak clusters were detected in these muscles at E16.5 (Figures 5B, 5D, and 5L). SCs and nerves were consistently positioned at a distance from occasional AChR accumulations. These findings show that AChR clusters in DeSyn muscles are more sensitive to the absence of agrin than in FaSyn muscles and that each type of AChR cluster maintains its own muscle type-specific properties during disassembly. In addition, when compared to embryos without MNs, where all fibers of a given muscle exhibited comparable AChR labeling patterns, more heterogeneity in focal AChR clustering was evident

in the presence of nerve and in the absence of agrin (Figure 5F). Therefore, motor nerves initially promoted cluster accumulation in the absence of agrin in FaSyn muscles, but a few days later, they also induced cluster dispersal in these muscles.

Selective Disassembly of NMJs in DeSyn Muscles Can Be Induced by Chronic Blockade of Synaptic Activity in Young Adult Mice

To determine whether muscle type-specific properties are maintained at mature synapses in FaSyn and DeSyn muscles, we attempted to destabilize synapses by blocking nerve-evoked activity. We carried out activity blockade experiments in 3-week-old and older mice by treating muscles with Botulinum toxin A (BotA), a toxin that blocks calcium-dependent transmitter release. Such treatments induce ultraterminal nerve sprouting in selected muscles (Frey et al., 2000).

A single application of BotA to the triceps surae muscle produced a pronounced blockade of neuromuscular transmission in hindlimb calf muscles, with the absence of stimulus-induced endplate potentials and greatly reduced frequencies (>90%) of spontaneous transmitter release that persisted for at least 2 weeks (data not shown). Under these experimental conditions, AChR labeling patterns between 5 and 30 days after application of the toxin were not substantially different from untreated controls (Figure 6G). In contrast, repeated applications of toxin over a period of 2 weeks led, in selected muscles, to a pronounced loss of postsynaptic AChRs (Figures 6D and 6G). 1 month after the onset of paralysis, postsynaptic disassembly was nearly complete at DeSyn muscles (Figures 6D and 6G) and absent at FaSyn muscles (Figures 6C and 6G). Concomitant with the disassembly of the original postsynaptic AChR cluster, numerous ectopic nerve-associated AChR clusters appeared in DeSyn muscles (data not shown). Ectopic clusters were absent in FaSyn muscles. To verify that the absence of nerve-evoked activity has distinct effects on AChR clusters in FaSyn and DeSyn muscles, we also analyzed AChR clusters in denervated muscles. Like chronic paralysis, denervation produced a disassembly of AChR clusters on DeSyn muscles, whereas those on FaSyn muscles resisted disassembly (Figures 6E, 6F, and 6G). Chronic paral-

ysis or denervation induced a complete loss of focal AChR clusters in DeSyn muscles in mice of up to not, vert, similar2–3 months of age. In older mice, this sensitivity to the absence of nerve-evoked activity decreased, and no disassembly was detected in mice 6 months and older (Figures 6G and 6P). Therefore, marked differences between NMJs of FaSyn and DeSyn muscles persist in young adult mice, where they can be revealed as differences in sensitivity to chronic transmitter release blockade or denervation. This sensitivity is gradually lost between 3 and 6 months of age, suggesting that the consolidation of NMJs in DeSyn muscles is a protracted process, extending from embryonic development into maturity.

To determine how chronic blockade of neuromuscular transmission affects the presynaptic components, we analyzed neuromuscular innervation in chronically paralyzed adult muscle using a combined silver esterase reaction. This histological method visualizes intramuscular nerves in black and the reaction product of acetylcholine esterase at the synapse in blue. Repeated applications of BotA to hindlimb muscles over a 2 week period led to a dramatic collateral sprouting reaction in DeSyn muscles, e.g., LGC and vastus lateralis in 1-month-old mice (Figures 6K and 6O), but not 1-year-old mice (Figures 6M and 6P). Starting about 2 weeks after the beginning of the treatment, numerous collaterals grew longitudinally along the paralyzed muscle fibers, extending for up to 0.5 mm on each side of the original synaptic site (Figures 6K and 6N). The longitudinal sprouts extended short transversal side branches that formed acetylcholine esterase-rich putative ectopic synaptic structures (data not shown). In marked contrast, the rectus femoris and tibialis anterior, two FaSyn muscles, did not exhibit this sprouting response (Figures 6J and 6O). Analysis of collateral sprouting and AChR cluster disassembly in the same muscles revealed that the two processes were closely correlated in their timing (Figure 6N), muscle specificity (Figure 6O), and age dependence (Figure 6P). The time course of AChR cluster disassembly in chronically paralyzed and denervated DeSyn muscles was comparable (data not shown), suggesting that as in the embryo, the status of focal clustering of AChRs influences the maintenance of the presynaptic nerve at the NMJ.

Roles of agrin in Stabilizing Adult Synapses

To investigate further the similarities between the factors that affect synapse formation during development and those that promote synapse maintenance in the adult, we explored the role of agrin in young adult mice. To investigate the possible relationship between agrin-mediated synapse maintenance and inactivity-mediated destabilization, we carried out chronic paralysis experiments with BotA in mice that express higher or lower than normal levels of agrin.

The expression of agrin in neurons, including spinal MNs, is substantially lower after birth than in early development (Cohen et al., 1997). To generate adult mice expressing high levels of agrin, we produced Thy1-agrin transgenics (Figure 7A) that overexpress chick z-agrin specifically and constitutively in adult neurons, including spinal MNs (Figures 7A–7D; Caroni, 1997). Two independent transgenic lines were used for this study, with comparable results (Figure 7D). In both lines, robust expression of the transgene started about 1 week after birth, and many neurons, including spinal MNs (Figure 7B), expressed transgenic agrin. When mouse and chick agrin cDNA probes were used to compare in situ hybridization signals in spinal MNs in the adult, transgene signals were more than 10-fold higher than those for endogenous agrin (data not shown).

Overexpression of z-agrin in Thy1-agrin mice protected AChR clusters and presynaptic nerves against destabilization induced by chronic blockade of nerve-evoked activity in the presence of BotA (Figures 7G–7I). Although a substantial fraction of neuromuscular synapses in DeSyn muscles did eventually disassemble in the transgenic mice, this reaction was delayed significantly. 25 days after beginning the BotA treatment, LGC (lateral compartment) muscle fibers with no detectable presynaptic structures and sprouts of more than 50 μm were found at >90% of wild-type values, but less than 30% of total in Thy1-agrin mice; values at 45 days were >98% and >70%, respectively. Taken together, these results provide evidence that z-agrin promotes

NMJ maintenance in the adult and suggest that agrin and synaptic activity may act in concert to maintain NMJs.

To decrease agrin expression, we made use of heterozygous z-agrin+/− mice. In these mice, significant AChR disassembly and collateral nerve sprouting characteristic of synapse disassembly was detected in both DeSyn (Figures 7F and 7I) and FaSyn (Figures 7E and 7I) muscles 1 month after the onset of the chronic BotA treatment. In addition, z-agrin+/−mice exhibited an accelerated sprouting response. Substantial sprouting was detected after a single treatment with BotA in DeSyn muscles, and occasional synapses with sprouts were observed in the absence of paralysis in DeSyn muscles (data not shown). Taken together, these results provide evidence that z-agrin promotes NMJ maintenance in the adult and suggest that agrin and synaptic activity act in concert to maintain NMJs.

Schwann Cell Sprouting in Denervated FaSyn and DeSyn Muscles

To further investigate whether in young adults, as in the embryo, a major contribution to the difference observed in DeSyn and FaSyn muscles resides in the muscle, we monitored tSC sprouting in lower hindlimb muscles 14 days after denervation using p75 expression (Reynolds and Woolf, 1992). Strong SC and tSC p75 immunoreactivity was detected in the absence of nerve (Figures 8C–8H), whereas p75 signals were nearly undetectable in innervated contralateral muscle (Figures 8A and 8B).

A comparison of tSCs sprouting at denervated NMJs of FaSyn and DeSyn muscles in 6-week-old mice revealed substantial differences in the two types of muscles. Thus, while strong tSC sprouting was detected at all NMJs in DeSyn muscles (Figure 8D), sprouting was weak to absent in FaSyn muscles (Figure 8C). Similar distributions of tSCs with sprouts were detected 7 days after denervation (data not shown). Like synapse disassembly after chronic paralysis, denervation-induced tSC sprouting was affected by the expression of agrin. Thus, in adult z-agrin+/−mice with only one wild-type agrin allele, tSC sprouting was much more pronounced and also detected at most

synapses in FaSyn muscles (Figures 8E and 8F). Moreover, denervation-induced tSC sprouting was reduced in adult Thy1-agrin mice (Figures 8G and 8H). In denervated soleus muscle, 168 (84%) out of 200 denervated NMJs exhibited at least one tSC process longer than 50 μm, and 105 (52%) had processes longer than 75 μm in wild-type mice (n = 4 mice). In Thy1-agrin transgenics, the corresponding values were 37/200 (18%) and 12/200 (6%) (n = 4 mice). These results demonstrate the existence of marked differences in the sprouting responses of tSCs to denervation in FaSyn and DeSyn muscles in the adult and suggest that chronic absence of activity and nerve promotes sprouting of tSC processes in DeSyn, but not in FaSyn, muscles.

10.4Discussion

In this study, we provide evidence that skeletal muscles can be subdivided into two previously unrecognized subtypes, designated FaSyn and DeSyn muscles. These muscles differ in the rate of neuromuscular synaptogenesis during embryonic development and in the maintenance of NMJs in the adult. As soon as neuromuscular synaptogenesis begins, FaSyn and DeSyn muscles exhibit marked differences in the morphology of AChR clusters and in the extent to which nerve terminals, SCs, and AChR clusters are associated with each other. In FaSyn muscles, a mature pattern is achieved within less than 1 day of development but, in DeSyn muscles, it requires 4–5 days. These differences in the timing and rate of synapse assembly appear to reflect muscle-intrinsic, nerve-independent programs of focal AChR clustering. FaSyn and DeSyn muscles differ in the extent to which they depend on agrin. In a DeSyn muscle (such as the diaphragm), focal AChR clustering and maintenance depends critically on nerve-derived factors, whereas this dependence is much more limited in FaSyn muscles. NMJs on FaSyn and DeSyn muscles continue to differ for several months after birth. Thus, after birth and up to 3–5 months of age, AChR clusters and presynaptic nerve terminals in DeSyn muscles are selectively vulnerable to the absence of nerve-evoked activity or reduced levels of agrin.

Here, we first discuss possible mechanistic bases for differences between FaSyn and DeSyn muscles. Second, we discuss how these findings provide new insight into the relative roles of muscle and nerve in neuromuscular synaptogenesis. Third, we discuss the selective vulnerability of synapses on DeSyn muscles in young adults and the protective roles of nerve-evoked activity and agrin during AChR cluster and synapse disassembly.

Intrinsically Distinct Patterns of Focal AChR Clustering in Different Muscles

FaSyn and DeSyn muscles differ in their abilities to form focal AChR clusters in the presence or absence of motor axons and to maintain AChR clusters in the presence or absence of agrin. The differences between the nature and rate of NMJ formation in the two muscle types may involve the general molecular steps that are thought to control focal AChR clustering. FaSyn and DeSyn muscles could, for example, express different levels of critical protein components that drive the assembly of the postsynaptic receptor complex (e.g., MuSK or rapsyn). However, we have not detected clear differences in the distribution of rapsyn or MuSK in FaSyn and DeSyn muscles between E14.5 and birth. Alternatively, the clustering processes for AChRs or associated molecules may differ qualitatively in the two types of muscle. This could involve the presence of different accessory proteins and/or variations in signal transduction pathways involved in complex assembly (Fuhrer et al. 1999 and Sanes and Lichtman 2001). One possible target of such differential pathways could be the primary MuSK-dependent scaffold (Apel et al., 1997) necessary to drive AChR clustering.

A recent study carried out in the sternomastoid muscle of young and adult mice (a DeSyn muscle) has provided evidence that blocking skeletal muscle TrkB receptor activity leads to a fragmentation of AChR clusters and to the disassembly of synapses (Gonzalez et al., 1999). TrkB receptor activity may also be required to prevent the fragmentation of agrin-induced AChR clusters on cultured myotubes (Gonzalez et al., 1999), raising the possibility that FaSyn and DeSyn muscles differ in their dependence

on signal transduction events downstream of TrkB receptor activation. Finally, differences in matrix components, such as laminins or proteoglycans, which are known to modulate effects of agrin, may be involved. Muscle specification and patterning are directed by cues originating in the local mesenchyme, so differences in the extracellular matrix or mesenchymal cells of FaSyn and DeSyn muscles might well exist.

Relative Roles of Focal AChR Clustering and Nerve-Derived Signals in Promoting Synaptogenesis in FaSyn and DeSyn Muscles

The striking correlation between AChR cluster patterns and the timing and rate of NMJ maturation at nascent synapses in FaSyn and DeSyn muscles raises the question of how pre- and postsynaptic differentiation are coordinated. On the one hand, presynaptic maturation might be controlled in a retrograde fashion by the postsynaptic differentiation process. Alternatively, different MN pools might also have independent programs that permit fast or delayed presynaptic maturation. Although our experiments do not address this question in the developing embyro, we detected selective AChR loss in the presence of BotA or denervation and selective tSC sprouting upon denervation in DeSyn muscles in the adult. Based on these findings, we favor the idea that the intrinsic mechanisms that influence AChR clustering in FaSyn and DeSyn muscles also have an impact on at least some aspects of presynaptic differentiation, maturation, and maintenance at the NMJ (Figure 9).

Whatever the sources of differences between FaSyn and DeSyn NMJs, our results are relevant to recent findings on the role of the presynaptic nerve and agrin in organizing postsynaptic AChR complexes. This is because nearly all previous studies have focused on the diaphragm, a DeSyn muscle. These studies led to the conclusion that the presence of the presynaptic nerve is necessary to maintain synaptic AChR clusters and to disperse nonsynaptic clusters. In all of the DeSyn muscles analyzed in this study, we found a similar dependence on the nerve for synaptogenesis. These findings are also consistent with the induction of ectopic AChR clusters by ectopic expression of z-agrin in an adult DeSyn muscle, the soleus (e.g., Jones et al., 1997). In FaSyn mus-

cles, however, the process of AChR cluster formation is much more rapid and independent of the nerve for a prolonged period. Thus, at least in FaSyn muscles, agrin does not appear to be essential for the initial formation of a synaptic complex of AChR cluster, nerve, and SC. Instead, agrin appears to have a critical role in augmenting focal AChR clustering, enhancing alignment of nerve and SC with the AChR cluster, and promoting NMJ maintenance. Thus, in the absence of agrin, alignment of nerve and SC with AChR clusters in FaSyn muscles were distinctly slower than in wild-type mice between E13.5 and E15.5, and NMJs began to disassemble from E15.5 on (Figure 5F). The presence of an efficient process of focal AChR clustering may initially be sufficient to protect nascent NMJs on FaSyn muscles from disassembly in response to the absence of agrin, whereas selective vulnerability in DeSyn muscles may be due to the low intrinsic efficiency of the clustering process in these muscles. In agreement with previous reports (Sanes and Lichtman, 1999), agrin may thus promote synapse maturation and maintenance by strengthening and sustaining the pathway for AChR clustering, presumably through MuSK (Figure 9).

A comparison of AChR clusters in the absence of MNs or agrin (Figure 4 and Figure 5) supports and extends the notion that the motor nerve can promote synaptogenesis in the absence of agrin (Lin et al. 2001 and Yang et al. 2001). Although in agrin-deficient mice most AChR clusters in FaSyn muscles are indistinguishable from those in wild-type before E15.5, these clusters are smaller and labeled less intensely in the absence of MNs . The motor nerves not only promote AChR cluster growth in the absence of agrin in FaSyn muscles, but also enhance cluster dispersal at ectopic sites in DeSyn muscles and at disassembling synapses in both DeSyn and FaSyn muscles. Thus, in mice lacking MNs, all muscle fibers of a given muscle exhibit comparable AChR labeling patterns, whereas in the absence of agrin, even FaSyn muscles contain increasing numbers of muscle fibers lacking detectable AChR clusters after E15.5. These findings are similar to the effects of synaptic and extra-synaptic activity on AChR gene expression and AChR cluster formation and stability (Sanes and Lichtman, 1999). They are also reminiscent of the effects of agrin and electrical activity on

the formation, growth, and stability of ectopic AChR clusters on living soleus muscle in adult rats (Skorpen et al., 1999).

Selective Vulnerability of NMJs on DeSyn Muscles in the Adult

The motor nerve continues to play an important role in maintaining AChR clusters and in synapse integrity postnatally. Our results show that in young adult mice, as in the embryo, this neural influence differs between FaSyn and DeSyn muscles, generally being greater in the latter. One pathway through which the nerve promotes synaptic maintenance involves muscle activity. Thus, the chronic paralysis experiments provide experimental evidence that a minimal amount of nerve-induced synaptic activity is required in the adult to maintain neuromuscular synapses on DeSyn muscles. These findings are consistent with those of a recent study on the turnover of AChRs at blocked NMJs of the sternomastoideum (Akaaboune et al., 1999), a DeSyn muscle. A similar role of nerve-evoked activity for maintenance of postsynaptic dendritic spines has been described in hippocampal neurons in slice cultures (McKinney et al., 1999). Z-agrin also protected synapses on DeSyn muscles from disassembly in the adult. Together, these results suggest that a low level of nerve-evoked activity may act together with z-agrin to protect synapses from the activation of an AChR cluster and synapse disassembly pathway in young adult mice.

There are several parallels between the processes of NMJ disassembly for FaSyn and DeSyn muscles in the embryo and in the adult. By analogy to its role in the adult, it is possible that during NMJ development, activity promotes focal AChR clustering at synapses and promotes AChR dispersal in the absence of agrin and at extra-synaptic sites. This interpretation is consistent with the finding that in the absence of transmitter release in Munc-18−/− mice, NMJ formation is initiated normally, but synapses disassemble after a few days (Verhage et al., 2000). A similar role for synaptic activity in promoting synapse maturation and maintenance has been suggested for developing retino-tectal synapses (e.g., O'Rourke et al., 1994).

Reciprocal Interactions between Nerve and Muscle during NMJ Formation and Maturation

We found a striking correlation between focal AChR clustering, synapse formation during development, and synapse maintenance in the adult in FaSyn and DeSyn muscles, raising the question of how these events are coordinated. One possibility is that focal postsynaptic AChR clustering plays a critical role in signaling retrogradely to promote synapse differentiation and prevent disassembly (Figure 9). During development, presynaptic differentiation involves the stopping, alignment, and thickening of the presynaptic nerve, and positioning of tSC bodies at the maturing synapse. The striking rearrangement of SCs to synapse-associated position may coincide with the aquisition of synapse-specific properties by tSCs. The tight association of tSCs with maturing presynaptic terminals may promote further synapse strengthening by enhancing the efficacy of synaptic transmission (Robitaille, 1998). Such heightened efficacy, in turn, may signal back from muscle to the presynaptic nerve to promote further presynaptic differentiation locally at the nerve terminal and through retrograde signaling pathways to the terminal arbor and on to the cell body (Fitzsimonds and Poo, 1998). This process would parallel local regulation at the developing NMJ in Drosophila, where postsynaptic differentiation and synaptic efficacy generate retrograde signals that control presynaptic differentiation (Davis and Goodman 1998 and Davis 2000). Through such retrograde signals, the assembly of the synaptic apparatus through processes intrinsic to particular postsynaptic muscles may affect the timing of presynaptic MN maturation.

In addition to affecting the timing of pre- and postsynaptic maturation, the differences in synaptogenesis and synapse maintenance in FaSyn and DeSyn muscles may confer distinct regulatory properties to forming and maturing synaptic connections in the two types of muscles. Thus, due to their relative instability in the embryo and in young mice, synapses on DeSyn muscles may be more sensitive to control through activity or trophic support than those on FaSyn muscles. Similar differences in maturation rate may also exist at central synapses, raising the possibility that intrinsically distinct sus-

ceptibilities to regulation may be a general principle to affect the plasticity of synaptic connections during development and the restriction of this plasticity in the adult.

10.5Experimental Procedures

Mouse Genetics

agrin mutant mice: z-agrin−/− mice were produced as described (Gautam et al., 1996) and were obtained through F. Rupp (Johns Hopkins University); agrin−/− mice were generated as described by Lin et al. (2001). Thy1-z-agrin transgenic mice overexpressing chick-z-agrin cDNA in adult neurons were produced using full-length chick neural agrin (Denzer et al., 1995) and the Thy1 expression cassette described by Caroni (1997) (see also Figure 7).

We produced mice lacking MNs from an early time in development and before the outgrowth of motor axons from the spinal cord using a specific genetic approach for diphtheria toxin-mediated ablation, as described inYang et al. (2001).
Paralysis and Denervation Experiments

To block transmitter release at the NMJ, purified Botulinum toxin A (Botox, clinical grade, Allergan AG, Lachen, Switzerland) was injected (0.01 U per g mouse) into either the triceps surae or quadriceps muscle. To produce chronic paralysis, toxin was applied every third day, for periods of up to 1 month. Hindlimb muscles were denervated by cutting the sciatic nerve at midthigh level.

Histology and Immunocytochemistry

Embryonic hindlimbs were fixed with 4% paraformaldeyde in PBS for 2 hr, and serial 12 μm cryostat sections were collected. Sections were incubated for 16 hr at 4°C in PBS with 1% BSA, 0.1% Triton X-100, and antibody, followed by secondary antibodies. Synapsing index values were based on three criteria: (1) the compactness of

AChR clusters, (2) the alignment of presynaptic nerves with AChR clusters, and (3) the alignment of SCs with AChR clusters. These parameters were scored on a scale of one (low) to five (high), and individual values were summed for each muscle. All sections were from one set of embryos, which included wild-type and mutant littermates, and were processed and analyzed at the same time. For samples between E13.75 and E14, only sections of muscle invaded by nerve were scored.

Skeletal muscle proteins were visualized with the following antibodies: skeletal α-actinin, monoclonal antibody EA-53 (Sigma); myosin heavy chain embryonic, monoclonal antibody WB-MHCe (Novocastra Labs., Newcastle-upon-Tyne, UK); and integrin-α7, rabbit antiserum (kind gift of U. Mueller, Friedrich Miescher Institut, Basel, Switzerland). RITC-α-Bungarotoxin and Alexa-labeled secondary antibodies were from Molecular Probes Inc., Eugene, OR.

Postsynaptic complexes (α-Bungarotoxin-positive areas) in 25-day-old and older mice were scored for their integrity on a five (control) to zero (disassembled) scale, as described in the Supplemental Experimental Procedures section. Postsynaptic complexes scoring three or less were defined as disassembling AChR clusters. Neuromuscular synapses and their innervation patterns in the adult were visualized with a combined silver esterase reaction, as described by Aigner et al. (1995). Disassembling synapses were defined as muscle fibers exhibiting nerves with no detectable terminal arborization and characteristically twisting collateral sprouts extending for more than 150 μm along the length of the muscle fiber.

Data analysis

AChR cluster compactness values were defined as follows: (1) prominent labeling along the central half of muscle fiber, multiple central clusters; (2) prominent extra-cluster labeling, central cluster fragmented; (3) detectable extra-cluster labeling, one uninterrupted central cluster; (4) no detectable extra-cluster label, variations in label-

ing intensity within central synaptic cluster; and (5) no detectable extra-cluster label and uniform labeling of central synaptic cluster.

The alignment of presynaptic nerves with AChR clusters was asessed as follows. (1) Less than 10% of NMJs exhibit any overlap between nerve and AChR cluster. (2) Less than one third of NMJs exhibit any overlap between nerve and AChR cluster. (3) At least one third of NMJs exhibit at least 25% alignment between nerve and AChR cluster; terminal nerve branches defasciculated. (4) At least 50% alignment between nerve and AChR cluster at more than half of NMJs; terminal nerve branches partially defasciculated. (5) Nerve and AChR cluster aligned over more than 75% of length, at more than 90% of the NMJs, and terminal nerve branches fasciculated.

The alignment of SCs with AChR clusters was assessed as follows. (1) No overlap between SCs and AChR clusters. (2) Less than one third of NMJs exhibit any overlap between SC and AChR cluster. (3) At least one third of NMJs exhibit at least 25% alignment between SC and AChR cluster. (4) 50% alignment between SC and AChR cluster at more than half of NMJs. (5) Nerve and AChR cluster aligned over more than 50% of length, at more than 90% of the NMJs.

Postsynaptic complexes (α-Bungarotoxin-positive areas) in 25-day-old and older mice were scored for their integrity on a five (control) to zero (disassembled) scale, according to the following criteria. Five: branches of uniform width and labeling intensity with bright edges; >50% of surface inside area defined by α-Bungarotoxin-positive branches (synaptic region) not labeled for AchR. Four: AChR-positive branches broader than in five, with variable width, uniform labeling intensity, but no prominently labeled edges; fraction of AChR-negative area inside synaptic region <50%. Three: as in four, but labeling intensity inside AChR-positive branches inhomogeneous (patchy); total synaptic region area 50% or less of that in four, presumably due to strong muscle atrophy. Two: as in three, but no well-defined AChR-negative areas inside synaptic region. One: as in two, but <50% of synaptic region outlines defined

as a discontinuity in α-Bungarotoxin labeling intensity; substantial (about half or more) fraction of the area inside synaptic region exhibits AChR labeling levels comparable to background. Zero: small, weakly labeled, nonconnected AChR-positive areas, with no defined synaptic region detectable.

10.6Acknowledgements

We thank Corinna Schneider and Lan Xu (Friedrich Miescher Institut) for help with the histology and electrophysiology of adult muscles, Simon Hippenmeyer (Biozentrum) for help with the figures, and Fabio Rupp (Johns Hopkins University) for z-agrin mutant mice. We are grateful to Yves-Alain Barde (Friedrich Miescher Institut) for valuable comments on the manuscript. S.A. is supported by a grant from the Swiss National Science Foundation. M.A.R. is supported by grants from the Swiss National Science Foundation and the Kanton of Basel-Stadt. J.R.S. is supported by the N.I.H.; T.M.J. is an investigator of HHMI. The Friedrich Miescher Institute for Biomedical Research is a branch of the Novartis Research Foundation.

10.7Figures

Figure 1. Distinct Patterns of AChR Clustering during Synapse Formation in Different Muscles of the Hindlimb in the Mouse(A) Labeling of AChR with α-Bungarotoxin in FaSyn (tibialis anterior) and DeSyn (LGC) muscles at embryonic day (E)16.5. Both a FaSyn and a DeSyn muscle are shown on the same low-magnification panel. The high-magnification images of AChR clusters in FaSyn and DeSyn muscle were processed in the same way. Note the bright, compact clusters and the very low levels of extrasynaptic signal in the FaSyn muscle; also note the more weakly labeled, noncompacted clusters and the presence of diffuse AChR labeling in the DeSyn muscle.(B–E) Double-labeling immunocytochemistry of FaSyn (adductor, [B and C]) and DeSyn (gracilis anterior, [D and E]) muscles at E14.5 for AChR (B and D) and rapsyn (C and E). The four images were processed at the same flourescent intensity. Note that rapsyn

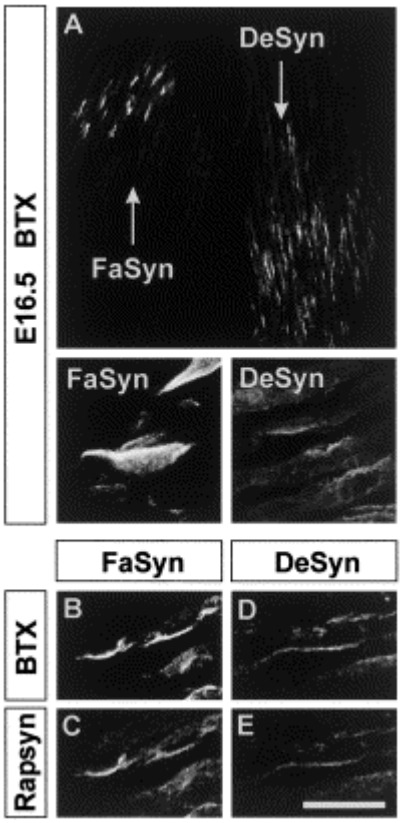

labeling patterns reflect AChR patterns in FaSyn and DeSyn muscle.Scale bar: 80 μm, (A) low magnification panel; 10 μm, (A) insets; and 7.5 μm (B–E).

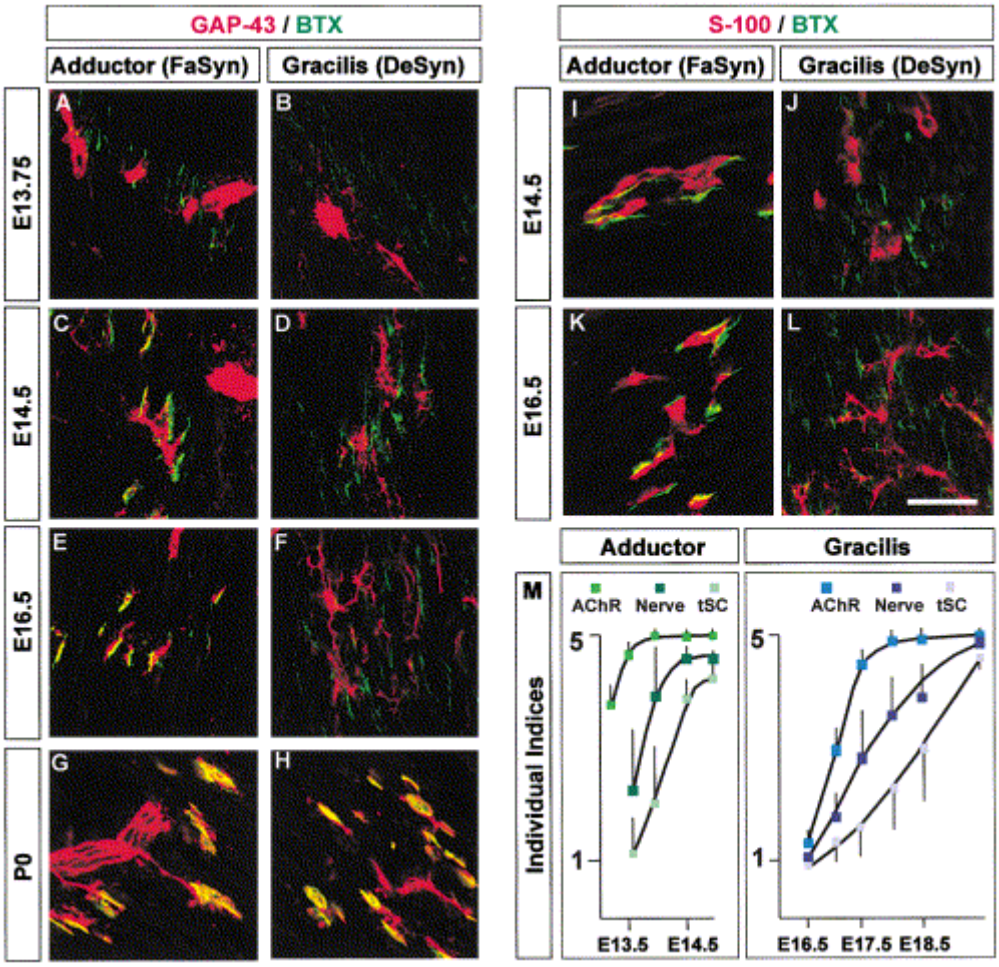

Figure 2. Distinct Patterns of Neuromuscular Synaptogenesis in Mouse FaSyn (Adductor) and DeSyn (Gracilis Anterior) Muscles(A–L) Double-labeling immunocytochemistry of FaSyn (A, C, E, G, I, and K) and DeSyn (B, D, F, H, J, and L) muscles at E13.75 (A and B), E14.5 (C, D, I, and J), E16.5 (E, F, K, and L), and at birth (G and H). Postsynaptic AChR was visualized with fluorescently labeled α-Bungarotoxin (BTX, green), nerve with an antibody against the axonal protein GAP-43 (red) and Schwann cells (SC) with an antibody against S-100 (red). Individual indices for the data shown in the panels are as follows (average value for AChR cluster/alignment of nerve or SC with AChR cluster): 4.4/1 (A), 1.2/1 (B), 4.8/4 (C), 1.4/1 (D), 4.9/5 (E), 1.4/1 (F), 4.9/5 (G), 4.9/5 (H), 4.8/5 (I), 1.5/1 (J), 4.9/4 (K), and 1.5/2 (L).(M) Individual indices (compactness of AChR cluster, alignment of nerve with AChR cluster, and alignment of SC with AChR cluster) as a function of developmental time during the transition phase to a mature synaptic configuration in a FaSyn (adductor) and DeSyn

(gracilis anterior) muscle. Data are averages from 50 NMJs (three embryos).Scale bar: 40 μm (A–L).

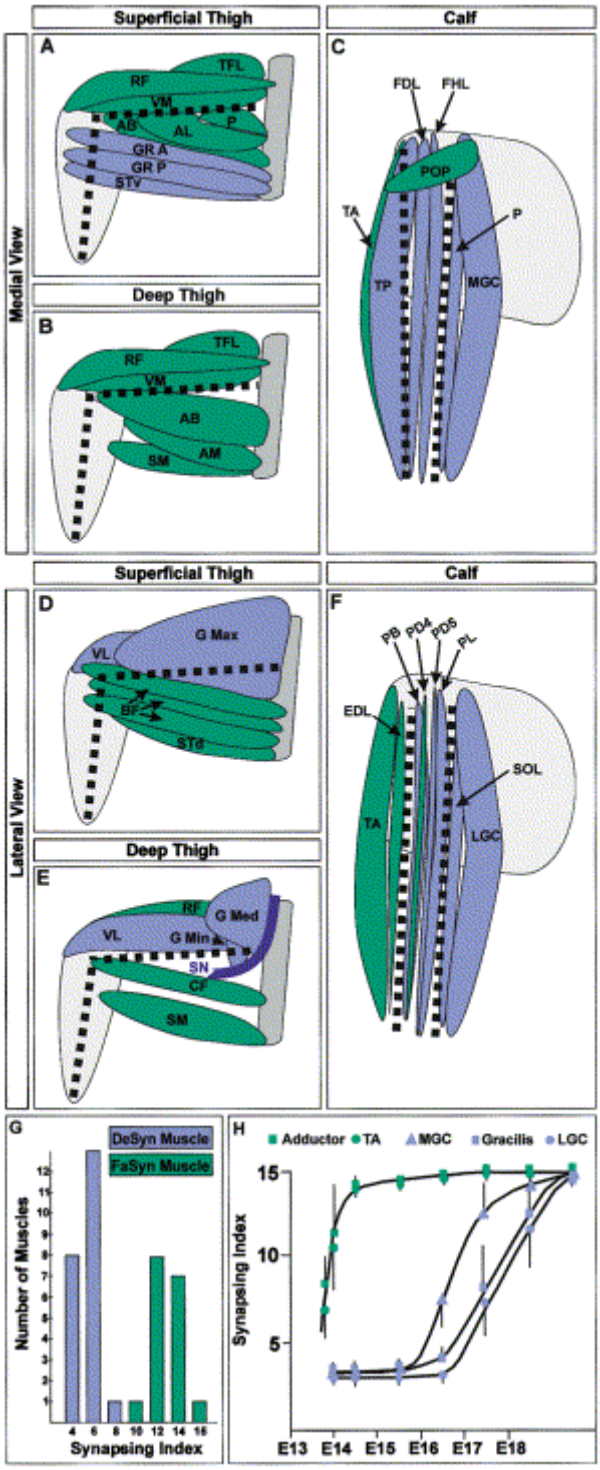

Figure 3. Distribution of FaSyn and DeSyn Muscles in the Hindlimb of the MouseConsecutive sections of E16.5 hindlimbs were double-labeled with α-Bungarotoxin and S-100 antibody. Schematic drawings of some of the muscles with their attachment points are shown in (A)–(F). DeSyn muscles (synapsing indices between three and nine) are in blue, and FaSyn muscles (synapsing indeces between 10 and 15) are in green. The dotted lines indicate the approximate positions of the bones. SN: sciatic nerve (E).(A–F) Medial (A–C) and lateral (D–F) views of thigh (A, B, D, and E) and calf (C and F). To reveal most of the thigh muscles, the medial and lateral views are further subdivided into superficial (A and D) and deep (B and E). The following is a list of thigh muscle abbreviations: AB, adductor brevis; AL, adductor longus; AM, adductor magnus; BF, biceps femoris; CF, caudofemoralis; GMax, gluteus maximus; GMed, gluteus medius; GMin, gluteus minimus; GRA, gracilis anticus; GRP, gracilis posticus; P, pectineus; RF, rectus femoris; Std, semitendinosus dorsal; Stv, semitendinosus ventral; SM, semimembranosus; TFL, tensor fascia lata; VM, vastus medialis; and VL, vastus lateralis. The following is a list of calf muscle abbreviations: EDL, extensor digitorum longus; FDL, flexor digitorum longus; FHL, flexor hallucis longus; LGC, lateral gastrocnemius; MGC, medial gastrocnemius; P, plantaris; PB, peroneus brevis; PD4, peroneus digiti quarti; PD5, peroneus digiti quinti; PL, peroneus longus; POP, popliteus; SOL, soleus; TA, tibialis anterior; and TP, tibialis posterior.(G) Frequency histogram of synapsing index values for 37 different muscles at E16.5. The bars represent the numbers of muscles with synapse index values of 3 or 4 (labeled as 4), 5 or 6 (labeled as 6), 7 or 8 (labeled as 8), 9 or 10 (labeled as 10), 11 or 12 (labeled as 12), 13 or 14 (labeled as 14), and 15 (labeled as 15).(H) Synapsing index values during embryonic development in two FaSyn muscles (adductor, TA), two DeSyn muscles (gracilis anterior, LGC), and one IntSyn muscle (MGC). Data are averages from three mice (at least 25 NMJs per muscle and mouse).

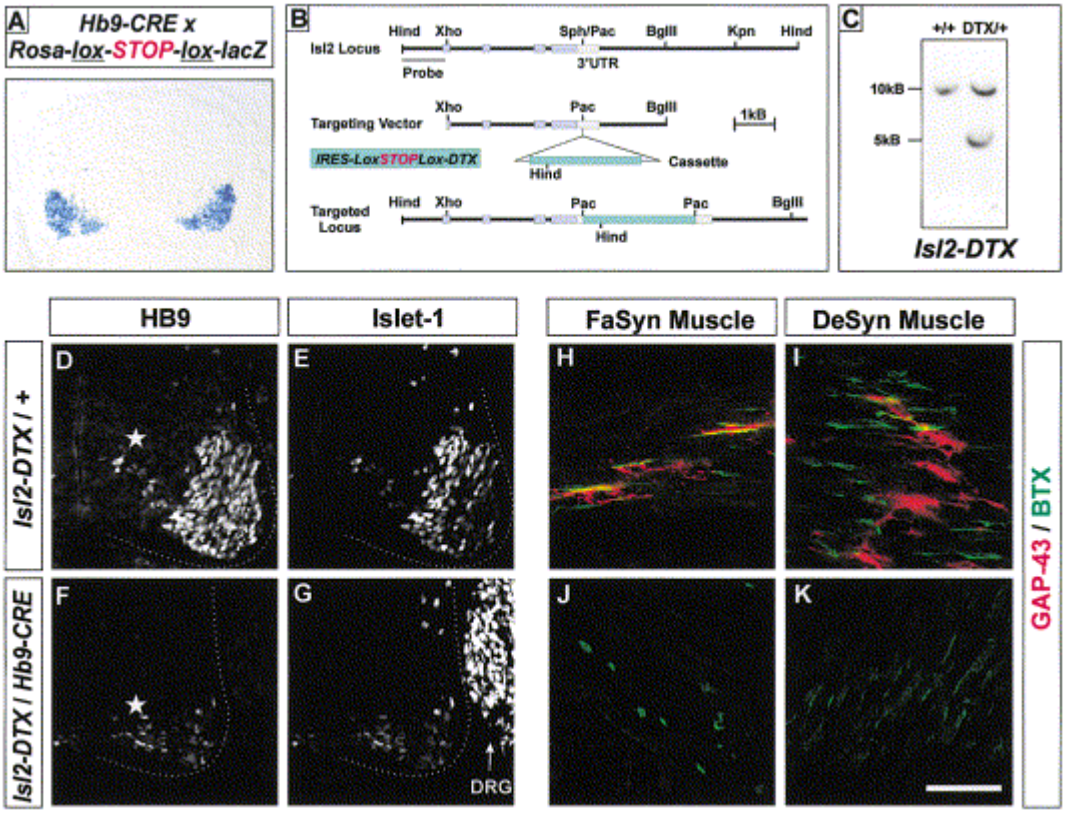

Figure 4. Distinct Patterns of Focal AChR Clustering Reflect Properties Intrinsic to FaSyn and DeSyn Muscles(A) MN specific expression of Cre recombinase in HB9-CRE mice is visualized by the blue β-galactosidase reaction product in ventral brachial spinal cord on a section from an E13.5 embryo double transgenic for the HB9-Cre allele and the Rosa-lox-STOP-lox-lacZ reporter line allele (Soriano, 1999).(B) Structure of the mouse Isl2 locus, Isl2-IRES-lox-STOP-lox-DTX targeting construct, and targeted Isl2 allele for inducible expression of Diphteria toxin in cells expressing Cre recombinase.(C) Wild-type (+/+) and targeted (DTX/+) Isl2 allele. Genomic Southern blot with a HindIII-XhoI probe 5′ to the targeting construct (B). The genomic DNA was digested with HindIII for analysis.(D–G) Specific ablation of spinal presynaptic motor neurons (MNs) in Isl2-DTX/HB9-Cre double-transgenic mice. Immunocytochemistry of E11 lumbar spinal cord ventral horns (dotted lines) with antibodies to HB9 (D and F) and Islet1 (E and G). Note the absence of most HB9- and Islet1-expressing MNs in double-transgenic (F and G), but not single-transgenic, Cre-negative (D and E) mice. The asterisks indicate medially located, late-born

MNs that have not been affected by DTX expression yet.(H–K) Characteristic patterns of AChR cluster distribution in FaSyn and DeSyn muscles in the presence and absence of motor nerves. Double-labeling immunocytochemistry for nerve and postsynaptic AChR clusters in FaSyn and DeSyn muscles at E16.5 in the presence (H and I) and absence (J and K) of motor innervation.Scale bar: 80 μm (D–G) and 40 μm (H–K).

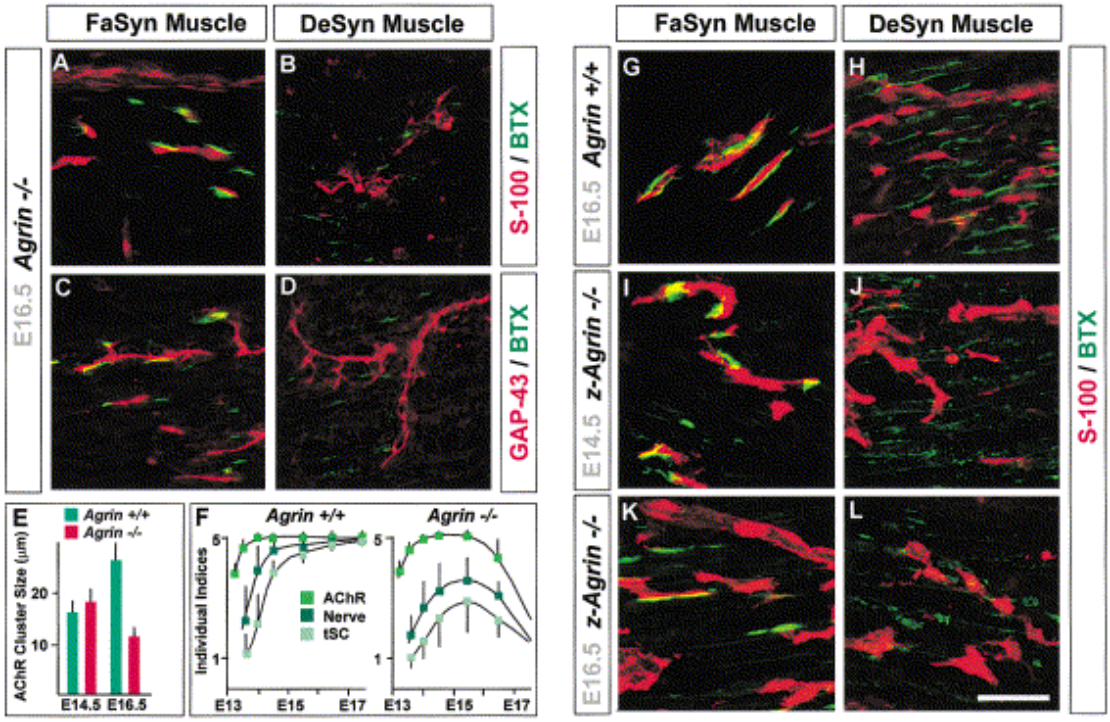

Figure 5. Role of agrin for Neuromuscular Synaptogenesis in FaSyn and DeSyn Muscles(A–D) Double labeling of FaSyn (adductor, [A and C]) and DeSyn (gracilis anterior, [B and D]) muscles of E16.5 agrin-deficient mice. AChR (BTX, green), SC (S-100, red), and nerve (GAP-43, red) were visualized as described in Figure 2. Note normal appearance of synaptic complexes in FaSyn muscles in the absence of agrin. Individual indices (see the figure legend for Figure 2): 4.2/3 (A), 1.0/1 (B), 3.7/3 (C), and 1.1/1 (D).(E) Average AChR cluster size (longest diameter) in adductor muscle (FaSyn) of agrin−/− mice and wild-type littermates at E14.5 and E16.5. Data are from two mice each (25 NMJs per muscle and mouse).(F) Individual AChR, nerve, and SC indices between E13.5 and E17.5 in adductor muscle (FaSyn) of agrin−/− mice and

wild-type littermates (sample size as in Figure 2M).(G–L) Double-labeling of FaSyn (adductor, G, I, and K) and DeSyn (gracilis anterior, H, J, and L) muscles of E16.5 wild-type (G and H), E14.5 z-agrin−/− (I and J), and E16.5 z-agrin−/− (K and L) mice. Individual indices: 4.5/5 (G), 1.6/1 (H), 4.7/4 (I), 1.1/1 (J), 3.8/3 (K), and 1.0/1 (L).Scale bar: 40 μm.

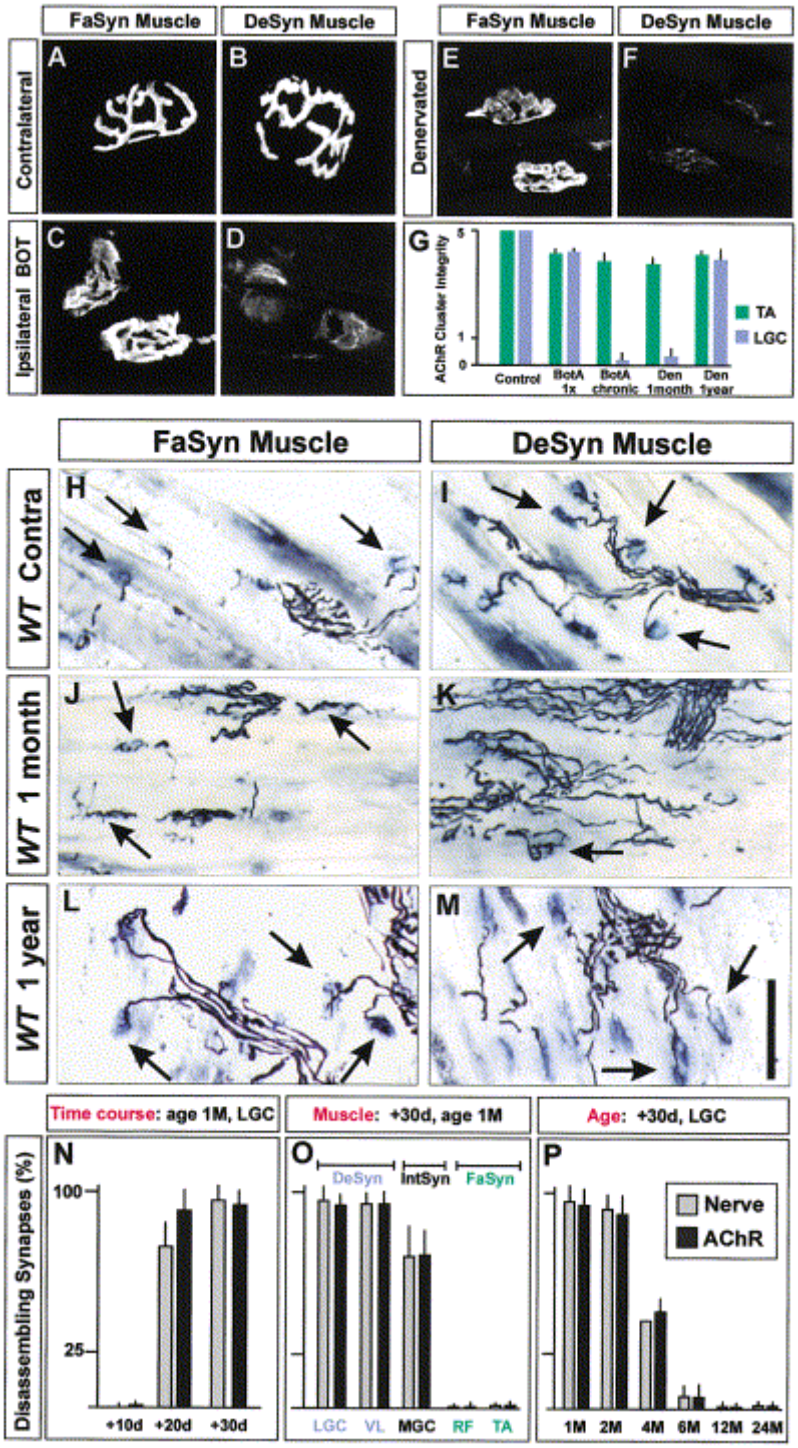

Figure 6. Selective Loss of AChR Clusters and Disassembly of NMJs in DeSyn Muscles Induced by Chronic Blockade of Nerve-Evoked Activity or Denervation in Young Adult Mice(A–D) BotA was repeatedly injected into the right calf at postnatal day (P)15, P19, P23, P27, and P31, and muscles were analyzed at P45. Representative

examples of NMJs (α-Bungarotoxin labeling) in rectus femoris (FaSyn) and lateral gastrocnemius (LGC, DeSyn) from nontreated contralateral hindlimb (A and B) and paralyzed hindlimb (C and D). The examples shown are from one experiment; all sections were processed the same way and scanned at equal confocal intensity.(E and F) representative examples of AChR clusters in TA (E) and LGC (F), 20 days after sciatic nerve transsection in a 1-month-old mouse.(G) Quantitative analysis of AChR cluster disassembly in paralyzed and denervated FaSyn and DeSyn muscles. The data are from two mice each (at least 30 NMJs per mouse). BotA, 1×: one application of BotA at P15, followed by analysis at P45; BotA chronic: repeated injections treatment, as described in (A)–(D). See Experimental Procedures for AChR cluster integrity criteria.(H–M) Combined silver esterase reactions of contralateral wild-type controls (H and I) and treated muscles (J–M); nerves are black, and acetylcholine esterase reaction product at the NMJ is blue. Chronic paralysis leads to a reduction in synaptic acetylcholine esterase activity.The arrows point to intact NMJs without (H, I, L, and M) and with (J) ultraterminal nerve sprouts. Note the extensive longitudinal sprouting of nerves indicative of synapse disassembly in chronically paralyzed DeSyn (LGC) muscle at 1 month (K), but not 1 year (M), of age and the absence of disassembly in FaSyn (rectus femoris) muscle (J and L).(N–P) Quantitative analysis of synapse disassembly induced by chronic paralysis with BotA. The data are from 100 NMJs each (two mice). For the time course experiments (N), the BotA treatment was initiated at P15, and LGC innervation was analyzed 10, 20, and 30 days later. Where disassembly was analyzed in different muscles (O) (VL, vastus lateralis; RF, rectus femoris; and TA, tibialis anterior), mice were treated as in (N) and analyzed 30 days later. The age-dependence of the disassembly response (P) was analyzed in LGC. In these experiments, treatments were initiated 15 days before the age indicated in the figure, and mice were analyzed 15 days after that age.Scale bar: 40 μm in (A)–(F) and 140 μm in (H)–(M).

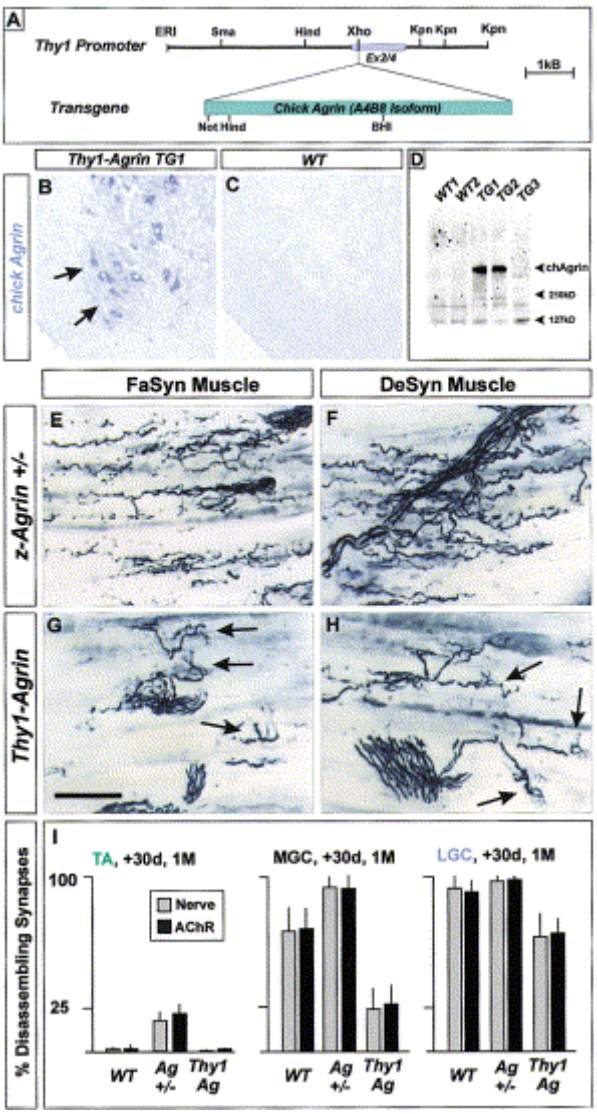

Figure 7. Dose-Dependent Protection against NMJ Disassembly in Young Adult Mice by agrin(A–D) Generation of transgenic mice overexpressing chick z-agrin constitutively in neurons, including α-MNs in the adult. (A) Map of Thy1-agrin transgenic construct. (B and C) In situ hybridization of adult lumbar spinal cord sections with chick agrin digoxigenin labeled RNA probe. (B) Adult transgenic mouse, line TG1; (C) Wild-type littermate control. Arrows point to spinal MNs expressing the chick agrin transgene. (D) Expression of transgenic chick z-agrin. Immunoblot of equivalent adult mouse brain homogenate samples probed with antibody against chick agrin. The line TG3 expressed low levels of transgene in very few neurons and was not further included in the analysis.(E–H) Protection by agrin against synapse disas-

sembly induced by chronic blockade of transmitter release. 1-month-old (1M) z-agrin+/− (E and F) and Thy1-agrin transgenic line TG1 (G and H) mice were treated as described in the legend to Figure 6. The arrows point to intact NMJs (AChE, characteristic pattern of presynaptic nerve terminal branching; see also AChR analysis in Figure 7I).(I) Quantitative analysis of synapse disassembly in wild-type, agrin+/− and Thy1-agrin mice. Labeling of the figure is as described in Figure 6G–6I.Scale bar: 140 μm.

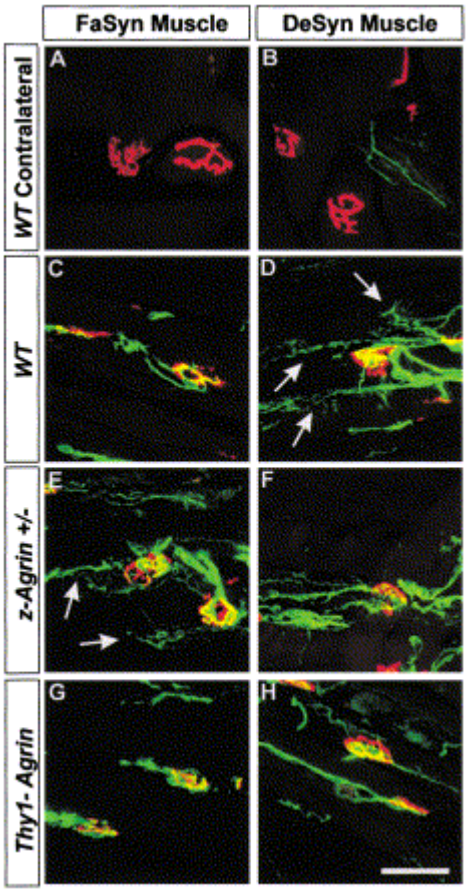

Figure 8. Selective Sprouting of tSCs at Denervated NMJs of DeSyn MusclesDouble-labeling immunocytochemistry of FaSyn (tibialis anterior) and DeSyn (LGC) muscles 2 weeks after denervation. Postsynaptic AChRs (α-Bungarotoxin) are in red, and activated SCs (p75 immunoreactivity) are in green. Arrows point to tSC sprouts.(A–D) Denervated hindlimb (C and D) and contralateral untreated control (A and B) of a wild-type mouse. Note the very low or absent p75 signals of SCs and tSCs in contact

with nerve and strong upregulation upon denervation. Also note the low incidence of tSC sprouting at denervated NMJs in FaSyn muscle (C) and strong response in DeSyn muscle (D).(E and F) Denervated hindlimb of z-agrin+/− mouse. Note sprouting of tSCs at denervated FaSyn NMJs.(G and H) Denervated hindlimb of Thy-agrin transgenic mouse. Note the strong reduction of tSC sprouting.Scale bar: 40 μm.

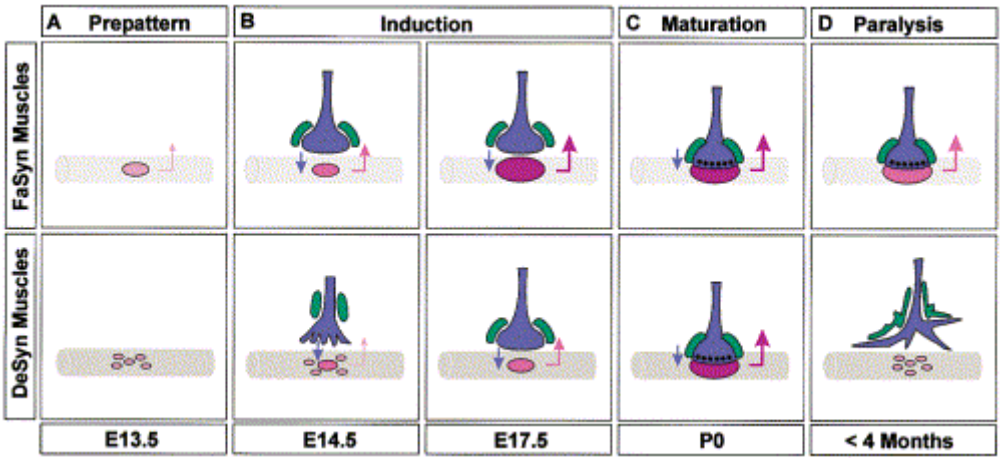

Figure 9. Proposed Model of Neuromuscular Synaptogenesis and Maturation in FaSyn and DeSyn Muscles(A) Nerve-independent prepatterning of postsynaptic AChRs (red) in FaSyn and DeSyn muscles exhibits characteristic differences in focal AChR clustering due to intrinsically distinct properties of these muscles. FaSyn muscles rapidly assemble one compact cluster that may reach a threshold to promote presynaptic differentiation through retrograde signals (red arrow). DeSyn muscles assemble loosely organized AChR clusters not sufficient (subthreshold) to induce presynaptic differentiation.(B) In the hindlimb, incoming motor nerves interact with AChR clusters on muscle to establish neuromuscular synapses through a cascade of reciprocal inductive interactions between E13.75 and birth. In FaSyn muscles, nerves may either contact preexisting clusters or promote the formation of focal clusters at sites of contact with muscle. Nerve-derived signals promoting synaptogenesis (blue arrows) include z-agrin. A further signal may involve transmitter release. Presynaptic differentiation depends on the presence of a supra-threshold focal AChR cluster on muscle and involves alignment of the nerve (blue) with the AChR cluster and association of Schwann cells (green) with the nascent synapse. Focal clusters on FaSyn muscles ini-

tiate this process effectively at E13.75, whereas the presence of nerve and nerve-derived agrin are necessary to bring about supra-threshold AChR clustering and initiate presynaptic differentiation in DeSyn muscles from E16.5 forward. In addition to these differences in onset times, rates of synaptic differentiation are substantially faster in FaSyn than in DeSyn muscles.(C) Synapse maturation involves further differentiation and strengthening of NMJs through reciprocal signals.(D) NMJs on FaSyn and DeSyn muscles continue to differ in their stability for several months after birth. Thus, in young adult mice, synaptic complexes in DeSyn muscles depend on the presence of synaptic activity for maintenance and are disassembled in its absence.

Supplementary Figures

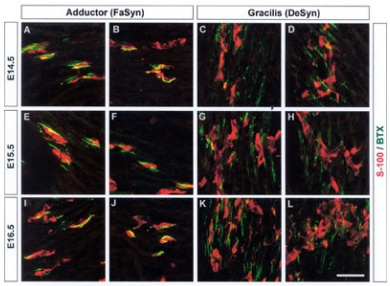

Sup. Fig. 1

Double-labeling immunocytochemistry of FaSyn (A, B, E, F, I, and J) and DeSyn (C, D, G, H, K, and L) muscles at embryonic day (E)14.5 (A–D), E15.5 (E–H), and E16.5 (I–L). Postsynaptic AChR was visualized with fluorescently labeled α -Bungarotoxin (BTX, green) and Schwann cells with an antibody against S-100 (red). Each panel is from a distinct embryo.
Bar: 40 µm.

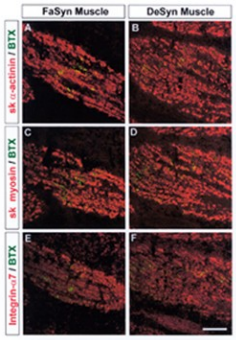

Sup. Fig. 2

Double-labeling immunocytochemistry of FaSyn (A, C, and E) and DeSyn (B, D, and F) muscles at E15.5. The skeletal muscle proteins skeletal muscle α -actinin (A and B), embryonic skeletal myosin heavy chain (C and D), and integrin-α 7 (E and F) were visualized with specific antibodies (red); postsynaptic AChR was visualized with fluorescently labeled α -Bungarotoxin (BTX, green). Pairs of panels (FaSyn and DeSyn) are from the same slide, and confocal images were processed in the same way.
Bar: 60 µm.

Chapter 11 - Anatomical Plasticity of Motor Axons Regulated Locally Through Accumulation state of Postsynaptic Receptor Clusters

Alexandre Ferrão Santos[1], Reto Portmann[1], Shao Lin[2], Craig S. Newman[3], Paul A. Krieg[4], Markus A. Ruegg[2], and Pico Caroni[1]

1 Friedrich Miescher Institute, Maulbeerstrasse 66, CH-4058 Basel, Switzerland
2 Biozentrum, Univ. of Basel, Klingelbergstrasse 70, CH-4000 Basel, Switzerland
3 Section of Neurobiology, Inst. of Neurosci., Univ. of Texas, Austin, TX 78712 USA
4 Dept. Cell Biology and Anatomy, Univ. of Arizona, Tucson, AZ 85724, USA

11.1Summary

Regulated processes of synapse assembly and disassembly, coupled to neurite remodeling (anatomical plasticity) play important roles in the plasticity of neuronal circuits, but the cellular mechanisms that control local circuit rearrangements are poorly understood. Here we exploit a distinction among different skeletal muscles to exhibit paralysis-induced anatomical plasticity at their neuromuscular junctions (NMJs), and show that postsynaptic muscle fibers control the local extent of presynaptic axon growth through a mechanism tightly coupled to the state of assembly of postsynaptic acetylcholine receptor (AChR) clusters. Permissiveness for presynaptic expansion involves a process leading to gradual AChR cluster disassembly, which is triggered in plastic muscles in the absence of transmitter release, and further depends on sustained mTOR1 and proteasome activities. Thus, in addition to controlling synaptogenesis, intrinsic processes of postsynaptic AChR clustering and dispersion regulate anatomical plasticity at NMJs, to determine the sizes of axonal arborizations onto their local targets.

11.2Introduction

The assembly and plasticity of neuronal circuits includes processes of regulated formation and disassembly of synaptic connections (anatomical plasticity). Thus, during development, the self-organization of local circuits involves protracted periods of synapse turnover coupled to local neurite outgrowth and retraction (e.g. Ruthauzer *et al.*, 2003). Likewise, a significant degree of synapse turnover, coupled in part to local process outgrowth, is thought to contribute to experience-related learning and memory in the adult, and to adaptation to dysfunction upon injury and in disease (Trachtenberg *et al.*, 2002, Galimberti *et al.*, 2006, Bareyre *et al.*, 2004). The stabilization and dismantling of individual synapses is coupled to the relative strength of their synaptic transmission, and to adhesion at the synapse (Biederer *et al.*, 2002, Yamagata *et al.*, 2003). In addition, there must be mechanisms controlling the numbers and distributions of synaptic contacts between sets of defined pre- and postsynaptic partners. This regulation involves anatomical plasticity on a larger scale than that controlling individual synapses, but little is known about the principles and cellular mechanisms controlling these processes. In particular, the relative contributions of presynaptic, postsynaptic and glial elements to control remodeling and ensure specificity in anatomical plasticity have remained unclear. The complexity of synapses in central neuropil has been a major obstacle in these studies, and there is a need for well-defined and experimentally accessible systems in which to elucidate these basic issues in plasticity.

Neuromuscular junctions (NMJs) have long provided accessible model systems to investigate mechanisms controlling the assembly and maintenance of defined synapses in vivo (Kummer *et al.*, 2006, Goda and Davis, 2003). Seminal studies by McMahan and his colleagues have established that extracellular matrix (ECM) at the NMJ contains information sufficient to stop ingrowing motor nerves, and to direct both post- and presynaptic differentiation9. Subsequent studies have assigned a central

role to assembled postsynaptic acetylcholine receptors (AChRs) in synaptogenesis (Kummer *et al.*, 2006, Panzer *et al.*, 2006, Flanagan-Steet *et al.*, 2005, Nguyen *et al.*, 2000), and shown that when AChR cluster accumulation is compromised due to the absence of MuSK, rapsyn or agrin in mice, presynaptic nerves extend long processes along muscle fibers, suggesting that stop signals for motoneuron axons might be associated with postsynaptic apparatus at the NMJ (Kummer *et al.*, 2006, Wang *et al.*, 2003, Hesser *et al.*, 2006, Terrado *et al.*, 2001, Banks *et al.*, 2001). The nature, and indeed existence of such signals has, however, remained unclear. In addition to contact-mediated mechanisms, recent studies have shown that synaptic activity is important to stabilize AChR clusters and NMJs, and to enhance focal clustering of AChRs (Kummer *et al.*, 2006, Akaaboune *et al.*, 1999, Misgeld *et al.*, 2002, Skorpen *et al.*, 1999, Lin *et al.*, 2005, Misgeld *et al.*, 2005). Taken together, these studies have provided evidence that mechanisms regulating the assembly and stability of postsynaptic AChR clusters play central roles in controlling NMJs assembly and maintenance.

NMJs have provided uniquely advantageous experimental systems to investigate anatomical plasticity in the target region (Santos and Caroni, 2003). Partial denervation experiments in the adult have established that nerves can sprout from spared NMJs, to efficiently reinnervate nearby synaptic sites in a process important for neuromuscular repair. This involves sprouting of “terminal” Schwann cell (tSC) processes from denervated synaptic sites, contact of neighboring innervated synapses by the tSC processes, and stimulation of sprout growth along those Schwann cell processes (Son and Thompson, 1995, Son *et al.*, 1996). In a significantly different experimental paradigm, blockade of neuromuscular transmission, e.g. with Botulinum toxin A (BotA), can induce motor nerve growth from NMJs, to induce ectopic AChR clusters and form new functional synapses on muscle fibers (Santos and Caroni, 2003, de Paiva *et al.*, 1999). The mechanisms controlling this dramatic form of anatomical plasticity are poorly understood, but release of sprout-promoting factors, and sprouting of tSCs in the absence of synaptic activity have been implicated (Santos and Caroni, 2003, English, 2003). Interestingly, while this represents an important adaptive mech-

anism to restore functional innervation of target muscle, it does not operate at all NMJs, in all muscles, or at all ages (Santos and Caroni, 2003, Frey *et al.*, 2000). This specificity in anatomical plasticity has raised the possibility that comparing stimulus-induced responses at "naturally" plastic versus non-plastic NMJs might provide deeper insights into mechanisms controlling anatomical plasticity.

As a first step towards elucidating what might distinguish plastic from non-plastic synapses, we could recently assign skeletal muscles to two novel subclasses, which did not reflect any previously known distinctions among muscles, but differed in the assembly patterns of their NMJs during development (Pun *et al.*, 2002). Thus, muscle fibers on FaSyn (Fast Synapsing) muscles exhibit focal AChR clusters before contact by nerve, and readily assemble focal NMJs upon neuromuscular contact (embryonic day (E) 13.75-14). In contrast, AChR clusters are dispersed, and nerves sprout on muscle fibers of DeSyn (Delayed Synapsing) muscles during 4 days of embryonic development (up to E18). Although NMJs on FaSyn and DeSyn muscles appear undistinguishable after E18, inducing chronic paralysis with BotA in young adult mice leads to dramatic nerve sprouting and ectopic synaptogenesis in DeSyn muscles, but to no comparable responses in FaSyn muscles (Pun *et al.*, 2002).

Here we exploited the differences between DeSyn and FaSyn muscles to elucidate cellular mechanisms controlling anatomical plasticity at the NMJ. We show that in BotA-induced plasticity it is postsynaptic muscles that control nerve sprouting and synapse remodeling. We further show that instead of regulating sprouting per se, muscles control the magnitude of presynaptic nerve expansion on individual muscle fibers. This regulation involves an inhibitory mechanism for local presynaptic arborization coupled to the accumulation state of postsynaptic apparatus on individual muscle fibers. Permissiveness for expanded terminal arborization involves a gradual process triggered in DeSyn muscles in the absence of transmitter release, further depending on sustained mTOR1 and proteasome activities, and leading to increasing AChR cluster disassembly. These results from experimentally accessible NMJs pro-

vide a conceptual framework to account for how factors intrinsic to postsynaptic targets combine with synaptic activity and contact-mediated mechanisms to locally control the size of axonal arborizations onto specific targets.

11.3Results

Gradual spread of motor nerves and ectopic synapses in young-adult DeSyn muscles treated with BotA

In a first series of experiments, we elucidated properties and requirements of paralysis-induced synapse remodeling in postnatal mouse muscles. We applied BotA locally in one hind limb of 1-month *Thy1-mGFP^{mu}* mice (De Paola *et al.*, 2003), and monitored AChR clusters (RITC-α-Bungarotoxin), and presynaptic nerves (membrane-targeted GFP) in DeSyn and FaSyn muscles (DeSyn: lateral gastrocnemius (LGC^{DeSyn}), medial gastrocnemius (MGC^{DeSyn}), soleus (SOL^{DeSyn}), gluteus maximus, vastus lateralis (VL^{DeSyn}); FaSyn: rectus femoris (RF^{FaSyn}), tibialis anterior (TA^{FaSyn}), extensor digitorum longus (EDL^{FaSyn})). We found that repeated applications of BotA every fourth day consistently induced presynaptic nerve growth and ectopic AChR clusters in DeSyn but not FaSyn muscles (**Figs. 1a, b**). The growth of terminal nerves beyond the original NMJ was clearly detectable at day +5 (i.e. 5 days after beginning of the treatment; **Fig. 1c**), and its extent increased gradually up to at least day +25 (**Figs. 1a, b**). Increasing nerve growth was correlated with a loss of postsynaptic "pretzel" configurations at original NMJs, a wider distribution of ectopic AChR clusters, and a diminishing labeling intensity and size of original and ectopic AChR clusters (**Fig. 1a**).

In addition to its specificity for DeSyn muscles, BotA-induced plasticity was age-dependent. Thus, BotA failed to induce significant nerve growth and ectopic AChR clusters during the first two postnatal weeks; in addition, the extent of the response to

BotA diminished beyond 2 months, and no significant remodeling could be induced in most DeSyn muscles of mice older than 4 months (**Fig. 1b**). Exceptions in which BotA-induced anatomical plasticity could be induced throughout life included SOL^{-DeSyn} and gluteus $maximus^{DeSyn}$ (not shown). Unlike repeated applications of BotA, a single application of BotA induced paralysis, but only transient nerve growth in LGC^{DeSyn}, possibly reflecting a requirement for persistent blockade of miniature events to induce robust remodeling, (**Fig. 1b; Suppl. Fig. 1**). Finally, BotA-induced remodeling was reversible. Thus, when the treatment was discontinued at day +20 and mice were analyzed at day +50, we detected very few sprouts and a restoration of adult-type focal innervation (**Suppl. Fig. 2**). We conclude that blockade of transmitter release with BotA induces a gradual and reversible expansion of presynaptic nerves beyond original NMJs, and ectopic AChR clusters specifically in young-adult DeSyn muscles.

To identify molecular counterparts of BotA-induced NMJ remodeling in young adult DeSyn muscles, we carried out a proteomic screen, comparing protein samples from seven different young-adult muscles, four DeSyn and three FaSyn muscles, with or without a repeated BotA treatment. We found that several proteins are induced with slow kinetics (8-20 days range) by a repeated BotA treatment in all muscles (**Suppl. Table 1**). In addition, the screen revealed the existence of a small set of proteins specifically upregulated in repeatedly paralyzed young-adult DeSyn muscles, but not FaSyn muscles (**Suppl. Fig. 3, Suppl. Table 1**). Several of these DeSyn specific proteins were embryonic isoforms of muscle-specific genes, suggesting that their induction reflected a specific response in DeSyn muscle fibers. As might have been expected, a repeated treatment with BotA led to a gradual and marked (6-20-fold) induction of the corresponding embryonic transcripts in DeSyn muscles, whereas control transcripts were not affected (**Suppl. Fig. 3**). Surprisingly, however, the transcripts were induced with comparable efficiencies in FaSyn or DeSyn muscles, and in P5, 1 month or 9 months old mice (**Suppl. Fig. 3**). Therefore, chronic blockade of transmitter release induces a gradual accumulation of certain embryonic muscle gene transcripts in

all muscles, at all ages, and with a kinetics resembling that of NMJ remodeling, but the accumulation of the corresponding proteins is restricted to young adult DeSyn muscles. Taken together, these findings reveal a correlation between BotA-induced anatomical plasticity and processes specifically induced in young-adult DeSyn muscles by the BotA treatment.

Control of BotA-induced anatomical plasticity by postsynaptic muscles

To investigate the relative contributions of presynaptic nerve and postsynaptic muscle in controlling presynaptic growth and synapse remodeling in the presence of BotA, we carried out cross-innervation experiments in young adult mice. In one set of experiments, the nerves to SOL^{DeSyn} and to EDL^{FaSyn} were cut at a position about 2 mm from their entry points to muscle, the proximal SOL nerve stump was placed in close vicinity to the distal stump of the EDL nerve, and the other nerve stumps were glued (see Methods). In parallel cross-innervation experiments, we forced reinnervation of SOL^{DeSyn} NMJs by EDL nerves. One month after these surgeries (2-months mice), when reinnervation appeared stable, we treated the muscles with BotA. We found that SOL motoneurons failed to exhibit sprouting when innervating EDL^{FaSyn} muscle, and EDL motoneurons exhibited efficient paralysis-induced sprouting on SOL^{DeSyn} muscle (**Fig. 2a**). These results suggested that paralysis-induced sprouting and synapse remodeling are controlled by properties intrinsic to postsynaptic muscles.

To provide independent evidence that postsynaptic muscle controls nerve growth and NMJ remodeling in the adult, we analyzed BotA-induced plasticity by individual motoneurons in *Thy1-mGFP*^{s} mice (De Paola *et al.*, 2003), which express the transgene in a small number of motoneurons innervating LGC^{DeSyn}. We had noticed the existence of age-dependent lateral gradients of responsiveness to paralysis-induced remodeling within the compartments of LGC^{DeSyn} and MGC^{DeSyn}, which might reflect corresponding gradients in age-related loss of plasticity in large muscles (Santos

and Caroni, 2003) (residual remodeling is first confined to the center of muscle compartments at 2-3 months, before being lost altogether at 4-5 months). Analysis of 2-months BotA-treated *Thy1-mGFP^s* mice revealed an obvious gradient in the growth behavior of individual presynaptic terminals along the medial-to-lateral axis (**Fig. 2b**), indicating that NMJs by the same motoneuron (see also **Suppl. Fig. 4**) remodeled according to their medio-lateral position along the LGC^{DeSyn} compartment. We conclude that BotA-induced nerve growth and NMJ remodeling are controlled locally, through properties intrinsic to postsynaptic muscles and muscle fibers.

To determine whether it is specifically sprout initiation, which is controlled locally, or whether the growth of sprouts is also controlled at the level of individual muscle fibers, we analyzed the patterns of sprout extension within regions of BotA-treated DeSyn muscles with the largest local differences in plasticity, focusing on individual sprouts extending onto several adjacent muscle fibers. A detailed analysis provided clear evidence that the extents and patterns of sprout growth were controlled locally by individual muscle fibers, and that this control was not restricted to the immediate vicinity of preexisting NMJs. Thus, we found that: 1) sprouts from different axons exhibited closely comparable arborization patterns and extents when growing onto the same muscle fiber (e.g. **Fig. 3**, top left, right), 2) the same sprout exhibited distinct arborization patterns onto different muscle fibers (e.g. **Fig. 3**, top left, bottom left), 3) arborization territories of sprouts onto the same muscle fiber often did not overlap (e.g. **Fig. 3** top left and bottom right). We conclude that in BotA-induced plasticity individual muscle fiber surfaces can differ in their non-permissiveness for nerve growth, and that the extent of sprout growth is determined locally for individual sprout branch / muscle fiber pairs.

In BotA-induced plasticity motor nerves control Schwann cell processes

BotA-induced nerve sprouting might reflect an initial induction of tSC sprouting in young-adult DeSyn muscles, which would then support nerve sprouting. Alternatively, paralyzed young-adult DeSyn muscles might signal directly to nerve to induce sprouting. To discriminate between these possibilities, we monitored tSCs during paralysis- or denervation-induced sprouting using transgenic mice in which cytosolic GFP (cGFP) was expressed in SCs and tSCs using an S100 promoter cassette[30] (*S100-cGFP* mice; see Methods). We found that BotA induced a slow growth of straight, thick tSC processes from NMJs in DeSyn but not FaSyn muscles (**Fig. 4a**). The tSC processes appeared to form chains of SCs and were closely associated with ectopic AChR clusters, suggesting that they were associated with nerve sprouts (**Fig. 4a**). In striking contrast, denervation rapidly induced growth of numerous long, thin, and radiating tSC processes in DeSyn and FaSyn muscles (**Fig. 4b**). The appearances of denervation-induced tSC sprouts in DeSyn or FaSyn muscles were closely comparable, and the tSC sprouts were not associated with ectopic AChR clusters (**Fig. 4b**). By showing that in the absence of motor nerves tSC sprouting is not affected by differences among DeSyn and FaSyn muscles (nor by age; not shown), these results suggested that in BotA-induced paralysis nerve sprouting involves control of presynaptic nerve growth by postsynaptic muscles, which in turn controls tSC process growth.

To provide independent evidence that when they are in contact with SCs, nerves control SC process outgrowth, we analyzed the growth patterns of axons regenerating onto paralyzed FaSyn or DeSyn muscles. In this experimental paradigm, tSCs sprout due to denervation, and regenerating axons reaching the sites of NMJs grow along tSC processes, forming "escaped sprouts" (not shown, but see Reynolds and Woolf, 1992, O'Malley *et al.*, 1999). To exclude effects that might be due to properties of presynaptic axons, we carried out this analysis in cross-innervation experiments, where "sprouting" (soleus) nerves reinnervated EDL^{FaSyn} and "non-sprouting" (EDL) nerves reinnervated SOL^{DeSyn}. In addition, to prevent axon stopping due to synaptic activity, we delivered a single dose of BotA locally nine days prior to analyzing the outcome of these experiments. We found that regenerating EDL nerves grew

extensively onto SOL^{DeSyn} muscle, and induced many small and faintly labeled ectopic AChR clusters under these experimental conditions (**Fig. 4c**). In contrast, regenerating soleus nerves induced a few large brightly labeled ectopic clusters, and stopped (and retracted; arrowheads) shortly beyond the original "pretzel-shaped" AChR clusters on EDL^{FaSyn} muscle fibers (**Fig. 4c**). We conclude that a property of FaSyn muscles is sufficient to stop regenerating motor nerves at synaptic apparatus in spite of the presence of profuse denervation-induced tSC processes and the absence of transmitter release, whereas paralyzed DeSyn muscles allow further growth of nerves and the establishment of small ectopic synapses under the same experimental conditions.

Disrupting postsynaptic clusters is sufficient to induce nerve growth on any muscle

Are stopping of presynaptic nerves and the state of aggregation of AChR clusters on muscle related causally? To test the hypothesis that assembled postsynaptic clusters might prevent anatomical plasticity on paralyzed FaSyn muscles, we carried out in vivo knockdown experiments, in which we reduced the expression of the critical kinase MuSK (Kummer *et al*., 2006, Hesser *et al.,*2006) in adult FaSyn muscles prior to carrying out chronic BotA treatment experiments. In control experiments we verified that a MuSK siRNA construct (Kong *et al.,* 2004) effectively interfered with agrin-induced AChR cluster assembly in C2C12 myotubes, whereas a control CD4 siRNA construct did not (**Suppl. Fig. 5**). We then expressed the same MuSK siRNA construct together with a GFP reporter construct in a 1-month FaSyn muscle (RF^{FaSyn}) using an in vivo electroporation procedure (Kong *et al.,* 2004) (see Methods). A repeated BotA treatment was initiated 7 days after the electroporation procedure, and the muscles were analyzed for GFP expression, the appearance of AChR clusters and nerve sprouting at day +10 of the BotA procedure. We found that nerves contacting FaSyn muscle fibers with disrupted AChR clusters (MuSK siRNA) exhibited pronounced sprouting, whereas nerves contacting FaSyn muscle fibers expressing the

control construct (CD4 siRNA) did not (**Fig. 5a**). Nerve sprouting was detected on 145/185 (MuSK siRNA) and on 0/185 (CD4 siRNA) GFP-positive muscle fibers (N= 3 mice each). Interestingly, side-branches of sprouts contacting neighboring FaSyn muscle fibers with intact NMJs induced ectopic AChR clusters on those fibers, and appeared to be stopped at those clusters (**Fig. 5a**, arrows). We conclude that AChR cluster disruption in the absence of MuSK is sufficient to promote sprouting in the presence of BotA in non-plastic FaSyn muscles. The results further suggested that contact by sprouts with clustering competent FaSyn muscle fibers might be sufficient to induce ectopic clusters and locally stop side-branches of the same sprouts.

To provide independent evidence that interfering with AChR cluster integrity is sufficient to promote nerve sprouting, we investigated treatments that compromise AChR cluster accumulation in all muscles in wild-type adults. We found that local applications of DMSO rapidly induced cluster disruption and growth of straight nerve sprouts in DeSyn and FaSyn muscles (**Fig. 5b**). This sprouting was induced locally at muscle fibers with disrupted clusters, whereas neighboring muscle fibers with intact clusters exhibited no sprouting from NMJs (**Fig. 5b**). Significantly, AChR cluster disruption had comparable effects on nerve sprouting in the presence or absence of BotA (**Fig. 5b**), suggesting that upon AChR cluster disruption motor nerves grow on muscle fibers irrespective of transmitter release and of muscle type. In further experiments, we found that a brief treatment with the DNA-breaks-inducing and transcription-blocking agent Actinomycin D (ActinoD; see Methods) led to a fragmentation of NMJs into separate domains in both DeSyn and FaSyn muscles (**Suppl. Fig. 6**). A single application of BotA induced a loss of AChR clusters in these ActinoD-treated DeSyn and FaSyn muscles, which was accompanied by a rapid and massive outgrowth of straight sprouts (**Suppl. Fig. 6**). At day +14 after the addition of BotA, unbranched nerve sprouts had grown all the way to the end of their (FaSyn) muscle fibers, and back (sprout lengths of 2000-4000 μm; **Suppl. Fig. 6**). Taken together, these results provide evidence that disrupting AChR clusters is sufficient to induce the growth of long straight sprouts along muscle fibers in any muscle in the adult.

TOR and proteasome dependence of BotA-induced anatomical plasticity

Having found that cluster dispersal is sufficient to induce sprouting in any muscle, we next aimed at determining whether the re-accumulation of AChR clusters during BotA-induced plasticity might also be sufficient to suppress sprouting in plastic muscles. To this end, we searched for ways to interfere with the dispersal of AChR clusters in BotA-treated young-adult DeSyn muscles. Since previous studies had related proteasome activity to anatomical plasticity and postsynaptic density rearrangements (DiAntonio and Hicke, 2004, Ehlers 2003), we investigated BotA-induced remodeling in the presence of the specific proteasome inhibitors Lactacystin or MG132. We found that the proteasome inhibitors suppressed BotA-induced remodeling of AChR clusters and nerve sprouting in young-adult DeSyn muscles (**Fig. 6a**). We further determined whether the TOR pathway, which has been implicated in plasticity at NMJs, might also be involved in BotA-induced remodeling. Indeed, the specific inhibitor of mTOR1 Rapamycin (Jessen and Mirsky, 2005) effectively suppressed AChR cluster remodeling and nerve sprouting at NMJs of DeSyn muscles (**Fig. 6a**). Lactacystin, MG132 and Rapamycin did not interfere with the induction of plasticity-related proteins in DeSyn muscles (**Fig. 6a**), suggesting that mTOR1- and proteasome-dependent processes are required for anatomical plasticity in parallel (or downstream) to the induction of specific molecular responses in DeSyn muscles.

To determine whether Lactacystin and Rapamycin interfered directly with nerve sprouting, or indirectly through regulatory pathways controlling plasticity, we applied the drugs to DMSO-treated muscles, where a disruption of AChR clusters is accompanied by rapid and BotA-independent growth of sprouts (see above). We found that neither Lactacystin nor Rapamycin interfered with DMSO-induced nerve sprouting (**Fig. 6b**). In further control experiments, the same drugs also did not affect sprouting of tSC processes in denervated muscles (not shown). These results thus sug-

gest that the inhibitors specifically interfere with processes in BotA-treated DeSyn muscles leading to AChR cluster remodeling and nerve sprouting.

Sprout lengths are coupled to the accumulation state of postsynaptic clusters

To determine whether and how cluster remodeling and/or nerve sprouting depended on the continued activities of the proteasome and mTOR1 in paralyzed DeSyn muscles, we carried out inhibitor application experiments late during the BotA treatment, when cluster dispersal, nerve sprouting and ectopic synaptogenesis were well advanced. We found that applications of Lactacystin or Rapamycin from day +15 on, and during the last 5-7 days of a 20-22-day BotA treatment, led to a dramatic accentuation and enlargement of nerve-associated ectopic AChR clusters (**Fig. 6c**). Remarkably, this strengthening of nerve-associated clusters was accompanied by a gradual retraction of motor nerves, and a loss of AChR clusters distal from the retracted nerves (**Fig. 6c**). Since in these experiments neuromuscular transmission continued to be blocked by BotA, these results provide evidence that continued proteasome and mTOR1 activities are required to sustain a cluster dispersion process in paralyzed young adult DeSyn muscles. The retraction of nerve sprouts that accompanied cluster growth in these experiments suggests that as the cluster accumulation process is again strengthened in the presence of the proteasome or mTOR1 inhibitors, the local lengths of sprouts on individual muscle fibers is adjusted through retraction. Taken together, these results thus suggest that the lengths of motor nerve processes on muscle fibers are causally linked to the accumulation state of AChR clusters.

Muscle fiber non-permissiveness determines the local magnitude of nerve growth

How might individual muscle fibers locally restrict sprout growth through a mechanism coupled to the assembly of postsynaptic AChRs? One scenario consistent with

the synaptic appearance of stopped sprouts in the experiments of Fig. 3 and Fig. 4 was that muscle fibers might restrict nerve growth upon the assembly of AChR clusters at the distal ends of sprouts; in this scenario, growing sprouts would be directly restrained by AChR clusters. Alternatively, muscle fibers might negatively control the magnitude of sprout growth through a mechanism coupled to the assembly state of AChR clusters; in this scenario, sprouting would be controlled by muscle signals restricting sprout size, and the magnitude of these signals would be coupled to AChR cluster accumulation on those muscle fibers. To investigate these possible mechanisms, we monitored how BotA-induced sprouts grew, and how they interacted with postsynaptic clusters. In a first set of experiments, we examined in detail nerve processes extending from NMJs during the early phases of BotA-induced sprouting. We found that even in untreated muscles, 1-3 thin, short and twisting processes extended beyond many NMJs, from apparently random positions (**Fig. 7a**). This thin process configuration was still maintained at most NMJs in chronically paralyzed FaSyn muscles at day +20 (**Fig. 7a**). In contrast, at day +5 upon the addition of BotA a distinct type of outgrowth consisting of a single (in some cases two), thicker and much longer process extended from many NMJs on DeSyn muscles (**Fig. 7a**); because of its exit point and orientation, this process resembled a prolongation of the motor nerve to the NMJ. While the lengths of these early sprouts varied among NMJs on DeSyn muscles, their ends or trajectories did not coincide with ectopic AChR clusters, which were not detectable 5 days upon initiation of the BotA treatment (**Fig. 7a**). Since under different experimental conditions much longer sprouts can grow 5 days upon the addition of BotA (**Fig. 5b** and **Suppl. Fig. 6**), these observations argued against the possibility that, at least at this early stage, AChR clusters at the distal ends of sprouts negatively regulated sprout growth.

To further investigate the relationship between sprout growth and the presence of AChR clusters along their path, we carried out in vivo time-lapse imaging experiments in BotA-treated muscles at more advanced stages of sprouting. For most of these experiments, we repeatedly imaged the same group of NMJs and sprouts at the

skin-facing surface of LGC^{DeSyn} at intervals of 2 days (see Methods). These live imaging experiments revealed important further features of the sprouting process in BotA-treated DeSyn muscles (**Fig. 7b**). First, while the ends of their main- and side-branches were rich in filopodia and dynamic, sprouts did not remodel on a large scale, but instead elongated gradually over many days; these observations further supported the notion that muscle fibers mainly regulate the magnitude of sprout growth, not sprout growth rates or sprout stability. Second, the distal ends of sprouts did not coincide with ectopic AChR clusters, and many sprouts were not associated with ectopic AChR clusters at most of the imaging sessions between day +10 and +16 of the BotA treatment (sprouts 2-4 in **Fig. 7b**); these observations further supported the notion that sprout extension is not limited by distal ectopic AChR clusters. Third, some sprouts established numerous ectopic AChR clusters throughout the imaging sessions (sprout 1), while nearby sprouts only did so at a later time point (sprout 3), and yet others did not (sprouts 2,4); because cluster-establishing sprouts also did so at a distance from their muscle fiber of origin (see side-branches by sprout 1), these observations suggested that the establishment of ectopic AChR clusters might reflect a property of individual sprouts, possibly related to their maturation. Finally, ectopic clusters appeared and disappeared along the length of cluster-establishing sprouts (sprout 1), suggesting that throughout the observation period most ectopic synapses were unstable. Taken together, these results provide strong evidence that sprout growth is not restricted through ectopic AChR clusters at the ends of sprouts. Furthermore, since most ectopic clusters were unstable and many sprouts lacked ectopic clusters, these results further argue against the possibility that ectopic clusters stabilize sprouts on muscle (see also **Fig. 6c**). Instead, the results suggest that muscle fibers negatively control the extent to which sprouts grow on them, and that this control involves a local mechanism coupled to cluster accumulation.

11.4Discussion

We have exploited a distinction in the susceptibilities of skeletal muscles to exhibit BotA-induced anatomical plasticity at the NMJ, and combinations of local treatments, genetic models, and molecular readouts, to elucidate cellular mechanisms controlling anatomical plasticity in the target region in vivo. We show that upon blockade of transmitter release, postsynaptic muscles control anatomical plasticity through an inhibitory mechanism for local presynaptic arborization, coupled to the accumulation state of postsynaptic apparatus. In the following sections we discuss the three main findings of this study: 1) how BotA-induced plasticity is fundamentally different from anatomical plasticity induced by denervation, and provides an experimental paradigm to investigate how anatomical plasticity is regulated in the absence of lesions in vivo; 2) how it involves control of local presynaptic arborization size by individual postsynaptic targets; 3) how inducing anatomical plasticity at NMJs involves altering the accumulation state of the postsynaptic apparatus, which is coupled to local postsynaptic non-permissiveness. These results are discussed in relation to those from previous studies, and to their implications for understanding how anatomical plasticity is regulated in neuronal circuits.

BotA- and denervation-induced anatomical plasticity are distinct processes

This study provides evidence that denervation- and BotA-induced anatomical plasticity involve distinct phenomena, which are controlled by distinct mechanisms. In doing so, it resolves previous inconsistencies among studies focusing on different muscles, animals of different ages, and using different protocols to investigate anatomical plasticity at NMJs. In good agreement with previous studies, we find that denervation induces a rapid outgrowth of tSC processes in any skeletal muscle and at any age (Son and Thompson, 1995, Reynolds and Woolf, 1992, O'Malley *et al*., 1999). Upon denervation, tSC processes are thin, and extend from NMJs in a radiating

pattern. In contrast, BotA-induced anatomical plasticity develops more gradually, and exhibits marked muscle- and age-dependent properties. BotA-induced nerve and tSC sprouts are thick, grow predominantly parallel to the orientation of muscle fibers, and induce ectopic AChR clusters. It is well established that SCs exhibit substantial phenotypic plasticity, and that their differentiation state is controlled through contact with axons.(Jessen and Mirsky, 2005). Accordingly, our results suggest that in the absence of axonal contact, tSCs switch to a phenotype involving profuse process extension, and characterized by the expression of growth-associated genes such as p75 and GAP-43(Reynolds and Woolf, 1992). In this mode, SC processes can efficiently induce sprouting of nerves from nearby NMJs or lesioned nerve stumps, and guide those processes to reinnervate denervated NMJs or to bridge gaps at lesioned nerves (Son and Thompson, 1995, Son *et al*., 1996). Denervation-induced anatomical plasticity thus leads to repair of disrupted connectivity (**Fig. 8**). In contrast, upon BotA-induced blockade of transmitter release nerve-SC contacts are not disrupted, tSCs do not re-express p75 and GAP-43 (not shown), and they only exhibit sprouting under experimental conditions that allow nerve sprouts to grow. In keeping with this, and unlike denervation, BotA-induced anatomical plasticity is controlled by postsynaptic muscles, which restrict nerve growth. In agreement with previous reports (Son *et al*., 1996), BotA-induced nerve sprouts were also associated with tSC processes, and our results do not rule out a permissive role for tSC processes in supporting nerve sprouts. However, while such a role would be consistent with previous evidence that the presence of tSCs is important to maintain neuromuscular innervation (Reddy *et al.*, 2003), our results show that when the presynaptic nerve is present, tSC processes remain associated with it, and do not extend isolated processes onto muscle fibers. We further show that unlike denervation, BotA-induced anatomical plasticity involves a gradual and local expansion of the extent of motor nerve arborization onto postsynaptic muscle fibers. The induction of ectopic synapses, which is associated with this motor nerve expansion likely serves to restore functional activation of target muscle fibers by motor nerves (**Fig. 8**). In addition to its value to investigate anatomical plasticity at NMJs, BotA-induced anatomical plasticity thus provides an experimental paradigm to

investigate mechanisms controlling the size and pattern of target innervation in the adult. The value of this paradigm is enhanced by the separate accessibility of plastic and non-plastic neuromuscular systems to experimental manipulation, live imaging and comprehensive molecular analysis.

Negative control of terminal arborization size at NMJs

Our results provide evidence that anatomical plasticity induced in the absence of denervation involves regulation of the extent of presynaptic growth locally onto individual postsynaptic targets. Thus: 1) disrupting postsynaptic AChR clusters was sufficient to induce a rapid growth of long straight sprouts extending along the length of individual muscle fibers on any muscle, indicating that in the absence of postsynaptic apparatus there was no restriction to the extent of sprout elongation on muscle; 2) in contrast, in BotA-treated DeSyn muscles sprouts exhibited slow elongation with little evidence of remodeling, suggesting that it was the extent to which sprouts elongated that augmented gradually in the presence of BotA; 3) applications of mTOR1 or proteasome inhibitors, which by themselves did not inhibit sprout growth on muscle in the absence of AChR clusters, led to a dramatic retraction of sprouts on BotA-treated muscles, suggesting that when postsynaptic cluster dispersal was reversed, presynaptic sprouts not only did not grow anymore, but were not maintained and shortened. Taken together, these results suggest that rather than controlling the number of their neuromuscular synapses in a direct manner during plasticity, postsynaptic muscle fibers might control synapse numbers indirectly through the extent of local terminal arborizations by presynaptic motor axons. An implication of this model is that each presynaptic nerve of the same kind would independently establish a contact of comparable size with a given postsynaptic target cell, irrespective of the presence of additional presynaptic nerves. The extent of that contact appears to depend on the particular state of postsynaptic non-permissiveness, which might be regulated through combinations of intrinsic factors and synaptic activity. According to this model, postsynaptic non-permissiveness would thus tend to scale the local size of separate presy-

naptic contacts onto a defined postsynaptic target. This relationship between local terminal arborization size and synapse numbers has, to our knowledge, not been reported before, and it will be of interest to determine whether it also applies to other pairs of pre- and postsynaptic partners.

Coupling between the accumulation state of postsynaptic apparatus and anatomical plasticity

This study has provided strong evidence that postsynaptic muscles control the extent of BotA-induced anatomical plasticity at NMJs through an inhibitory mechanism, which prevents nerve growth at non-permissive FaSyn muscles, and couples plasticity to the accumulation state of postsynaptic complexes on DeSyn muscles. These observations tie in well with the relative distributions of AChR clusters and nerve sprouts during embryonic development in DeSyn and FaSyn muscles (Sun *et al.*, 2002), with the fact that muscles lacking agrin, MuSK or rapsyn are covered with long motor nerve processes at birth (Kummer *et al.*, 2006), and with the relative arrangements of AChR clusters and nerves in mice with mutations that compromise the normal state of assembly of postsynaptic apparatus at NMJs (Grady *et al.*,2000, Martin, 2003). The notion that synaptic sites prevent motor nerve growth on muscle is not novel, and entirely consistent with the results of previous studies on neuromuscular synaptogenesis during development and in the adult (Kummer *et al.*, 2006, Wang *et al.*, 2003, Hesser *et al.*, 2006, Terrado *et al.*, 2001, Banks *et al.*, 2001). But our results extend those studies on synaptogenesis by showing that when plasticity is induced, an inhibitory mechanism for nerve growth is gradually attenuated in those muscles, where anatomical plasticity can occur. Elucidating the mechanism through which the accumulation state of AChR clusters controls presynaptic arborization lengths will require further studies, but our findings are consistent with two types of models. In one scenario, direct interactions between motor nerves and AChR clusters might restrict the extent of nerve extension distally to those clusters through a mechanism analogous to contact-mediated inhibition of growth (Edgar, 2006). Alternatively, the state of

AChR cluster assembly processes might be coupled to muscle surface non-permissiveness through intracellular compartments involved in trafficking of cell interaction components to the muscle surface. The first scenario envisions a direct involvement of interactions at synapses in regulating nerve growth, whereas the alternative scenario does not. Irrespective of the particular mechanism involved, our results suggest that sprout-promoting factors might enhance, but are not critically required for BotA-induced anatomical plasticity. These models further imply that, within the limits imposed by postsynaptic non-permissiveness, presynaptic mechanisms influencing local interactions along the muscle surface or at the synapse (Yee and Pestronk, 1987) could play a significant role in determining how individual presynaptic nerves arborize and distribute their synapses onto their target muscles.

Finally, our results provide first insights about the mechanisms leading to permissiveness for plasticity in young adult DeSyn muscles, and suggest that regulation ultimately targets the efficiency of postsynaptic cluster assembly (Kummer *et al.*, 2006, Kishi *et al.*, 2005). This does not seem to involve the half-lives of synaptic AChRs (Akaaboune *et al.*, 1999, Brunneau *et al.* 2005), since these were affected to a comparable extent by BotA in DeSyn and FaSyn muscles (not shown). The requirement for proteasome function is reminiscent of the role of ubiquitination and proteasome-mediated degradation to modify the composition and plasticity of the postsynaptic apparatus at central glutamatergic synapses (DiAntonio and Hicke, 2004, Ehlers, 2003). Permissiveness for plasticity may involve the expression of specific ubiquitin ligases in chronically paralyzed young adult DeSyn muscles, and proteasome-dependent degradation of selected postsynaptic apparatus components (Ehlers, 2003). Such a regulatory process through levels of critical cytosolic factors in muscle fibers could account for the observation that AChR clusters on the same muscle fiber exhibited comparable sizes and labeling intensities during plasticity. However, our results would also be consistent with a presynaptic requirement of mTOR1 and/or proteasome activity in BotA-induced plasticity. According to such a scenario, the regulatory pathways might be required to produce a dispersion of permissive AChR clusters by

the presynaptic nerve (Yee and Pestronk, 1987), e.g. by preventing the assembly of adhesive complexes at the presynaptic terminal. Presynaptic modulation of anatomical plasticity through mTOR1 and/or proteasome-mediated degradation pathways would provide for further flexibility in how individual presynaptic nerves exhibit anatomical plasticity in their target regions.

11.5Outlook

There is evidence to suggest that the principles for regulation of anatomical plasticity in the target region revealed in this study might also apply to circuit assembly and plasticity in the CNS. Thus: 1) coordinate regulation of sprouting and synapse remodeling by synaptic activity and postsynaptic differentiation has been reported for the assembly of circuits during development (Ruthazer *et al.*, 2003, Zou and Cline, 1999); 2) slowly developing anatomical plasticity has been demonstrated in the adult as a result of chronic functional alterations (Bareyre *et al.*, 2004, Darian-Smith and Gilbert, 1994). We find that the requirements for anatomical plasticity in the adult can vary among individual postsynaptic targets (e.g. LGC^{DeSyn} versus SOL^{DeSyn}), and that at some systems pronounced rearrangements in local connectivity take place in the presence of synaptic activity (e.g. hippocampal mossy fiber terminals (Galimberti *et al.*, 2006)). The results of this study might thus provide a general conceptual framework to investigate the relative roles of intrinsic postsynaptic factors, synapse-assembling mechanisms and synaptic activity in locally regulating anatomical plasticity in the target region.

11.6Experimental Procedures

Reagents and mouse strains

The reporter transgenic mouse lines *Thy1-mGFP^{mu}* and *Thy-mGFP^{s}* were as described[29]. *S100-GFP* mice expressing an EGFP transgene in SCs were generated us-

ing an S100-based expression cassette[30] and standard transgenic technology. Reagents used in this study: Lactacystin, Rapamycin, Actinomycin D, MG132 (Sigma); Botulinum toxin A (Allergan AG, Lachen, Switzerland); Rompun (Bayer); Ketamine (sold as Narketan, Chassot); RITC-α-Bungarotoxin (Molecular Probes).

Surgery and in vivo treatments

For surgery, mice were anaesthetized with 100 µl/10g body mass of Ketamine (12%)/Rompun (8%) in 0.9% NaCl. For crossinervation experiments, the nerves to EDL^{FaSyn} and SOL^{DeSyn} were exposed and cut to maximize the lengths of the distal (to the host muscle, about 2 mm) and proximal nerve stumps (from the donor motor pool). The opposite stumps (donor distal, host proximal) were plugged close with glue (Histoacryl; B. Braun, surgical). To ensure reliable innervation of host nerve stump by donor axons, the corresponding nerves were positioned facing each other, and fixed to muscle with a small amount of Histoacryl. By using this procedure we achieved efficient reinnervation of host muscle NMJs by 3-4 weeks after the surgery in more than $2/3^{rd}$ of the mice.

Drugs were injected locally, subcutaneously (50 µl/mouse injection volumes). Concentrations of drugs in the injection solution (PBS) were: 2 mM (Lactacystin), 1 mM (MG132), 2 mM (Rapamycin), 0.2 mM (Actinomycin D); Botulinum toxin A was applied at 0.02 U/g body weight (either a single injection, or every 4^{th} day). Unless stated otherwise, drugs were applied daily for 5 days.

For in vivo imaging, BotA-treated Thy1-$mGFP^{mu}$ mice were anaesthetized, the surfaces of RF^{FaSyn} or LGC^{DeSyn} were exposed locally, bathed for 10 min with 10 µl of 5 µg/ml RITC-α-Bungarotoxin, washed as described[47], and imaged for nerve (mGFP) and AChR (RITC) using a confocal microscope (see below). Following image acquisition, the skin wound was sewed shut. First images were acquired at day +10 (BotA treatment), and the same NMJs were imaged again at days +12, +14 and +16.

In vivo siRNA experiments were carried out using an ECM 830 electroporation system (Harvard Apparatus, Holliston, MA), as described[33]. Briefly, RF^{FaSyn} was ex-

posed in anaesthetized 1-month mice, 5-10 µl of vector mix (2 µg/µl each, including NLS-GFP reported construct) were applied (longitudinally) into RF^{FaSyn} with a 50 µl Hamilton syringe, and eight 20 msec pulses were applied at 1 Hz (voltage of 200 V/cm). BotA treatments were initiated 7 days after the electroporation procedure.

Histology and immunocytochemistry

For most experiments, we analyzed muscle innervation patterns using reporter mice expressing mGFP in neurons, and whole mount preparations of muscles. Briefly, identified muscles were dissected, fixed in PBS with 3.5% formaldehyde (30 min, room temperature), washed, and counterstained with RITC-α-Bungarotoxin (2µg/ml). In other experiments, cryostat sections of unfixed muscles were postfixed (10 min, 3.5% formaldehyde in PBS) and labeled for immunocytochemistry as described (Pun *et al.*, 2002).

Fluorescent data were imaged and acquired using an Olympus (BX61) confocal microscope and Fluoview 4.1 software. Sprout lengths were quantified using NeuroJ software. Unless specified otherwise, sprouting in LGC^{DeSyn} was always analyzed within the central third of the lateral or medial compartments, where it was strongest.

The protocol for the combined silver esterase method to visualize nerves and AChE in muscles was as described (Aigner *et al.*, 1995).

Electrophysiology

EDL^{FaSyn} or SOL^{DeSyn} preparations were pinned out in a Sylgard-coated chamber, and perfused with (in mM): 150 NaCl, 5.4 KCl, 1.55 CaCl, 4.88 $MgCl_2$, 10 Hepes-NaOH, and 13 Glucose (pH 7.4) at room temperature (22-24 ^{o}C). Phrenic or soleus nerves were drawn into a fine capillary-stimulating electrode. Intracellular recordings were made with microelectrodes (12-15 MOhm) filled with 3M KCl. Voltage clamp recordings were performed using an AxoClamp 2B in bridge mode (Axon Instruments). Spontaneously occurring MEPPs were first recorded, and then series of 30 EPPs (1 Hz) were collected. Recordings were selected for data acquisition only when

resting membrane potentials were between –60 to –80mV. Data were digitized, recorded to disk and analyzed using a Digidata 1200 series Interface and Axoscope software (Axon Instruments).

Molecular biology

Muscle samples for proteomic analysis were reduced to powder in liquid nitrogen, solubilized in IEF equilibration buffer, cleared by centrifugation (50k, 1h), and protein amounts were determined with the RCDC protein assay from Bio-Rad. Equal protein amounts were loaded to IEF strips, and isoelectric focusing was performed in an IPGphor strip holder (Amersham, Uppsala SE). Second dimension SDS gel electrophoresis was performed on an Ettan Dalt II gel running box (Amersham) and gels were stained with the LSB colloidal Coomassie blue staining method. Stained gels were scanned with the GS-800 calibrated densitometer (Bio-Rad) and spot intensity was analyzed with ProteomWeaver v2.2.3 (Definiens, Munich DE). Peak intensity values were corrected by background subtraction and normalization for gel loading variations. In order to sequence gel spots, gel fragments were sampled with the handspot picker GelPal (Genetix, Hampshire UK), trypsinized and analyzed with a LCQ Deca XP (Thermo-Finnigan, Waltham MA) mass spectrometer. The resulting spectra were analyzed using the SeQuest v27 (Thermo-Finnigan) search database algorithm.

To analyze transcript contents, RNA was purified using the Trizol kit (Invitrogen), and reverse transcribed with AMV reverse transcriptase (Promega). The following primers were used for quantitative RT-PCR analysis: TnIs forward: ACCTGGTCAAGGCAGAACAGA; TnIs reverse: CCCCCATATAGTCGATGTTCA;

TnT3 universal forward: AAAAGGCTCTGTCCTCCATGG; TnT3 universal reverse: TTGTCCCTCAGCTTGTCATCG; TnT3 Fetal forward: ATGAAGATGCTGTCGCCGA; TnT3 Fetal reverse: AGTCTACTTTCTCCCCTTCCGG. Amplified sequences were detected and quantified using the 7000 Sequence detection system (Applied Biosystems). Calibration and linearity controls were carried out for all determinations.

Vectors for RNA interference were constructed using the loop sequence TTCAAGAGA; they included M2 (MuSK), and CD4, as described (Kong et al., 2004). The vec-

tors Dyg1 and Dyg2 included the murine 21 nt target sequences 1085-1105 (Dyg1) and 1105-1125 (Dyg2) of Dystroglycan (NCBI accession: NM_010017). Knockdown vectors were first tested in an agrin-induced AChR aggregation assay using C2C12 myotubes. Briefly, myoblasts were transfected with vector and mGFP construct using 3 µl of Lipofectamine 2000 (Invitrogen) in 1 ml of OptiMEM (GIBCO). Cells were then allowed to differentiate for 5 days, AChR clustering was induced by adding agrin overnight, and myotubes were processed for immunocytochemistry.

Acknowledgments

We thank Corinna Schneider and Lan Xu (FMI) for help with the histology and electrophysiology of adult muscles. We are particularly grateful to Anne Ulvestad (Proteomics facility of the Friedrich Miescher Institut) for precious help with the quantitative proteomics experiments. We further thank Silvia Arber (Univ. of Basel, Switzerland) for valuable comments on the manuscript. The Friedrich Miescher Institut for Biomedical Research is part of the Novartis Research Foundation.

11.7Figures

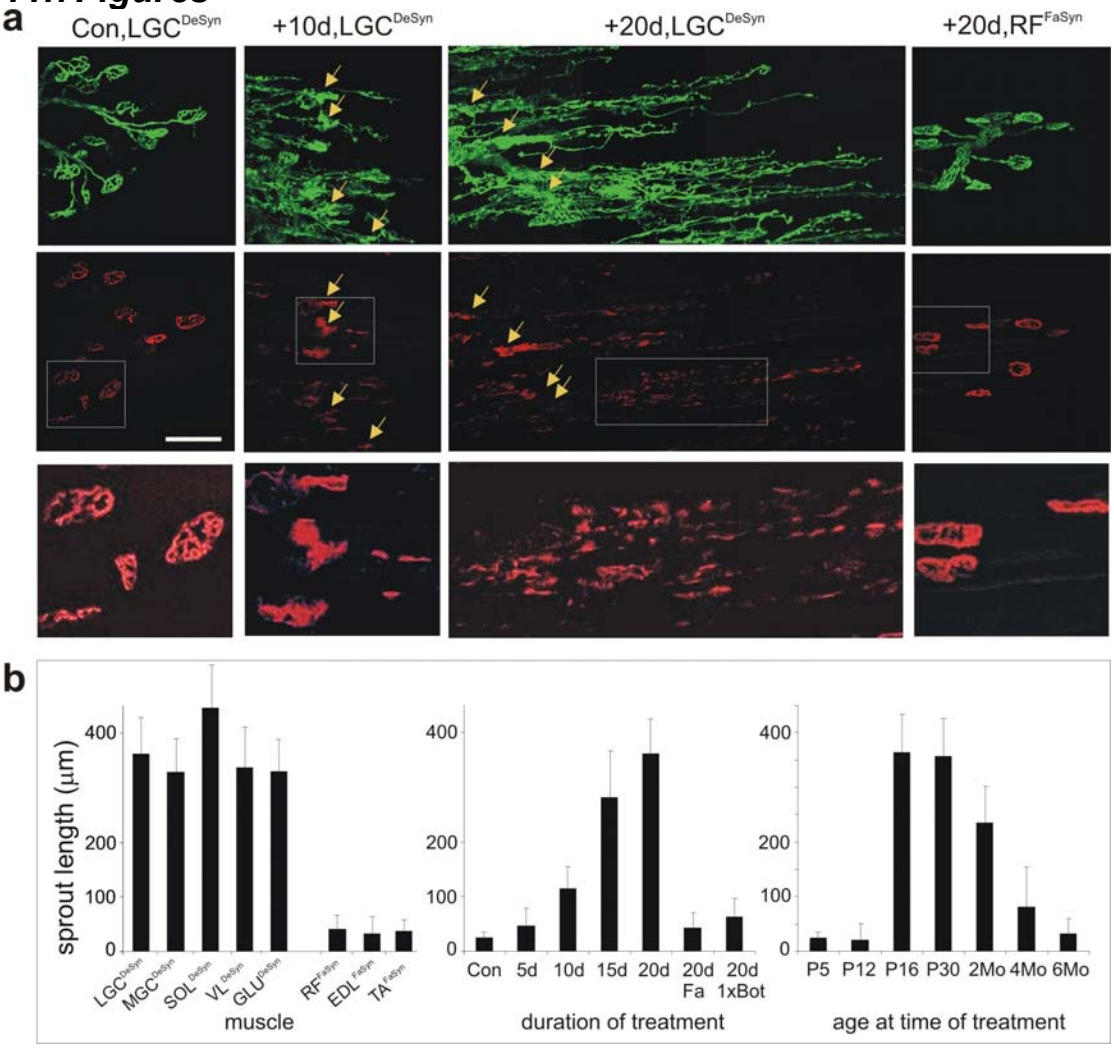

Figure 1

Gradual spread of motor nerves and ectopic synapses in young-adult DeSyn muscles treated with BotA. a, Nerve sprouting and ectopic synaptogenesis in BotA-treated muscles. Presynaptic nerves (upper row): GFP fluorescence (*Thy1-mGFP^{mu}* mice); postsynaptic apparatus (middle and lower row): RITC-α-Bungarotoxin. Arrows point to initial locations of some NMJs. Lower row: higher magnification views of the fields in the boxes. Note how sprouting is negatively correlated with AChR cluster organization and accumulation. **b**, BotA-induced sprouting is restricted to DeSyn mus-

cles (left, 20d BotA), depends on a long lasting blockade of synaptic transmission (center, LGC^{DeSyn}, except for sample labeled as Fa (RF^{FaSyn})), and is restricted to young adult DeSyn muscles (right, 20d BotA, LGC^{DeSyn}). N= 120 NMJs; 3 mice. Bar: 100 µm.

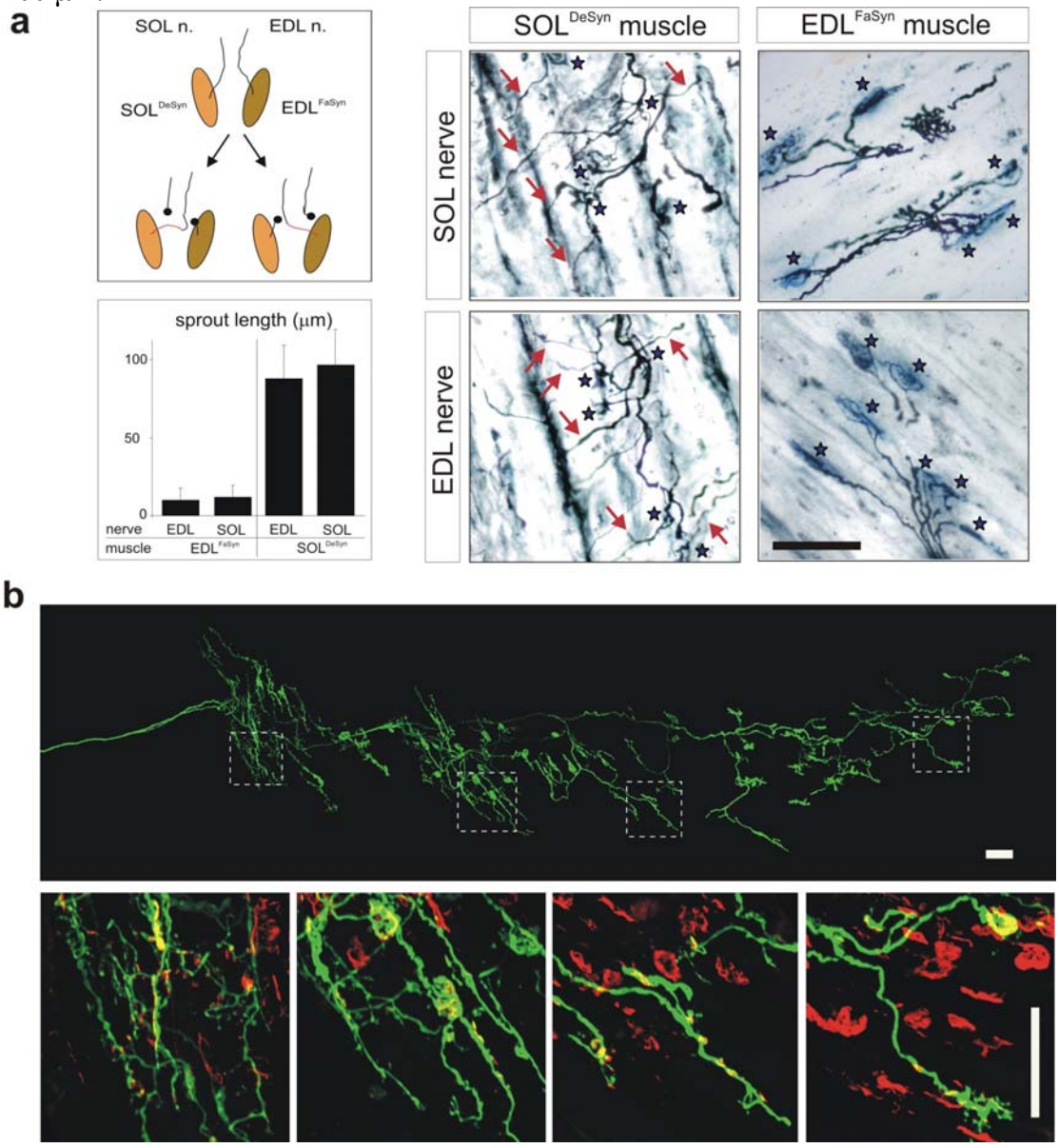

Figure 2

Postsynaptic muscles control BotA-induced plasticity at NMJs. a, Crossinervation experiments: host muscle determines whether or not nerves sprout upon paralysis.

Left: Schematic of the surgeries (top), and quantitative analysis of BotA-induced sprouting upon crossinervation (bottom; 7d BotA; N=450, 3mice)). Right: Representative examples of BotA-induced sprouting upon crossinervation (7d BotA, 1 month after surgeries; left labeling: donor nerve; top labeling: host muscle). Combined silver-esterase reaction (nerve black, AChE blue). Stars: positions of original NMJs; arrows: sprouts. For comparisons, note that sprouting in paralyzed SOL^{DeSyn} is more rapid than in LGC^{DeSyn}. **b**, NMJs by the same motoneuron sprout according to their position along a lateral gradient on LGC^{DeSyn}. Individual mGFP-expressing motoneuron (*Thy1-mGFP*^{s} mouse) innervating lateral-most compartment of LGC^{DeSyn} (lateral end of muscle to the right; motoneuron main axon runs from left to right) after 20d of BotA treatment. Boxes: positions of higher magnification panels. Note extensive sprouting at the medial section of the LGC^{DeSyn} subcompartment (left), and absence of sprouting at its distal end (right). Bars: 100 µm.

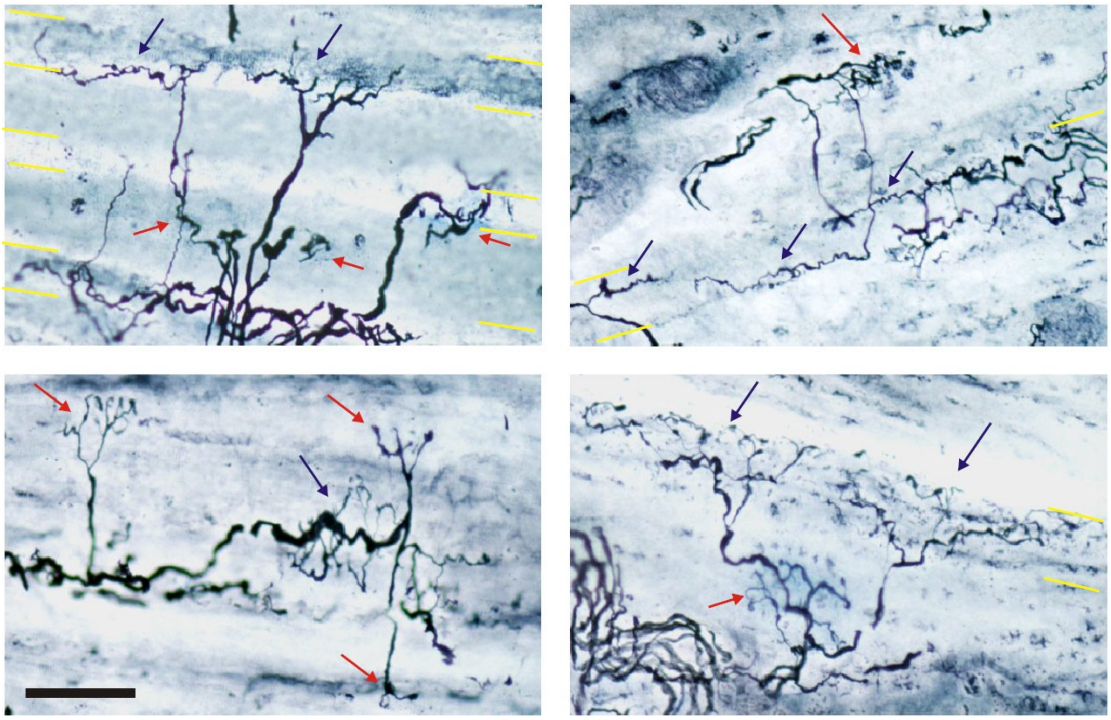

Figure 3

The extent of sprout growth on muscle is determined locally, at the level of individual muscle fibers. Combined silver esterase reaction (black: nerves; blue: acetylcholine-esterase reaction product); 1.5-months mouse, medial compartment of LGC^{DeSyn}, +20d BotA. The panels show examples of sprouts extending across muscle fiber boundaries (the levels and orientations of some of the boundaries are indicated by the yellow lines), and arborizing on distinct muscle fibers. Blue arrows: arborizations by sprouts on comparatively permissive muscle fibers (the central muscle fiber in the upper right panel is particularly permissive); red arrows: arborizations on comparatively non-permissive muscle fibers (see also intense synaptic esterase reaction product; the central muscle fiber in the upper left panel is particularly non-permissive). Note how sprout arborization patterns reflect individual muscle fibers, not presynaptic nerves. See text for a more detailed description of these data. Bar: 50 μm.

Figure 4

In BotA-induced plasticity, muscles control nerves, which control tSCs. a, Gradual extension of tSC processes in BotA-treated DeSyn, but not FaSyn muscles. *S100-GFP* mice. Arrows in +5d LGC^{DeSyn} muscle point to ends of sprouts. Note thick tSC processes in +16d LGC^{DeSyn} muscle, and their association with ectopic AChR clusters (arrows). **b**, Rapid and undistinguishable growth of thin radiating tSC processes in DeSyn and FaSyn muscles upon denervation. *S100-GFP* mice. **c**, Regenerating nerves are arrested (and retract) at large AChR clusters on FaSyn muscles (arrows), in spite of denervation-induced tSC sprouting. Crossinnervation experiments: EDL nerve onto SOL^{DeSyn} muscle (left), or soleus nerve onto EDL^{FaSyn} muscle (right). Analysis 40 days after surgeries (last 9 days +BotA). Bars: 50 μm.

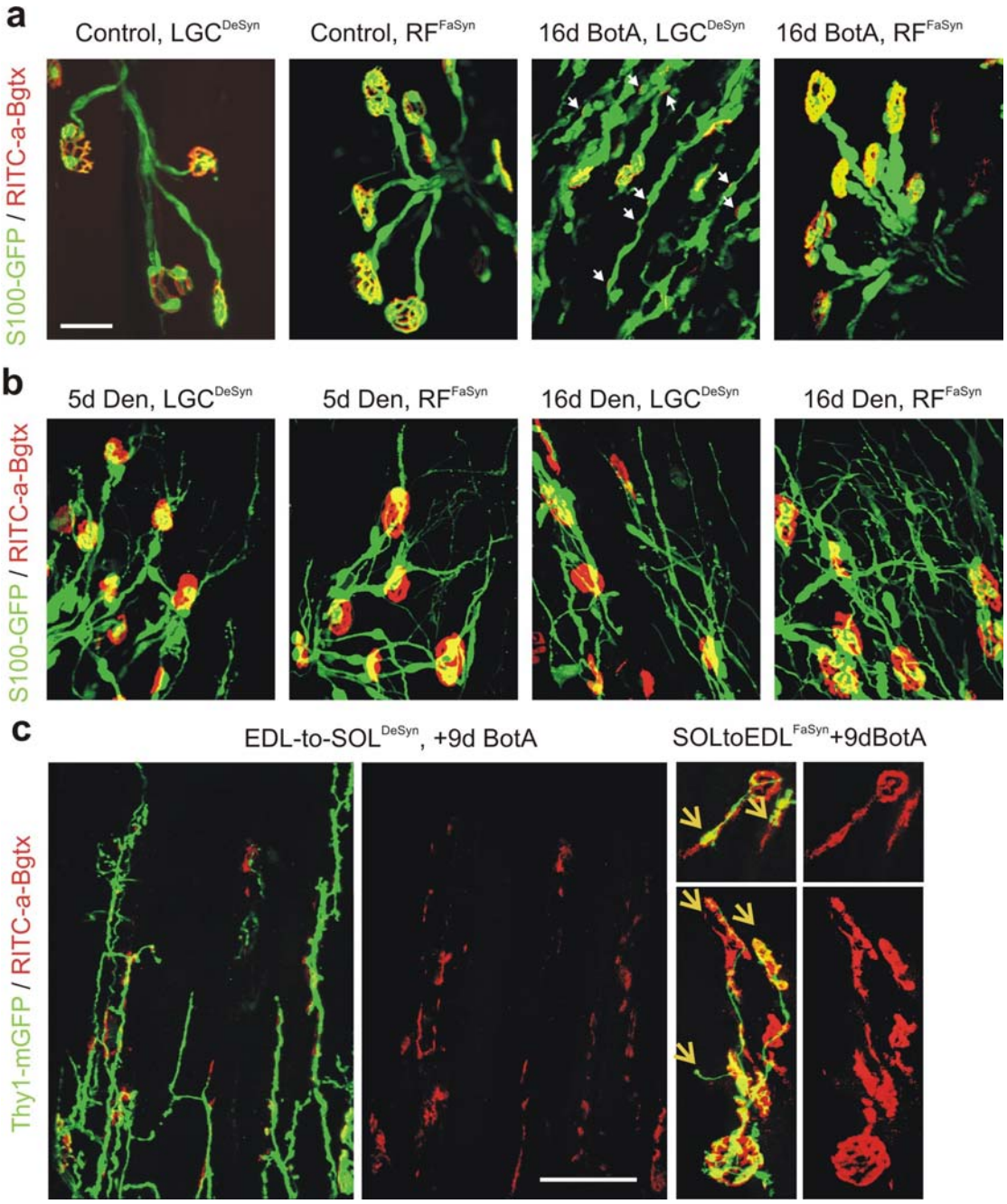
a
Control, LGC DeSyn
Control, RF FaSyn
16d BotA, LGC DeSyn
16d BotA, RF FaSyn
S100-GFP / RITC-a-Bgtx
b
5d Den, LGC DeSyn
5d Den, RF FaSyn
16d Den, LGC DeSyn
16d Den, RF FaSyn
S100-GFP / RITC-a-Bgtx
c
EDL-to-SOL DeSyn, +9d BotA
SOLtoEDL FaSyn+9dBotA
Thy1-mGFP / RITC-a-Bgtx

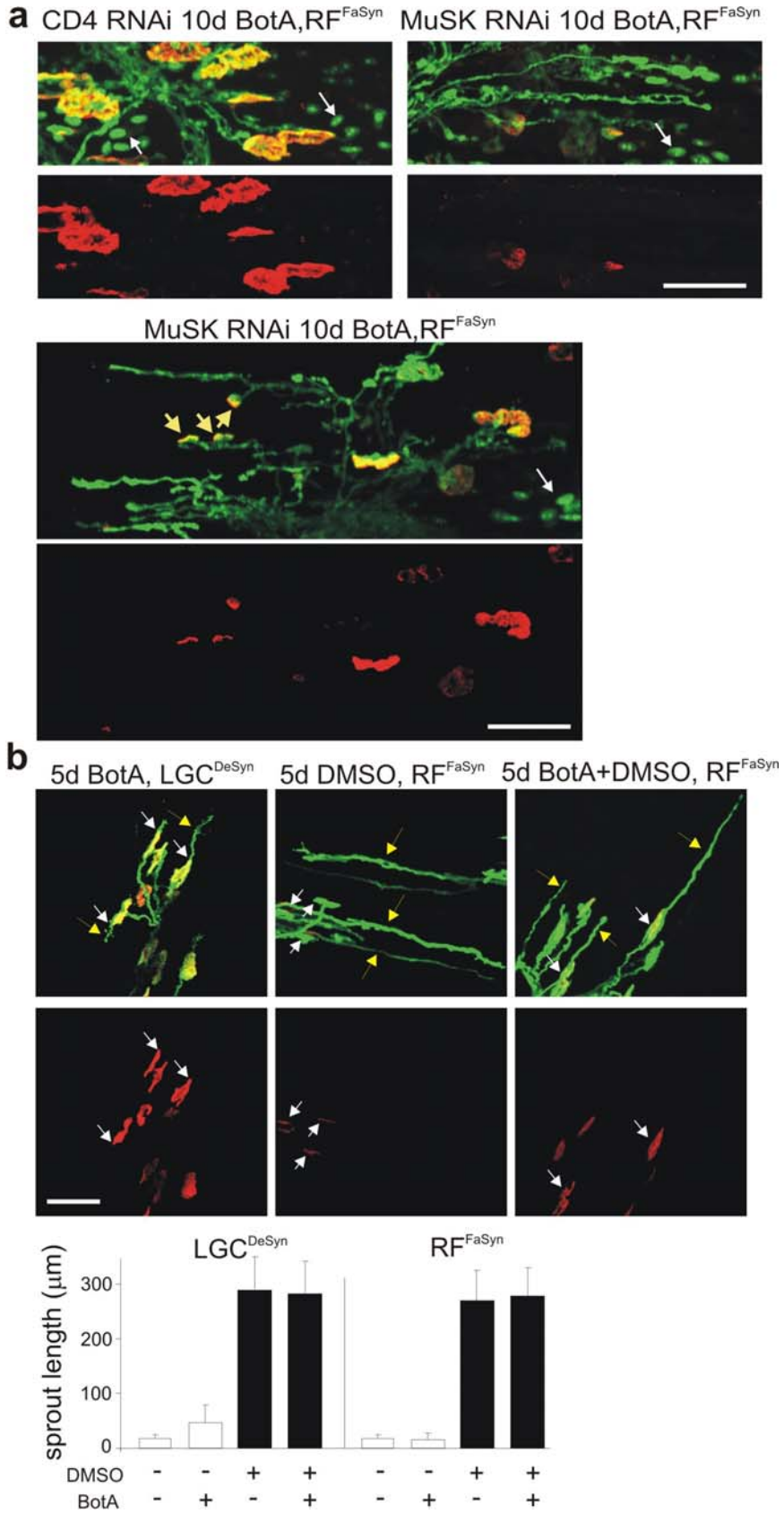
a
CD4 RNAi 10d BotA,RF^FaSyn
MuSK RNAi 10d BotA,RF^FaSyn
MuSK RNAi 10d BotA,RF^FaSyn
b
5d BotA, LGC^DeSyn
5d DMSO, RF^FaSyn
5d BotA+DMSO, RF^FaSyn
LGC^DeSyn
RF^FaSyn
sprout length (µm)
300
200
100
0
DMSO - - + + - - + +
BotA - + - + - + - +

Figure 5

Disrupting postsynaptic clusters is sufficient to induce nerve growth on any muscle. Green: nerves (mGFP); red: AChR (α-Bungarotoxin). **a**, Postsynaptic AChR cluster disruption is sufficient to induce sprouting with BotA in a FaSyn muscle. In vivo knockdown experiments with MuSK siRNA (2 examples), and control CD4 siRNA. Note extensive sprouting on muscle fibers with disrupted AChR clusters; also note cluster induction and stopping by sprout side branches (yellow arrows) contacting muscle fibers with intact clusters (intact NMJs on the left). White arrows: NLS-GFP-positive nuclei (reporter construct; many positive nuclei were positioned outside of the frames shown in the figure). **b**, Induction of rapidly growing sprouts upon AChR cluster disruption in DeSyn and FaSyn muscles. 1-month *Thy1-mGFP^{mu}* mice. Note short sprouts (arrows) in +5d BotA LGC^{DeSyn}, and much longer sprouts (yellow arrows) with or without BotA in DMSO-treated RF^{FaSyn}. Also note weakening of AChR clusters (white arrows) upon DMSO treatment. Quantitative analysis: 5d treatments, 1-month mice, N= 120 NMJs, 3 mice each. Bars: 50 μm.

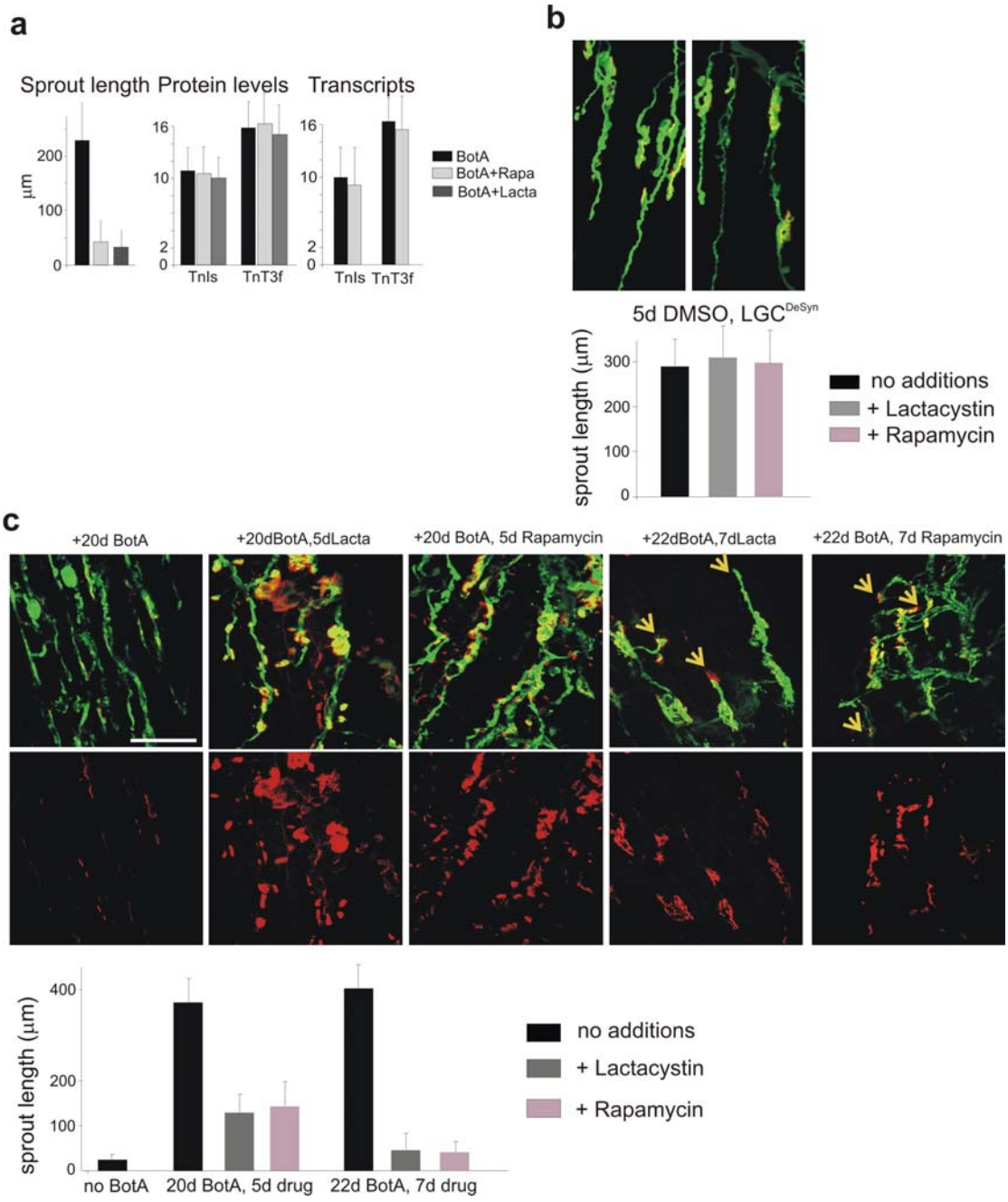

Figure 6

Re-accumulation of AChR clusters and retraction of sprouts in BotA-treated muscles exposed to Lactacystin or Rapamycin. Green: nerves (mGFP); red: AChR (α-Bungarotoxin). **a**, Application of Rapamycin (Rapa) or Lactacystin (Lacta) to chronically paralyzed DeSyn muscles inhibits BotA-induced sprouting, but not the up-regulation of embryonic transcripts, nor that of embryonic proteins (LGC^{DeSyn}). Pro-

tein and transcript levels: +20d BotA data; sprout lengths: +15d BotA data; drug applications during last 5 days of each experiment. N=3 mice each. **b**, Lactacystin or Rapamycin do not interfere with nerve sprouting induced by DMSO. 1-month LGC^{DeSyn}. N=120 NMJs, 3 mice each. **c**, Accumulation of nerve-associated AChR clusters and retraction of sprouts upon the addition of Lactacystin or Rapamycin to BotA-treated LGC^{DeSyn}. Where indicated, drugs were applied from day +15 on. Arrows: ectopic clusters associated with retracting sprouts. Note how Lactacystin or Rapamycin fail to stabilize AChR clusters that are not associated with sprouts (compare +20d to +22d data). Quantitative analysis: N=120 NMJs, 3 mice each. Bar: 50 µm.

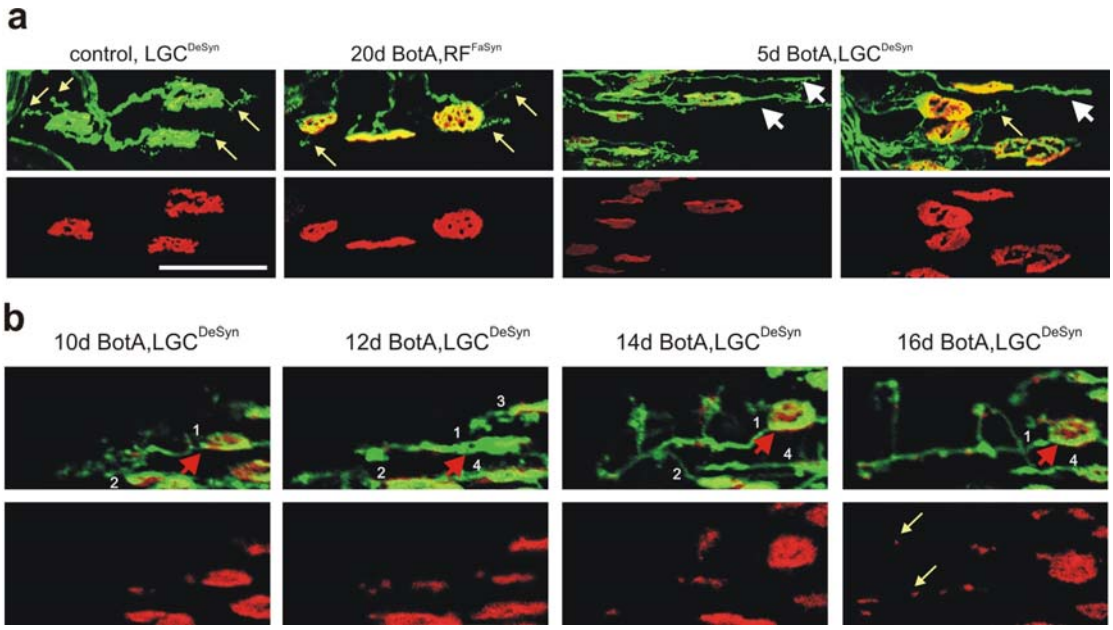

Figure 7

Relationship between sprout extension and ectopic AChR clusters in BotA-treated DeSyn muscles. Green: nerves (mGFP); red: AChR (α-Bungarotoxin). **a**, Absence of ectopic AChR clusters during the early stages of BotA-induced sprouting. NMJs exhibit several short twisted sprouts (thin arrows) in the absence of BotA (left), or in BotA-treated FaSyn muscles (second panel); 1-2 straight sprouts (larger arrows) grow from many NMJs on DeSyn muscles at day +5 of the BotA treatment, but at this early

time sprouts are not associated with ectopic AChR clusters. **b**, In vivo time-lapse imaging of nerves and AChR clusters in BotA-treated LGC^{DeSyn} and RF^{FaSyn}. Note gradual elongation of sprouts (indicated by separate numbers) on LGC^{DeSyn}, changing patterns of ectopic AChR clusters along sprout-1, and absence of clusters at distal ends of most sprouts. For orientation, a red arrowhead marks the same LGC^{DeSyn} NMJ in the panels; small arrows (+16d, AChR, LGC^{DeSyn}) indicate examples of two ectopic clusters that were not detectable at day +14. See text for a more detailed description of these data. Bars: 50 µm.

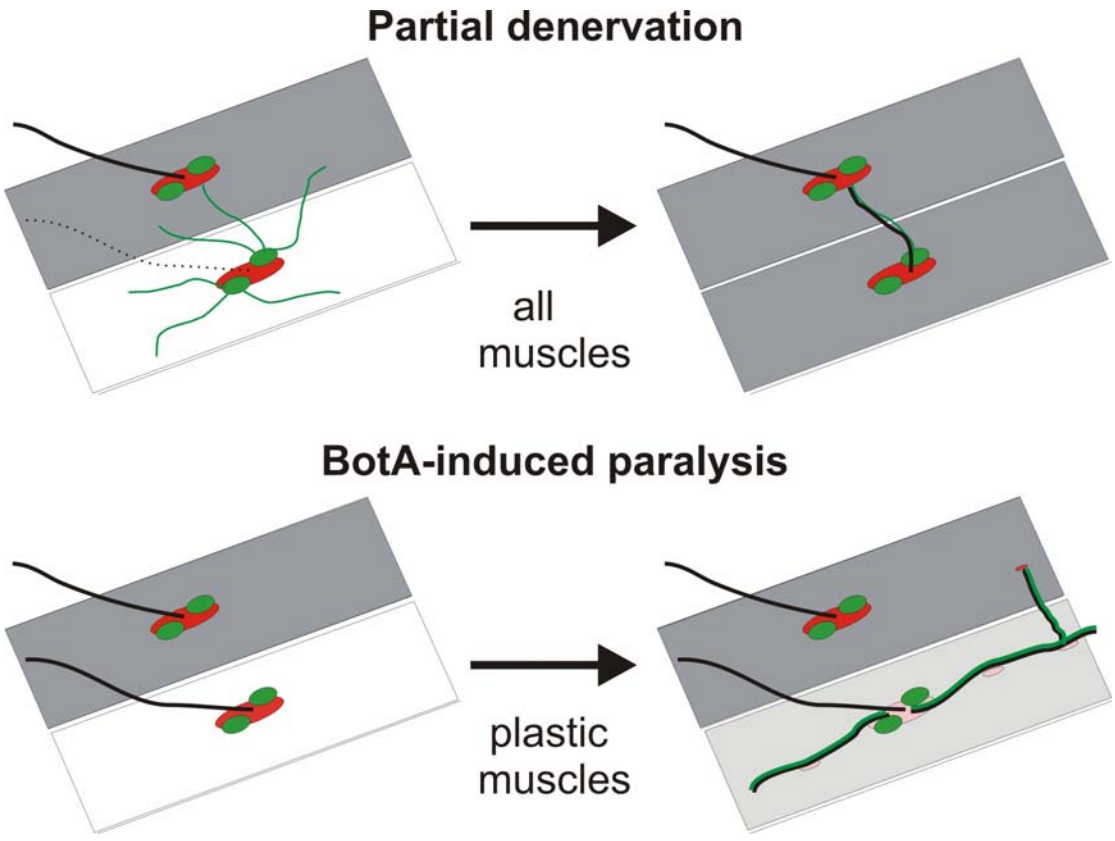

Figure 8

Denervation- and BotA-induced anatomical plasticity at NMJs involve distinct mechanisms and produce distinct rearrangements of connectivity. The schematics represent two muscle fibers innervated by two separate MNs each. The intensity of the gray shading represents the strength of muscle fiber activation by innervating motor

nerves. AChR clusters are indicated in red; the intensity of the red color represents the state of AChR accumulation at postsynaptic clusters. tSCs and their processes are in green. Partial denervation leads to sprouting of radial tSC processes from denervated sites in all muscles, and growth of motor nerve sprouts along tSC processes from nearby NMJs, to reinnervated synaptic sites through preserved motor axons. BotA-induced paralysis leads to a reduction in AChR cluster accumulation in plastic muscles, which is associated with a gradual elongation of motor nerve sprouts on muscle fibers, and the establishment of ectopic synaptic sites.

11.8Supplementary material

Suppl. Table 1

Proteins induced by a chronic BotA treatment in 1-month LGC^{DeSyn} and/or RF^{FaSyn}

Proteins induced in LGC^{DeSyn} and RF^{FaSyn}:

Desmin Des (P31001)

14-3-3 protein epsilon Ywhae (P62259)

14-3-3 protein gamma Ywhae (P61982)

Superoxide dismutase [Cu-Zn] Sod1 (P08228)

ubiquitin carboxyl-terminal hydrolase isozyme L1 Uchl1 (Q9R0P9) (aka PGP 9.5)

Annexin A5 Anxa5/Anx5 (P48036) (aka Lipocortin V, Thromboplastin inhibitor)

Serpinb6 Serpin B6 (Q60854) (aka Placental thrombin inhibitor)

Sarcalumenin Srl/SAR (Q7TQ48)

Sarcosin Krp1/ Kbtbd10 (Q9ER30) (aka Kelch-related protein 1)

Proteins induced in LGC^{DeSyn}, but not in RF^{FaSyn}:

CapZ alpha-2 Capza2 (P47754) (aka F-actin capping protein alpha-2)

L-lactate dehydrogenase B chain Ldhb/Ldh-2/Ldh2 (P16125) (aka LDH-H)

TnT3f (Q9QZ47)

TnIs (O88346)

MLC1SB (P09542) (aka Ventricular/slow twitch myosin alkali light chain)

Proteins induced in RF^{FaSyn}, but not in LGC^{DeSyn}:

Alpha crystallin B chain Cryab/Crya2 (P23927)

Glycogen phosphorylase, muscle form Pygm: (Q9WUB3) (aka Myophosphorylase)

The chronic BotA treatment was initiated at 1 month (N=3), and muscle samples were collected at day +20. Levels of all the proteins included in the lists were upregulated more than 2-fold in muscles of all mice analyzed (at least three). Each protein entry includes protein name, gene name, protein database code (Swissprot, as in http://ca.-expasy.org/sprot/) and, were appropriate, aliases.

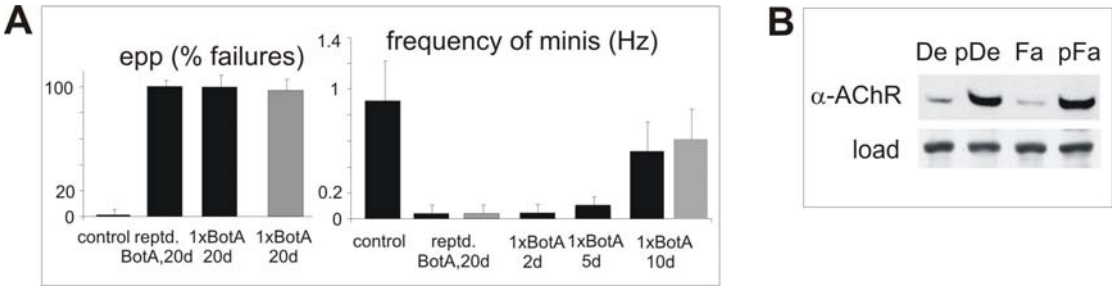

Suppl. Figure 1

Distinct requirements for persistent blockade of evoked release and miniature events by BotA. a, One application (1x) of BotA induces a long lasting blockade of evoked release (epp), but blockade of miniature events (minis) requires repeated applications of BotA. Nerve-muscle preparations from EDL^{FaSyn} (dark bars) or SOL^{DeSyn} (light bars). Days: time after beginning of the treatment. N= 60 NMJs; 3 mice. **b**, Rapid induction of activity-regulated proteins by BotA in LGC^{DeSyn} (De) and RF^{FaSyn} (Fa). Immunoblot for α-subunit of AChR and loading control (P_i-Tyrosine band

at 50 kD). Ispilateral BotA-treated (p) and contralateral controls 4 days after toxin treatment.

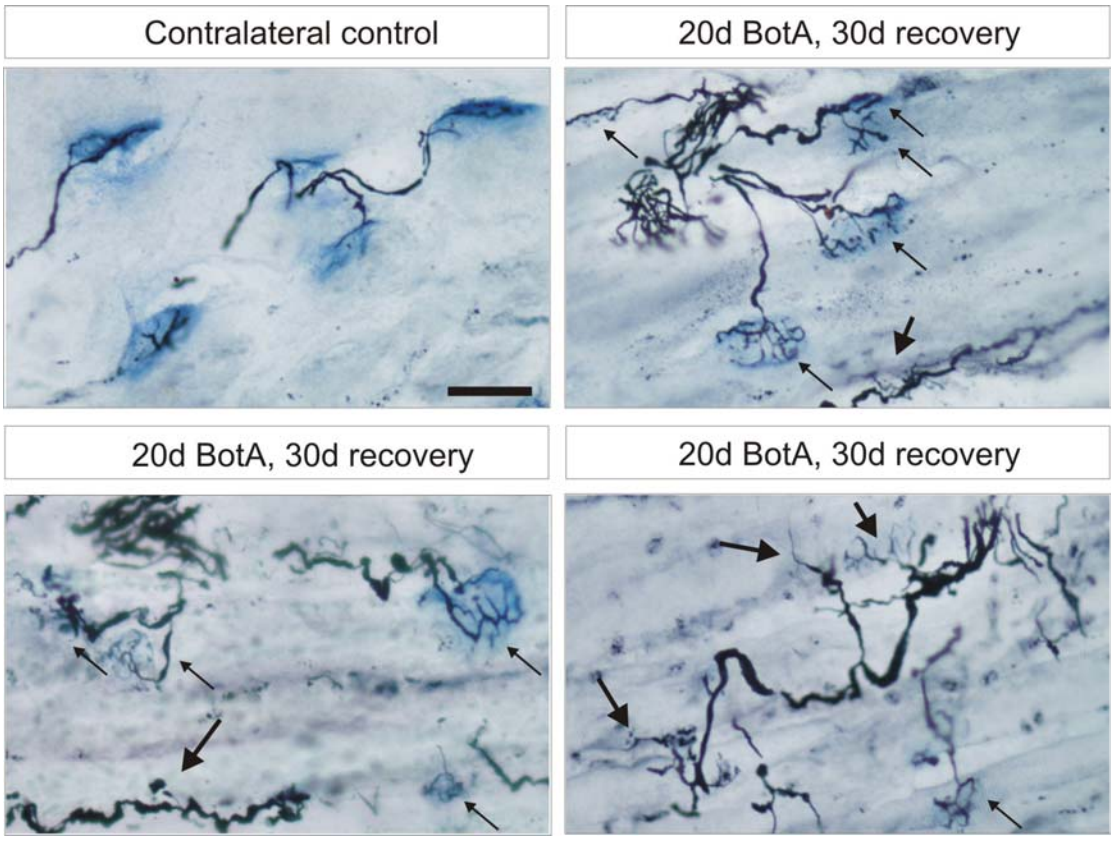

Suppl. Figure 2

Recovery from sprouting and NMJ remodeling induced by a chronic BotA treatment. The treatments were initiated at 1 month, and the last drug application was at day +20 (LGC^{DeSyn}; each row shows two panels from the same mouse). Combined silver esterase reaction (nerves black, AChE blue). NMJs have recovered a focal appearance (thin arrows); some of the long processes have persisted 30d later (thicker arrows), and have established NMJs through side-branches (thick arrows in bottom row, right). For comparison, an equivalent region of LGC^{DeSyn} at day +20 can be seen in Fig. **1a**. Bar: 50 µm.

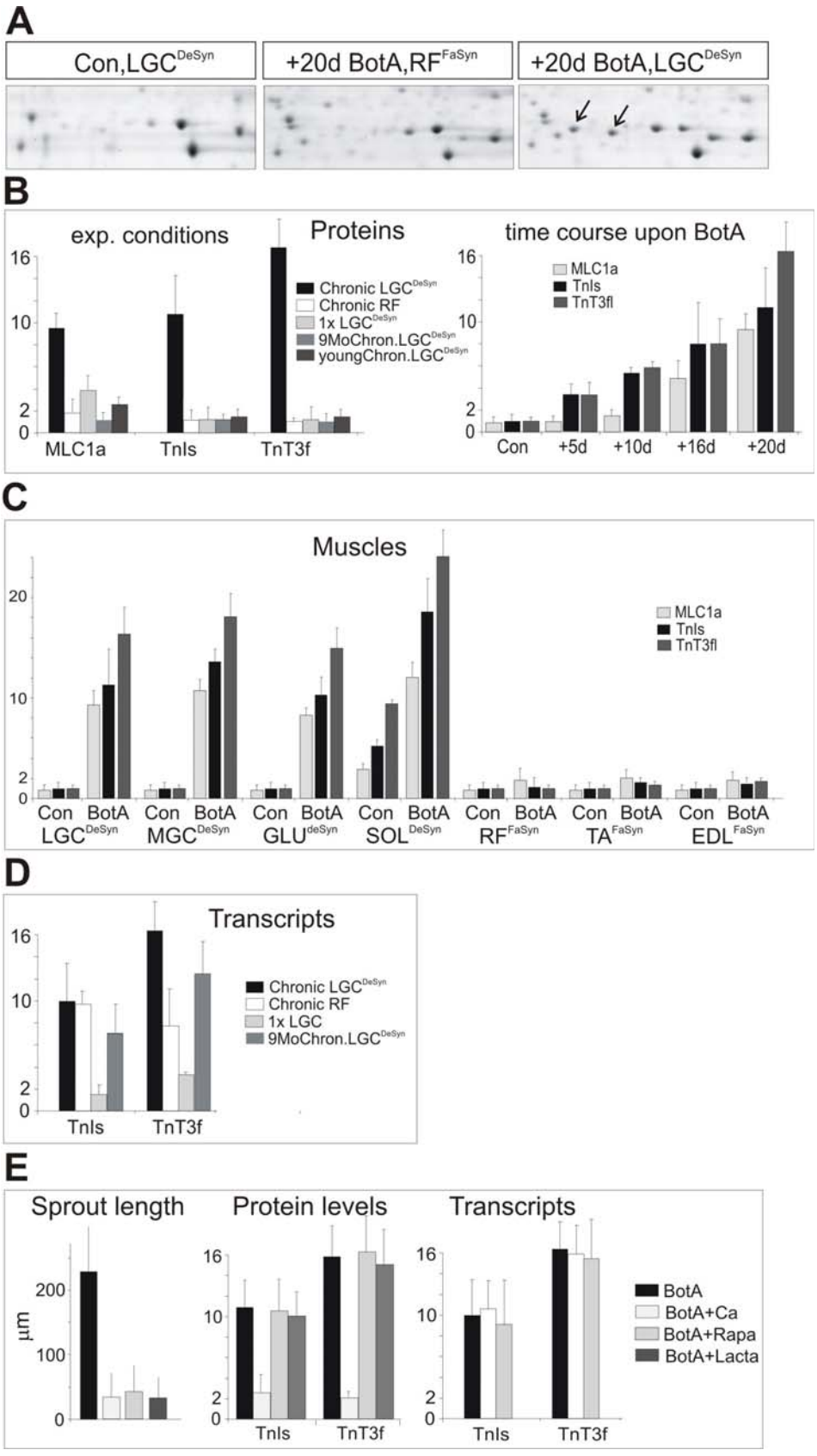
A
Con,LGC DeSyn
+20d BotA,RF FaSyn
+20d BotA,LGC DeSyn
B
exp. conditions
Proteins
Chronic LGC DeSyn
Chronic RF
1x LGC DeSyn
9MoChron.LGC DeSyn
youngChron.LGC DeSyn
MLC1a
TnIs
TnT3f
time course upon BotA
MLC1a
TnIs
TnT3fl
Con
+5d
+10d
+16d
+20d
C
Muscles
MLC1a
TnIs
TnT3fl
Con BotA LGC DeSyn
Con BotA MGC DeSyn
Con BotA GLU deSyn
Con BotA SOL DeSyn
Con BotA RF FaSyn
Con BotA TA FaSyn
Con BotA EDL FaSyn
D
Transcripts
Chronic LGC DeSyn
Chronic RF
1x LGC
9MoChron.LGC DeSyn
TnIs
TnT3f
E
Sprout length
Protein levels
Transcripts
µm
BotA
BotA+Ca
BotA+Rapa
BotA+Lacta
TnIs
TnT3f

Suppl. Fig. 3

A long-lasting blockade of synaptic transmission induces embryonic muscle genes in all muscles, but the proteins accumulate selectively in young adult DeSyn muscles. a, Selective upregulation of embryonic Troponin splice forms and isoforms (arrows) in DeSyn muscles treated chronically with BotA. Representative Coomassie-stained 2-D gel details including Troponin isoforms. **b**, Selective upregulation of embryonic muscle proteins in chronically paralyzed young adult LGC^{DeSyn} (exp. conditions), correlating with NMJ plasticity (time course). Quantitative analysis of protein contents from 2-D gels; young: BotA treatment initiated at P5 (20d, repeated). N=3 mice. **c**, Selective upregulation of embryonic muscle proteins in DeSyn, but not FaSyn muscles (20d BotA, start at 1-month). N=3 mice. **d**, Chronic blockade of miniature events leads to upregulation of embryonic muscle transcripts in all muscles and at all ages. Analysis of qRT-PCR data; N=3 mice.

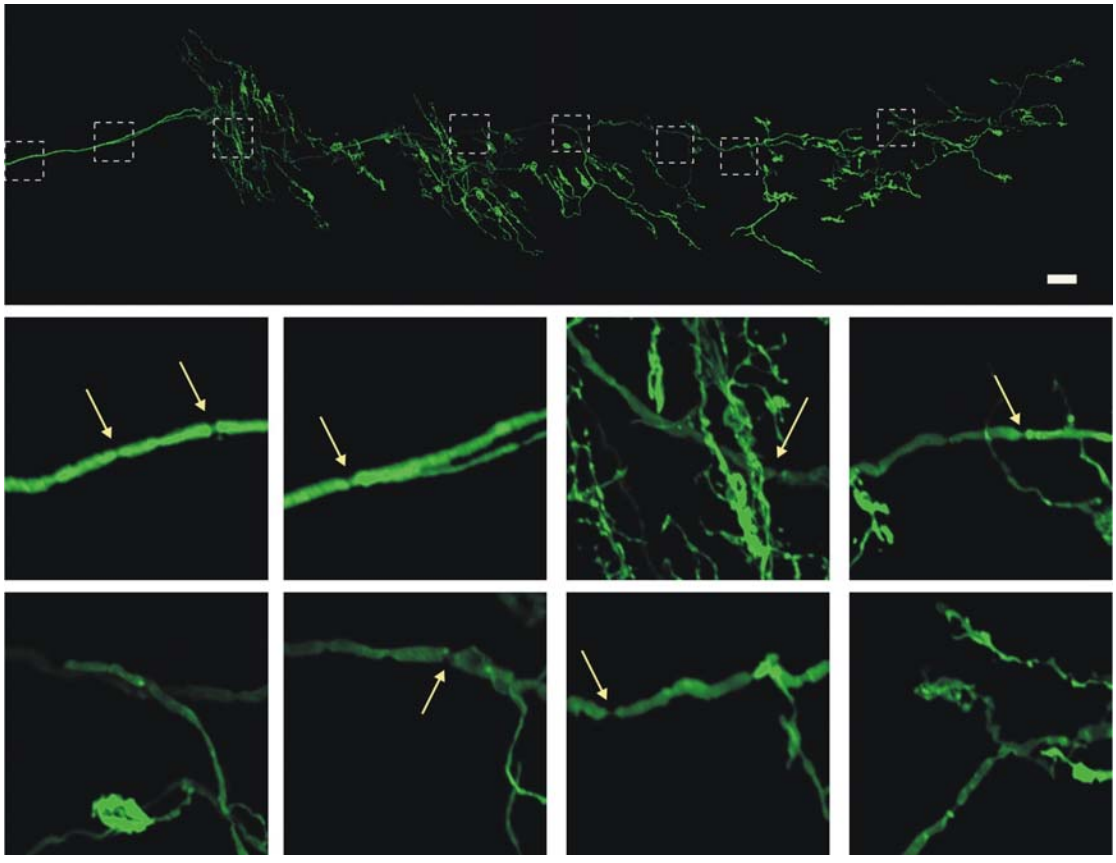

Suppl. Figure 4

High magnification views of main axon by single mGFP-positive motoneuron shown in Fig. 2b, as it runs through its LGC^{DeSyn} subcompartment (from left to right). The boxes in the low magnification panel (top) indicate the positions of the high-magnification views (ordered from left to right, top row first). Small arrows point to nodes; the panels were selected in part to document branch points by side-branches to NMJs (e.g. second high-magnification panel).

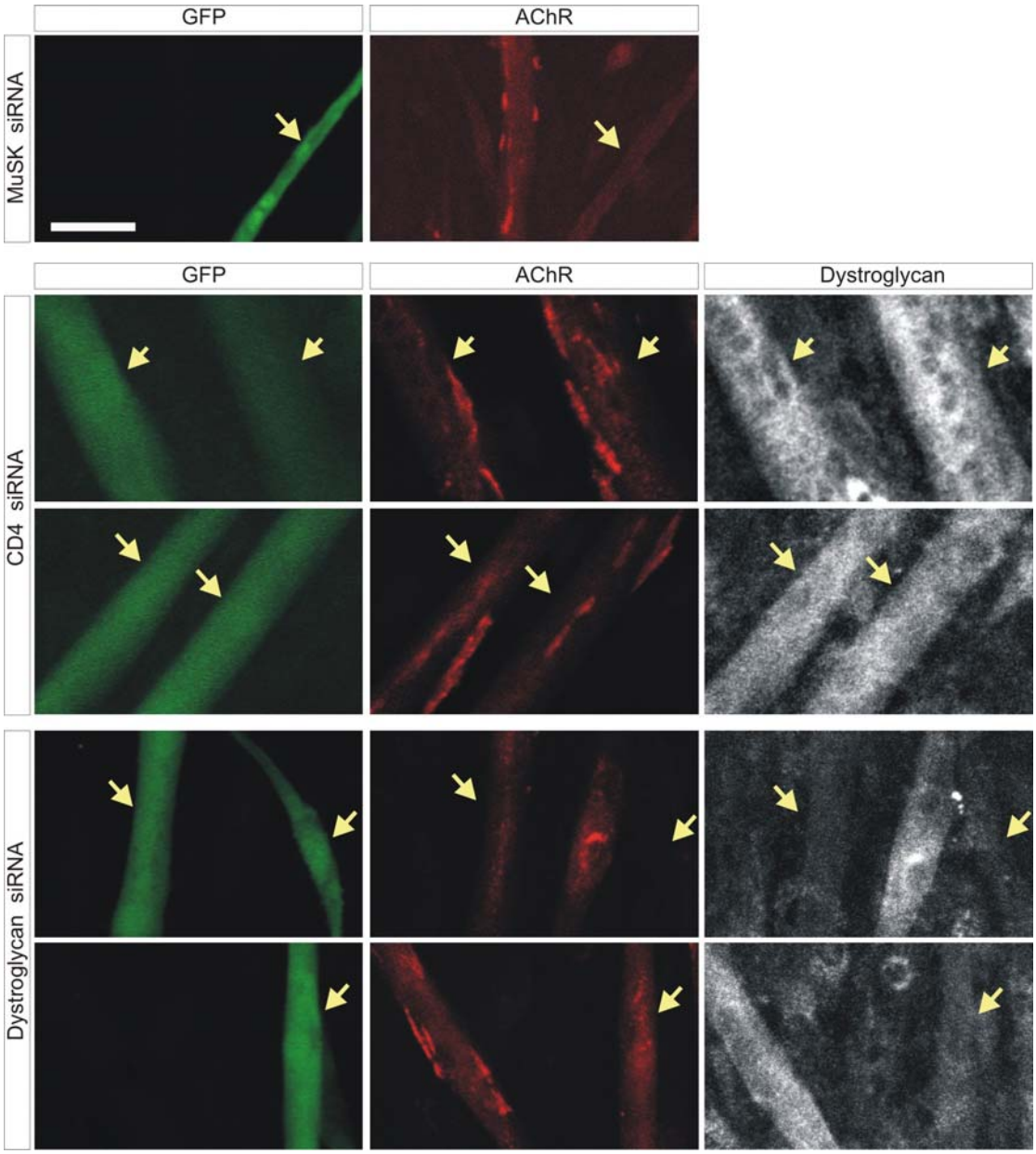

Suppl. Figure 5

Knockdown of MuSK in C2C12 myotubes. The positions of GFP-positive myotubes (co-transfected reporter plasmid) are indicated by arrows. MuSK siRNA[33] led to a suppression of agrin-induced AChR clusters and smaller myotubes. CD4 siRNA documents the lack of effects on AChR clusters when expressing a control RNAi plasmid. Bar: 30 µm.

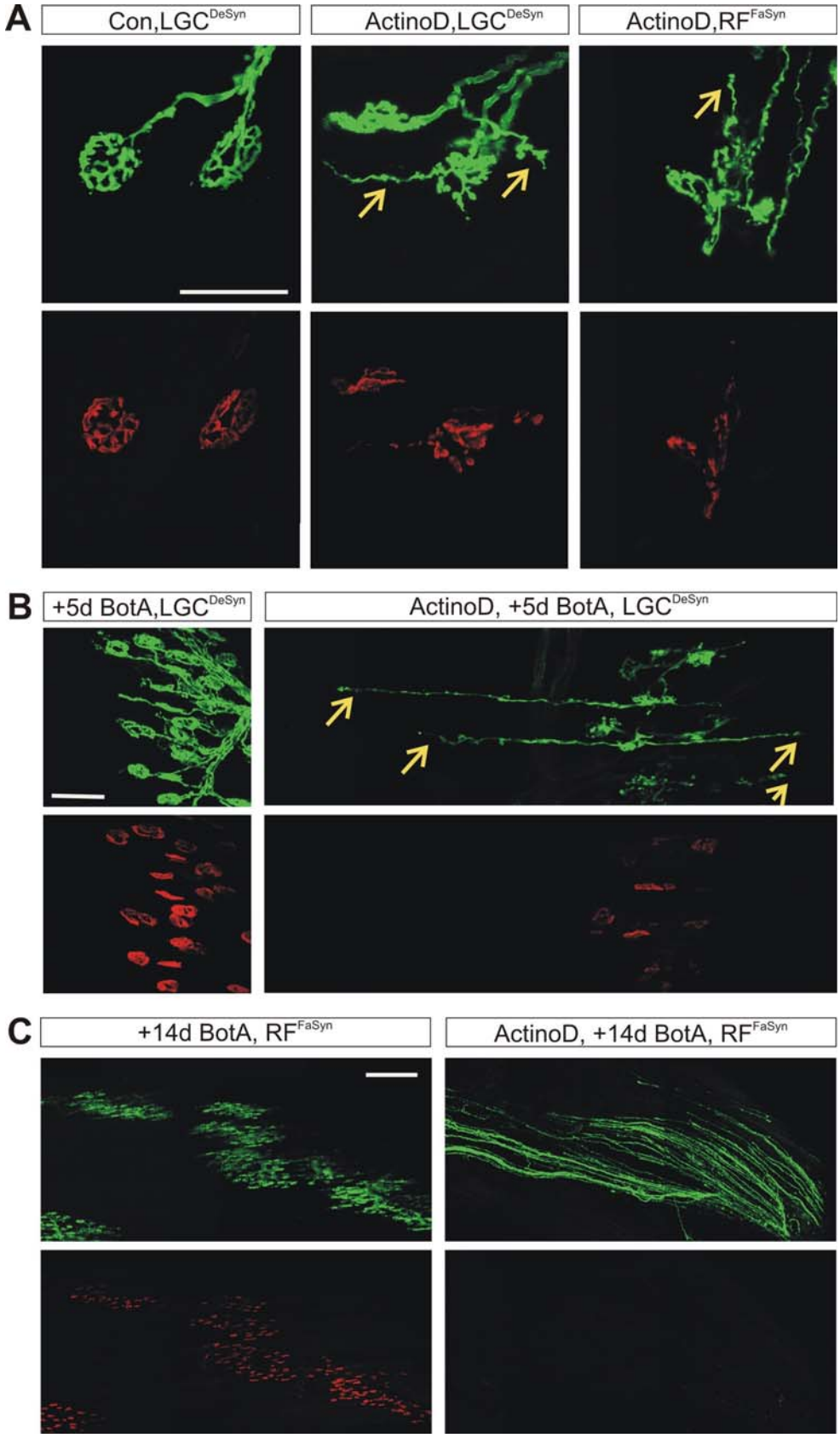
A
Con,LGC DeSyn
ActinoD,LGC DeSyn
ActinoD,RF FaSyn
B
+5d BotA,LGC DeSyn
ActinoD, +5d BotA, LGC DeSyn
C
+14d BotA, RF FaSyn
ActinoD, +14d BotA, RF FaSyn

Suppl. Figure 6

A treatment interfering with the assembly state of postsynaptic apparatus in the adult leads to rapid and unrestricted BotA-induced sprouting in DeSyn and FaSyn muscles. a, Local application of ActinoD leads to a reduction in the assembly state of postsynaptic apparatus in DeSyn and FaSyn muscles. ActinoD was applied daily for 4 days, and NMJs were analyzed 20d after beginning of the treatment. Note fragmentation of postsynaptic apparatus and nerve sprouts inducing ectopic AChR clusters (arrows) in ActinoD-treated muscles. **b**, Rapid induction of sprouting by BotA in ActinoD-treated muscles. Experimental conditions as in (a), except for the addition of BotA 5 days before the end of the experiment. Note long straight sprouts in ActinoD- plus BotA-treated DeSyn muscle (arrows). Comparable sprouting was induced in ActinoD-treated FaSyn muscles (not shown). **c**, Unrestricted BotA-induced sprouting in ActinoD-treated FaSyn muscles. Experimental conditions as in (a), except for the addition of BotA 14d before the end of the experiment. Note long straight sprouts with no ectopic AChR clusters and loss of original postsynaptic apparatus at +14d BotA in ActinoD-treated FaSyn muscle. Bars: 100 (a, b) and 300 μm (c).

Chapter 12 - Selective Vulnerability and Pruning of Phasic Motoneuron Axons Alleviated by CNTF in Motoneuron Disease

Nature Neuroscience (2006), 9 (3), p. 408-19.

San Pun, Alexandre Ferrao Santos, Smita Saxena, Lan Xu, and Pico Caroni

Friedrich Miescher Institut, Maulbeerstrasse 66, CH-4058 Basel, Switzerland

12.1Summary

Neurodegenerative diseases involve long preclinical phases and insidious progression patterns, but the mechanisms of disease progression are poorly understood. Quantitative accounts of neuronal circuitry affected by disease have been lacking. Consequently, it has remained unclear whether disease progression reflects stochastic gradual loss processes, or temporally defined selective vulnerabilities of distinct synapses or axons. Here we derive a quantitative topographic map of muscle innervation in the hindlimb, and show that in two mouse models of motoneuron (MN) disease, axons of fast-fatiguable MNs are affected synchronously, long before symptoms; axons of fast-fatigue-resistant MNs are affected at symptoms, whereas axons of slow MNs resist. Axonal vulnerability leads to synaptic vesicle stalling and Bcl2A1-a accumulation, is alleviated by CNTF, and triggers proteasome-dependent pruning of all peripheral axon branches. Thus, neurodegeneration involves predictable selective vulnerability patterns by physiological subtypes of axons, episodes of abrupt pruning in the target region, and compensation by resistant axons.

12.2 Introduction

In neurodegenerative diseases, years of slowly progressing and clinically undetectable alterations and losses set the stage for devastating clinical phases, when treatments produce disappointing results. Synapses are lost early in disease, but the mechanisms underlying this vulnerability are not understood (Walsh and Selkoe, 2004; Coleman and Yao, 2003). It is not clear whether particular synapses are lost selectively, gradually or abruptly, and whether it is synapses, axons or dendrites, which are targeted by disease. The complexities of adult brain circuitry pose formidable challenges to elucidating mechanisms of early disease progression. However, in animal models of motoneuron (MN) disease (Gurney et al., 1994; Bruijn et al., 2004), more accessible synapses between MNs and muscles are also lost early on, and in reproducible patterns (Frey et al., 2000; Fischer et al., 2004). MN disease models thus provide uniquely advantageous systems to investigate pathways of vulnerability and disease progression in neurodegeneration. Such information is essential for early detection, and the development of more effective treatments against these diseases.

Transgenic mice expressing human SOD1 point mutant proteins associated with familial amyotrophic lateral sclerosis (FALS) (Rosen et al., 1993) develop paralytic MN disease closely resembling human ALS. The mechanism through which mutant SOD1 triggers disease appears to involve pathogenic processes in the local environment of MNs (Lino et al., 2002; Clement et al., 2003), and mitochondrial accumulation of mutant SOD1 in affected MNs (Liu et al., 2004; Pasinelli et al., 2004). Early MN dysfunction includes mitochondrial pathology (Wong et al., 1995; Kong and Xu, 1998), axonal deficits such as the accumulation of neurofilaments and slowing of axonal transport (Collard et al., 1995; Zhang et al., 1997; Williamson et al., 1999; Jablonka et al., 2004), and failure (Pinter et al., 1995) and loss of peripheral synapses (Frey et al., 2000; Fischer et al., 2004). Mice expressing high levels of human SOD1(G93A) provide a particularly valuable model of MN disease due to their remarkably predictable pattern of disease progression (Gurney et al., 1994). The mice develop first clinical signs of MN disease at postnatal day (P) 80-90, and die at P136$\pm$5. Loss of MNs is a

late event in disease (detectable from P90-100), and interventions inhibiting or preventing MN loss have a modest impact on the timing of paralytic disease progression and death (Fischer et al., 2004; Sagot et al., 1995; Kostic et al., 1997). In contrast, the local application of axon protecting agents such as CNTF delays deficits in axonal transport, losses in muscle strength and death (Sagot et al., 1998; Sendtner et al., 1992). Likewise, removal of neurofilament (NF) side-chains by a knock-in approach, or alterations in axonal NF composition in transgenic mice reduce axonal pathology and delay disease progression. By providing evidence that deficits in axon function are specifically associated with disease progression in ALS, these findings have raised the issue of how such deficits relate to the gradual and highly predictable patterns of muscle strength losses associated with disease.

Recent studies have established that many peripheral synapses between MNs and muscles (neuromuscular junctions, NMJs) are lost in SOD1(G93A) mice from P50 on, before detectable losses of motor axons in ventral roots exiting the spinal cord, and long before any clinical sign of disease (Frey et al., 2000; Fischer et al., 2004). In addition, a detailed study revealed reproducible differences in the timing of denervation of individual muscles, and distinct topographic patterns of denervation in individual hindlimb muscles, suggesting that NMJs were being lost according to defined albeit still unknown principles (Frey et al., 2000). Taken together, the currently available evidence thus suggested that a process of selective and progressive loss of peripheral synapses linked to axonal dysfunction might be a critical determinant of disease progression in ALS. However, because they could not relate individual NMJs to particular axons and MNs, these studies could not elucidate whether individual axons lose their NMJs gradually or all at once, and whether particular types of axons and/or NMJs are selectively vulnerable to disease-associated loss. Furthermore, and for the same reasons, mechanistic investigations of the disease process have suffered from an inability to distinguish affected from non-affected axons and MNs at any stage of the disease.

Here we exploited a combination of Thy1-transgenic mice expressing GFP fusion proteins in only few neurons (De Paola et al., 2003), together with established histological procedures, to quantitatively map the innervation of hindlimb muscle compartments by MNs and their functional subtypes in the mouse. We then applied these maps and procedures to elucidate principles and mechanisms of early disease progression in FALS mice. Our results identify axons of phasically (infrequently) firing motoneurons as being selectively vulnerable at well-defined times early in disease, and show that where present, tonic ones resist and compensate through sprouting and reinnervation. Axonal vulnerability involves absence of neurofilament adjustments, synaptic vesicle stalling, loss of synaptic vesicles from all peripheral synapses, and upregulation of Bcl2A1-a in MNs; this is followed by Lactacystin-sensitive pruning of all peripheral synapses and terminal axon branches. The axonal vulnerability process can be alleviated by peripheral applications of CNTF. Since early defects in axonal transport have also been associated with Alzheimer's (Stokin et al., 2005) and Huntington's (Gunawardena and Goldstein, 2005) disease, these findings may reflect general principles of disease progression and treatment in neurodegeneration, independent of the molecular pathways triggering particular forms of disease.

12.3 Results

A quantitative topographic map of gastrocnemius innervation by MNs

To investigate in a quantitative manner whether and how the patterns of synapse loss in SOD1(G93A) mice might relate to individual MNs and their particular subtypes, we first mapped the distribution of all synapses made by individual MNs in lateral gastrocnemius muscle (LGC) using transgenic mice expressing membrane-targeted GFP (mGFP) in only few neurons (*Thy1-mGFP*^{s} mice; De Paola et al., 2003). LGC is subdivided into three non-overlapping compartments (lateral (l), intermediate (i), me-

dial (m)), which are innervated by separate nerve branches, established by non-overlapping subsets of MNs within the LGC pool (Burke, 1994) (Fig. 1a). We found that at the first 1-2 branch points made by the nerve entering any of the three LGC compartments, individual MN axons extended into only one of the alternative nerve branches (Fig. 1b,c). The same axons then extended into most (>90%) subsequent intramuscular branches of their muscle nerve. We found the same type of arrangement for other large muscles in the hindlimb (gluteus maximus, medial gastrocnemius (MGC), vastus lateralis, rectus femoris, tibialis anterior (TA); not shown). Branch selection by MNs thus defines subcompartments of muscles innervated by non-overlapping sets of MNs. The subcompartments partition LGC into 8 subterritories with respect to a medio-lateral gradient (l1-2; i1-3; m1-3; Fig. 1a). Within these 8 subcompartments, many MNs arborize throughout the bone-to-skin axis (Fig. 1c), but some MNs restrict their innervation to either the inner or outer 2/3rd of LGC (Fig. 1d). When numbers of large myelinated axons within intramuscular nerve branches were counted using combined silver-esterase preparations (see Fig. 2a), these were found to be stereotyped, and in good agreement with motor unit (MU; one MN and all muscle fibers it innervates; Burke, 1994) number estimates based on the extent of subcompartment innervation by individual MNs (Fig. 1d). Remarkably, this MU arrangement and the numbers of MUs per subcompartment were highly reproducible among different mice (Fig. 1d), allowing us to provide a quantitative topographic account of the MUs innervating LGC in the mouse (Fig. 1e).

Three classes of muscle subcompartments with respect to denervation in SOD1(G93A) mice

We next reanalyzed hindlimb muscle denervation patterns in SOD1(G93A) mice as a function of age, relating these patterns to the distribution of muscle subcompartments, and the numbers of motor nerves in corresponding intramuscular nerve branches. We found that disease induced two temporally well-defined episodes of axon losses in muscle, and that muscle subcompartments could be assigned to one of

three distinct classes (Class-1, -2, -3), which differed dramatically in their patterns of denervation (Fig. 2b). In Class-1 subcompartments (in LGC: l1, m3; in TA: skin-oriented subcompartment), all NMJs became abruptly and permanently denervated between P48 and P52, and all large MN axons in intramuscular nerve branches (see Methods) were lost between P50 and P55 (Fig. 2a-c; Class-1 subcompartments were also identified in MGC, rectus femoris and vastus lateralis (not shown)). In Class-2 subcompartments (LGC: i3, m1), a fraction of intramuscular nerves was lost permanently between P50 and P55 (Fig. 2c). NMJs that became denervated between P48 and P55 were reinnervated in part at P60, but this innervation was not stable (Fig. 2c), and a second episode of abrupt denervation between P80 and P90 led to a permanent loss of axons and innervated NMJs in Class-2 subcompartments (Fig. 2b,c). Defined fractions of axons were also permanently lost during the first (P50-55), and second (P80-90) episode of axon loss in Class-3 subcompartments (LGC: l2, i1, i2, m2; Fig. 2b, c). However, although we did detect significant fractions of denervated NMJs between P48 and P55, there was little detectable denervation from P60 to P120, and only little denervation up to the terminal phase of disease, suggesting that resisting axons in Class-3 subcompartments efficiently and stably reinnervated NMJs through collateral sprouts (Fig. 2c).

Taken together, these results would be consistent with the existence of three types of hindlimb MUs, which would differ in their distribution among muscle subcompartments, and with respect to vulnerability to disease progression in this animal model of FALS: Class-1 subcompartments would be exclusively innervated by the most vulnerable MNs (first denervation episode), and only Class-3 subcompartments would also be innervated by resistant MNs. We next determined whether there might be a relationship between functional subtypes of MUs (Burke, 1994) and denervation in the SOD1(G93A) model.

Synchronous peripheral pruning of FF, and then FR MN axons in SOD1(G93A) mice

To determine whether MU subtypes, as defined by their vulnerability to the disease process, might reflect known subtypes of MNs as defined by physiological properties (Burke, 1994), we compared the distribution of muscle fiber subtypes to that of the subcompartments (see Methods). This analysis was based on the fact that MNs of any subtype (fast-fatiguable (FF), fast-fatigue resistant (FR), slow (S)) exclusively innervate muscle fibers of their own subtype (FF: type-IIb; FR: type-IIa: S: type-I). We found that Class-1 subcompartments were devoid of type-I or -IIa muscle fibers, and were thus exclusively innervated by FF MNs (FF/-/-; Fig. 3a,b). Class-2 subcompartments contained type-IIb and type IIa fibers, but were devoid of type-1 muscle fibers, and were thus innervated by FF and FR, but not S MNs (FF/FR/-; Fig. 3b). In contrast, Class-3 subcompartments were all partially innervated by S-type MNs ((FF)/FR/S; Fig. 3b). Soleus (SOL), which exhibited no denervation or nerve losses before P85-90 lacks IIb muscle fibers, and is thus exclusively innervated by FR and S MNs (-/FR/S). These relationships between patterns of denervation and MU subtype distributions were found in all hindlimb muscles analyzed in this study (LGC, SOL, TA (Figs. 2c, 3b), MGC, gluteus maximus, vastus lateralis, rectus femoris (not shown)).

It is well established that muscle fibers reinnervated by collateral sprouts are converted to the subtype of the reinnervating MN, a process leading to muscle fiber type grouping after nerve injury and in disease (Burke, 1994). Accordingly, to provide direct evidence that it is specifically S MNs that resist and compensate through sprouting and reinnervation of vacated NMJs, we analyzed type-I fiber contents (MHC type-1 positive fibers) as a function of disease state. We found that in LGC subcompartments i1 and i2 (Class-3) of SOD1(G93A) mice, median type-I fiber contents were 8-9% at P50, 35-55% at P70, and 76-90% at P100 (N=3 mice), whereas no MHC type-I positive fibers appeared in Class-2 and Class-1 subcompartments at any stage of disease. In control experiments, no age-dependent alterations in type-I fiber contents were detected in Class-3 subcompartments of wildtype mice (contents in i1/2 were 8-9% at 2 and at 10 months).

We conclude that in SOD1(G93A) mice, FF MNs innervating hindlimb muscles abruptly disconnect their peripheral synapses at P48-52, and loose their intramuscular nerve branches at P50-55 (first loss episode). FR MNs innervating the same muscle subcompartments initially sprout to partially reinnervate NMJs on IIb muscle fibers, but are decreasingly competent to maintain additional NMJs, and prune their intramuscular nerve branches at P80-90 (second loss episode). In contrast, S MNs compensate efficiently through sprouting, and continue to maintain greatly expanded MUs up to the time when mice die.

Selective vulnerabilities to disease of FF and FR MN axons

To determine whether the early selective vulnerability to disease of FF MUs was due to a property of the presynaptic FF MNs or of the postsynaptic IIb muscle fibers, we carried out cross-innervation experiments in SOD1(G93A) mice, in which we forced soleus MNs to innervate TA muscle (see Methods). These surgeries were carried out at P55, when all innervation to the 2/3rd of TA facing skin has been lost (Class-1 subcompartment), innervation of the remaining 1/3rd of TA was maintained by FR MNs (Class-2 subcompartment), and no nerve losses were detected in soleus (Fig. 2c). We found that soleus MNs stably innervated NMJs on TA in a pattern that did not depend on whether crossinervation was carried out in wild type or SOD1(G93A) mice, and that this pattern had no resemblance to that of the residual innervation in contralateral MN disease TA (Fig. 4a).

Next, to determine whether selective axonal defects can also be detected in the absence of contact to muscle, we carried out crush-reinnervation experiments at times preceding the denervation episodes. We found that sciatic nerve crush at P30 led to undistinguishable reinnervation of hindlimb muscles in wildtype and SOD1(G93A) mice at P37 (Fig. 4b). In contrast, when nerves were crushed at P38 (i.e. before disease-related denervation), no axons reinnervated Class-1 subcompartments, whereas nerves did reinnervate Class-2 subcompartments (Nguyen et al., 2002) (Fig. 4b). The results thus reveal a selective reinnervation deficit in FF axons from P38-45 on, i.e. 6-

12 days before denervation. Crushing of peripheral nerve at P60, long before denervation of Class-2 subcompartments, revealed a marked delay in peripheral nerve regeneration (Fig. 4c), and greatly reduced reoccupation of NMJs by regenerating axons, which were more pronounced for Class-2 than Class-3 subcompartments (Fig. 4c-e). The reinnervation deficits did not reflect impaired transmitter release at vulnerable axons, as reoccupation of NMJs by regenerating axons in wildtype mice was not affected by Botulinum toxin A, which suppresses calcium-induced secretion (Fig. 4b). Taken together, these results provide evidence that the patterns of denervation in FALS mice reflect selective vulnerability properties of the corresponding presynaptic MN axons, not their target muscles, nor their peripheral synapses.

Axonal vulnerability involves synaptic vesicle stalling and depletion

To investigate the targets of selective vulnerability in FF and FR MN axons, we searched for early signs of selective axonal transport impairments, which have been linked by previous studies to early vulnerability in motoneuron diseases (Collard et al., 1995; Zhang et al., 1997; Williamson and Cleveland, 1999; Jablonka et al., 2004). We found synaptic vesicle (SV) accumulations paired to low diffuse axonal SV signals, i.e. the characteristic signs of SV stalling within intramuscular nerve branches in Class-1 subcompartments (Fig. 5a). These axonal deficits were first detectable from P35-38 on, and their distribution was well correlated with that of FF MN axons (affected axon (clumped SV signal) fractions in SOD1(G93A) mice at P38: >90% in subcompartment l1, 46-62% in subcompartment l2, 0-3% in soleus (N=3 mice); no comparable clumping was detected in subcompartment l1 of wild-type mice).

To determine how the early and selective defects in axonal SV transport relate to selective losses of peripheral synapses and intramuscular axon arborization in disease, we analyzed the distribution of presynaptic components at NMJs as a function of subcompartment and age in SOD1(G93A) mice. We found that NMJs in Class-1 subcompartments lost all detectable SVs (detected with the three distinct markers SV2, Synaptophysin and Synapsin I) between P38 and P46, i.e. 4-10 days before denerva-

tion (Figs. 5b, c), whereas the presynaptic active zone component Synthaxin-1b was lost together with presynaptic nerve (Fig. 5b). In addition, SV depletion from NMJs tended to be more advanced towards skin-facing parts of muscle subcompartments. In one set of experiments (N=3 mice), NMJs in TA (third facing skin) with detectable SV signal (SV2) at P46 were 3/500 (SOD1(G93A)), versus 474/500 (wild-type littermates). Analysis of NMJs during the naturally occurring process of synapse elimination did not reveal an early loss of SVs in retracting nerves and bulbs (not shown). Likewise, developmental pruning of axons is not preceded by SV depletion, and when peripheral nerves were crushed in adult wildtype mice, or in $Wld^{s/s}$ mice with retarded Wallerian degeneration, no early loss of SV signal from NMJs was detected (not shown). These results thus suggest that although its final outcome resembles developmental or lesion-induced pruning, the "dying back" process in the FALS model is specifically associated with a selective vulnerability of axonal transport first in FF and then in FR axons, leading to SV stalling and loss from NMJs. Neither impaired reinnervation following nerve crush (Fig. 4b) nor synaptic vesicle stalling were detectable in FF axons before P35-38, or in FR axons before P55-60, suggesting that these age windows might coincide with the onset of MN axon vulnerabilities, i.e. the times at which defined axon subtypes become impaired by disease in this FALS model.

Comparable phases of axonal vulnerabilities in distinct models of FALS

To determine whether and to what extent the characteristic patterns and time-courses of axonal vulnerability in SOD1(G93A) mice might generalize to mouse models of FALS, we next analyzed muscle innervation in SOD1(G85R) (line 148) transgenic mice. This model differs from its SOD1(G93A) counterpart in two important ways: 1) disease is caused by a SOD1 mutant with significantly different stability and toxicity properties; 2) disease onset is greatly delayed, i.e. SOD1(G85R) mice exhibit axonal and astrocytic pathology at ca. 6.5 months, clinical onset at 7.5 months, and end-phase at 9.5 months, whereas the corresponding ages for SOD1(G93A) mice are 1.75

months, 2.5 months, and 4.5 months. We found that at 6.5 months the SOD1(G85R) line exhibited triceps surae innervation patterns closely comparable to those of SOD1(G93A) mice at P85-90, including a complete loss of FF motor axons, of most FR axons, and of synaptic vesicles from residual innervated NMJs in Class-2 subcompartments, combined with a good preservation of Class-3 subcompartment innervation (Fig. 6a, b). In striking contrast, only 40 days earlier (i.e. at 5 months) SOD1(G85R) triceps surae muscles exhibited no denervation, no axon loss, and only a mild disruption in the occupancy of NMJs by synaptic vesicles in Class-1 subcompartments (Fig. 6a-c). Therefore, in spite of distinct SOD1 mutations and very different disease onset times, the patterns and time courses of selective peripheral losses are very similar in SOD1(G93A) and SOD1(G85R) mice: the two models of FALS thus differ in the durations of their pre-axonal-vulnerability phases, but then exhibit closely comparable phases of selective MN axon vulnerabilities leading to paralysis and death.

We also analyzed triceps surae innervation patterns in homozygous *pmn/pmn* mice, a juvenile and particularly aggressive form of MN disease unrelated to FALS, and involving a mutant tubulin chaperone. These mice are symptomatic at P15-17 and reach end-stage at P30-40. We found that in early symptomatic P12 or P17 *pmn/pmn* mice, many NMJs (15-60%, depending on subcompartment and position along bone-skin axis) in Class-1 and Class-2 subcompartments were denervated, no motor nerves of normal thickness were present in intramuscular nerves, and all innervated NMJs were reinnervated by sprouts (thin nerves, partial occupancy, escaped sprouts) (not shown). In contrast, Class-3 subcompartments and soleus still contained thicker motor nerves, and their numbers were consistent with them being S-MN axons (soleus: 8-10; LGC i2: 1-2). The mice also exhibited signs of partial synaptic vesicle depletion at NMJs of Class-1 and -2 subcompartments, but normal synaptic vesicle accumulation at many soleus NMJs (not shown). Selective denervation by FF and FR axons in *pmn/pmn* mice thus resembles that in the FALS models, but peripheral SV accumulation and reinnervation by vulnerable axons is much more efficient, suggesting that although FF (and FR) axons are again more vulnerable than S axons, the specific process of axonal vulnerability is different in this cell-autonomous model of early-onset MN disease.

CNTF specifically alleviates axonal vulnerability in FALS

MN axons can be partially protected in FALS and *pmn/pmn* mice by intramuscular applications of CNTF (Sendtner et al., 1992) (but not GDNF; Sagot et al., 1998), which preserves retrograde transport and delays disease progression[21]. Consistent with the notion that a defect in axonal transport selectively in FF axons lies upstream of the "dying back" pathology in the MN disease model, we found that daily applications of CNTF (but not GDNF) from P38 to P68 effectively protected FF axons from SV stalling, SV loss, NMJ loss and peripheral pruning (Fig. 7a). Furthermore, CNTF applications from P55 to P80 protected FR MUs by maintaining their expanded size, and the occupancy state of innervated NMJs (fraction of postsynaptic apparatus faced by presynaptic nerve; Fig. 7b). When added at the onset of SV stalling and depletion, CNTF is thus effective in protecting against several aspects of disease-associated vulnerability in FF and FR MN axons, suggesting that CNTF activates processes counteracting the mechanism of axonal vulnerability in FALS.

To investigate candidate targets of CNTF protection, we analyzed the organization of NFs, i.e. the axonal cytoskeletal system that has been causally linked to axonal vulnerability in FALS. To distinguish between axons of distinct vulnerabilities to disease, we used electron microscopy to compare large myelinated MN axons of intramuscular nerve to l1-LGC (purely FF) to those to SOL (FR and S). We found that although bundled NFs were more frequent in SOL nerve (not shown), the average densities of NFs in cross-sections of the two distinct peripheral nerves were undistinguishable in wild-type mice (Fig. 7c). Furthermore, we found no differences between NF organizations and densities of wild-type versus SOD1(G93A) mice at P30 (Fig. 7c). In contrast, NF densities were reduced to 73% of control in SOL nerve axons of SOD1(G93A) mice at P45, whereas those of FF axons were slightly elevated (Fig. 7c). Significantly, treatment with CNTF for 10 days induced a reduction of NF densities to 79% of control at P45 in FF axons of SOD1(G93A) mice, a further reduction of NF densities to 66% of control at P45 in SOL axons, but no differences in the densities of

NFs in either nerve at P30 (Fig. 7c). These findings suggest that resistant SOL axons might adapt to a disease-associated axonal burden at P45 (but not P30) by reducing NF densities, and that CNTF boosts axonal resistance to disease, facilitating NF density reductions in both FF and SOL axons at P45.

To further investigate how CNTF alleviates axonal vulnerability in MN disease, we searched for molecular markers upregulated in MNs at the time of peripheral axon pruning using a microarray approach (see methods; S.S. and P.C., unpublished results). One of the upregulated transcripts coded for Bcl2A1-a, an anti-apoptotic protein that can be upregulated in stressed lymphocytes in response to NF-κB activation. Consistent with a regulation of Bcl2A1-a by stress in MNs, we found that the transcript was transiently upregulated during 2 days in ipsilateral lumbar MNs following sciatic nerve crush (not shown). In situ hybridization and immunocytochemical analysis of SOD1(G93A) spinal cord sections at levels projecting to hindlimb muscles (L3-L5) revealed low signals comparable to wildtype at ages up to P40, but pronounced upregulation in 25-35% of MNs retrogradely labeled from triceps surae muscle at P44, and upregulation in higher numbers of lumbar MNs from P70 and beyond (Fig. 7d; Suppl. Fig. 1). Consistent with upregulation in FF MNs, Bcl2A1-a positive MNs at P44 were particularly prominent in L4/5 lateral pools including early affected TA (Fig. 7d). Daily applications of CNTF unilaterally to hindlimb muscles from P38 on prevented the upregulation of Bcl2A1-a in ipsilateral MNs (Fig. 7d). Therefore, disease-related accumulation of Bcl2A1-a in MNs of SOD1(G93A) mice coincides in time with the depletion of SVs from NMJs, and the application of CNTF to muscle prevents both, SV stalling and depletion in axons, and upregulation of Bcl2A1-a in MN cell bodies. The upregulation of Bcl2A1-a in about a third of triceps surae MNs at P44 might thus reflect the onset of a stress response to axonal vulnerability in FF MNs, and its downregulation by CNTF further supports the notion that CNTF specifically alleviates axonal vulnerability in FALS.

A transition from axonal vulnerability to Lactacystin-sensitive pruning in FALS

To further define the process of axonal vulnerability in FALS, we investigated its relationship to NMJ denervation and peripheral axon pruning. We found that in contrast to earlier applications of the cytokine, CNTF applications initiated at P45 or later, i.e. 4-6 days before the first innervation losses, but when many NMJs were depleted of SVs, were ineffective in preventing the loss of peripheral innervation and intramuscular axons at FF MUs (Fig. 8a). The same regimen of CNTF was however still effective in preventing Bcl2A1-a upregulation in MN cell bodies at P55 (Fig. 8a), suggesting that CNTF from P45 on still counteracted aspects of vulnerability in FF axons, but could not anymore prevent a peripheral pruning process. The swiftness of the selective pruning process in FALS suggested that it might reflect an active mechanism similar to the pruning of axons during development, and in lesioned-induced Wallerian degeneration. Since the latter processes depend on proteasome function, we determined whether the specific proteasome inhibitor Lactacystin, a drug of established effectiveness and specificity in vivo, might interfere with peripheral axon pruning in FALS. We found that daily applications of Lactacystin to triceps surae from P45 on effectively prevented NMJ denervation up to at least P55 (Fig. 8b). In contrast, Lactacystin from P35 or P45 was ineffective in preventing SV stalling and depletion from NMJs, or Bcl2A1-a upregulation in MNs (Fig. 8b). We conclude that CNTF specifically alleviates axonal vulnerability in FALS, but fails to prevent Lactacystin-sensitive peripheral pruning of NMJs and intramuscular nerves late in the vulnerability process. This transition to lack of effectiveness by CNTF might reflect activation of a CNTF-insensitive pruning process at P45, or the peripheral accumulation of axonal damages beyond CNTF-supported axonal repair mechanisms, leading to peripheral pruning.

Discussion

We have provided, for the first time, a quantitative account of identified neuronal circuitry affected during disease progression in a model of a human neurodegenerative disease. The analysis has revealed that the disease phases affecting MNs in FALS can be reduced to a small series of predictable and well-defined axonal vulnerability and pruning processes; exploiting this surprisingly stereotype map of disease progression, we provide novel insights into the mechanisms underlying these diseases. In the following paragraphs we discuss mechanisms of selective axonal vulnerability in FALS, how the distinct vulnerabilities of FF, FR and S axons relate to disease progression, and how these findings can likely be generalized to further major neurodegenerative diseases and their treatment.

The results of this study provide insights into the mechanisms of selective vulnerability in FALS, and their alleviation by CNTF. The close correspondences between the timings of detectable deficits in axonal transport, of selective peripheral axon pruning, and of disease progression phases support the notion that selective axonal vulnerabilities, e.g. in axonal transport are causally related to disease progression in FALS. Our results do not formally discriminate between disease progression models involving distinct progression rates of deficits in FF, FR and S MN cell bodies, versus scenarios involving selective vulnerability to the disease process by the axons themselves. However, by revealing that the subtypes of axons exhibit distinct progressions of CNTF-sensitive axonal deficits during disease, the results are most consistent with an axonal site of selective vulnerability in MN disease. A selective axonal involvement is fully consistent with reports of specific deficits in axonal transport and of axonal dysfunction in MN diseases (Jablonka et al., 2004; Pinter et al., 1995; Sagot et al., 1995; Warita et al., 1999), of selective vulnerability of FF and FR axons to toxic chemicals (Delio et al., 1992), of a causal relationship between deficits in fast axonal transport mechanisms and MN degeneration (LaMonte et al., 2002; Xia et al., 2003; Shah and Cleveland, 2002), and of an axonal site of action for CNTF(De Paola et al., 2003; English, 2003). Should the MN axons indeed be primary sites of selectively vulnerability

to disease, then MN cell bodies might not even be more vulnerable to FALS than other types of neurons in the CNS. Selective axonal vulnerabilities might involve selective primary damages to subtypes of axons, or failure by vulnerable axons to compensate for disease-related burdens. Although these mechanisms are not mutually exclusive, and are both consistent with our findings, we favor inadequate compensation as a critical factor in selective vulnerability. Thus, the detection of disease-related reductions in NF density in resistant SOL but not vulnerable FF axons, and the observation that CNTF stimulates disease-related reductions in both FF and SOL axons are consistent with a scenario in which disease affects all MN axons, more vulnerable axons exhibit less effective adaptive responses, and protection by CNTF specifically involves a boosting of adaptive responses in disease-affected axons. The latter interpretation is consistent with the fact that: 1) CNTF augments protective processes in stressed neurons through phosphorylation of STAT3; 2) that while both GDNF (which was ineffective in protecting axons) and CNTF activate MAP-kinase and PI3-kinase pathways, only CNTF activates protective JAK/STAT pathways; 3) that CNTF prevented the upregulation of the stress-related gene Bcl2A1-a in FALS MNs independent of the peripheral pruning process; and 4) that preventing peripheral pruning with Lactacystin did not affect SV accumulation or Bcl2A1-a upregulation. Recent genetic studies have established that CNTF is not a modifier gene in ALS, suggesting that it is not critical for the activation of protective pathways in FALS. One possible explanation for this finding is that related cytokine-like growth factors such as LIF and Cardiotrophin-1 might produce similar protective effects in MN disease. Alternatively, the gradual nature of the disease progression process and/or a compromised local environment might produce a failure to activate protective cytokine pathways. Finally, the fact that axonal protection with exogenous CNTF delays, but does not prevent disease progression in FALS mice might relate to the existence of further disease-related influences impairing MN function. More effective treatments might therefore need to combine factors boosting axon-protecting pathways such as CNTF with factors alleviating disease-associated toxicities by the microenvironment.

Our results provide evidence that in FALS mice FF axons in the hindlimb are affected selectively, synchronously and early on, leading to an abrupt loss of their peripheral synapses and intramuscular arborization. These selective and complete losses of innervation in exclusively FF subcompartments are of potential value as diagnostic tools. That they have not yet been detected clinically is likely due to the specific recruitment of FF MUs only for brief tasks requiring extreme force (Burke, 1994). Where present, FR axons in the same subcompartments can compensate to a limited extent through sprouting and reinnervation initially, although they then weaken progressively, and prune their peripheral arborization when clinical symptoms are first detected in FALS mice. Compensation by FR axons in Class-2 subcompartments (FF/FR/-) does not appear to be a decisive factor contributing to their weakening in disease, since in soleus muscle (-/FR/S), which does not exhibit denervation at P50-55 (SOD1(G93A) mice), the phase of FR axon pruning is also taking place at P80-90. In contrast to axons of phasic MNs, axons of S MNs are particularly resistant to disease: they compensate efficiently, and maintain expanded MUs up to the final phase of disease. However, delayed regeneration after nerve crush, and a slowly progressing reduction in the innervation extent of Class-3 subcompartments late in disease suggest that, albeit to a much lesser extent, S MN axons are also vulnerable to disease. Taken together, our results thus suggest that in MN disease the onset of the clinical phase coincides with the weakening and loss of FR innervation, and the progressive weakening of S MN axons determines clinical progression during the end-phase of the disease. The very similar patterns and time courses of selective axonal vulnerabilities in SOD1(G93A) and SOD1(G85R) mice suggest that the disease processes in the different forms of SOD1-related FALS converge onto a shared final pathway of selective axonal vulnerabilities by MN subtypes, leading to paralysis and death. Consistent with the results of recent studies, differences in the onset times of FALS might thus reflect distinct toxicities of disease-causing mutants towards cells in the local environment of MNs, upstream of conditions affecting MNs and their axons.

This study identifies physiological subtypes of related neurons and axons differing in their vulnerability to disease, suggesting that differences among these neurons (Burke, 1994; Raoul et al., 2002) are critically important to disease progression. Selective vulnerability by FF and FR MN axons is consistent with clinical observations on ALS and post-polio syndrome patients (Dengler et al., 1990; Larsson et al., 1995). FF MN axons exhibit the largest diameters, and innervate the largest numbers of muscle fibers among α-MNs (Burke, 1994). These large sizes might result in higher demands on axonal transport, and higher vulnerability to its dysfunction. However, while axonal neurofilament contents have been linked to axonal vulnerability (Lobsiger et al., 2005), one study has provided experimental evidence against a simple relationship between axonal diameter and vulnerability in disease (Nguyen et al., 2000). A further attractive possibility is that the selective vulnerability of FF (and to a lesser extent FR) MN axons, and the relative resistance of S MN axons might relate to their dramatically different patterns of action potential firing (Burke, 1994) (phasic (FF<<FR) versus tonic (S)). Frequent spiking by tonic MNs might be accompanied by more efficient ion and energy homeostasis mechanisms in their axons. Accordingly, factors affecting the selective vulnerability of phasic MN axons might include mitochondrial functions (Liu et al., 2004; Pasinelli et al., 2004; Wong et al., 1995; Kong and Xu, 1998), and the homeostasis of energy and ions in the axon (Shaw and Eggett, 2000; Palecek et al., 1999; Kuo et al., 2004), upstream of axonal transport.

Finally, the available evidence from previous studies is consistent with the possibility that the principles of selective axonal vulnerabilities and disease progression uncovered by this study might apply to further major neurodegenerative diseases associated with early axonopathy. Thus, in addition to further forms of MN disease (Frey et al., 2000; Sagot et al., 1995; De Paola et al., 2003), Alzheimer's, Parkinson's and Huntington's disease have also been linked to early defects in axonal transport (Stokin et al., 2005; Gunawardena and Goldstein, 2005) and early losses of synapses (Walsh and Selkoe, 2004; Coleman and Yao, 2003). Indeed, investigations of pathogenic mechanisms in Drosophila models have provided evidence that loss of huntingtin, overex-

pression of polyQ proteins, or overexpression of amyloid precursor protein mutants all specifically induce disruptions of axonal transport (Gunawardena and Goldstein, 2001; Gunawardena et al., 2003). Detailed investigations of axonal circuitry affected in other animal models of neurodegenerative disease might therefore uncover shared principles of selective vulnerability, as well as early markers of disease progression. With respect to clinical implications of these findings, the association of distinct axonal compartments with early vulnerability and with resilience to disease, points to therapeutic strategies aimed at boosting the resistance and repair potential of more resistant axons during early clinical phases of disease, using axon-protecting factors such as CNTF. Currently available evidence suggests that such therapeutic strategies might be effective in many different neurodegenerative diseases that target axons.

Methods

Labeling and histology procedures

Mice overexpressing high copy numbers of human SOD1(G93A; Gurney et al., 1994) associated with familial ALS were obtained from Jackson Laboratories. These mice tend to lose transgene copies across successive generations, leading to unpredictable slowing down of disease progression. Because a predictable time course of disease progression was essential to this study, we routinely verified that mice included in the analysis did exhibit denervation and/or SV loss patterns as predicted by their age, and replaced mutant mice stocks all 8-12 months.

We monitored the outlines of individual MNs using transgenic mice overexpressing membrane-targeted mGFP in few neurons (Thy1-mGFP^{s}; De Paola et al., 2003). For some experiments, we visualized synaptic vesicles using Thy1-spGFP^{mu} transgenic mice (De Paola et al., 2003), overexpressing a synaptophysin-GFP fusion protein in most neurons. For whole mount analysis of innervation patterns by individual MNs, muscles from Thy1-mGFP^{s} mice were briefly fixed (3.5% formaldehyde in PBS,

30min, room temperature), washed, counterstained with RITC-α-Bungarotoxin (2μg/ml) to visualize postsynaptic AChRs, and imaged in PBS. Confocal images were acquired using an Olympus (BX61) confocal microscope and Fluoview 4.1 software. To analyze thicker muscles (e.g. LGC) along their entire bone-to-skin axis, muscles were partitioned into 2-3 longitudinal sections using a surgical scalpel.

Intramuscular nerves and their NMJs were analyzed using a combined silver-esterase reaction[5]. Histology was carried out on 50 μm cryostat sections; section planes and orientation landmarks for the analysis of triceps surae muscles were as described (Frey et al., 2000).

For immunocytochemistry, cryostat sections were mounted on gelatin-coated glass slides, postfixed for 10 min in 4% paraformaldehyde at RT, and permeabilized in PBS, 1% Triton X-100, 4% BSA (1h, RT). Antibody incubations were carried out in PBS, with 0.3% BSA and 0.1% Triton X-100. The antibodies were: rabbit-anti-synapsin I (Calbiochem), rabbit-anti-synaptophysin (DAKO), SV2 monoclonal (Developmental Studies Hybridoma Bank), mouse-anti-neurofilament-160 (Sigma), rabbit-anti-synthaxin1B (Synaptic Systems, Goettingen). Monoclonal antibodies against myosin heavy chain isoforms IIb, IIa and I were from Sigma (F3, D9, D5), and labeling involved an additional digestion step after postfixation with 0.1% trypsin in PBS (3min, room temperature), followed by permeabilization with 0.5% NP40. In double-labeling experiments, we verified that antibodies to SV components and spGFP transgene all yielded undistinguishable patterns of losses and partial NMJ occupancies in the disease model.

Analysis of innervation patterns

For the analysis of neuromuscular innervation and muscle fiber composition on longitudinal cryostat sections of muscle, LGC subcompartments and their boundaries were identified as follows. Compartment boundaries were readily defined through the arrangement of tendon material and the turning points of the synapse-rich band on longitudinal sections[5] (see Fig. 1a). Within the 3 LGC compartments, the relative posi-

tions of subcompartment boundaries were defined using Thy1-mGFP^s whole mounts (see Fig. 1b, c). These positions varied significantly depending on the relative position along the skin-to-bone axis of LGC. Consequently, all LGC muscles were mounted and sectioned with their bone-facing surface at the bottom of the block[5], all muscle sections were collected for histology, and most of the analysis was restricted to sections within the 65-85% range of muscle along the skin-to-bone axis (skin level set as 0%), where subcompartment boundary positions did not vary significantly. In addition, this range of muscle was most representative of innervation status, since it included arborization by all LGC MUs. Within this range of muscle, the l1/l2 boundary was at 58% of the lateral compartment (lateral muscle edge: 0%), the i1/i2 and i2/i3 boundaries were at 32% and 68% of intermediate compartment (edge adjacent to lateral compartment: 0%), and the m1/m2 and m2/m3 boundaries were at 35% and 62% of medial compartment (edge adjacent to intermediate compartment: 0%). Finally, unlike those of compartments, subcompartment boundaries include a zone of innervation overlap between adjacent MN subpools. Consequently, to avoid ambiguities due to this overlap, a muscle width of 6% (3% each side of the medial subcompartment boundary) was excluded from the analysis.

Numbers of myelinated (thick) axons in intramuscular nerve branches were derived from silver-esterase preparations, in which labeled axons could be followed throughout the thickness of the section (20x objective and bright-field illumination). The analysis was based on the observation that in whole mount preparations from Thy1-mGFP^s mice with several mGFP-positive MNs in an individual subcompartment, individual MNs extended their axons into most (consistently >90%) subcompartment nerve branches. Sprouts and most sensory nerves yielded thin silver-stained profiles, which were excluded from the analysis. Rare sensory nerves to muscle spindles were thickest, were apparently not altered in disease, and were excluded from the analysis when unambiguous identification (diameter or tracing to a spindle) was possible. Individual values were derived from nerve branches along which axon numbers could be derived at 2-3 distinct positions, with closely comparable outcomes; the higher of these 2-3 values was retained. Nerve branches with substantially lower axon counts (less than

20% of total) were excluded based on the assumption that they reflected nerves not entirely included inside the sections. In general, these counts yielded remarkably comparable values among different sections and mice (Figs. 1d, 2c, 6b). Innervation patterns in disease changed abruptly across subcompartment boundaries, greatly facilitating the analysis.

To estimate total numbers of MUs innervating defined subcompartments (e.g. Fig. 1e), we combined the information about the total number of putative motor axons inside intramuscular nerves, the extension of any MU through the bone-to-skin axis, and the fraction of postsynaptic AChRs innervated by any individual MN (total AChR clusters/number of clusters innervated by one MN; total of 126 individual LGC MUs analyzed in this study; see Fig. 1d). Because MUs either extended throughout the bone-to-skin axis, or through approximately 2/3rd of its extension, values for total numbers of nerves inside the middle third of muscle usually yielded good estimates for the total number of MUs (Figs. 1d,e). Likely due to a lower frequency of Thy1-driven transgene expression in S-type MUs (A.F.S and P.C., unpublished results), these comparisons yielded best matches for subcompartments devoid of S-type MUs. MU size values in LGC ranged between 240 innervated NMJs for the largest MUs (in l1) to 25 innervated NMJs for the smallest ones.

Percentages of NMJs innervated only partially (Fig. 6b) were defined as fractions of innervated AChR clusters in which SV labeling was absent from at least a third of the AChR-positive area (see examples in Fig. 4e).

In vivo experiments

For crossinervation experiments, the nerves to TA and soleus were exposed and cut to maximize the lengths of the distal (to the host muscle, about 2 mm) and proximal nerve stumps (from the donor motor pool). The opposite stumps (donor distal, host proximal) were plugged close with glue (Histoacryl; B. Braun, surgical). To ensure reliable innervation of host nerve stump by donor axons, the corresponding nerves were positioned facing each other, and fixed to muscle with a small amount of

Histoacryl applied some distance away from the stump end. By using this procedure we achieved reinnervation of TA NMJs by about 3 weeks after the surgery in more than 2/3rd of the mice. The innervation state of TA NMJs was then analyzed on cryo-stat sections (cut perpendicular to the bone-to-skin axis) using neurofilament plus SV2 labeling for nerve, and RITC-α-Bungarotoxin for synaptic sites. Due to a disease-associated impairment to regenerate FF (and FR) axons (Fig. 4b, c), and technical difficulties associated with carrying out cross-innervation experiments in young (<P25) mice, reciprocal cross-innervation experiments involving TA nerve and soleus muscle have not been included in the analysis.

For crush-reinnervation experiments, the sciatic nerve was crushed at mid-thigh level, and reinnervation of LGC subcompartments was assessed as described for cross-innervation experiments. In some of these experiments, in order to prevent transmitter release by reinnervating axons, ipsilateral calf muscles were treated with two local applications of Botulinum toxin A (Allergan AG, Lachen, Switzerland; 0.02 U/g body weight), 4 and 6 days after the nerve crush surgery.

CNTF (Sigma rat recombinant protein) or GDNF (Sigma human recombinant protein) were reconstituted with 0.1%BSA/PBS (working solutions: 1 μg/ml);100 μl of this solution were injected into triceps surae, and 50 μl into TA every second day.

Acknowledgments

We are grateful to C. Schneider for excellent technical assistance, and to Silvia Arber (FMI and Biozentrum, Univ. of Basel) for valuable comments on the manuscript. The Friedrich Miescher Institut is part of the Novartis Research Foundation.

12.4 Figure legends

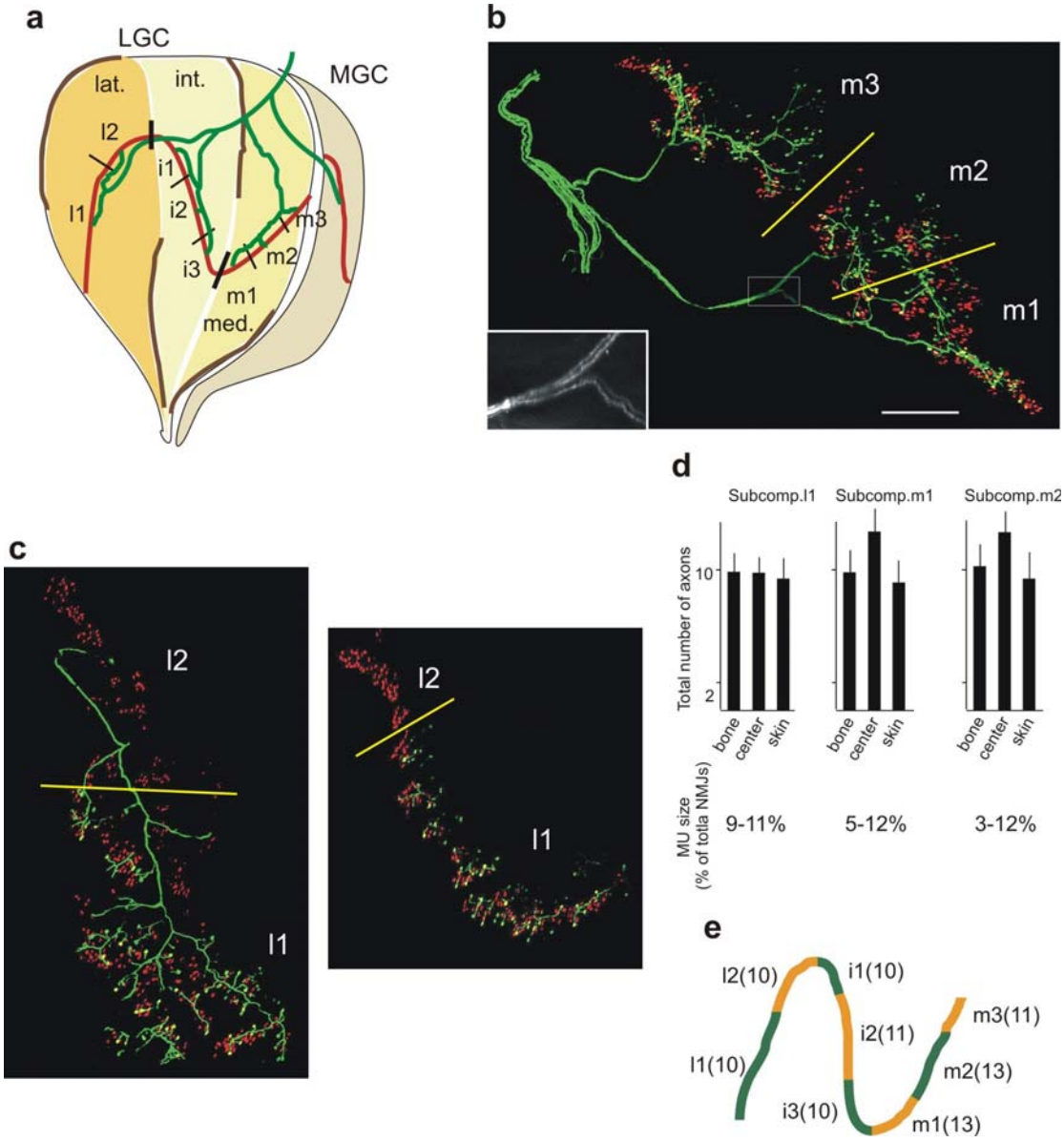

Figure 1

Quantitative topographic map of the MUs innervating the LGC muscle in the mouse. **a**, Schematic of nerves (green), NMJs (red), compartments (colored surfaces) and sub-compartments (labels along synaptic band) in mouse LGC. **b,** Arborization pattern of axons innervating the medial compartment of LGC. Whole mount preparation from Thy1-mGFP^{s} transgenic mouse (Clement et al., 2003) , expressing mGFP (green) in few MNs, and counterstained with RITC-α-Bungarotoxin to visualize NMJs. Axon bundles branch out from LGC/SOL nerve (left), to innervate subcompartments m3,

m2 and m1 (boundary regions indicated by bars). Individual axons project to only one subcompartment (inset: branch point to m2/m1 (4 axons before branch point, 2 axons each to m2 and m1). Bar: 1 mm (a,b). **c**, Arborization pattern of one axon innervating subcompartment l1 of LGC; the two panels show its entire projection within the half of LGC-l facing bone (left) and facing skin (right). **d**, Average number of silver esterase-stained axons in intramuscular nerve branches (top; N=60 nerves, from 4 mice), and range of MU sizes (fraction of total NMJs innervated by individual mGFP-positive axons) in LGC subcompartments. **e**, Schematic of LGC subcompartments, with corresponding total numbers of MUs.

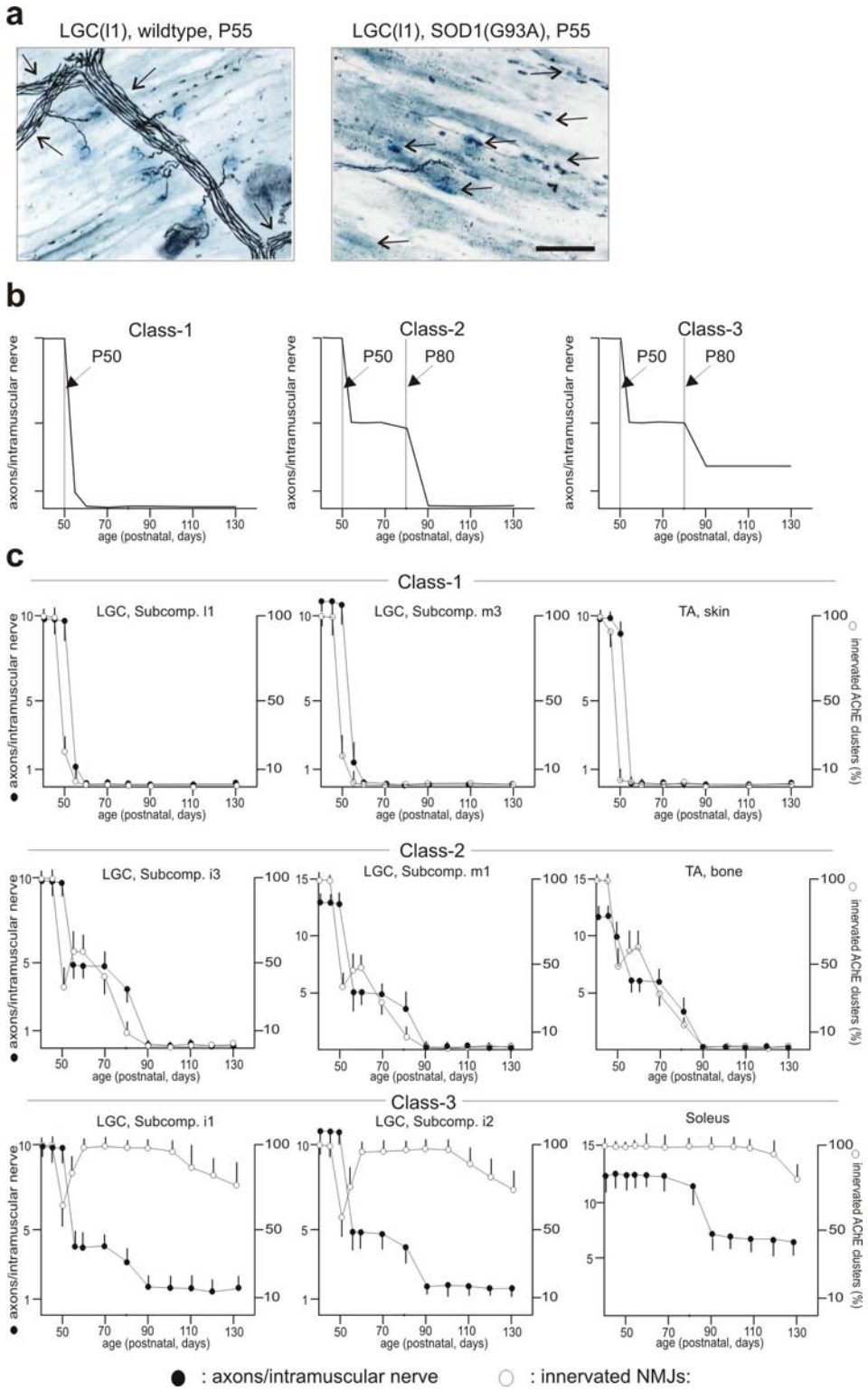
a
LGC(I1), wildtype, P55
LGC(I1), SOD1(G93A), P55
b
Class-1
Class-2
Class-3
P50
P80
axons/intramuscular nerve
age (postnatal, days)
c
Class-1
LGC, Subcomp. I1
LGC, Subcomp. m3
TA, skin
Class-2
LGC, Subcomp. i3
LGC, Subcomp. m1
TA, bone
Class-3
LGC, Subcomp. i1
LGC, Subcomp. i2
Soleus
innervated AChE clusters (%)
● : axons/intramuscular nerve
○ : innervated NMJs:

Figure 2

Analysis of subcompartment denervation patterns in hindlimb muscles of SOD1(G93A) mice reveals grouping into three distinct classes. a, Intramuscular nerves (arrows left, consisting of axon (black) bundles) and postsynaptic sites (Acetylcholine esterase, blue) in LGC subcompartment l1 of wild-type and SOD1(G93A) mouse at P55. Note complete denervation (arrows right) and absence of thick motor axons in the mutant mouse. Bar: 100 µm. **b,** Schematic of intramuscular axon loss patterns for Class-1, -2 and-3 subcompartments as a function of age in SOD1(G93A) mice. **c**, Axon numbers in intramuscular nerve branches (filled circles) and innervated synaptic sites (empty circles) as a function of age in individual Class-1, -2 and -3 subcompartments. For LGC, the analysis was restricted to silver-esterase processed sections from the central third along the bone-to-skin axis; TA: third facing skin or bone. N=3 mice, 45 intramuscular nerves, 450 AChE sites.

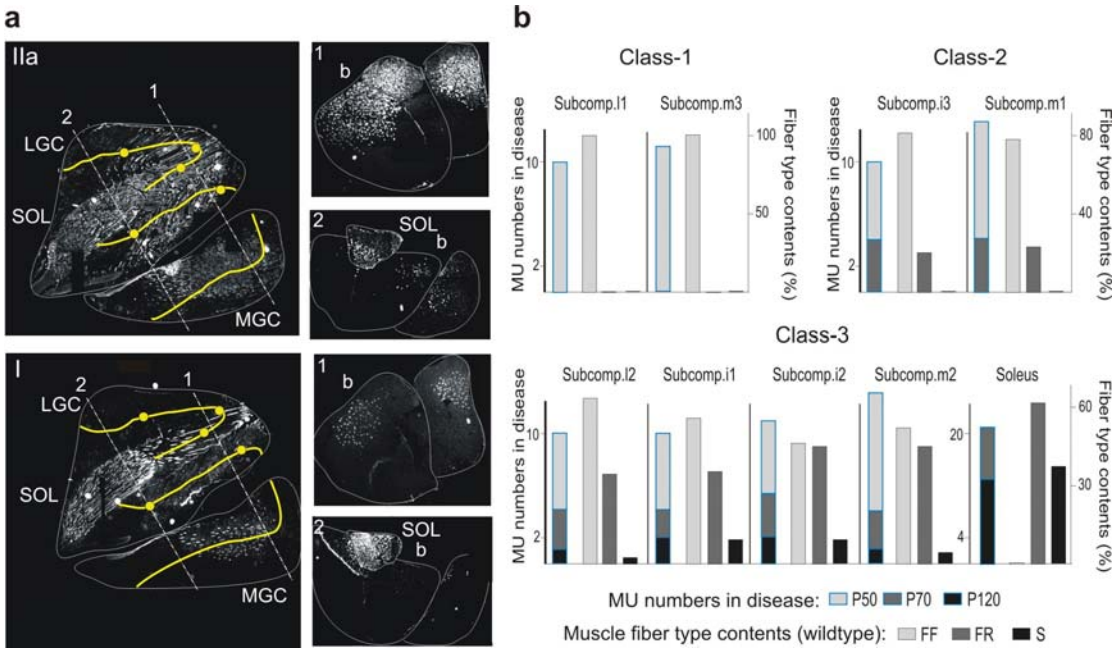

Figure 3

Identification of MN subtypes vulnerable and resistant to axon pruning in SOD1(G93A) mice. a, Distribution of type IIa (innervated by FR MNs) and type I (innervated by S MNs) muscle fibers in LGC, MGC and SOL muscle. The longitudinal sections on the right (parallel to bone) are from the bone-facing third of the muscle

group. Yellow line: position of synaptic band; yellow dots: approximate position of subcompartment boundaries. Dotted lines (1,2) indicate the positions of the vertical sections shown in the right panels (b: bone-facing side). The white lines highlight the borders of individual muscles. **b**, Axon (MU) numbers as a function of age (left bars, blue outlines), and muscle fiber subtype compositions (bone-facing half) for Class-1, -2 and -3 subcompartments. Class-1: innervation by FF MNs only (no IIa or I fibers); Class-2: innervation by FF and FR MNs (no I fibers); Class-3: innervation by FF, FR and S MNs. Only Class-3 subcompartments with S MUs retain innervation beyond P90.

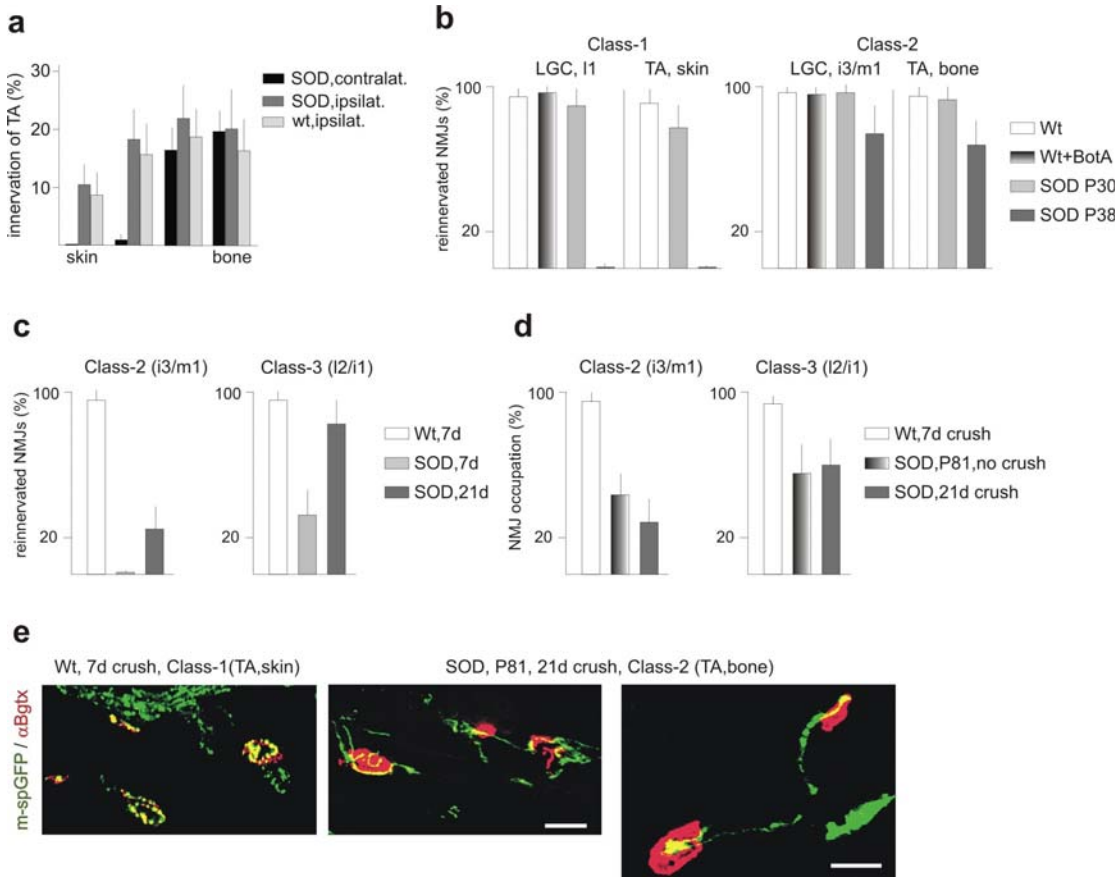

Figure 4

Selective vulnerability of phasic MN axons in disease. a, Selective vulnerability by presynaptic MNs. Crossinervation by soleus MNs in SOD (SOD, ispilat.) and wild-type (wt, ispilat.) mice, versus residual innervation by TA MNs (SOD, contralat.). In-

nervation of synaptic sites in P80 TA muscle along the skin-to-bone axis. N= 60 NMJs, 2 mice. **b,** Competence for reinnervation after axonal crush is lost in parallel with disease-related denervation. Reinnervation in wildtype mice (crush at P38) was not affected by Botulinum toxin A (see Methods). Sciatic nerve crush at P30 led to normal reinnervation of Class-1 subcompartments, whereas no reinnervation was detected upon crush at P38. The reduced reinnervation after crush at P38 in Class-2 subcompartments was likely due to a specific impairment of FF MNs. Reinnervation was assessed 7d after crush; N=150 NMJs from 3 mice. **c-e,** A defect in crushed-induced regeneration and NMJ re-occupancy before denervation in FR MNs of SOD1(G93A) mice. Sciatic nerves were crushed at P60, and reinnervation (**c**, 7d or 21d after crush**)** or occupancy of innervated NMJs (**d,e**) were assessed as indicated. m-spGFP: axonal signal from mouse expressing mGFP and spGFP. N=150 NMJs from 3 mice. Bars: 40 µm.

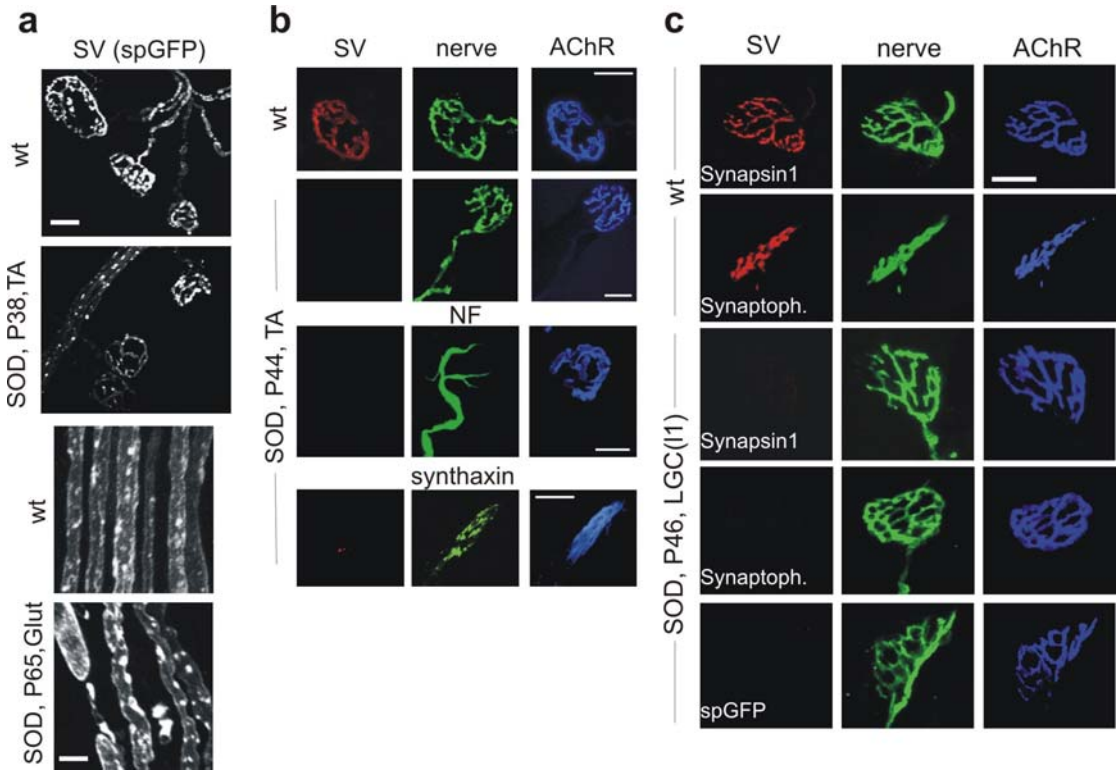

Figure 5

Early stalling and loss of SVs from intramuscular axons and NMJs in MN disease. a, Early SV stalling in intramuscular nerves and at NMJs in SOD1(G93A) mice. Upper panels: TA: skin-facing third of TA muscle (Class-1); lower panels: Gluteus (Class-2 subcompartment); SV: synaptophysin-GFP fusion protein signal from Thy1-spGFP^{mu} mouse (Clement et al., 2003). Note SV accumulations and lower diffuse intra-axonal SV signals, and swellings in some of the intramuscular axons (lower panels) in FALS mice. **b**, SV loss preceding axon loss from synaptic sites of SOD1(G93A) mice. SV: SV2; nerve: mGFP; NF: Neurofilament-160; Synthaxin: synthaxin-1b. **c,** SV loss as detected with integral and SV-associated proteins precedes denervation of NMJs. In the Thy1-spGFP transgenic mice, more than 95% of NMJs exhibited spGFP signals undistinguishable from those of endogenous SV2. Nerve: mGFP (or NF-160 for spGFP mouse). Bars: 20 μm (lower panels in a: 5 μm).

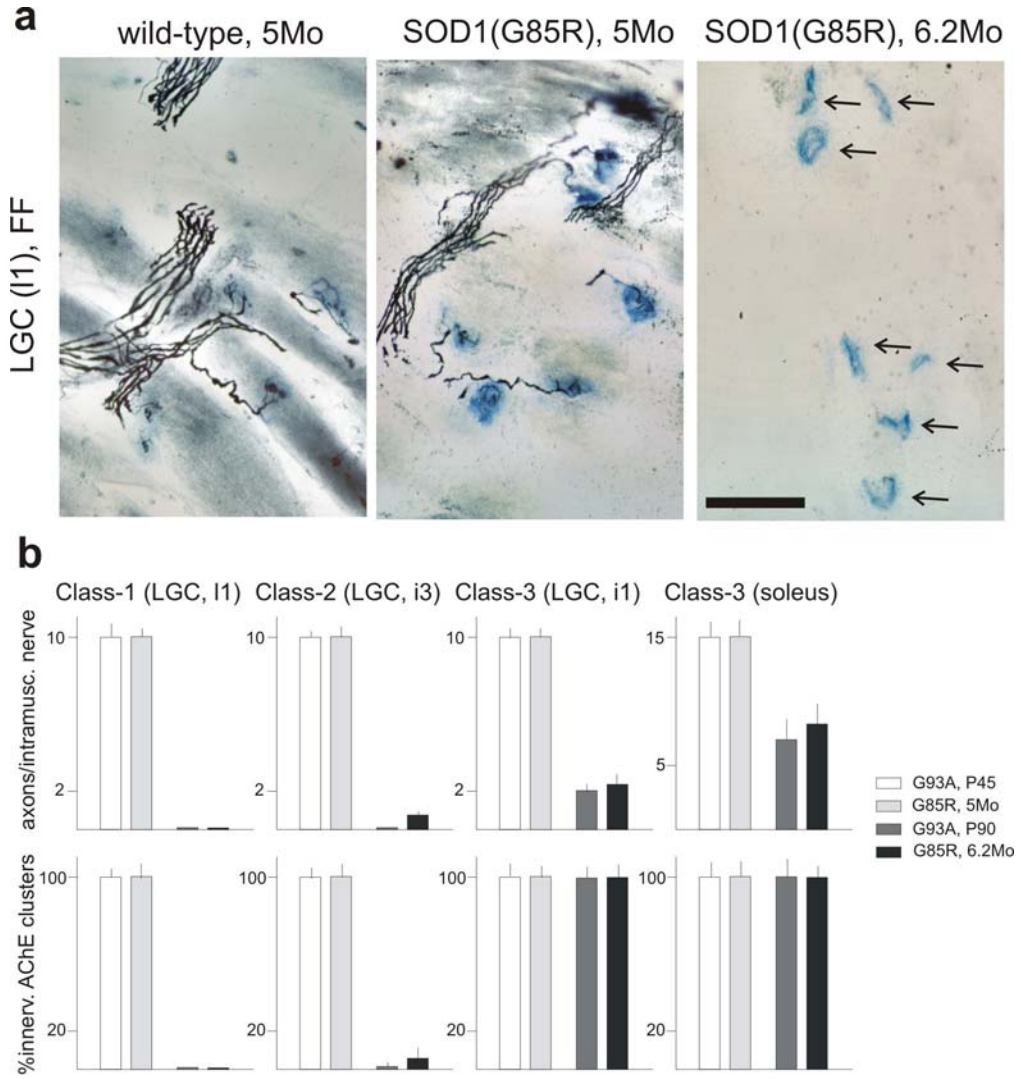

Figure 6

Local applications of CNTF prevent disease-associated SV stalling and peripheral axon pruning. a, CNTF prevents SV loss and pruning of FF MN axons in SOD1(G93A) mice. TA muscle (skin-facing third) at P68; mutant mice were treated with CNTF (SOD,+CNTF) or vehicle (SOD,+veh.) from P38 on. Bar: 100 μm. **b**, CNTF (from P55 on) supports expanded MUs by FR MNs. Analysis at P80; N= 150 NMJs, 3 mice. Fully innervated / total: fraction (%) of innervated NMJs with more than 80% of AChR surface faced by SV signal.

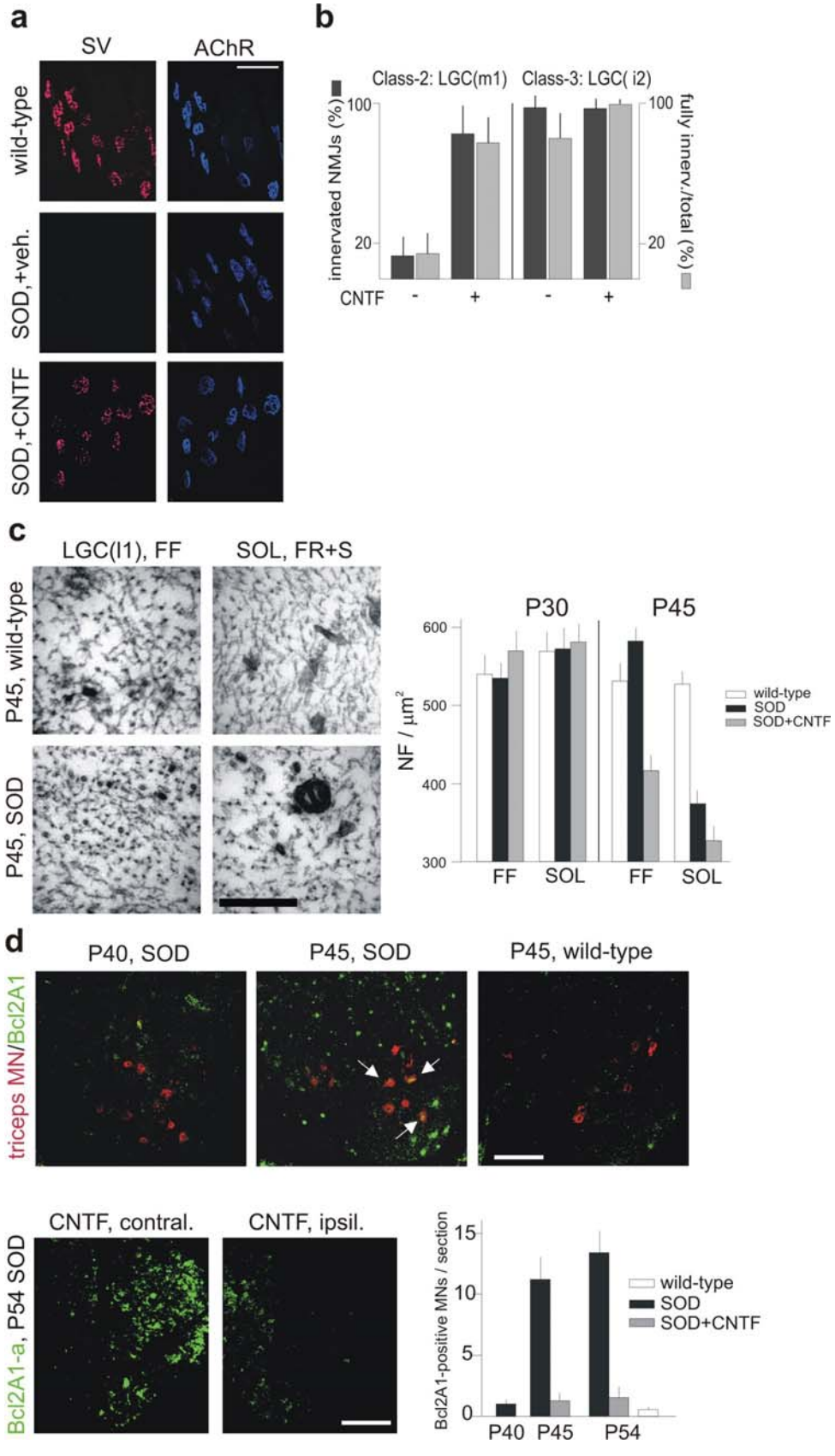
a
SV
AChR
wild-type
SOD,+veh.
SOD,+CNTF
b
Class-2: LGC(m1)
Class-3: LGC(i2)
innervated NMJs (%)
fully innerv./total (%)
100
20
CNTF
-
+
c
LGC(l1), FF
SOL, FR+S
P45, wild-type
P45, SOD
P30
P45
NF / µm²
600
500
400
300
FF
SOL
wild-type
SOD
SOD+CNTF
d
P40, SOD
P45, SOD
P45, wild-type
triceps MN/Bcl2A1
CNTF, contral.
CNTF, ipsil.
Bcl2A1-a, P54 SOD
Bcl2A1-positive MNs / section
15
10
5
0
P40
P45
P54

Figure 7

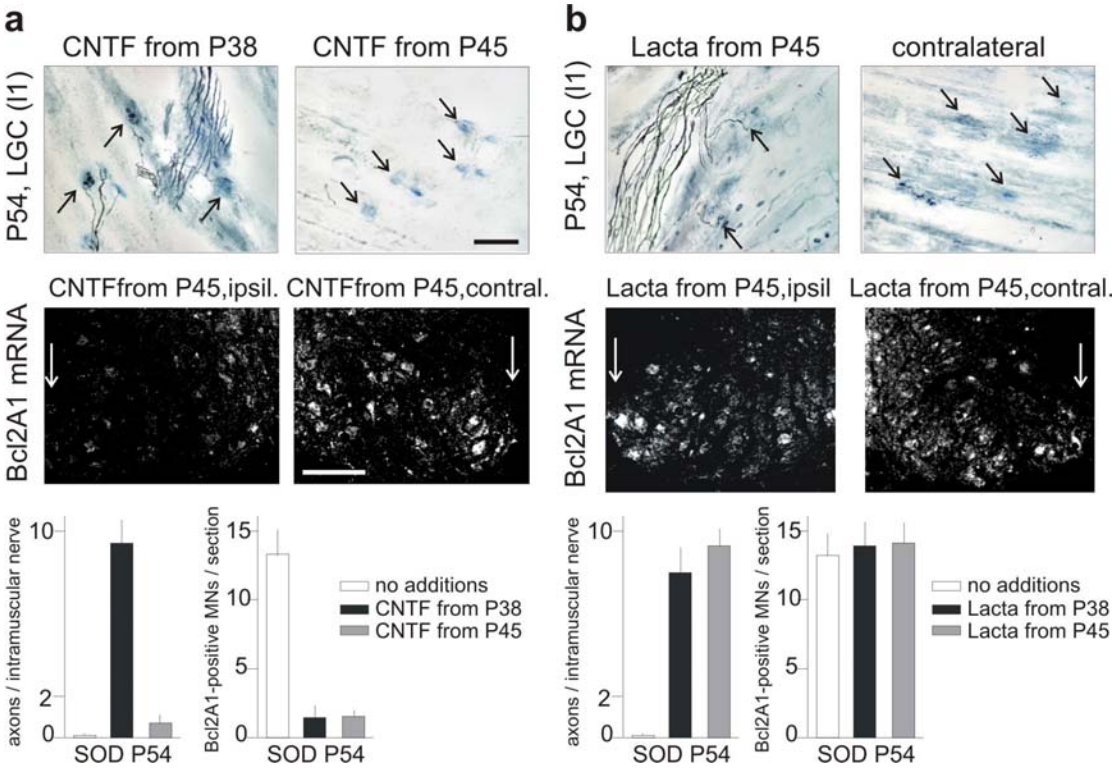

Figure 8

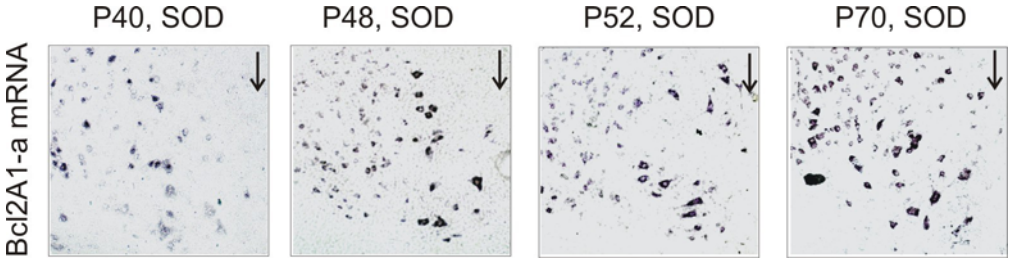

Supplementary figure 1

Chapter 13 - General discussion

13.1 Postsynaptic control of local network connectivity

Results from the analysis of synaptogenesis during development and synaptic plasticity in the adult NMJ show that postsynaptic control of input connectivity is a general feature in the regulation of anatomical synaptic plasticity.

First, the postsynaptic target is pre-patterned for connectivity, since receptor clustering and postsynaptic differentiation can take place in the absence of nerve. Second, patterns of synaptogenesis and adult plasticity are also determined by the postsynaptic target. The muscle fiber is able to control whether synapses will be stabilized or removed depending on the activity input it receives.

By allowing or preventing formation of stable contacts, the muscle fiber is also able to control local growth of the axons. Once a productive contact is established, growth is arrested and the axon processes are contained within the endplate.

A similar model of axon growth and pruning controlled by the production of stable synapses could take place during episodes of network connectivity refinement such as critical periods, or rewiring events occurring in motor cortex after amputations, both types of events being heavily dependent on activity patterns.

Since during adult life synaptic reorganization events are restricted to a subpopulation of labile synapses, mechanisms controlling the creation and maintenance of these synapses could play an important role in defining the long-term cognitive functions of the nervous system.

13.2 Synapse management via regulation of postsynaptic apparatus stability

Control by the postsynapse of synapse management could involve a number of mechanisms, which have been put forward in the past: secretion of growth factors, contact-mediated mechanisms, release of proteases. We found that the ability of the postsynaptic muscle fiber to control axon growth and synapse formation or removal is achieved by modifications in the stability of the postsynaptic apparatus.

DeSyn muscles display anatomical plasticity by destabilizing the postsynaptic endplate, whereas FaSyn NMJs remain stable during paralysis. However, specific destabi-

lization of the postsynaptic endplate (via MuSK siRNA) in FaSyn muscles is sufficient to enable anatomical plasticity.

The changes observed in the organization of the synapse are probably not due to differences in the proteins constituting the postsynaptic complex, but in the regulation of their assembly, distribution and stability. During development, DeSyn and FaSyn muscles show similar patterns of MuSK and rapsyn expression. In both cases the proteins remain tightly co-localized with AChR clusters. During chronic paralysis in the young adult, there are indeed changes in the composition of the postsynaptic cluster, but they do not appear to be specific to DeSyn muscles: rapidly after paralysis, there is an increase in the expression of the α subunit of AChR in both types of muscles.

The mechanism leading to destabilization of the postsynaptic complex assembly during chronic paralysis could be related to maintenance mechanisms observed in development (chapter 10) and tissue culture (annex 1).

The *in vivo* and tissue culture experiments in annex 1 have shown that lipid rafts play an important role in regulating the assembly of the postsynaptic endplate: removal of cholesterol, a major lipid raft component, results in the destabilization of postsynaptic endplate, whereas cholesterol enrichment enhances AChR clusters stability.

Src and Fyn play a key role in the formation of lipid rafts and correct targeting of postsynaptic proteins to the rafts. Src-/-;fyn-/- myotubes have less rafts than wild-type cells, and the post-synaptic proteins are less enriched in lipid rafts. It is not clear weather the effect of Src and Fyn in lipid raft targeting of postsynaptic proteins is specific or a consequence of a lipid raft enrichment. But the finding that cholesterol addition rescued the raft partitioning of AChRs and MuSK in src-/-;fyn-/- myotubes suggests the later possibility.

How do lipid rafts modify the postsynaptic organization and stability? Since the signalling pathways leading to MuSK dependent AChR cluster assembly are independent from those regulating lipid rafts mediated stabilization, and that this effect is independent from lipid raft accumulation at the cell surface, it is possible that lipid rafts could affect the postsynaptic endplate via regulation of protein trafficking to and from the surface. Lipid rafts are present in transport vesicles shuttling from the Golgi apparatus to the plasma membrane (Simons and Ikonen, 1997), and in endocytic vesicles

formed at the cell surface through raft-associated caveolae, which merge with intracellular caveosomes and with endosomes (Pelkmans et al., 2004).
Alterations in lipid raft organization could modify trafficking to and from the postsynaptic endplate, changing the point of dynamic equilibrium in the postsynaptic protein organization and thus altering the postsynaptic endplate stability.

13.3 Role of cell adhesion in anatomical plasticity

Experiments such as *in vivo* knock down of MuSK, but also *in vivo* manipulation of rafts show that the stability of the postsynaptic endplate is crucial in regulating anatomical plasticity. But how could different conditions of postsynaptic assembly affect axon and Schwann cell behavior?
Because the synapse is a tight assembly of cells, adhesion mechanisms could not only provide structural stability but also regulate growth. According to this view, a failure in the capacity of the postsynapse to provide a valid contact target (i.e. ultimately a contact-mediated signal) could release repression of growth in the nerve and Schwann cell.
If the stability of the postsynaptic endplate regulates anatomical plasticity via adhesion mechanisms, direct targeting of adhesion should be sufficient to allow anatomical plasticity.
Analysis of the myd mutants lends support for this view. In myd mice the defective glycosylation of dystroglycan leads to loss of function. Dystroglycan is a key structural component of the postsynaptic endplate. It anchors the postsynaptic cluster to the actin cortex via utrophin and dystrophin, and its extracellular domain binds to ECM scaffolds such as agrin and laminin.
Loss of function of Dystroglycan leads to disorganization of the postsynaptic endplate, but also to increased anatomical plasticity under chronic paralysis, showing that the bridge to ECM is an essential relay in the regulation of anatomical plasticity.
The fact that both in myd mutants and in Actinomycin D treated muscles, lack of activity is required to allow extrasynaptic nerve growth, suggests that not only removal of adhesion but also lack of activity is required for anatomical plasticity.

The role of the ECM as mediator of adhesion regulated anatomical plasticity is underlined by the fact that in plastic synapses there are specific modifications of the synaptic ECM (agrin re-organization, loss of WFA staining). Inhibition of extracellular proteases shows that these changes in ECM organization are required to allow anatomical plasticity.

The ECM has also been shown to play an important role in regulating synaptic plasticity in the mature CNS. *In vivo* injections of chondroitinase ABC, an enzyme which degrades chondroitin sulfate proteoglycans is sufficient to trigger a new phase of synaptic plasticity similar to the "critical period" (Pizzorusso et al., 2002). It would be interesting to investigate if also in the CNS, the ECM regulates plasticity through adhesion mechanisms.

13.4 Role of Schwann cells

Although the results of our studies clearly establish that the postsynapse regulates pre- and post-synaptic anatomical rearrangements during synaptogenesis and chronic paralysis, they do not address the potential role of the Schwann cell in regulating or modifying plasticity.

Thompson's experiments have indicated that in partially denervated muscles, nerve growth along muscle is supported by Schwann cell processes originating from denervated NMJs (Son et al., 1995; Love et al., 1999). Furthermore, EM pictures of BotA treated muscles show that the growing nerve remains associated to Schwann cell processes (data not shown).

It is then possible that nerve growth in muscle is a secondary effect to tSC plasticity controlled postsynaptically. Such a mechanism fits well with recent results on the impact of glia on circuit formation and maintenance. In C. Elegans, some glial cells have been shown to direct network connectivity (Shen et al., 2004). Astrocytes and Schwann cells have also been shown to promote synaptogenesis in the mammalian cortex (Christopherson et al., 2005; Ullian et al., 2004).

In order to test the potential role of the tSC in NMJ anatomical plasticity we compared paralysis and denervation in transgenic mice expressing GFP under the control of the S100 promoter (Annex 3). We found that whereas during paralysis Schwann cells remodel extensively only in DeSyn muscles but not FaSyn, in denervation tSCs sprout

rapidly (5 days) and extensively in both muscles. Extensive sprout 5 days after denervation in both muscles shows that tSCs are competent for vigorous anatomical remodeling, but that this growth potential remains suppressed in the presence of nerve.

Strikingly, the type of tSC remodeling in the presence or absence of nerve is qualitatively different. Whereas in denervation the tSCs grow processes while their soma remain associated with the postsynaptic endplate, during paralysis tSCs migrate and multiply, closely associated with nerve and without growing sprouts. This data is consistent with the idea that the nerve offers an attractive surface for tSC migration and growth, probably through the expression of neuregulin (Taveggia et al., 2005). In the absence of nerve the tSCs remain associated with the postsynaptic endplate and fail to proliferate. But as in DeSyn the cluster disassembles during denervation, the tSCs gradually abandon the former synaptic endplate and de-differentiate into long chains of elongated cells.

Our findings support the idea that tSCs have a permissive rather than instructive role in the regulation of nerve growth during chronic paralysis. The fact that in the absence of nerve tSC response does not differentiate between DeSyn and Fasyn muscles indicates that the nerve has a strong instructive role in the behavior of tSCs.

13.5 Role of nerve

Although regulation of synaptogenesis in development and anatomical plasticity in the adult are determined by the postsynaptic muscle fiber, which then influences tSCs, the nerve does play an important role in the management of synapses.

First, DeSyn muscles require constant activity input to maintain their synapses. Second, under conditions of anatomical plasticity and despite extensive tSC growth, ectopic clusters will not be formed in the absence of nerve-muscle contact.

But the axon can also affect synapse stability through its ability to remodel the ECM, or depending on its intrinsic competence for growth and adhesion.

In transgenic mice overexpressing agrin in the nerve, plasticity induced by chronic paralysis is attenuated, indicating that the nerve can affect synaptic stability by shaping the ECM at the synaptic cleft.

Transgenic mice overexpressing GAP-43 in nerves also showed a more limited synaptic plasticity under chronic paralysis. GAP-43 is an intracellular protein that promotes

growth cone adhesion and is usually expressed during periods of synaptogenesis. These results indicate that the ability of nerve to grow and form functional adhesion platforms will have an impact on the anatomical plasticity of the synapse by affecting both pre- and postsynaptic processes.

13.6 Motoneuron specific sensitivity during disease

The stereotyped innervation of MNs and the accessibility of the NMJ allow the detailed study of the biological processes leading to progressive neurodegeneration. Using transgenic mice expressing human SOD1 point mutant proteins and with single GFP labeled MNs, we could perform a quantitative study of the disease progression. We found that disease progression follows a series of stereotyped stages and that there are three MN populations with different sensitivities to disease.

Steps of disease progression included stalling of synaptic vesicle trafficking along the axon, a decrease in the number of synaptic vesicles at the synapse, and anomalies in the neurofilament organization in the axon. Later stages of the disease included loss of synapse and axon pruning in FF and FR axons, followed by a period of axon regeneration and compensated innervation by FR and S axons. A second period of axonal pruning results in the loss of the FR axons, and only the S axons regenerate efficiently until the death of the animal.

It is important to note that although FF, FR and S MNs follow a very different evolution during the disease, all MNs are affected (e. g. neurofilaments modifications can be noted early in S axons). So the difference in sensitivity is more probably due to differences in reaction or adaptation of the MN to the disease conditions than a temporal difference in exposure to injury. Investigations in the mechanisms of disease resistance of FR and S MNs could thus open the way to novel therapeutic approaches.

A critical observation is that the disease processes observed in the SOD1(G93A) line used for this study are also observed in other disease models. Thus the SOD1(G85R) line has a delayed disease onset, but analysis of mice between 5 and 6 months of age showed a similar pattern of specific vulnerability of each type of MN. Similar patterns

of specific MN vulnerability could also be observed in pmn/pmn mice, which are affected early on by a MN disease unrelated to FALS. This would suggest that different types of stress, affecting intrinsically the MN or its environment, eventually converge to a common pathway of neurodegeneration.

A common pathway of disease progression combined with the observation that different types of MNs show a very different ability to resist disease imply that therapeutic strategies targeting common steps of disease evolution and supporting axon responses to disease could be clinically relevant to a wide variety of conditions, despite not targeting the initial cause of disease. In this context rescue of FR axons would be particularly important to prolong life quality and expectancy of patients.

In the meantime, more direct applications of these findings could include a more precocious detection of early signs of disease by specifically analyzing FF axons or muscle compartments enriched in IIb muscle fibers.

MNs in FALS seem to be more affected by an axon transport problem (synaptic vesicle stalling, NF anomalies, positive effect of peripherally applied CNTF) rather than by a soma pathology (inefficiency of approaches inhibiting or preventing MN loss in preventing disease progression; Fischer et al., 2004; Sagot et al., 1995; Kostic et al., 1997). Early losses of synapses and defects in axon transport have also been reported in pathologies such as Alzheimer's and Huntington's disease (Walsh and Selkoe, 2004; Coleman and Yao, 2003; Stokin et al., 2005; Gunawardena and Goldstein, 2005). It is thus possible that insights gleaned from studies of diseases of an approachable system such as the MNs could lead to progress in the understanding of CNS pathologies, which is currently hampered by lack of access and the complexity of the affected regions.

Chapter 14 - Outlook

The results presented in this work provide new insights into the mechanisms of synapse formation and maintenance both in development and in the adult. But they also raise numerous questions, and point towards new directions of investigation.

A major question raised by the discovery of two new classes of muscles, DeSyn and FaSyn, concerns the cellular mechanisms underlying the differences in postsynaptic endplate organization and stability during development and in the adult. Because the locus of control is the organization of the postsynaptic complexes, it will be interesting to study cellular processes likely to affect them. Good candidates are regulation of lipid rafts by proteins such as Src and Fyn, but also cellular trafficking mechanisms, which can change the composition and distribution of the postsynaptic platform. Other attractive candidates are mechanisms affecting cytoskeletal organization and stability.

The second issue raised by the differences in synaptogenesis and anatomical plasticity in DeSyn and FaSyn muscles is the putative functional role of the distinct regulatory pathways in the two classes of muscles. It is not clear why during development DeSyn muscles exhibit a delayed assembly of focal synapses, and why in the adult FaSyn muscles fail to react to absence of activity. Possible explanations might involve differences in the mechanical function of these muscles, differences in their capacity to adapt to changes in usage, or differences in their exposure to environmental stress or disease.

Another important question would be to elucidate the role of the Schwann cell in mediating the changes leading to synaptic plasticity. Are Schwann cells activated by disassembly of the postsynaptic endplate? Are they the main actors in the remodeling of the synaptic ECM?

More fundamentally, it would also be interesting to explore if mechanisms regulating NMJ anatomical plasticity are also used by CNS synapses. Are the postsynaptic targets the main regulators of anatomical plasticity at central synapses? Are there major differences in activity-dependent plasticity among closely related synapse systems? Are glia important players to control anatomical plasticity of synapses in the CNS? So far, principles discovered at NMJs have been generally useful in guiding studies of central synapses. It therefore seems reasonable to anticipate that determining to what

extent principles developed in this thesis apply to synapse assembly and plasticity in the CNS will provide for further productive lines of research in the study of neuronal circuits.

Chapter 15 - Bibliography

Aigner, L., Arber, S., Kapfhammer, J.P., Laux, T., Schneider, C., Botteri, F., Brenner, H.R. and Caroni, P., 1995. Overexpression of the neural growth-associated protein GAP-43 induces nerve sprouting in the adult nervous system of transgenic mice. Cell 83, 269–278.

Akaaboune, M., Culican, S.M., Turney, S.G. and Lichtman, J.W., 1999. Rapid and reversible effects of activity on acetylcholine receptor density at the neuromuscular junction in vivo. Science 286, 503–507.

Anderson, M.J. and Cohen, M.W., 1977. Nerve-induced and spontaneous redistribution of acetylcholine receptors on cultured muscle cells. J. Physiol. (Lond.) 268, 757–773.

Antonini, A., Gagiolini, M. & Stryker, M.P. 1999 Anatomical correlates of functional plasticity in mouse visual cortex. Journal of Neuroscience 19, 4388-4406.

Apel, E.D., Glass, D.J., Moscoso, L.M., Yancopoulos, G.D. and Sanes, J.R., 1997. Rapsyn is required for MuSK signaling and recruits synaptic components to a MuSK-containing scaffold. Neuron 18, 623–636.

Arber, S., Han, B., Mendelsohn, M., Smith, M., Jessell, T.M. and Sockanathan, S., 1999. Requirement for the homeobox gene Hb9 in the consolidation of motor neuron identity. Neuron 23, 659–674.

Balice-Gordon, R.J., Chua, C.K., Nelson, C.C., and Lichtman, J.W., 1993. Gradual loss of synaptic cartels precedes axon withdrawal at developing neuromuscular junctions. Neuron 11, 801-815.

Banks, G.B., Chau, T.N., Bartlett, S.E. and Noakes, P.G. Promotion of motoneuron survival and branching in rapsyn-deficient mice. J Comp Neurol. 429, 156-165 (2001).

Bareyre, F.M. et al. The injured spinal cord spontaneously forms a new intraspinal circuit in adult rats. Nat.Neurosci. 7, 269-277 (2004).

Barrantes, F.J., 1993. Structural-functional correlates of the nicotinic acetylcholine receptor and its lipid microenvironment. Faseb J. 7, 1460-7.

Bezakova G., Helm J.P., Francolini M. and Lomo T., 2001. Effects of purified recombinant neural and muscle agrin on skeletal muscle fibers in vivo. J. Cell Biol. 153(7), 1441-52.

Biederer, T., Sara, Y., Mozhayeva, M., Atasoy, D., Liu, X., Kavalali, E.T., and Sudhof, T.C., 2002. SynCAM, a synaptic adhesion molecule that drives synapse assembly. Science 297, 1525-1531.

Bisby, M.A. & Tetzlaff, W., 1992. Changes in cytoskeletal protein synthesis following axon injury and during axon regeneration. Molecular Neurobiology 6, 107-123.

Bommel, H. et al., 2002. Missense mutation in the tubulin-specific chaperone E (Tbce) gene in the mouse mutant progressive motor neuronopathy, a model of human motoneuron disease. J.Cell.Biol. 159, 563-569.

Bomze, H.M., Bulsara, K.R., Iskandar, B.J., Caroni, P. & Skene, J.H., 2001. Spinal axon regeneration evoked by replacing two growth cone proteins in adult neurons. Nature Neuroscience 4, 38-43.

Borges, L.S., and M. Ferns. 2001. agrin-induced phosphorylation of the acetylcholine receptor regulates cytoskeletal anchoring and clustering. J Cell Biol. 153:1-12.

Brandon, E.P., Lin, W., D'Amour, K.A., Pizzo, D.P., Dominguez, B., Sugiura, Y., Thode, S., KO, C.P., Thal, L.J., Gage, F.H. and Lee, K.F., 2003. Aberrant patterning of neuromuscular synapses in choline acetyltransferase-deficient mice. Journal of Neuroscience 23, 539-549.

Brown, D.A., and E. London. 1998. Functions of lipid rafts in biological membranes. Annu Rev Cell Dev Biol. 14:111-36.

Brown, M.C., 1984. Sprouting of motor nerves in adult muscles: a recapitulation of ontogeny. Trends Neuroscience 7, 10-14.

Bruneau, E., Sutter, D., Hume, R.I. and Akaaboune, M. Identification of nicotinic acetylcholine receptor recycling and its role in maintaining receptor density at the neuromuscular junction in vivo. J.Neurosci. 26, 9949-9959 (2005).

Bruijn, L.I., Miller, T.M. and Cleveland, D.W., 2004. Unraveling the mechanisms involved in motor neuron degeneration in ALS. Annu.Rev.Neurosci. 27, 723-749.

Bruses, J.L., N. Chauvet, and U. Rutishauser. 2001. Membrane lipid rafts are necessary for the maintenance of the (alpha)7 nicotinic acetylcholine receptor in somatic spines of ciliary neurons. J Neurosci. 21:504-12.

Burgess, R.W., Nguyen, Q.T., Son, Y.J., Lichtman, J.W. and Sanes, J.R., 1999. Alternatively spliced isoforms of nerve- and muscle-derived agrin: their roles at the neuromuscular junction. Neuron 23, 33–44.

Burke, R.E., 1994. The physiology of motor units. In: Second Edition, A.G., Engel and, C. and Franzini-Armstrong, Editors, 1994. Myology, McGraw-Hill, Inc, New York 464–483.

Carlisle, H.J., and Kennedy M.B., 2005. Spine architecture and synaptic plasticity. Trends Neurosci. 28:182-7.

Caroni, P., Becker, M., 1992. The downregulation of growth-associated proteins in motoneurons at the onset of synapse elimination is controlled by muscle activity and IGF1. Journal of Neuroscience 12, 3849-3861.

Caroni, P., 1997a. Overexpression of growth-associated proteins in the neurons of adult transgenic mice. Journal of Neuroscience Methods 71, 3-9.

Caroni, P., 1997b. Intrinsic neuronal determinants that promote axonal sprouting and elongation. Bioessays 19, 767-775.

Caroni, P., Aigner, L., Schneider, C., 1997. Intrinsic neuronal determinants locally regulate extrasynaptic and synaptic growth at the adult neuromuscular junction. Journal of Cell Biology 136, 679-692.

Chih, B., H. Engelman, and P. Scheiffele. 2005. Control of excitatory and inhibitory synapse formation by neuroligins. Science. 307:1324-8.

Chiu, A.Y., Zhai, P., Dal Canto, M.C., Peters, T.M., Kwon, Y.W., Prattis, S.M. & Gurney, M.E., 1995. Age-dependent penetrance of disease in a transgenic mouse model of familial amyotrophic lateral sclerosis. Molecular Cellular Neuroscience 6, 349-362.

Christopherson K.S., Ullian E.M., Stokes C.C., Mullowney C.E., Hell J.W., Agah A., Lawler J., Mosher D.F., Bornstein P. and Barres B.A., 2005 Thrombospondins are astrocyte-secreted proteins that promote CNS synaptogenesis.Cell. 120(3),421-33.

Clement A.M., Nguyen M.D., Roberts E.A., Garcia M.L., Boillee S., Rule M., McMahon A.P., Doucette W., Siwek D., Ferrante R.J., Brown R.H. Jr., Julien J.P., Goldstein L.S. and Cleveland D.W., 2003. Wild-type nonneuronal cells extend survival of SOD1 mutant motor neurons in ALS mice. Science 302, 113-117.

Cohen, N.A., Kaufmann, W.E., Worley, P.F. and Rupp, F., 1997. Expression of agrin in the developing and adult rat brain. Neuroscience 76, 581–596.

Cohen-Cory, S. 2002. The developing synapse: construction and modulation of synaptic structures and circuits. Science. 298:770-6.

Coleman, P.D. and Yao, P.J., 2003. Synaptic slaughter in Alzheimer's disease. Neurobiol.Aging 24, 1023-1027.

Collard, J.F., Cote, F. and Julien, J.P., 1995. Defective axonal transport in a transgenic mouse model of amyotrophic lateral sclerosis. Nature 375, 61-64.

Cote, P.D., Moukhles, H., Lindenbaum, M., and Carbonetto, S., 1999. Chimaeric mice deficient in dystroglycans develop muscular dystrophy and have disrupted myoneural synapses. Nat.Genet. 23, 338-342.

Cox, M.E., and P.F. Maness. 1993. Tyrosine phosphorylation of alpha-tubulin is an early response to NGF and pp60v-src in PC12 cells. J Mol Neurosci. 4:63-72.

Dalva, M.B., M.A. Takasu, M.Z. Lin, S.M. Shamah, L. Hu, N.W. Gale, and M.E. Greenberg., 2000. EphB receptors interact with NMDA receptors and regulate excitatory synapse formation. Cell. 103:945-56.

Darian-Smith, C., and Gilbert C.D., 1994. Axonal sprouting accompanies functional reorganization in adult cat striate cortex. Nature 368, 737-740.

Davis, G.W., 2000. The making of a synapse: target-derived signals and presynaptic differentiation. Neuron 26, 551–554.

Davis, G.W. and Goodman, C.S., 1998. Synapse-specific control of synaptic efficacy at the terminals of a single neuron. Nature 392, 82–86.

Davis, G.W., 2000. The making of a synapse: target-derived signals and presynaptic differentiation. Neuron 26, 551-554.

DeChiara, T.M., Bowen, D.C., Valenzuela, D.M., Simmons, M.V., Poueymirou, W.T., Thomas, S., Kinetz, E., Compton, D.L., Rojas, E., Park, J.S. et al., 1996. The receptor tyrosine kinase MuSK is required for neuromuscular junction formation in vivo. Cell 85, 501–512.

De Harven E. and Coërs C., 1959. Electron microscope study of the human neuromuscular junction. J. Biophys. Biochem. Cytol. 6(1):7-10

Delio, D.A., Fiori, M.G. and Lowndes, H.E., 1992. Motor unit function during evolution of proximal axon swellings. J.Neurol.Sci. 109, 30-40.

Del Pozo, M.A., N.B. Alderson, W.B. Kiosses, H.H. Chiang, R.G. Anderson, and M.A. Schwartz., 2004. Integrins regulate Rac targeting by internalization of membrane domains. Science. 303:839-42.

Dengler, R. et al., 1990. Amyotrophic lateral sclerosis: macro-EMG and twitch forces of single motor units. Muscle Nerve 13, 545-550.

Denzer, A.J., Gesemann, M., Schumacher, B. and Ruegg, M.A., 1995. An amino-terminal extension is required for the secretion of chick agrin and its binding to extracellular matrix. J. Cell Biol. 131, 1547–1560.

de Paiva, A., Meunier, F.A., Molgo, J., Aoki, K.R., and Dolly J.O., 1999. Functional repair of motor endplates after botulinum neurotoxin type A poisoning: biphasic switch of synaptic activity between nerve sprouts and their parent terminals. Proc.-Natl.Acad.Sci.USA. 96, 3200-3205.

De Paola, V., Arber, S., and Caroni, P., 2003. AMPA receptors regulate dynamic equilibrium of presynaptic terminals in mature hippocampal networks. Nat.Neurosci. 6, 491-500.

DiAntonio, A., and Hicke L., 2004. Ubiquitin-dependent regulation of the synapse. Annu.Rev.Neurosci. 27, 223-46.

Edgar, B.A. From cell structure to transcription: Hippo forges a new path. Cell 124, 267-273 (2006).

Ehlers, M.D., 2003. Activity level controls postsynaptic composition and signaling via the ubiquitin-proteasome system. Nat.Neurosci. 6, 231-42.

English, A.W., 2003. Cytokines, growth factors and sprouting at the neuromuscular junction. J.Neurocytol. 32, 943-60.

Ferns, M., M. Deiner, and Z. Hall., 1996. agrin-induced acetylcholine receptor clustering in mammalian muscle requires tyrosine phosphorylation. J Cell Biol. 132:937-44.

Fischer, L.R. et al., 2004. Amyotrophic lateral sclerosis is a distal axonopathy: evidence in mice and man. Exp.Neurol. 185, 232-40.

Fitzsimonds, R.M. and Poo, M.M., 1998. Retrograde signaling in the development and modification of synapses. Physiol. Rev. 78, 143–170.

Flanagan-Steet, H., Fox, M.A., Meyer, D. and Sanes, J.R. Neuromuscular synapses can form in vivo by incorporation of initially aneural postsynaptic specializations. Development 132, 4471-4481 (2005).

Frank, E. and Fischbach, G.D., 1977. ACh receptors accumulate at newly formed nerve-muscle synapses in vitro. Soc. Gen. Physiol. Ser. 32, 285–291.

Frey, D., Schneider, C., Xu, L., Borg, J., Spooren, W. and Caroni, P., 2000a. Early and selective loss of neuromuscular synapse subtypes with low sprouting competence in motoneuron diseases. Journal of Neuroscience 20, 2534-2542

Frey, D., Laux, T., Xu, L., Schneider, C. and Caroni, P., 2000b. Shared and unique roles of CAP23 and GAP43 in actin regulation, neurite outgrowth, and anatomical plasticity. Journal of Cell Biology 149, 1443-1454.

Froehner S. C., Luetje C. W., Scotland P. B. and Patrick, J., 1990. The postsynaptic 43K protein clusters muscle nicotinic acetylcholine receptors in Xenopus oocytes. Neuron 5, 403-410.

Frugier, T., Nicole, S., Cifuentes-Diaz, C. and Melki, J., 2002. The molecular bases of spinal muscular atrophy. Current Opinion in Genetics and Development 12, 294-298.

Fuhrer, C., and Z.W. Hall., 1996. Functional interaction of Src family kinases with the acetylcholine receptor in C2 myotubes. J Biol Chem. 271:32474-81.

Fuhrer, C., J.E. Sugiyama, R.G. Taylor, and Z.W. Hall., 1997. Association of muscle-specific kinase MuSK with the acetylcholine receptor in mammalian muscle. Embo J. 16:4951-60.

Fuhrer, C., Gautam, M., Sugiyama, J.E. and Hall, Z.W., 1999. Roles of rapsyn and agrin in interaction of postsynaptic proteins with acetylcholine receptors. J. Neurosci. 19, 6405–6416.

Galbiati, F., B. Razani, and M.P. Lisanti., 2001. Emerging themes in lipid rafts and caveolae. Cell. 106:403-11.

Galimberti, I. et al. Long-term rearrangements of hippocampal mossy fiber terminal connectivity in the adult regulated by experience. Neuron 50, 749-763 (2006).

Gautam, M., Noakes, P.G., Mudd, J., Nichol, M., Chu, G.C., Sanes, J.R. and Merlie, J.P., 1995. Failure of postsynaptic specialization to develop at neuromuscular junctions of rapsyn-deficient mice. Nature 377, 232–236.

Gautam, M., Noakes, P.G., Moscoso, L., Rupp, F., Scheller, R.H., Merlie, J.P. and Sanes, J.R., 1996. Defective neuromuscular synaptogenesis in agrin-deficient mutant mice. Cell 85, 525–535.

Gervasio, O.L., and W.D. Phillips., 2005. Increased ratio of rapsyn to ACh receptor stabilizes postsynaptic receptors at the mouse neuromuscular synapse. J Physiol. 562:673-85.

Gillingwater, T.H., Ingham, C.A., Coleman, M.P. and Ribchester, R.R., 2003. Ultrastructural correlates of synapse withdrawal at axotomised neuromuscular junctions in mutant and transgenic mice expressing the Wld gene. J.Anat. 203, 265-276.

Glass, D.J., Bowen, D.C., Stitt, T.N., Radziejewski, C., Bruno, J., Ryan, T.E., Gies, D.R., Shah, S., Mattsson, K., Burden, S.J. et al., 1996. agrin acts via a MuSK receptor complex. Cell 85, 513–523.

Goda, Y., and Davis, G.W., 2003. Mechanisms of synapse assembly and disassembly. Neuron 40, 243-264.

Goldberg, J.L., Klassen, M.P., Hua, Y., Barres, B.A., 2002a. Amacrine-signaled loss of intrinsic axon growth ability by retinal ganglion cells. Science 296, 1860-1864.

Goldberg, J.L., Espinosa, J.S., Xu, Y., Davidson, N., Kovacs, G.T., Barres, B.A., 2002b. Retinal ganglion cells do not extend axons by default: promotion by neurotrophic signaling and electrical activity. Neuron 33, 689-702.

Golub, T., S. Wacha, and P. Caroni., 2004. Spatial and temporal control of signaling through lipid rafts. Curr Opin Neurobiol. 14:542-50.

Golub, T., and Caroni, P., 2005. PI(4,5)P2-dependent microdomain assemblies capture microtubules to promote and control leading edge motility. J.Cell Biol. 169, 151-165.

Gonzalez, M., Ruggiero, F.P., Chang, Q., Shi, Y.J., Rich, M.M., Kraner, S. and Balice-Gordon, R.J., 1999. Disruption of Trkb-mediated signaling induces disassembly of postsynaptic receptor clusters at neuromuscular junctions. Neuron 24, 567–583.

Goritz, C., D.H. Mauch, and F.W. Pfrieger., 2005. Multiple mechanisms mediate cholesterol-induced synaptogenesis in a CNS neuron. Mol Cell Neurosci. 29:190-201.

Grady, R.M., H. Teng, M.C. Nichol, J.C. Cunningham, R.S. Wilkinson, and J.R. Sanes., 1997. Skeletal and cardiac myopathies in mice lacking utrophin and dystrophin: a model for Duchenne muscular dystrophy. Cell 90:729-38.

Grady, R.M., Zhou, H., Cunningham, J.M., Henry, M.D., Campbell, K.P., and Sanes, J.R., 2000. Maturation and maintenance of the neuromuscular synapse: genetic evidence for roles of the dystrophin--glycoprotein complex. Neuron 25, 279-293.

Graf, E.R., X. Zhang, S.X. Jin, M.W. Linhoff, and A.M. Craig., 2004. Neurexins induce differentiation of GABA and glutamate postsynaptic specializations via neuroligins. Cell. 119:1013-26.

Gunawardena, S. and Goldstein, L.S., 2001. Disruption of axonal transport and neuronal viability by amyloid precursor protein mutations in Drosophila. Neuron 32, 389-401.

Gunawardena, S. et al., 2003. Disruption of axonal transport by loss of huntingtin or expression of pathogenic polyQ proteins in Drosophila. Neuron 40, 25-40.

Gunawardena, S. and Goldstein, L.S., 2005. Polyglutamine diseases and transport problems: deadly traffic jams on neuronal highways. Arch.Neurol. 62, 46-51.

Gurney, M.E. et al., 1994. Motor neuron degeneration in mice that express a human Cu,Zn superoxide dismutase mutation. Science 264, 1772-1775.

Hay, N., and Sonenberg, N., 2004. Upstream and downstream of mTOR. Genes Dev. 18, 1926-1945.

Harris, A.J., 1981. Embryonic growth and innervation of rat skeletal muscles. III. Neural regulation of junctional and extra-junctional acetylcholine receptor clusters. Philos. Trans. R. Soc. Lond. B Biol. Sci. 293, 287–314.

Heathcote, R.D., Ekman, J.M., Campbell, K.P. & Godfrey, E.W., 2000. Dystroglycan overexpression in vivo alters acetylcholine receptor aggregation at the neuromuscular junction. Developmental Biology 227, 595-605.

Henry, M.D., and Campbell, K.P., 1998. A role for dystroglycan in basement membrane assembly. Cell. 95, 859-70.

Herbst R., Avetisova E., Burden S.J., 2002. Restoration of synapse formation in Musk mutant mice expressing a Musk/Trk chimeric receptor. Development 129(23), 5449-60.

Hering, H., C.C. Lin, and M. Sheng., 2003. Lipid rafts in the maintenance of synapses, dendritic spines, and surface AMPA receptor stability. J Neurosci. 23:3262-71.

Herrera, A.A., Qiang, H., KO, C.P., 2000. The role of perisynaptic Schwann cells in development of neuromuscular junctions in the frog (Xenopus laevis). Journal of Neurobiology 45, 237-254.

Hesser, B.A., Henschel, O. and Witzemann, V. Synapse disassembly and formation of new synapses in postnatal muscle upon conditional inactivation of MuSK. Mol.Cell.Neurosci. 31, 470-480 (2006).

Houseweart, M.K. and Cleveland, D.W., 1999. Bcl-2 overexpression does not protect neurons from mutant neurofilament-mediated motor neuron degeneration. J.Neurosci. 19, 6446-6456.

Huh, K.H., and C. Fuhrer., 2002. Clustering of nicotinic acetylcholine receptors: from the neuromuscular junction to interneuronal synapses. Mol Neurobiol. 25:79-112.

Incardona, J.P., and S. Eaton., 2000. Cholesterol in signal transduction. Curr Opin Cell Biol. 12:193-203.

Jablonka, S., Wiese, S. and Sendtner, M. Axonal defects in mouse models of motoneuron disease. J.Neurobiol. 58, 272-86 (2004).

Jacobson, C., Cote, P.D., Rossi, S.G., Rotundo, R.L., and Carbonetto, S., 2001. The dystroglycan complex is necessary for stabilization of acetylcholine receptor clusters at neuromuscular junctions and formation of the synaptic basement membrane. J.Cell Biol. 152, 435-450.

Jessen, K.R. and Mirsky, R. The origin and development of glial cells in peripheral nerves. Nat.Rev.Neurosci. 6, 671-682 (2005).

Jones, C.L., 1979. The morphogenesis of the thigh of the mouse with special reference to tetrapod muscle homologies. J. Morphol. 162, 275–309.

Jones, G., Meier, T., Lichtsteiner, M., Witzemann, V., Sakmann, B. and Brenner, H.R., 1997. Induction by agrin of ectopic and functional postsynaptic-like membrane in innervated muscle. Proc. Natl. Acad. Sci. USA 94, 2654–2659.

Kanagawa, M., Saito, F., Kunz, S., Yoshida-Moriguchi, T., Barresi, R., Kobayashi, Y.M., Muschler, J., Dumanski, J.P., Michele, D.E., Oldstone, M.B., and Campbell, K.P., 2004. Molecular recognition by LARGE is essential for expression of functional dystroglycan. Cell 117, 953-964.

Khan A.A., Bose C., Yam L.S., Soloski M.J. and Rupp F., 2001. Physiological regulation of the immunological synapse by agrin. Science 292(5522), 1681-6.

Kishi, M., Kummer, T.T., Eglen, S.J. and Sanes, J.R. LL5beta: a regulator of postsynaptic differentiation identified in a screen for synaptically enriched transcripts at the neuromuscular junction. J.Cell.Biol. 25, 355-366 (2005).

Kong, J. and Xu, Z., 1998. Massive mitochondrial degeneration in motor neurons triggers the onset of amyotrophic lateral sclerosis in mice expressing a mutant SOD1. J. Neurosci. 18, 3241-3250.

Kong, X.C., Barzaghi, P., and Ruegg, M.A., 2004. Inhibition of synapse assembly in mammalian muscle in vivo by RNA interference. EMBO Rep. 5, 183-188.

Kostic, V., Jackson-Lewis, V., de Bilbao, F., Dubois-Dauphin, M. and Przedborski, S., 1997. Bcl-2: prolonging life in a transgenic mouse model of familial amyotrophic lateral sclerosis. Science 277, 559-562.

Kummer, T.T., Misgeld, T., Lichtman, J.W., and Sanes, J.R., 2004. Nerve-independent formation of a topologically complex postsynaptic apparatus. J.Cell.Biol. 164, 1077-1087.

Kuo, J.J. et al., 2004. Hyperexcitability of cultured spinal motoneurons from presymptomatic ALS mice. J. Neurophysiol. 91, 571-575.

Kusumi, A., I. Koyama-Honda, and K. Suzuki., 2004. Molecular dynamics and interactions for creation of stimulation-induced stabilized rafts from small unstable steady-state rafts. Traffic. 5:213-30.

LaMonte, B.H. et al., 2002. Disruption of dynein/dynactin inhibits axonal transport in motor neurons causing late-onset progressive degeneration. Neuron 34, 715-727.

LaRochelle W. J. and Froehner S. C., 1986. Determination of the tissue distributions and relative concentrations of the postsynaptic 43-kDa protein and the acetylcholine receptor in Torpedo. J. Biol. Chem. 261, 5270-5274.

Larsson, L., Li, X., Tollback, A. and Grimby, L., 1995. Contractile properties in single muscle fibers from chronically overused motor units in relation to motoneuron firing properties in prior polio patients. J.Neurol.Sci. 132, 182-192.

Lee, H.H., Dadgostar, H., Cheng, Q., Shu, J. and Cheng, G., 1999. NF-kappaB-mediated up-regulation of Bcl-x and Bfl-1/A1 is required for CD40 survival signaling in B lymphocytes. Proc.Natl.Acad.Sci.USA. 96, 9136-9141.

Levi, S., Grady, R.M., Henry, M.D., Campbell, K.P., Sanes, J.R., and Craig, A.M., 2002. Dystroglycan is selectively associated with inhibitory GABAergic synapses but is dispensable for their differentiation. J.Neurosci. 22, 4274-4285.

Lin, W., Burgess, R.W., Dominguez, B., Pfaff, S.L., Sanes, J.R. and Lee, K.F., 2001. Distinct roles of nerve and muscle in postsynaptic differentiation of the neuromuscular synapse. Nature 410, 1057–1064.

Lino, M.M., Schneider, C. and Caroni, P., 2002. Accumulation of SOD1 mutants in postnatal motoneurons does not cause motoneuron pathology or motoneuron disease. J.Neurosci. 22, 4825-4832.

Liu, J. et al., 2004. Toxicity of familial ALS-linked SOD1 mutants from selective recruitment to spinal mitochondria. Neuron 43, 5-17.

Livet, J., Sigrist, M., Stroebel, S., DePaola., V., Price, S.R., Henderson, C.E., Jessell, T.M., Arber, S., 2002. ETS gene Pea3 controls the central position and terminal arborization of specific motor neuron pools. Neuron 35, 877-892.

Lobsiger C.S., Garcia M.L., Ward C.M. and Cleveland D.W., 2005. Altered axonal architecture by removal of the heavily phosphorylated neurofilament tail domains strongly slows superoxide dismutase 1 mutant-mediated ALS. Proc. Natl. Acad. Sci. U S A. 102(29),10351-6.

Love, F.M., Thompson, W.J., 1999. Glial cells promote muscle reinnervation by responding to activity-dependent postsynaptic signals. J. Neurosci. 19, 10390-10396.

Ma, L., Y.Z. Huang, G.M. Pitcher, J.G. Valtschanoff, Y.H. Ma, L.Y. Feng, B. Lu, W.C. Xiong, M.W. Salter, R.J. Weinberg, and L. Mei., 2003. Ligand-dependent recruitment of the ErbB4 signaling complex into neuronal lipid rafts. J Neurosci. 23:3164-75.

Marangi, P.A., J.R. Forsayeth, P. Mittaud, S. Erb-Vogtli, D.J. Blake, M. Moransard, A. Sander, and Fuhrer C., 2001. Acetylcholine receptors are required for agrin-induced clustering of postsynaptic proteins. Embo J. 20:7060-73.

Marangi, P.A., Wieland, S.T. and Fuhrer, C., 2002. Laminin-1 redistributes postsynaptic proteins and requires rapsyn, tyrosine phosphorylation, and Src and Fyn to stably cluster acetylcholine receptors. Journal of Cell Biology 157, 883-895.

Marchand, S., A. Devillers-Thiery, S. Pons, J.P. Changeux, and Cartaud J., 2002. Rapsyn escorts the nicotinic acetylcholine receptor along the exocytic pathway via association with lipid rafts. J Neurosci. 22:8891-901.

Martin, P.T., 2003. Glycobiology of the neuromuscular junction. J.Neurocytol. 32, 915-929.

Mataga, N., Mizuguchi, Y., and Hensch, T.K., 2004. Experience-dependent pruning of dendritic spines in visual cortex by tissue plasminogen activator. Neuron 44, 1031-1041.

Mauch, D.H., K. Nagler, S. Schumacher, C. Goritz, E.C. Muller, A. Otto, and F.W. Pfrieger, 2001. CNS synaptogenesis promoted by glia-derived cholesterol. Science. 294:1354-7.

McKinney, R.A., Capogna, M., Durr, R., Gaehwiler, B.H. and Thompson, S.M., 1999. Miniature synaptic events maintain dendritic spines via AMPA receptor activation. Nat. Neurosci. 2, 44–49.

McMahan, U.J., 1990. The agrin hypothesis. Cold Spring Harb Symp Quant Biol. 55:407-18.

Misgeld, T., Burgess, R.W., Lewis, R.M., Cunningham, J.M., Lichtman, J.W., and Sanes, J.R., 2002. Roles of neurotransmitter in synapse formation: development of neuromuscular junctions lacking choline acetyltransferase. Neuron. 36, 635-648.

Misgeld, T., Kummer, T.T., Lichtman, J.W. and Sanes, J.R. Agrin promotes synaptic differentiation by counteracting an inhibitory effect of neurotransmitter. Proc.Natl.Acad.Sci.U.S.A. 102, 11088-11093 (2005).

Mittaud, P., A.A. Camilleri, R. Willmann, S. Erb-Vogtli, S.J. Burden, and C. Fuhrer., 2004. A single pulse of agrin triggers a pathway that acts to cluster acetylcholine receptors. Mol Cell Biol. 24:7841-54.

Mittaud, P., P.A. Marangi, S. Erb-Vogtli, and C. Fuhrer., 2001. agrin-induced activation of acetylcholine receptor-bound Src family kinases requires Rapsyn and correlates with acetylcholine receptor clustering. J Biol Chem. 276:14505-13.

Montanaro, F., Gee, S.H., Jacobson, C., Lindenbaum, M.H., Froehner, S.C., and Carbonetto, S., 1998. Laminin and alpha-dystroglycan mediate acetylcholine receptor aggregation via a MuSK-independent pathway. J. Neurosci. 18, 1250-1260.

Moransard, M., L.S. Borges, R. Willmann, P.A. Marangi, H.R. Brenner, M.J. Ferns, and C. Fuhrer., 2003. agrin regulates rapsyn interaction with surface acetylcholine receptors, and this underlies cytoskeletal anchoring and clustering. J Biol Chem. 278:7350-9.

Muller, G., 2002. Dynamics of plasma membrane microdomains and cross-talk to the insulin signalling cascade. FEBS Lett. 531:81-7.

Muller, G., N. Hanekop, W. Kramer, W. Bandlow, and W. Frick., 2002a. Interaction of phosphoinositolglycan(-peptides) with plasma membrane lipid rafts of rat adipocytes. Arch Biochem Biophys. 408:17-32.

Muller, G., C. Jung, W. Frick, W. Bandlow, and W. Kramer., 2002b. Interaction of phosphatidylinositolglycan(-peptides) with plasma membrane lipid rafts triggers insulin-mimetic signaling in rat adipocytes. Arch Biochem Biophys. 408:7-16.

Nguyen, M.D., Lariviere, R.C. and Julien, J.P., 2000. Reduction of axonal caliber does not alleviate motor neuron disease caused by mutant superoxide dismutase 1. Proc.Natl.Acad.Sci. U.S.A. 97, 12306-12311.

Nguyen, Q.T., Son, Y.J., Sanes, J.R., and Lichtman, J.W., 2000. Nerve terminals form but fail to mature when postsynaptic differentiation is blocked: in vivo analysis using mammalian nerve-muscle chimeras. J.Neurosci. 20, 6077-6086.

Nguyen, Q.T., Sanes, J.R. and Lichtman, J.W., 2002. Pre-existing pathways promote precise projection patterns. Nat.Neurosci. 5, 861-867.

Nishimune, H., Sanes, J.R., and Carlson, S.S., 2004. A synaptic laminin-calcium channel interaction organizes active zones in motor nerve terminals. Nature 432, 580-587.

Nishio, M., S. Fukumoto, K. Furukawa, A. Ichimura, H. Miyazaki, S. Kusunoki, and T. Urano., 2004. Overexpressed GM1 suppresses nerve growth factor (NGF) signals by modulating the intracellular localization of NGF receptors and membrane fluidity in PC12 cells. J Biol Chem. 279:33368-78.

Noakes P. G., Phillips W. D., Hanley T. A., Sanes J. R. and Merlie J. P., 1993. 43K protein and acetylcholine receptors colocalize during the initial stages of neuromuscular synapse formation in vivo. Dev. Biol. 155, 275-280.

O'Brien, R., D. Xu, R. Mi, X. Tang, C. Hopf, and P. Worley., 2002. Synaptically targeted narp plays an essential role in the aggregation of AMPA receptors at excitatory synapses in cultured spinal neurons. J Neurosci. 22:4487-98.

O'Brien, R.J., D. Xu, R.S. Petralia, O. Steward, R.L. Huganir, and P. Worley., 1999. Synaptic clustering of AMPA receptors by the extracellular immediate-early gene product Narp. Neuron. 23:309-23.

O'Malley, J.P., Waran, M.T. and Balice-Gordon, R.J. In vivo observations of terminal Schwann cells at normal, denervated, and reinnervated mouse neuromuscular junctions. J.Neurobiol. 38, 270-286 (1999).

Oray, S., Majewska, A., and Sur, M., 2004. Dendritic spine dynamics are regulated by monocular deprivation and extracellular matrix degradation. Neuron 44, 1021-1030.

O'Rourke, N.A., Cline, H.T. and Fraser, S.E., 1994. Rapid remodeling of retinal arbors in the tectum with and without blockade of synaptic transmission. Neuron 12, 921–934.

Ostrom, R.S., R.A. Bundey, and P.A. Insel., 2004. Nitric oxide inhibition of adenylyl cyclase type 6 activity is dependent upon lipid rafts and caveolin signaling complexes. J Biol Chem. 279:19846-53.

Palazzo, A.F., C.H. Eng, D.D. Schlaepfer, E.E. Marcantonio, and G.G. Gundersen, 2004. Localized stabilization of microtubules by integrin- and FAK-facilitated Rho signaling. Science. 303:836-9.

Palecek, J., Lips, M.B. and Keller, B.U., 1999. Calcium dynamics and buffering in motoneurones of the mouse spinal cord. J.Physiol. 520, 485-502.

Panzer, J.A., Song, Y. and Balice-Gordon, R.J. In vivo imaging of preferential motor axon outgrowth to and synaptogenesis at prepatterned acetylcholine receptor clusters in embryonic zebrafish skeletal muscle. J.Neurosci. 26, 934-947 (2006).

Park, K., Luo, J.M., Hisheh, S., Harvey, A.R. and Cui, Q., 2004. Cellular mechanisms associated with spontaneous and ciliary neurotrophic factor-cAMP-induced survival and axonal regeneration of adult retinal ganglion cells. J.Neurosci. 24, 10806-10815.

Pasinelli, P. et al., 2004. Amyotrophic lateral sclerosis-associated SOD1 mutant proteins bind and aggregate with Bcl-2 in spinal cord mitochondria. Neuron 43, 19-30.

Pelkmans, L., T. Burli, M. Zerial, and A. Helenius., 2004. Caveolin-stabilized membrane domains as multifunctional transport and sorting devices in endocytic membrane traffic. Cell. 118:767-80.

Peng, H.B., Xie, H., Rossi, S.G., and Rotundo, R.L., 1999. Acetylcholinesterase clustering at the neuromuscular junction involves perlecan and dystroglycan. J.Cell Biol. 145, 911-21.

Peterson, W.M., Wang, Q., Tzekova, R. and Wiegand, S.J., 2000. Ciliary neurotrophic factor and stress stimuli activate the Jak-STAT pathway in retinal neurons and glia. J.Neurosci. 20, 4081-4090.

Phillips W.D., Kopta C., Blount P., Gardner P.D., Steinbach J.H. and Merlie JP, 1991. ACh receptor-rich membrane domains organized in fibroblasts by recombinant 43-kilodalton protein. Science 251, 568-570.

Pike, L.J.. 2004. Lipid rafts: heterogeneity on the high seas. Biochem J. 378:281-92.

Pinter, M.J., Waldeck, R.F., Wallace, N., Crok, L.C., 1995. Motor unit behavior in canine motor neuron disease. J. Neurosci. 15, 3447-3457.

Pinter, M.J., Waldeck, R.F., Cope, T.C. & Cork, L.C., 1997. Effects of 4-aminopyridine on muscle and motor unit force in canine motor neuron disease. Journal of Neuroscience 17, 4500-4507

Pizzorusso, T., Medini, P., Berardi, N., Chierzi, S., Fawcett, J.W., and Maffei, L., 2002. Reactivation of ocular dominance plasticity in the adult visual cortex. Science 298, 1248-1251.

Pun, S., Sigrist, M., Santos, A.F., Ruegg, M.A., Sanes, J.R., Jessell, T.M., Arber, S., and Caroni P., 2002. An intrinsic distinction in neuromuscular junction assembly and maintenance in different skeletal muscles. Neuron 34, 357-370.

Raff, M.C., Whitmore, A.V. and Finn, J.T., 2002. Axonal self-destruction and neurodegeneration. Science 296, 868-871.

Raoul, C, et al., 2002. Motoneuron death triggered by a specific pathway downstream of Fas: Potentiation by ALS-linked SOD1 mutations. Neuron 35, 1067-1083.

Reddy, L.V., Koirala, S., Sugiura, Y., Herrera, A.A., and Ko C.P., 2003. Glial cells maintain synaptic structure and function and promote development of the neuromuscular junction in vivo. Neuron 40, 563-380.

Resh, M.D., 1999. Fatty acylation of proteins: new insights into membrane targeting of myristoylated and palmitoylated proteins. Biochim Biophys Acta. 1451:1-16.

Rhainds, D., P. Bourgeois, G. Bourret, K. Huard, L. Falstrault, and L. Brissette., 2004. Localization and regulation of SR-BI in membrane rafts of HepG2 cells. J Cell Sci. 117:3095-105.

Reynolds, M.L. and Woolf, C.J., 1992. Terminal Schwann cells elaborate extensive processes following denervation of the motor endplate. J. Neurocytol. 21, 50–66.

Rich, M.M., Wang, X., Cope, T.C. & Pinter, M.J., 2002a. Reduced neuromuscular quantal content with normal synaptic release time course and depression in canine motor neuron disease. Journal of Neurophysiology 88, 3305-3314.

Rich, M.M., Waldeck, R.F., Cork, L.C., Balice-Gordon, R.J., Fyffe, R.E., Wang, X., Cope, T.C. and Pinter, M.J., 2002b. Reduced endplate currents underlie motor unit dysfunction in canine motor neuron disease. Journal of Neurophysiology 88, 3293-32304.

Riddell, D.R., G. Christie, I. Hussain, and C. Dingwall., 2001. Compartmentalization of beta-secretase (Asp2) into low-buoyant density, noncaveolar lipid rafts. Curr Biol. 11:1288-93.

Robitaille, R., 1998. Modulation of synaptic efficacy and synaptic depression by glial cells at the frog neuromuscular junction. Neuron 21, 847–855.

Rodgers, W., D. Farris, and S. Mishra., 2005. Merging complexes: properties of membrane raft assembly during lymphocyte signaling. Trends Immunol. 26:97-103.

Rosen, D.R. et al., 1993. Mutations in Cu/Zn superoxide dismutase gene are associated with familial amyotrophic lateral sclerosis. Nature 362, 59-62.

Ruegg, M.A., and Bixby, J.L., 1998. agrin orchestrates synaptic differentiation at the vertebrate neuromuscular junction. Trends Neurosci. 21, 22-27.

Ruthazer, E.S., Akerman, C.J., and Cline, H.T., 2003. Control of axon branch dynamics by correlated activity in vivo. Science 301, 66-70.

Sagot, Y. et al., 1995. Bcl-2 overexpression prevents motoneuron cell body loss but not axonal degeneration in a mouse model of a neurodegenerative disease. J. Neurosci. 15, 7727-7733.

Sagot, Y., Tan, S.A., Hammang, J.P., Aebischer, P. and Kato, A.C., 1996. GDNF slows loss of motoneurons but not axonal degeneration or premature death of pmn/pmn mice. Journal of Neuroscience 16, 2335-2341

Sagot, Y., Rosse, T., Vejsada, R., Perrelet, D. and Kato, A.C., 1998. Differential effects of neurotrophic factors on motoneuron retrograde labeling in a murine model of motoneuron disease. J. Neurosci. 18, 1132-41.

Sandrock, A.W. Jr., Dryer, S.E., Rosen, K.M., Gozani, S.N., Kramer, R., Theill, L.E., Fischbach, G.D., 1997. Maintenance of acetylcholine receptor number by neuregulins at the neuromuscular junction in vivo. Science 276, 599-603

Sanes, J.R., Marshall, L.M., and McMahan, U.J. (1978). Reinnervation of muscle fiber basal lamina after removal of myofibers. Differentiation of regenerating axons at original synaptic sites. J.Cell Biol. 78, 176-198.

Sanes, J.R. and Lichtman, J.W., 1999. Development of the vertebrate neuromuscular junction. Annu. Rev. Neurosci. 22, 389–442.

Sanes, J.R. and Lichtman, J.W., 2001. Induction, assembly, maturation and maintenance of a postsynaptic apparatus. Nat. Rev. Neurosci. 2, 791–805.

Santos, A.F., and Caroni, P., 2003. Assembly, plasticity and selective vulnerability to disease of mouse neuromuscular junctions. J.Neurocytol. 32, 849-862.

Seeds, N.W., Siconolfi, L.B., and Haffke, S.P., 1997. Neuronal extracellular proteases facilitate cell migration, axonal growth, and pathfinding. Cell Tissue Res. 290, 367-370.

Sendtner, M. et al., 1992. Ciliary neurotrophic factor prevents degeneration of motor neurons in mouse mutant progressive motor neuronopathy. Nature 358, 502-504.

Siegel, S.G., Patton, B. and English, A.W., 2000. Ciliary neurotrophic factor is required for motoneuron sprouting. Experimental Neurology 166, 205-212.

Simons, K., and E. Ikonen., 1997. Functional rafts in cell membranes. Nature. 387:569-72.

Simons, K., and D. Toomre., 2000. Lipid rafts and signal transduction. Nat Rev Mol Cell Biol. 1:31-9.

Shah, J.V. and Cleveland, D.W., 2002. Slow axonal transport: fast motors in the slow lane. Curr.Opin.Cell Biol. 14, 58-62.

Shaw, P.J. and Eggett, C.J., 2000. Molecular factors underlying selective vulnerability of motor neurons to neurodegeneration in amyotrophic lateral sclerosis. J.Neurol. 247, I17-I27.

Shen K., Fetter R.D. and Bargmann C.I., 2004. Synaptic specificity is generated by the synaptic guidepost protein SYG-2 and its receptor, SYG-1. Cell. 116(6),869-81.

Skene, J.H.P., 1989. Axonal growth-associated proteins. Annual Reviews Neuroscience 12, 127-156

Skorpen, J., Lafond-Benestad, S. and Lomo, T., 1999. Regulation of the size and distribution of ectopic neuromuscular junctions in adult skeletal muscle by nerve-derived trophic factor and electrical muscle activity. Mol. Cell. Neurosci. 13, 192–206.

Smith, C.L., P. Mittaud, E.D. Prescott, C. Fuhrer, and S.J. Burden., 2001. Src, Fyn, and Yes are not required for neuromuscular synapse formation but are necessary for stabilization of agrin-induced clusters of acetylcholine receptors. J Neurosci. 21:3151-60.

Son, Y.J., Thompson, W.J., 1995. Nerve sprouting in muscle is induced and guided by processes extended by Schwann cells. Neuron 14, 133-141.

Son, Y.J., Trachtenberg, J.T., and Thompson, W.J., 1996. Schwann cells induce and guide sprouting and reinnervation of neuromuscular junctions. Trends Neurosci. 19, 280-285.

Song, K.S., S. Li, T. Okamoto, L.A. Quilliam, M. Sargiacomo, and M.P. Lisanti., 1996a. Co-purification and direct interaction of Ras with caveolin, an integral membrane protein of caveolae microdomains. Detergent-free purification of caveolae microdomains. J Biol Chem. 271:9690-7.

Song, K.S., P.E. Scherer, Z. Tang, T. Okamoto, S. Li, M. Chafel, C. Chu, D.S. Kohtz, and M.P. Lisanti., 1996b. Expression of caveolin-3 in skeletal, cardiac, and smooth muscle cells. Caveolin-3 is a component of the sarcolemma and co-fractionates with dystrophin and dystrophin-associated glycoproteins. J Biol Chem. 271:15160-5.

Soriano, P., 1999. Generalized lacZ expression with the ROSA26 Cre reporter strain. Nat. Genet. 21, 70–71.

Sternlicht, M.D., and Werb, Z., 2001. How matrix metalloproteinases regulate cell behavior. Ann.Rev.Cell Dev.Biol. 17, 463-516.

Stokin, G.B. et al., 2005. Axonopathy and transport deficits early in the pathogenesis of Alzheimer's disease. Science 307, 1282-1288.

Sugiyama, J.E., Glass, D.J., Yancopoulos, G.D., and Hall, Z.W., 1997. Laminin-induced acetylcholine receptor clustering: an alternative pathway. J.Cell Biol. 139, 181-191.

Tam, S.L., Archibald, V., Tyreman, N., Gordon, T., 2001. Increased neuromuscular activity reduces sprouting in partially denervated muscles. Journal of Neuroscience 21, 654-667.

Taniuchi, M., Clark, H.B., and E.M. Johnson Jr., 1986. Induction of nerve growth factor receptor in Schwann cells after axotomy. Proc.Natl.Acad.Sci. U.S.A. 83:4094-8.

Tansey, M.G., R.H. Baloh, J. Milbrandt, and E.M. Johnson, Jr., 2000. GFRalpha-mediated localization of RET to lipid rafts is required for effective downstream signaling, differentiation, and neuronal survival. Neuron. 25:611-23.

Taveggia C., Zanazzi G., Petrylak A., Yano H., Rosenbluth J., Einheber S., Xu X., Esper R.M., Loeb J.A., Shrager P., Chao M.V., Falls D.L., Role L. and Salzer J.L., 2005. Neuregulin-1 type III determines the ensheathment fate of axons. Neuron. 2005, 47(5),681-94.

Terrado, J. et al. Motoneuron survival is enhanced in the absence of neuromuscular junction formation in embryos. J.Neurosci. 21, 3144-3150 (2001).

Trachtenberg, J.T. et al. Long-term in vivo imaging of experience-dependent synaptic plasticity in adult cortex. Nature 420, 788-794 (2002).

Ullian E.M., Harris B.T., Wu A., Chan J.R. and Barres B.A., 2004. Schwann cells and astrocytes induce synapse formation by spinal motor neurons in culture. Mol. Cell. Neurosci., 25(2),241-51.

Umemori, H., Linhoff, M.W., Ornitz, D.M., and Sanes, J.R., 2004. FGF22 and its close relatives are presynaptic organizing molecules in the mammalian brain. Cell 118, 257-270.

Verhage, M., Maia, A.S., Plomp, J.J., Brussard, A.B., Heeroma, J.H., Vermeer, H., Toonen, R.F., Hammer, R.E., van den Berg, T.K., Missler, M. et al., 2000. Synaptic assembly of the brain in the absence of neurotransmitter secretion. Science 287, 864–869.

Walsh, D.M. and Selkoe, D.J., 2004. Deciphering the molecular basis of memory failure in Alzheimer's disease. Neuron 44, 181-193.

Wang, Z.Z. et al. Aberrant development of motor axons and neuromuscular synapses in MyoD-null mice. J.Neurosci. 23, 5161-5169 (2003).

Warita, H., Itoyama, Y. and Abe, K., 1999. Selective impairment of fast anterograde axonal transport in the peripheral nerves of asymptomatic transgenic mice with a G93A mutant SOD1 gene. Brain Res. 819, 120-131.

Watts, R.J., Hoopfer, E.D. and Luo, L., 2003. Axon pruning during Drosophila metamorphosis: evidence for local degeneration and requirement of the ubiquitin-proteasome system. Neuron 38, 871-885.

Weaver A.M., Karginov A.V., Kinley A.W., Weed S.A., Li Y., Parsons J.T. and Cooper J.A., 2001. Cortactin promotes and stabilizes Arp2/3-induced actin filament network formation. Curr Biol. 11(5):370-4.

Weed S.A. and Parsons J.T., 2001. Cortactin: coupling membrane dynamics to cortical actin assembly.Oncogene 20(44):6418-34.

Weston, C., Yee B, Hod, E. and Prives, J., 2000. agrin-induced acetylcholine receptor clustering is mediated by the small guanosine triphosphatases Rac and Cdc42. Journal of Cell Biology 150, 205-212.

Widmer, F., Caroni, P., 1990. Identification, localization, and primary structure of CAP-23, a particle-bound cytosolic protein of early development. Journal of Cell Biology 111, 3035-3047.

Williamson, T.L., et al., 1988. Absence of neurofilaments reduces the selective vulnerability of motor neurons and slows disease caused by a familial amyotrophic lateral sclerosis-linked superoxide dismutase 1 mutant. Proc.Natl.Acad.Sci U.S.A. 95, 9631-9636.

Williamson, T.L. and Cleveland, D.W., 1999. Slowing of axonal transport is a very early event in the toxicity of ALS-linked SOD1 mutants to motor neurons. Nat.Neurosci. 2, 50-56.

Willmann, R., and C. Fuhrer., 2002. Neuromuscular synaptogenesis: clustering of acetylcholine receptors revisited. Cell Mol Life Sci. 59:1296-316.

Woldeyesus, M.T., Britsch, S., Riethmacher, D., Xu, L., Sonnenberg-Riethmacher, E., Abou-Rebyeh, F., Harvey, R., Caroni, P. & Birchmeier, C., 1999. Peripheral nervous system defects in erbB2 mutants following genetic rescue of heart development. Genes and Development 13, 2538-2548.

Wong, P.C. et al., 1995. An adverse property of a familial ALS-linked SOD1 mutation causes motoneuron disease characterized by vacuolar degeneration of mitochondria. Neuron 14, 1105-1116.

Xia, C.H. et al., 2003. Abnormal neurofilament transport caused by targeted disruption of neuronal kinesin heavy chain KIF5A. J.Cell Biol. 161, 55-66.

Yamagata, M., Sanes, J.R., and Weiner, J.A., 2003. Synaptic adhesion molecules. Curr.Opin.Cell Biol. 15, 621-632.

Yang, X., Li, W., Prescott, E.D., Burden, S.J. and Wang, J.C., 2000. DNA topoisomerase IIbeta and neural development. Science 287, 131–134.

Yang, J.F., Cao, G., Koirala, S., Reddy, L.V., Ko, C.P., 2001a. Schwann cells express active agrin and enhance aggregation of acetylcholine receptors on muscle fibers. Journal of Neuroscience 21, 9572-9584.

Yang, X., Arber, S., William, C., Li, L., Tanabe, Y., Jessell, T.M., Birchmeier, C., Burden, S.J., 2001b. Patterning of muscle acetylcholine receptor gene expression in the absence of motor innervation. Neuron 30, 399-410.

Yee, W.C. and Pestronk, A. Mechanisms of postsynaptic plasticity: remodeling of the junctional acetylcholine receptor cluster induced by motor nerve terminal outgrowth. J.Neurosci. 7, 2019-2024 (1987).

Yoshihara, C.M., and Z.W. Hall., 1993. Increased expression of the 43-kD protein disrupts acetylcholine receptor clustering in myotubes. J Cell Biol. 122:169-79.

Zhai, Q. et al., 2003. Involvement of the ubiquitin-proteasome system in the early stages of Wallerian degeneration. Neuron 39, 217-225.

Zhang, B., Tu, P., Abtahian, F., Trojanowski, J.Q. and Lee, V.M., 1997. Neurofilaments and orthograde transport are reduced in ventral root axons of transgenic mice that express human SOD1 with a G93A mutation. J.Cell.Biol. 139, 1307-1315.

Zhang, X.L., N. Topley, T. Ito, and A. Phillips., 2005. Interleukin-6 regulation of transforming growth factor (TGF)-beta receptor compartmentalization and turnover enhances TGF-beta1 signaling. J Biol Chem. 280:12239-45.

Zhen, G.L., Wang, Q., Zhou, J.Z., Wang, J., Luo, Z., Liu, M., HE, X., Wynschaw-Boris, A., Xiong, W.C., Lu, B., Mei, L., 2002. Regulation of AChR clustering by dishevelled interacting with MuSK and PAK1. Neuron 35, 489-505.

Zhou, H., Glass, D.J., Yancopoulos, G.D. and Sanes, J.R., 1999. Distinct domains of MuSK mediate its abilities to induce and to associate with postsynaptic specializations. J. Cell Biol. 146, 1133–1146.

Zito, K. and Svoboda, K., 2002. Activity-dependent synaptogenesis in the adult Mammalian cortex. Neuron 35, 1015-1017.

Zou, D.J., and Cline, H.T., 1999. Postsynaptic calcium/calmodulin-dependent protein kinase II is required to limit elaboration of presynaptic and postsynaptic neuronal arbors. J.Neurosci. 19, 8909-8918.

Zuo, Y. et al. Fluorescent proteins expressed in mouse transgenic lines mark subsets of glia, neurons, macrophages and dendritic cells for vital examination. J.Neurosci. 24, 10999-11009 (2004).

Appendix 1 Cholesterol and rafts stabilize the postsynapse at the neuromuscular junction

EMBO J. (2006), 25 (17), 4050-60.

Raffaella Willmann*, San Pun§, Lena Stallmach*, Gayathri Sadasivam*, Alexandre Ferrao Santos§, Pico Caroni§, and Christian Fuhrer*

*Department of Neurochemistry, Brain Research Institute, University of Zürich, Winterthurerstrasse 190, CH-8057 Zürich, Switzerland

§Friedrich Miescher Institute for Biomedical Research, Maulbeerstrasse 66, CH-4058 Basel, Switzerland

Summary

Stabilization and maturation of synapses are important for the development and function of the nervous system, but the underlying in vivo mechanisms remain poorly characterized. We found that cholesterol stabilizes clusters of synaptic acetylcholine receptors (AChRs) in denervated muscle in vivo and in nerve-muscle explants in vitro. In paralyzed muscles cholesterol stabilized synaptic AChRs and triggered maturation of nerve-sprout induced AChR clusters into pretzel shape. Cholesterol also stabilized AChR clusters in cultured src-/-;fyn-/- myotubes, while disruption of lipid rafts by cholesterol-sequestering methyl-β-cyclodextrin disassembled AChR clusters in wild-type myotubes and nerve-muscle explants. Postsynaptic proteins including AChRs, rapsyn, MuSK and Src-family kinases were stronlgy enriched in rafts prepared from wild-type myotubes. Raft contents and the enrichment of postsynaptic proteins into rafts were decreased in src-/-;fyn-/- myotubes, in which AChR cluster stability is compromised, but were normalized by cholesterol treatment. These results provide evidence that cholesterol, lipid rafts and Src-kinases are critical components of a mechanism for the stabilization of postsynaptic apparatus at neuromuscular junctions.

Introduction

Synaptogenesis is a key process in the development and function of the nervous system. In a first phase of synaptogenesis, postsynaptic neurotransmitter receptors and associated proteins accumulate underneath active zones of nerve terminals to form a postsynaptic density important in regulating further signaling at the forming synapse. In cultured neurons, some protein signals triggering postsynaptic differentiation are known, e.g. neurexins and neuroligins (Chih et al., 2005; Graf et al., 2004), ephrinB and EphB receptors (Dalva et al., 2000), or Narp (O'Brien et al., 2002; O'Brien et al., 1999). Non-protein factors such as cholesterol are also important: glia-derived cholesterol induces synaptogenesis in cultured retinal ganglion cells (Goritz et al., 2005; Mauch et al., 2001), although its specific role in postsynaptic assembly has not been analyzed. The in vivo relevance of the protein signals and of cholesterol, and many aspects of their mechanism of action remain unknown. In a second phase of the synaptogenesis process, some synapses and postsynaptic densities mature and are stabilized, while others are eliminated. While neural activity is known to regulate this process (Carlisle and Kennedy, 2005; Cohen-Cory, 2002), the effector machinery in synapse stabilization is poorly understood.

Cholesterol, along with sphingolipids, is enriched in subcompartments of the cellular membrane system, also known as lipid rafts. These regulate signal transduction through association with signalling proteins (Brown and London, 1998; Golub et al., 2004; Simons and Toomre, 2000). Rafts can act as floating platforms able to diffuse laterally within the plasma membrane, bringing together activated receptors and transducer molecules. In addition, specific trafficking pathways specifically involve lipid raft compartments. Lipid rafts are involved in aspects of synaptic function in cultured cells. Thus, depletion of cholesterol leads to loss of surface AMPA receptors and of synapses in hippocampal neurons (Hering et al., 2003). In ciliary neurons, lipid rafts are necessary for the maintenance of α7 neuronal nicotinic acetylcholine receptors (AChRs) in synapse-associated clusters (Bruses et al., 2001). Furthermore, at the neuromuscular junction (NMJ), the presence of plasmalemmal cholesterol is necessary for proper AChR gating functions (Barrantes, 1993), and AChRs depend on lipid rafts for

their trafficking toward the plasma membrane in transfected heterologous cells (Marchand et al., 2002). However, the relevance of rafts and cholesterol for synaptogenesis in vivo, and the identity of the signaling pathways operating through rafts, have remained unclear.

During NMJ formation, myotubes respond to neural agrin, assembling AChRs at nascent synapses (Gautam et al., 1996; McMahan, 1990). This scaffolding function is assigned to MuSK, the trans-membrane kinase that translates agrin into a clustering signal (Apel et al., 1997; Glass et al., 1996). Besides MuSK and AChR, rapsyn is the third essential protein for the AChR clustering process (Gautam et al., 1995; Marangi et al., 2001). Its association to AChR increases in response to agrin, mediates binding to cytoskeletal proteins (Gervasio and Phillips, 2005; Moransard et al., 2003), and is important for clustering (Yoshihara and Hall, 1993).

During the maturation of NMJs, plaque-shaped AChR clusters are stabilized, and mature into pretzel-shaped configurations, with AChRs located at the crests of postjunctional folds. AChR half-life time is highly increased during NMJ maturation, and proteins associated with this synapse are selectively produced by subsynaptic nuclei (Sanes and Lichtman, 2001). The mechanisms mediating postsynaptic stabilization differ from those involved in synapse induction, and much less is known about them (Huh and Fuhrer, 2002; Willmann and Fuhrer, 2002). Essential players include the utrophin-complex with its components dystroglycan and dystrobrevin (Grady et al., 1997; Grady et al., 2000; Jacobson et al., 2001). In addition, Src-family kinases (SFKs) play an important role in the maturation process. These kinases are activated by agrin (Mittaud et al., 2004; Mittaud et al., 2001), and in cultured src-/-;fyn-/- myotubes, agrin- or laminin-induced AChR clusters are unstable and disassemble rapidly after withdrawal of these factors (Marangi et al., 2002; Smith et al., 2001). Since SFKs functions are specifically associated with lipid rafts, these results have raised the possibility that raft-dependent processes might be involved in postsynaptic apparatus maturation and maintenance through SFKs.

To investigate mechanisms of postsynaptic maturation, we determined whether, and through what signaling molecules, cholesterol and lipid rafts might stabilize NMJs in vivo and in vitro. We found that the addition of cholesterol stabilizes NMJs, and pro-

motes their maturation from patch- to pretzel-type configurations in vivo. Cholesterol also stabilizes AChR clusters in cultured src-/-;fyn-/- myotubes. AChRs, rapsyn, MuSK and members of the utrophin-complex reside in cholesterol-rich lipid rafts in cultured myotubes, and raft disruption disassembles AChR clusters. In src-/-;fyn-/- myotubes, raft association of AChRs and MuSK is reduced but normalized by cholesterol addition.

Results

Cholesterol stabilizes AChR clusters in vivo

To investigate a possible role of cholesterol and lipid rafts in promoting postsynaptic apparatus maintenance in vivo, we analyzed the state of assembly of AChR clusters at denervated NMJs in the absence or presence of exogenous cholesterol. The sciatic nerve was cut in 1-month old mice, and AChR clusters were visualized 12 days later in two DeSyn muscles (lateral gastrocnemius and medial gastrocnemius), which exhibit substantial postsynaptic cluster disassembly under these experimental conditions (Pun et al., 2002). To visualize denervated synaptic sites, we counterstained muscle sections with an antibody against p75, a protein upregulated in Schwann cells in the absence of nerve contact (Taniuchi et al., 1986) As expected, denervated synaptic sites exhibited only remnants of AChR clusters after 12 d of denervation (Fig. 1A; note irregular AChR labeling patterns, with only small regions of intense labeling). In contrast, when cholesterol was applied daily to denervated muscles, starting 5 days after denervation, AChR signals at denervated synaptic sites were much better preserved (Fig. 1A; note that p75 signals were not affected by the cholesterol treatment). These AChR signals were comparable to clusters in non-denervated control animals (not shown, but see Pun et al., 2002). A quantitative analysis of AChR labeling intensities revealed that synaptic sites had lost most of their AChR signal 12 d after denervation, but that the synaptic signal was largely preserved in the presence of exogenous cholesterol (Fig. 1C).

To investigate AChR cluster protection by cholesterol under more challenging experimental conditions, we analyzed nerve-muscle explant preparations of soleus maintained at 37ºC in Ringer solution supplemented with calcium. To reliably identify synaptic sites, we carried out these experiments using transgenic mice expressing a synaptophysin-GFP construct in neurons (Thy1-spGFPmu; De Paola et al., 2003). Under these experimental conditions, many synaptic sites lost most of their AChR signal after 3 h ex vivo, such that only about half the synapses appeared normal while the others had only low-intensity AChR label (Fig. 1B, C). Inclusion of the cholesterol sequestering agent methyl-β-cyclodextrin, which disrupts lipid rafts (Ma et al., 2003; Simons and Toomre, 2000; Tansey et al., 2000), accelerated the loss of AChR signal (Fig. 1B, C). In contrast, inclusion of cholesterol in the culture medium protected most AChR clusters (Fig. 1B, C).

To determine whether cholesterol might also promote the assembly of new AChR clusters in vivo, we carried out cholesterol supplementation experiments in lateral gastrocnemius muscle chronically treated with Botulinum toxin A. These experimental conditions (lateral gastrocnemius in 1-month old mice, toxin applications every 4th day for a total of 20 days) induce the disassembly of postsynaptic apparatus at NMJs, a massive nerve sprouting response, and induction of small ectopic AChR plaques along the nerve sprouts (Fig. 2A, B, left panels; see also Santos and Caroni , 2003). Daily local applications of cholesterol from day 10 of the BotA treatment, i.e. at a time when NMJ disassembly and nerve sprouting were not yet pronounced (Santos and Caroni, 2003), led to a suppression of the AChR cluster disassembly process, which was accompanied by a suppression of nerve sprouting and of ectopic AChR plaque induction by sprouts in these paralyzed muscles (Fig. 2A, right panels). The resulting AChR signals appeared very similar to those in non-treated control animals (not shown; but see Santos and Caroni, 2003). Significantly, initiation of the cholesterol treatment at day 15, when sprouting was well advanced (Santos et al., 2005), led to the assembly of large, pretzel-shaped ectopic AChR clusters along the sprouts (Fig. 2B).

Taken together, these data provide evidence that local applications of exogenous cholesterol in vivo protect AChR clusters against denervation-induced disassembly,

and promote the maturation of sprout-induced ectopic AChR clusters in paralyzed muscles from an embryonic-type plaque shape into a pretzel shape. We conclude that cholesterol is an important factor for the maturation and stabilization of the NMJ in vivo.

Cholesterol stabilizes AChR clusters in cultured src-/-;fyn-/- myotubes

To analyze the mechanism of action of cholesterol in stabilizing AChR clusters, we turned to aggregation assays in cultured myotubes. Furthermore, we took advantage of cells from mice lacking Src and Fyn, where AChR clusters are normally induced by agrin or laminin treatment, but disassemble within a few hours after removal of these factors from the medium (Marangi et al., 2002; Smith et al., 2001). We treated src-/-;fyn-/- myotubes with agrin, withdrew agrin upon completion of the clustering process, and determined whether the addition of cholesterol might stabilize AChR clusters in the mutant myotubes. We found that after 5 h, cholesterol-treated cells showed the same number of AChR clusters as cells from which agrin was not withdrawn (Fig. 3). Cells from which agrin was withdrawn for 5 h, without addition of cholesterol, showed a low cluster number, comparable to the level of spontaneous clustering. In wild-type cells, clusters were very stable following removal of agrin, as published previously (Ferns et al., 1996; Marangi et al., 2002; Smith et al., 2001). This stability prohibited assessing significant effects of cholesterol.

We next determined whether cholesterol might compensate for agrin withdrawal by enhancing signaling processes involved in the formation of the NMJ. Cholesterol addition to wild-type myotubes did not induce formation of AChR clusters (Fig. 4A). In addition, cholesterol did not lead to phosphorylation of MuSK or the β subunit of AChRs, unlike agrin (Fig. 4B, C). AChR β phosphorylation is a known requirement of efficient receptor clustering and cytoskeletal linkage (Borges and Ferns, 2001). Taken together, our data show that cholesterol stabilizes AChR clusters in cultured myotubes without activating agrin/MuSK signaling.

The proteins involved in AChR clustering reside in cholesterol-rich lipid rafts in muscle

Cholesterol is a key component of lipid rafts, and its action in cluster stabilization might involve raft-dependent processes. We therefore prepared and analyzed rafts from cultured wild-type myotubes using a well-established protocol (Muller, 2002; Muller et al., 2002a; Muller et al., 2002b; Nishio et al., 2004; Ostrom et al., 2004; Rhainds et al., 2004; Riddell et al., 2001; Song et al., 1996a; Zhang et al., 2005). Cell homogenates were floated on a discontinuous sucrose gradients, and fractions were analyzed by immunoblots. The raft fraction was found at the interface between 5% and 35% sucrose and further defined by typical raft markers such as caveolin-3, flotillin-2, cholesterol and the shingolipid, ganglioside GM1. All these markers, including cholesterol, were highly enriched in fractions 4-6 (Fig. 5A, B), which we therefore designated the raft fractions, also because they contain the border between 5% and 35% sucrose. Measurement of protein concentration showed that fractions 4-6 contain little overall protein, and that most protein was found at the bottom of the gradient, in fractions 8-12 which contained free (non-raft associated) cellular proteins (Fig. 5C). Another negative control was α-tubulin, which does not associate with rafts and was mostly recovered in the free fractions (Fig. 5A). These controls established the validity of the method for preparation of cholesterol-enriched lipid rafts from myotubes.

We probed fractions for the content of postsynaptic proteins. We found the AChR highly enriched in rafts, as 70% of the total receptor present in all fractions of the gradient resided in fractions 4-6 (Fig. 5D, E). Elements of the agrin signaling pathway such as MuSK and rapsyn were similarly enriched in rafts. The same was true for SFKs (Fig. 5D, E), which are known from other cell types to be typical constituents of lipid rafts(Resh, 1999). Finally, β-dystroglycan and α-dystrobrevin-2, members of the utrophin-complex important for NMJ stabilization (Grady et al., 2000; Jacobson et al., 2001), were also recovered efficiently in rafts. An overnight incubation with agrin, sufficient to produce maximal AChR clustering, did not detectably affect the fractions of AChR, rapsyn and MuSK partitioning into lipid rafts (data not shown).

Disruption of lipid rafts disassembles AChR clusters

Besides raft-association of proteins, another standard tool to investigate the role of lipid rafts in a given cellular process is to disrupt the rafts by methyl-β-cyclodextrin (MβCD). We treated wild-type myotubes with agrin to induce maximal AChR clusters and then added MβCD for 1-1.5 hrs. The number of clusters of normal size and morphology was strongly reduced by MβCD (Fig. 6). Upon MβCD treatment, we noticed many smaller clusters and areas containing cluster fragments. The myotube morphology was unaffected, and following removal of MβCD the myotubes lived for extended periods of time, like untreated controls (not shown). This indicates that the MβCD effect was specific and not a consequence of impaired myotube health. These data show that the integrity of cholesterol-containing rafts is required to maintain AChR clusters.

Impaired partitioning of postsynaptic proteins into rafts in the absence of Src and Fyn, and rescue by cholesterol

To understand the molecular mechanism through which cholesterol and rafts stabilize AChR clusters, we analyzed the composition of rafts prepared from src-/-;fyn-/- myotubes, in which clusters are unstable. Although rafts from mutant myotubes were strongly enriched for ganglioside GM1, caveolin-3, flotillin-2 and cholesterol (Fig. 7A, B), their protein contents were strongly reduced (Fig. 7C). Interestingly, significantly less of the total AChR, rapsyn and MuSK were in rafts from src-/-;fyn-/- myotubes compared to wild-type. The decrease was 30% for AChRs, 40% for rapsyn and 23% for MuSK (Fig. 7D).

This decreased raft association could have two reasons: Src and Fyn may recruit postsynaptic proteins into rafts and/or maintain normal numbers of rafts in a myotube. To investigate these possibilities, we quantitated raft partitioning of typical raft markers. 19% less of total cholesterol were found in the raft fractions 4-6 in src-/-;fyn-/- myotubes when compared to wild-type (Fig. 7E) and the trend was similar for caveolin-3 (Fig. 7F). Overall cellular levels of cholesterol, quantified per μg of cellular protein, were normal in the mutants, excluding overall nonspecific effects from the lack of Src and Fyn (Fig. 7G). These data suggest that src-/-;fyn-/- myotubes have less rafts than wild-type cells. A 19% reduction of rafts does not fully explain a 30% reduction of

raft-AChRs in the mutants, hence Src and Fyn most likely also contribute to recruitment of AChRs (and rapsyn and MuSK) into rafts.
Importantly, cholesterol addition to src-/-;fyn-/- myotubes not only stabilized AChR clusters (Fig. 3), but restored the raft partitioning of AChRs and MuSK back to normal (Fig. 7D). Likewise, the raft enrichment of cholesterol itself and of caveolin was normalized by cholesterol treatment (Fig. 7E, F). Thus, while the absence of Src and Fyn decreases the number of rafts and the recruitment of postsynaptic proteins into rafts, cholesterol addition overcomes this, normalizing the enrichment of AChR and MuSK in rafts. These data provide loss- and gain-of-function correlations that strongly implicate a role of intact rafts in AChR cluster stabilization.

Discussion

We have shown that cholesterol is an important factor for the stabilization and maturation of the NMJ in vivo and in vitro. This involvement of cholesterol does not stem from activation of the agrin/MuSK signaling pathway, but instead from promoting the incorporation of postsynaptic proteins into lipid rafts. We further provide evidence that Src and Fyn promote postsynaptic apparatus stabilization by enhancing the association of critical postsynaptic proteins with lipid rafts. We thus provide gain- and loss-of-function data indicating that a common mechanism comprising cholesterol, rafts and SFKs is at the core of stabilization of the NMJ postsynaptic apparatus.

Cholesterol promotes postsynaptic stabilization in vivo and in cultured myotubes
Our data are the first to show that cholesterol promotes synaptic stability in vivo. Cholesterol addition to denervated adult DeSyn gastrocnemius muscle during 12 days prevented the postsynaptic disassembly that would normally occur. Furthermore, soleus nerve-muscle explants exhibited substantial AChR pretzel disassembly within 3 hours, which was largely prevented by cholesterol treatment. Finally, Botulinum toxin A caused massive nerve sprouting and induction of plaque-shaped AChR clusters along the sprouts. When applied before this response, cholesterol stabilized exist-

ing AChR pretzels at NMJs; when applied after massive sprouting had started, cholesterol treatment promoted maturation of sprout-induced AChR cluster to adopt adult-type pretzel shape. Cholesterol addition, at the time of agrin withdrawal, also stabilized AChR clusters in cultured src-/-;fyn-/- myotubes.

Conversely, sequestering cholesterol by MβCD treatment, leading to disruption of lipid rafts, accelerated the disassembly of AChR pretzels in explants of soleus muscle, and disrupted clusters of AChRs in wild-type myotubes in culture. These data establish cholesterol as a factor for stabilization and maturation of the postsynaptic apparatus at the NMJ.

Cholesterol action in postsynaptic stabilization occurs via lipid rafts

To investigate the mechanism of action of cholesterol, we used myotubes in culture. We found that AChRs, rapsyn, MuSK, SFKs, α-dystrobrevin-2 and β-dystroglycan were highly concentrated in rafts, and the degree of concentration, ca. 70% of total, was similar to cholesterol. Importantly, cholesterol addition to cultured src-/-;fyn-/- myotubes increased the raft association of AChRs and MuSK. It also augmented raft participation of cholesterol in these cells, suggesting that the cholesterol treatment increased the number of lipid rafts.

These observations, together with the stabilizing effect of cholesterol on AChR clusters and the disassembly of clusters by the raft-disrupting agent MβCD, lead to the conclusion that cholesterol and lipid rafts are key players in stabilizing the NMJ postsynaptic apparatus, by promoting the raft-association of postsynaptic proteins.

Cholesterol, lipid rafts and SFKs: a core mechanism for stabilization of the postsynapse

We used src-/-;fyn-/- myotubes to investigate signaling pathways by which cholesterol and lipid rafts stabilize clusters of AChRs. The following observations indicate that cholesterol and rafts act in concert with SFKs in postsynaptic stabilization. First, the absence of Src and Fyn causes disassembly of AChR clusters in cultured myotubes (Marangi et al., 2002; Smith et al., 2001), similar to the effects of disrupting lipid rafts by MβCD. We have recently found that SFKs stabilize adult NMJs in vivo, since elec-

troporation of dominant-negative, kinase-inactive Src constructs into adult mouse soleus muscle leads to disassembly of pretzel-shaped AChR clusters (G. Sadasivam, R. Willmann, M.A. Rüegg, C. Fuhrer, unpublished observations). The stabilizing action of SFKs in vivo is similar to the effect of cholesterol addition as reported in Figures 1 and 2. Second, SFKs themselves are enriched in lipid rafts, suggesting that their action in postsynaptic stabilization may occur through the rafts. We have recently shown that in cultured src-/-;fyn-/- myotubes, cytoskeletal linkage of AChRs is weakened and, following agrin withdrawal, AChR β phosphorylation and AChR-rapsyn interaction rapidly decrease, suggesting that SFKs stabilize cytoskeletal links, phosphorylation and protein interactions of the AChR in maintaining the postsynaptic apparatus (G. Sadasivam, R. Willmann, M.A. Rüegg, C. Fuhrer, unpublished observations). The present data suggest that such SFK-action occurs through lipid rafts, in which all of the involved protein partners are enriched. Third, in src-/-;fyn-/- myotubes raft association of postsynaptic proteins is reduced due to a decrease in the raft number and loss of Src-Fyn-dependent recruitment of postsynaptic proteins into the rafts. Fourth, cholesterol addition to src-/-;fyn-/- myotubes restores raft numbers, raft association of postsynaptic proteins and stability of AChR clusters.

The emerging model is that Src and Fyn mediate raft integrity and recruitment of postsynaptic apparatus components into rafts, in the process of NMJ stabilization. Bringing postsynaptic proteins together in a common cellular compartment, rafts, may then allow Src and Fyn to act upon AChRs by phosphorylating the β subunit and maintaining interaction of the AChR with rapsyn and the cytoskeleton.

Both SFKs and lipid rafts are known in other cell types to assemble signaling steps that locally organize the cytoskeleton, e.g. by favoring activation of Rho-like GTPases and promoting actin assembly (Golub et al., 2004; Rodgers et al., 2005), or by organizing microtubules (Cox and Maness, 1993; del Pozo et al., 2004; Palazzo et al., 2004). Thereby specialized domains can be formed at the cell surface as represented by focal adhesion sites, and these specializations are stabilized through many participating cytoskeletal elements. as I understand it, what you find is that Src/Fyn enhance raft contents - it seems to me confusing to attribute downstream events at cluster as-

sembly to Src/Fyn (more consistent with the data: that the downstream event are due to higher raft contents)

Interestingly, the mechanism of cholesterol action in postsynaptic stabilization does not involve a re-activation of those pathways that lead to formation of the NMJ: we find that cholesterol addition to myotubes does not cause AChR clustering, activation of MuSK or phosphorylation of AChR βsubunits. Since cholesterol nonetheless stabilizes AChR clusters, this show that the pathways for stabilization of postsynaptic clusters are different from those for induction of cluster formation.

Lipid rafts may act dynamically in cluster stabilization

Data discussed above describe what cholesterol, rafts and SFKs do in postsynaptic stability, but where in a muscle cell do they act? We find 70% of all AChRs in rafts in myotubes and this is more than the surface pool of AChRs (60% in myotubes; Moransard et al., 2003) and more than the intracellular receptor pool (40%). Most likely, surface as well as intracellular AChRs associate with lipid rafts, and this opens many possibilities for the subcellular location of raft action.

At NMJ, rafts do not seem to act by forming a membrane-bound stable platform that increasingly incorporates postsynaptic proteins like a scaffold. Although cholesterol addition normalizes the defective raft association of AChRs and MuSK in src-/-;fyn-/- myotubes, rapsyn is unaffected and overall remains less raft-associated (Fig. 7D), yet under the same conditions, AChR clusters are stabilized to normal levels (Fig. 3). An equal raft association of AChRs and rapsyn, expected if rafts were to act like a static scaffold, is thus not necessary for a cluster to remain stable. At the same time, rapsyn:AChR stoichiometry and regulation of their interaction by agrin are important aspects in clustering (Moransard et al., 2003; Yoshihara and Hall, 1993). Taken together, these studies suggest that AChRs might not themselves be associated with a platform-like cluster of rafts, but with rapsyn and interacting proteins in a subsynaptic protein complex. Rafts appear as a more dynamic subcellular compartment, required for cluster stabilization without necessarily being part of the visible cluster, for example by serving as a continuous delivery zone for interacting proteins into the clusters.

The following observations support these notions. First, rafts not only reside at the plasma membrane, but also intracellularly, in the trans-Golgi network and in exocytic transport vesicles from the Golgi apparatus to the plasma membrane (Simons and Ikonen, 1997). In heterologous cells, rapsyn and AChRs are transported in such rafts to reach the cell surface (Marchand et al., 2002). Endocytosed vesicles, formed at the surface through raft-associated caveolae, merge with intracellular caveosomes and to a lesser degree with endosomes (Pelkmans et al., 2004). Thus rafts can act in intracellular trafficking pathways, not only by forming stable platforms at the surface. Second, overnight agrin treatment, sufficient to induce maximal AChR clustering, does not change the raft partitioning of postsynaptic proteins (Willmann and Fuhrer, unpublished observations). This is incompatible with the idea that rafts may stably coalesce at the surface and successively incorporate postsynaptic proteins to form a cluster. Third, along the same line, we have stained rafts in cultured myotubes with filipin (an autofluorescent ligand for cholesterol) or fluorescence-coupled cholera toxin and failed to see prominent colocalization with AChR clusters. Rather, raft signals were small and colocalized partially with markers of endosomes (Golub, Stallmach, Fuhrer and Caroni, unpublished observations). In muscle sections, cholera toxin did reveal an NMJ-like staining, but this was not visible in muscle that had been denervated for 2 days, a time interval when AChR clusters were still normal, implying that the synaptic raft staining was pre-synaptic originating from the nerve terminal (T. Golub and P. Caroni, unpublished observations).

Such observations imply two possibilities: the critical rafts of muscle, operating in cluster stabilization, may be a subpool not visible at clusters since they are inaccessible for staining with filipin or cholera toxin due to their intimate association with AChRs causing steric hindrance. In agreement with this, rafts in a cell are indeed known to exist in different subpopulations (Galbiati et al., 2001; Pike, 2004); the lipidic environment of AChRs does affect receptor channel properties, implying close receptor-lipid association (Barrantes, 1993); and raft association of AChRs in src-/-;fyn-/- myotubes is not reduced to zero but by 30%. More likely however, rafts themselves are not clustered at the postsynapse but present in other surface or intracellular membrane compartments, perhaps transport vesicles, that ensure delivery, incorpora-

tion and interactions of proteins into the postsynaptic apparatus. In such a way, rafts, containing cholesterol, SFKs, AChRs and other proteins, could ensure SFK-mediated steps that maintain the postsynaptic apparatus.

The interdependence and requirement of cholesterol, lipid rafts and SFKs in promoting stability at the NMJ is clear from data presented in this study. It remains to be investigated, *in vitro* and *in vivo*, how exactly these partners achieve postsynaptic stabilization and maturation, particularly with respect to trafficking pathways.

Materials and Methods

In vivo and ex vivo experiments.

Thy1-mGFPs and Thy1-spGFPmu reporter mice were as described (De Paola et al. 2003); all treatments were initiated when mice were 1-month old. Drugs were injected locally, subcutaneously (100 µl/mouse injection volumes). Botulinum toxin A (Allergan AG, Lachen, Switzerland) was applied at 0.02 U/g body weight every 4th day. Where indicated, cholesterol was applied daily (50 µm in injection solution). Nerve-muscle explants of soleus were maintained at 37ºC in calcium-supplemented Ringer for 3 hours, and then labeled with RITC-α-BT (2 µg/ml) for the analysis of AChR clusters. Where indicated, drugs in the incubation medium were 50 µm (cholesterol) and 10 mM (MβCD). Cryostat sections of unfixed muscles were postfixed (10 min, 3.5% formaldehyde in PBS) and labeled for immunocytochemistry as described (Pun et al., 2002). Fluorescent data were imaged and acquired using an Olympus (BX61) confocal microscope, Fluoview 4.1 software, and identical settings for all experiments belonging to one set (denervation, nerve-muscle explants, paralysis experiments). NMJ labeling intensities (integral of RITC-α-BT signal at individual NMJs) were derived from z-stacks using ImageJ software. Only NMJs lying en-face with respect to the plane of imaging were included in the analysis. For paralysis experiments, we analyzed muscle innervation patterns using reporter mice expressing mGFP in neurons, and whole mount preparations of muscles. Briefly, identified muscles were dissected, fixed in PBS with 3.5% formaldehyde (30 min, room temperature), washed, and counterstained with RITC-α-BT (2µg/ml).

Cell cultures and treatments. C2C12, src-/-;fyn-/- (clones DM11 and DM15), and their corresponding wild-type cells (clones SW5 and SW10) were propagated and fused to form myotubes as described earlier (Fuhrer et al., 1997; Marangi et al., 2002; Smith et al., 2001). To induce maximal AChR cluster formation, cells were treated with 1 nM recombinant neural agrin C-Ag12,4,8 (Fuhrer et al., 1997) overnight for 16 h. To withdraw agrin, cells were washed and incubated in agrin-free medium; this procedure was used before and shown to be efficient in removing the vast majority of agrin from cells (Mittaud et al., 2004). For cholesterol treatment, water-soluble cholesterol (Sigma; Fluka, Switzerland) was aliquoted in PBS, diluted in fusion medium immediately prior to use, and used at a final concentration of 50 µm if not specified otherwise. In methyl-β-cyclodextrin (MβCD) treatments, MβCD (Sigma) was diluted in fusion medium at 100 mM and used at a final concentration of 10 mM or 5 mM. We confirmed effective depletion of cholesterol from the cell membrane after incubation with 5 mM MβCD for 40-60 min: total cellular cholesterol content was reduced to 50-65% of untreated controls, and the use of fetal bovine serum-containing medium during the treatment had no effect on the cholesterol depletion (data not shown).
C2C12, SW5 and SW10 cells gave identical results in all assays and we refer to them commonly as wild-type cells. Likewise, DM11 and DM15 showed no clonal variation in all methods.

Preparation of lipid rafts.
We used a method that was shown before to be efficient for preparing lipid rafts from C2C12 myotubes (Song et al., 1996b), with slight modifications. Briefly, cells grown in 10 cm dishes were washed 2 times with ice-cold PBS containing 1 mM Na-orthovanadate (NaO). After addition of 1.5 ml Buffer A (Na-carbonate 0.5 M, pH 11; inhibitors cocktail as follows: NaO 1 mM, phenylarsine oxide 50 µm, p-nitrophenylphosphate 10 mM, NaF 50 mM, aprotinin 25 µg/ml, leupeptin 25 µg/ml), cells were quickly scraped and suspended using the pipette tip, then homogenized 2 times in a dounce homogenizer and finally sonicated 2 times for 10 seconds. The inhibitors were always prepared freshly and added to buffers just before use. The total extract (final volume: 2 ml) was quickly mixed with 2 ml 90% sucrose in Buffer B (Mes 25

mM, pH 6.5, NaCl 150 mM + inhibitor cocktail as above) at the bottom of a 13-ml tube and overlaid with 4 ml of 35% sucrose in Buffer C (buffer B + Na-carbonate 250 mM) and then with 4 ml of 5% sucrose in Buffer C, for a total volume of 12 ml. Samples were centrifuged for 17 h at 37'000 rpm in a Sorvall TH-641 rotor at 4°C. 1 ml-fractions were collected from the top and transferred into 3 ml ultraclear-tubes (Beckman). Samples for protein determination (50 µl), cholesterol determination (30 µl) and ganglioside GM1 detection (2 µl) were taken before diluting each fraction with 2 ml Buffer C. Fractions were then centrifuged for 50 min at 100'000 rpm in a Beckman TLA-100.3 rotor, supernatants were discarded and pellets were resuspended in Lämmli-buffer for SDS-Gel electrophoresis and Western blot.

Cell labeling and immunoprecipitation. For AChR stain, cells were incubated 40 minutes with rhodamine-coupled α-BT at 37°C, washed once in PBS at room temperature and then fixed in ice-cold methanol for 7 minutes at -20°C. Conventional fluorescence imaging was done using a Zeiss Axioskop 2 microscope equipped with a Hamamatsu Orcacam digital camera. For quantitation, compact clusters with intensities clearly higher than background and a minimal size of 5 µm were considered as detailed previously (Marangi et al., 2001; Marangi et al., 2002). Clusters were counted in at least 15 fields and experiments were repeated at least 3 times.
For precipitation of MuSK or AChRs, cell lysates were prepared. MuSK-antibodies followed by protein A-sepharose beads or biotin-α-BT followed by streptavidin-beads (Tox-P) were added as described before (Mittaud et al., 2004; Mittaud et al., 2001).

Protein and lipid detection.
Antibodies against phosphotyrosine (mixture of PY20 and 4G10); the conserved C-terminus of Src, Fyn, and Yes (src-CT); MuSK; rapsyn (Rap-1); β-dystroglycan; the AChR β subunit (mAb124); and the AChR α subunit (mAb35) were all used in Western blots as described previously (Fuhrer et al., 1999; Fuhrer and Hall, 1996; Marangi et al., 2001; Mittaud et al., 2001; Moransard et al., 2003). Antibodies against α-dystrobrevin-2 were a gift from Dr. D. Blake (Oxford, United Kingdom). Anti-caveolin-3 (Santa Cruz Biotechnology) was used at 1:2000, anti-flotillin 2/ESA clone 29 (Trans-

duction Laboratories) at 1:1000, and anti-α-tubulin clone DM1A (Sigma) at 1:500. Anti-p75 was as described (Pun et al, 2002). Densitometric analysis of Western blot signals was performed as done before (Marangi et al., 2001) using the software Image J (NIH, USA); the distribution of proteins in the lipid rafts fractions was quantitated by adding up the relative band densities of the raft fractions (4-6) and relating it to the sum of bands in all fractions within each experiment.

For detection of ganglioside GM1, 2µl of each fraction was applied to a nitrocellulose membrane, blocked with 5% milk in PBS and probed with horseradish peroxidase-coupled cholera-toxin subunit B (10ng/ml; Sigma; (Hering et al., 2003)). To measure cholesterol, 50µl of each fraction was analyzed with the Amplex Red cholesterol assay kit (Molecular Probes, Eugene, OR (Hering et al., 2003)) according to the manufacturer's instruction. Protein concentration was determined using the BCA protein assay kit (Pierce).

Statistical analysis.

All values are given as mean ± SEM. Significance was calculated with a t-Test (two-tailed, unequal variance) and is indicated as $p< 0.05$ (*) or $p< 0.01$ (**). In Figure Legends, n refers to the number of experiments.

Acknowledgements

We are grateful to Susanne Erb-Vögtli for cell culture. This work was supported by grants from the Swiss National Science Foundation, the Swiss Foundation for Research on Muscle Diseases, the Zürich Neuroscience Center (to C.F.), and the Novartis Research Foundation (to SP, AFS, PC).

Figure Legends

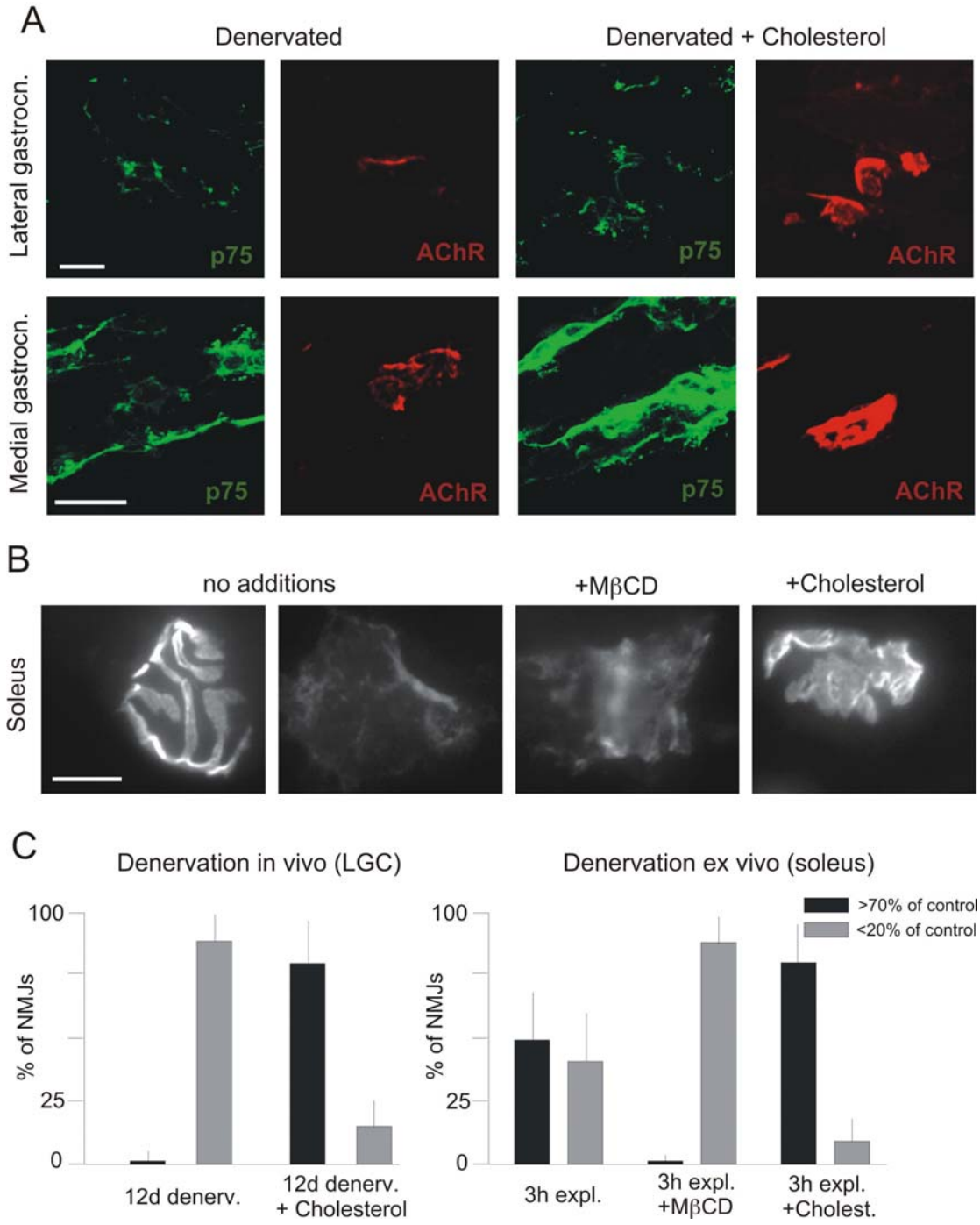

Fig. 1. Cholesterol stabilizes AChR clusters in denervated muscles. (A) Appearance of AChR clusters in two DeSyn muscles 12 days after denervation. Sciatic nerves were cut in 1-month mice; the absence of intact axons is confirmed by the expression of p75 in Schwann cells. Where indicated, cholesterol was applied daily, starting 5 days after denervation. (B) Examples of AChR clusters (RITC-α-BT) in soleus nerve-

muscle explants after 3 hours in vitro. (C) Quantitative analysis of data as shown in (A) (left) and (B) (right). AChR labeling intensities (RITC-α-BT) compared to controls; fractions of NMJs with signal at least 70%, or les than 20% of control values. N=300 AChR clusters (from 3 mice each). Bars: 40 (A) and 20 μm (B).

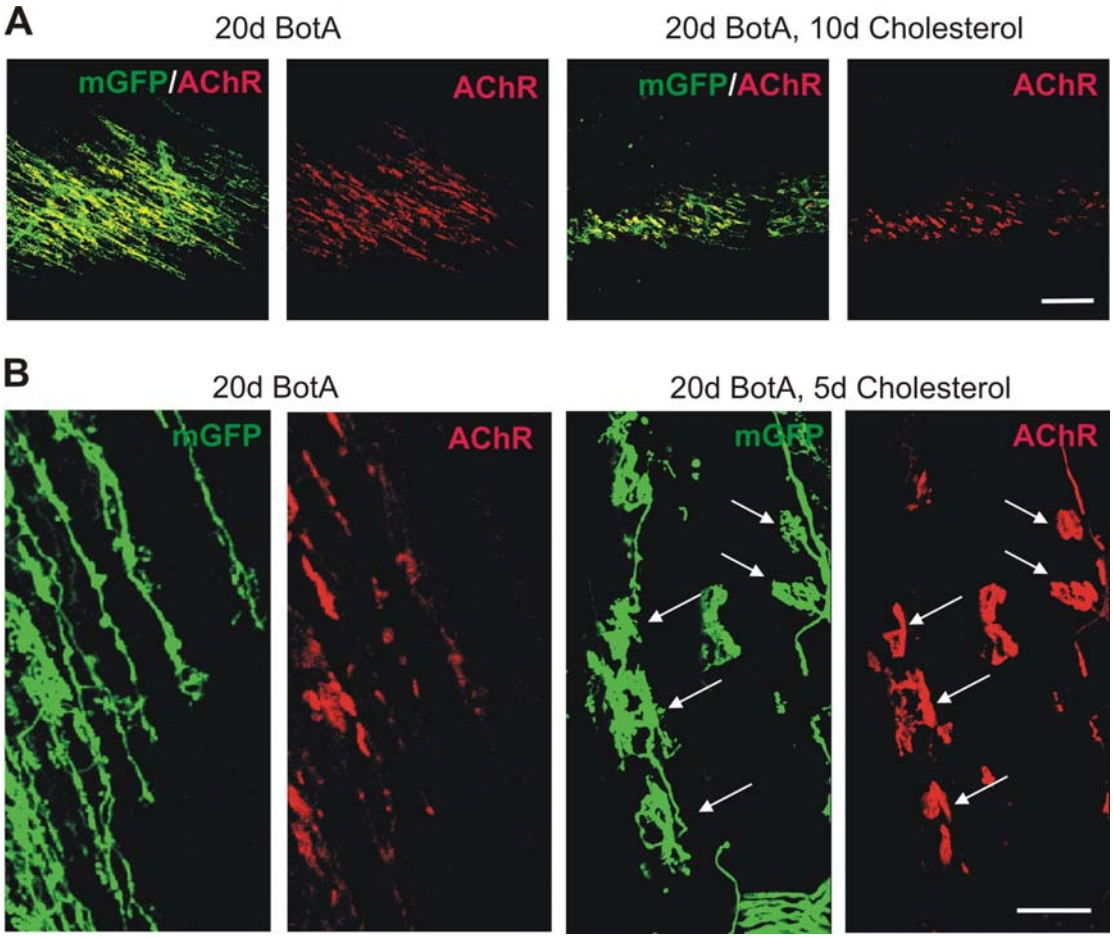

Fig. 2. Cholesterol promotes AChR cluster assembly at original and ectopic NMJs in paralyzed DeSyn muscles. Low- (A) and high-magnification (B) views of presynaptic nerves (mGFP) and postsynaptic AChR clusters (RITC-α-BT) in lateral gastrocnemius muscles treated with Botulinum toxin A (BotA). The chronic BotA treatment elicited a massive nerve sprouting response in this DeSyn muscle; cholesterol promoted AChR cluster assembly, and inhibited nerve sprouting. Note pretzel-shaped AChR clusters (arrows, right) induced by sprouts (arrows left) in the presence of exogenous cholesterol. Bars: 200 (A) and 40 μm (B).

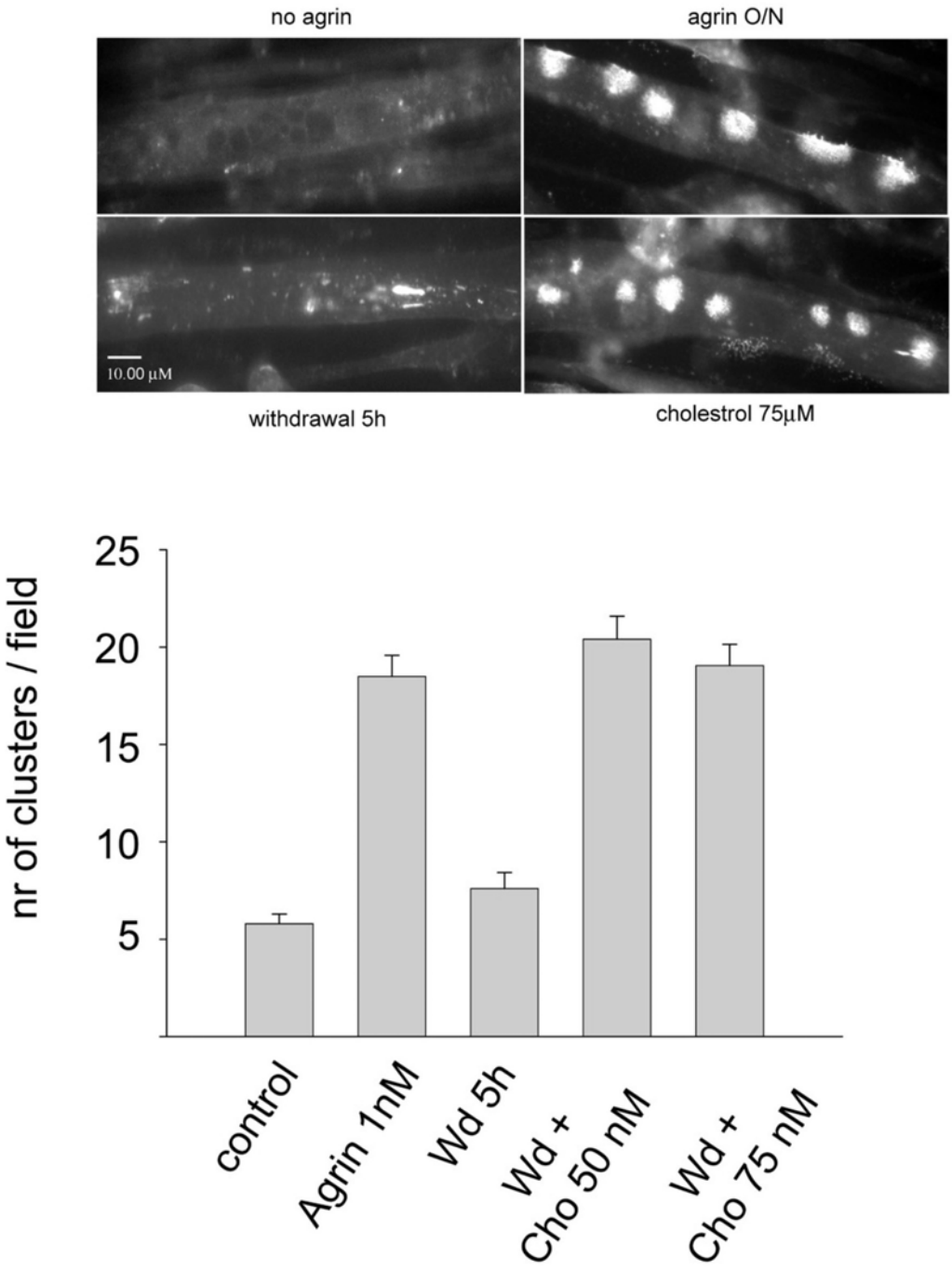

Fig. 3. Cholesterol stabilizes AChR clusters in src-/-;fyn-/- myotubes. (A) Cells were not treated or stimulated overnight with 1 nM agrin to induce AChR clusters (top

row). agrin was withdrawn, cells were washed and incubated for 5 h in agrin-free medium lacking (bottom left) or containing (bottom right) 75 µm cholesterol. Myotubes were stained with rhodamine-α-BT to visualize AChR clusters. (B) For cluster quantification, visual fields covering about 3 times the area of a panel shown in A were taken, and only compact clusters with a mimimum size of 5 µm were counted.

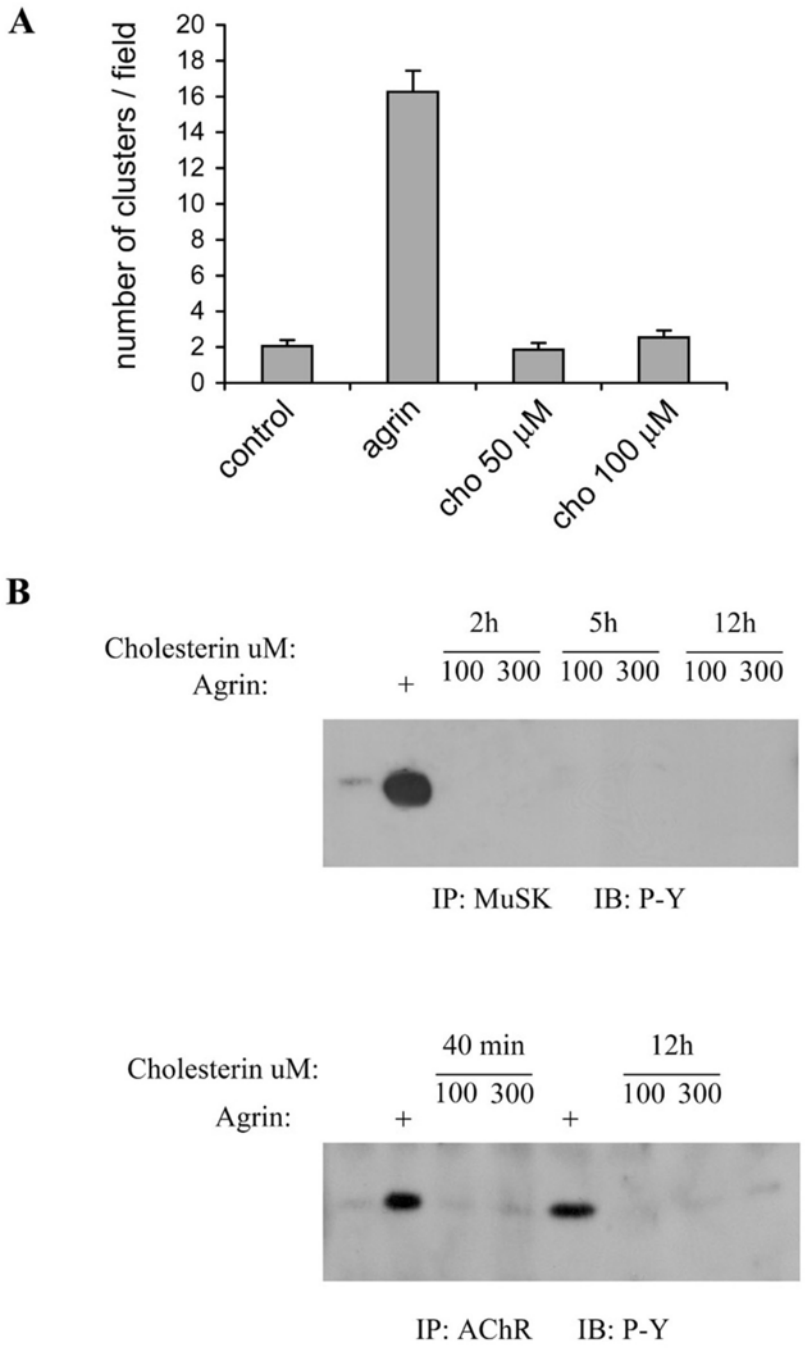

Fig. 4. Cholesterol does not induce AChR clustering and phosphorylation of MuSK and AChR β subunits. (A) Cholesterol or 1 nM agrin were added overnight to C2C12 myotubes. Cells were stained with rhodamine-α-BT and AChR clusters quantitated as in Figure 3. (B and C) C2C12 myotubes were treated with different doses of cholesterol, or with 1 nM agrin for 40 min, as indicated; c, untreated control. From cell

lysates, MuSK was immunoprecipitated (B) or AChRs were precipitated using biotin-α-BT and streptavidin-agarose (Tox-P, C). Phosphotyrosine immunoblotting detected phosphorylation of MuSK and AChR β subunits. The identity of these phosphoproteins was confirmed by reprobing with MuSK- or AChR β-specific antibodies (not shown).

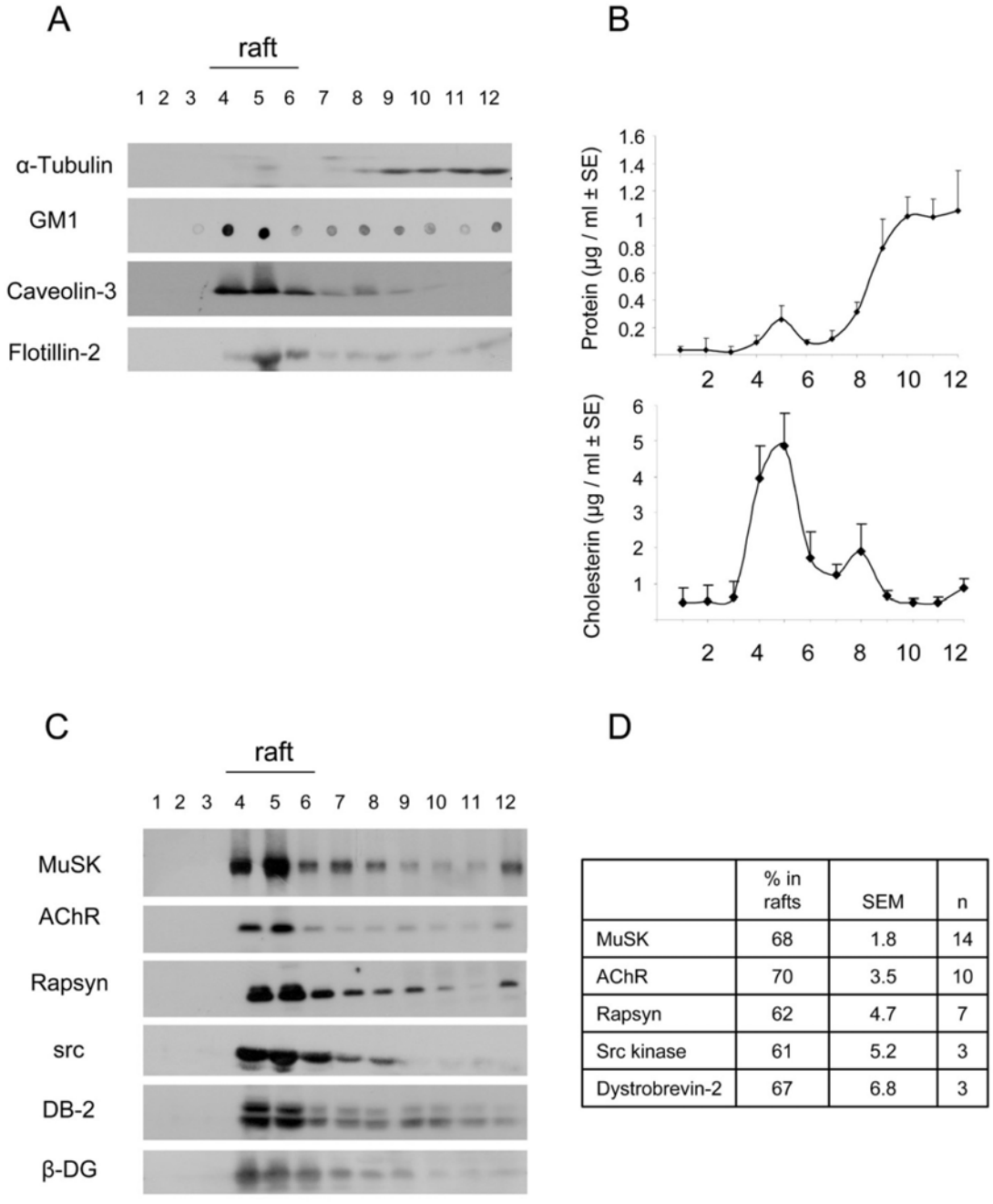

	% in rafts	SEM	n
MuSK	68	1.8	14
AChR	70	3.5	10
Rapsyn	62	4.7	7
Src kinase	61	5.2	3
Dystrobrevin-2	67	6.8	3

Fig. 5. Postsynaptic proteins associate with cholesterol-rich lipid rafts in myotubes. Rafts were prepared from wild type myotubes (C2C12 or clones SW10 and SW5), and fractions of the discontinuous sucrose gradients were collected. Fractions 9-12 represent the bottom gradient step (45% sucrose) containing the total cell extract. Fractions 5-8 represent the 35% sucrose layer and fractions 1-4 the top layer (5% sucrose). (A) Fractions were analyzed by immunoblotting (α-tubulin, caveolin-3, flotillin-2) or dot blotting (ganglioside GM1). Fractions 4-6 contain lipid rafts and α-tubulin served as a negative control. (B) Fractions were analyzed for the content of cholesterol, showing high enrichment in raft fractions 4-6 (n=4). (C) Protein assays of gradient fractions reveal the bulk of protein in the bottom fractions, illustrating the specificity of the raft preparation (n=4). (D) Fractions were subjected to immunoblotting, showing that MuSK, AChRs (β-subunit), rapsyn, SFKs, α-dystrobrevin-2 (α-DB-2) and β-dystroglycan (β-DG) all partition efficiently into rafts. (E) Blots as shown in D were quantitated by densitometric scanning. For each protein, the intensities of bands in raft fractions 4-6 were related to the sum of all fractions to quantify the percentage in rafts.

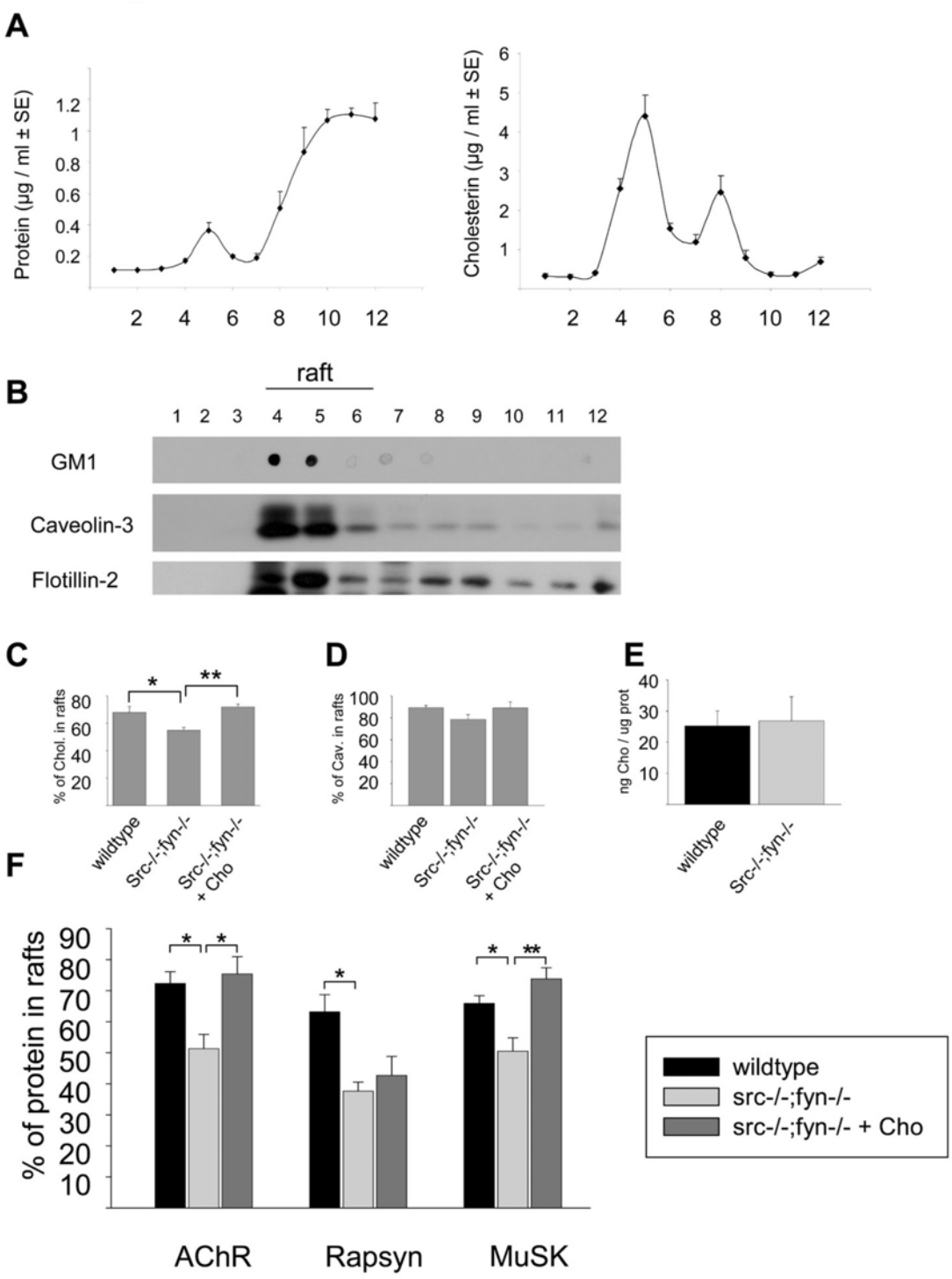

Fig. 6. Methyl-β-cyclodextrin (MβCD) disrupts AChR clusters in C2C12 myotubes. (A) C2C12 myotubes where first treated overnight with agrin (Ag) to induce AChR clusters. MβCD was then added in the continued presence of agrin, causing AChR

clusters to fragment and disappear, as revealed using rhodamine-α-BT staining. (B) Clusters of 5 μm minimal size were quantitated.

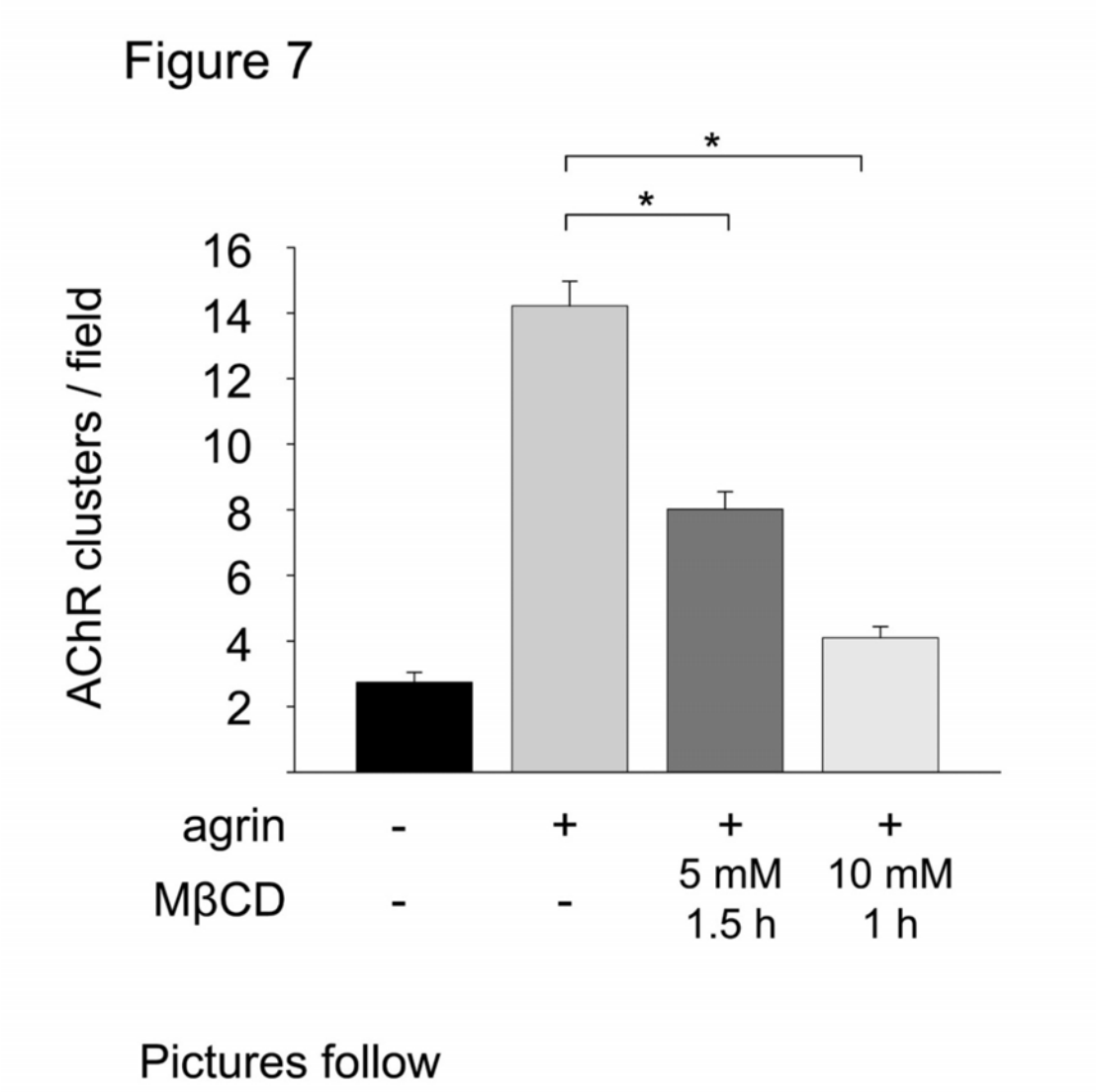

Fig. 7. to enhance the impact of this figure I would label graphs to emphasize that the data are from src/fyn mutant myotubes; I would also suggest to include profiles for control myotubes in (B) and (C)

In src-/-;fyn-/- myotubes, raft association of postsynaptic proteins is reduced but restored by cholesterol. (A-C) Characterization of rafts in src-/-;fyn-/- myotubes. Rafts were prepared from clones DM11 or DM15, and the content, in gradient fractions, of

ganglioside GM1, caveolin-3, flottilin-2 (A), cholesterol (B, n=12) and total protein (C, n=4) was analyzed. Markers are concentrated in raft fractions 4-6, with overall protein enriched at the gradient bottom (negative control). (D) Gradient fractions were analyzed for the content of AChR, rapsyn and MuSK, and the percentage of these proteins in raft fractions 4-6 was quantified as in Figure 5E. Wild-type cells (C2C12 or clones SW5 and SW10; n=3-7), src-/-;fyn-/- myotubes (n=4-6) and src-/-;fyn-/- myotubes treated with cholesterol (n=4-5) were used. src-/-;fyn-/- myotubes have significantly lower percentages of proteins in rafts, and cholesterol restores this in the case of AChR and MuSK. (E) Cells were treated as in D and the percentage of cholesterol in raft fractions 4-6 was quantitated. Raft association of cholesterol is lower in src-/-;fyn-/- myotubes (n=12) than in wild-type myotubes (n=8). Addition of cholesterol to the cell culture medium restores the amount of cholesterol in the raft fractions to the levels of wild-type myotubes (n=6). (F) Analysis as in E, examining caveolin-3 (Cav.). (G) The total amount of cholesterol, detected in total cell extracts, is the same in wild-type and src-/-;fyn-/- myotubes (n=8).

Appendix 2 Assembly, plasticity and selective vulnerability to disease of mouse neuromuscular junctions

Alexandre Ferrão Santos and Pico Caroni

J. Neurocytol. 2003, 32(5-8), 849-62.

Summary

Although physiological differences among neuromuscular junctions (NMJs) have long been known, NMJs have usually been considered as one type of synapse, restricting their potential value as model systems to investigate mechanisms controlling synapse assembly and plasticity. Here we discuss recent evidence that skeletal muscles in the mouse can be subdivided into two previously unrecognized subtypes, designated FaSyn and DeSyn muscles. These muscles differ in the pattern of neuromuscular synaptogenesis during embryonic development. Differences between classes are intrinsic to the muscles, and manifest in the absence of innervation or agrin. The distinct rates of synaptogenesis in the periphery may influence processes of circuit maturation through retrograde signals. While NMJs on FaSyn and DeSyn muscles exhibit a comparable anatomical organization in postnatal mice, treatments that challenge synaptic stability result in nerve sprouting, NMJ remodeling, and ectopic synaptogenesis selectively on DeSyn muscles. This anatomical plasticity of NMJs diminishes greatly between 2 and 6 months postnatally. NMJs lacking this plasticity are lost, selectively and very early on, in mouse models of motoneuron disease, suggesting that disease-associated motoneuron dysfunction may fail to initiate maintenance processes at "non-plastic" NMJs. Transgenic mice overexpressing growth-promoting proteins in motoneurons exhibit greatly enhanced stimulus-induced sprouting restricted to DeSyn muscles, supporting the notion that anatomical plasticity at the NMJ is primarily controlled by processes in the postsynaptic muscle. The discovery that entire muscles in the mouse differ substantially in the anatomical plasticity of their synapses establishes NMJs as a uniquely advantageous experimental system to investigate mechanisms controlling synaptic rearrangements at defined synapses in vivo.

1) Introduction: NMJs as model systems to study anatomical plasticity at identified synapses in vivo.

Due to its unique anatomical properties, the NMJ has long served as a model system to study principles of synapse assembly, remodeling, physiology and pathology. This model role took on new dimensions with the discovery of a signaling pathway leading from nerve-derived agrin, to MuSK- and rapsyn-dependent AChR clustering and synapse assembly, a mechanism that has served as a guiding principle for molecular investigations of synaptogenesis at central synapses (Sanes and Lichtman, 1999; Sanes and Lichtman, 2001). However, as the mechanisms governing the assembly and regulation of central synapses have emerged, apparent differences from those found at NMJs have raised doubts about the extent to which NMJs may be representative of synapses in the brain. Thus, for example, the apparently passive role of postsynaptic muscle during the initial process of NMJ assembly appeared to contrast to a more prominent role of postsynaptic mechanisms in controlling assembly and remodeling at glutamatergic synapses. In addition, although physiological differences among motor units, including their NMJs have long been known, NMJs have been considered as essentially one type of synapse in most studies. As a consequence, it has seemed unlikely that NMJs could also provide valuable information about mechanisms underlying the differences in assembly, plasticity and vulnerability properties among central synapses. In this review we discuss recent evidence that the assembly and anatomical plasticity of NMJs is largely controlled through processes at postsynaptic muscles, and that NMJs on different types of muscles differ substantially in the rates at which they assemble during development, and in their potential for remodeling in the adult. These findings support the notion that NMJs continue to provide excellent model systems to investigate principles of synapse assembly in vivo. In addition, they show how NMJs on different muscles may serve as model systems to elucidate mechanisms controlling the plasticity and selective vulnerability of synapse subtypes in the adult.

2) Distinct patterns of neuromuscular synaptogenesis in mouse muscles.

Although it has seemed reasonable to suppose that all NMJs develop in similar ways, in fact it is well known that NMJs vary substantially in size and shape, and that muscles differ greatly in physiology, metabolism and patterns of gene expression (Burke, 1994). To determine whether the steps in synapse formation and maturation exhibit muscle-type specific features, we carried out a detailed analysis of synaptogenesis and synaptic disassembly in identified hind-limb muscles in the mouse (Pun et al., 2002). This analysis spanned the period from E13.5, when motor axons in the mouse embryo start to invade individual cleaved muscle masses (Jones, 1979), to birth, by which time NMJs have matured considerably (Sanes and Lichtman, 1999). Most muscles exhibited one of two patterns of synapse assembly, which we call FaSyn (Fast Synapsing) and DeSyn (Delayed Synapsing). At E13.75, when the majority (ca. 95%) of motor nerves are not yet associated with AChR clusters, muscles differed significantly in the appearance and intensity of nascent AChR clusters, which were already compact in FaSyn muscles, but diffuse and weaker in DeSyn muscles. AChR clusters on DeSyn muscles remained poorly compacted between E14.5 and E16.5, when they consisted of arrays of discrete small clusters, possibly reflecting the microclusters (a.k.a. primary MuSK-dependent scaffolds) thought to represent elementary units of AChR clustering. Microcluster assembly depends on the function of the receptor tyrosine kinase MuSK (Apel et al., 1997; Zhen et al., 2002), the adapter protein rapsyn (Gautam et al., 1995), and the Rho-type GTPases Cdc42 and Rac (Weston et al., 2000). The distinct rates of appearance of focal AChR clusters coincided with marked differences in the relative arrangements of nerves, Schwann cells and AChR clusters in these muscles. Thus, presynaptic nerves in FaSyn-muscles were unbranched and confined to the AChR cluster region, and S100-positive terminal Schwann cells (tSCs) exhibited a compact configuration, in close association with regions of AChR clusters from E14.5 on (Fig. 1). In contrast, between E14.5 and E16.5, terminal nerves in DeSyn-muscles were extensively branched and not aligned with AChR clusters, and SC cell bodies were not positioned over AChR clusters (Fig. 1). In all muscles,

focal clustering of AChRs preceded alignment of the nerve with the cluster, and alignment of the nerve preceded that of the SC. From birth on, NMJs on all muscles had comparable appearances.

A detailed analysis of E13.5-17.5 embryos revealed that individual skeletal muscles in the mouse hind-limb can be subdivided into two main categories, that exhibit distinct rates of NMJ assembly (Fig. 1). Among the muscles that have been used extensively in other studies, diaphragm, soleus and sternomastoideum have DeSyn properties, whereas intercostals and tibialis anterior have FaSyn properties. The distinct patterns of NMJ assembly in FaSyn and DeSyn muscles are not related to rates of muscle maturation, physiological subtypes or relative position in the embryo. Thus, two muscles with predominantly fast-fatiguable motor units, the lateral gastrocnemius (LGC) and the rectus femoris, exhibited different innervation patterns. The rectus femoris is a FaSyn-muscle, whereas the LGC is a DeSyn-muscle. In addition, within any individual mixed-type muscle, FaSyn- and DeSyn-type innervation patterns were comparable among muscle fibers, further arguing against the possibility that these differences reflect the formation of functional subtypes of motor units. Second, no correlation was found between the proximo-distal location of a muscle and the type of innervation. But there was a clear tendency for muscles of the same type to occur in groups (Pun et al., 2002). Third, during this developmental period, and up to birth, relative labeling intensities for myosin heavy chain isoforms were undistinguishable in FaSyn and DeSyn muscles, arguing against the possibility that they reflect differences in the rate of differentiation of individual muscles. Together, these findings suggest that the innervation pattern is a specific property of an entire muscle, or of the corresponding motor pool innervating the muscle.

The mechanisms underlying these differences have not been elucidated yet, but the striking grouping of FaSyn and DeSyn muscles in the hind-limb (Pun et al., 2002) would be consistent with the possibility that they reflect early distinctions in mesenchyme composition, e.g. its extracellular matrix. Such distinctions may influence the differentiation properties of otherwise equivalent myoblasts and myotubes. It is

also possible that somewhat different myoblast lineages migrate to distinct prospective muscle territories during development.

3) In young adult mice, NMJs on DeSyn muscles remodel upon blockade of synaptic transmission, whereas those on FaSyn muscles do not.

Challenging mature NMJs by blocking nerve-evoked activity with Botulinum toxin A (BotA), a toxin that blocks calcium-dependent transmitter release, revealed that muscle-type specific properties are maintained at mature synapses in FaSyn and DeSyn muscles (Pun et al., 2002). Repeated applications of toxin every fourth day over a period of two weeks (chronic blockade of transmitter release) led to a pronounced loss of postsynaptic AChRs, and a dramatic collateral sprouting reaction in DeSyn muscles, e.g. LGC and vastus lateralis in mice younger than 4-6 months (Fig. 3). Single applications of BotA induced ultraterminal nerve sprouting in some muscles (Frey et al., 2000a), but failed to induce NMJ remodeling. This may reflect a requirement for continuous, full blockade of transmitter release to induce and sustain NMJ remodeling. Starting about 2 weeks after the beginning of the chronic treatment, numerous collaterals grew longitudinally along the paralyzed muscle fibers, extending for up to 0.5 mm on each side of the original synaptic site. The longitudinal sprouts extended short transversal side-branches that formed acetylcholine-esterase rich putative ectopic synaptic structures. In marked contrast, the rectus femoris and extensor digitorum longus (EDL), two FaSyn muscles, did not exhibit this sprouting response. Analysis of collateral sprouting and AChR cluster disassembly in the same muscles revealed that the two processes are closely correlated in their timing, muscle specificity and age-dependence. Like chronic paralysis, denervation produced a disassembly of AChR clusters on DeSyn muscles, whereas those on FaSyn muscles were more resistant. In addition, the time course of AChR cluster disassembly in chronically paralysed and denervated DeSyn muscles were comparable, suggesting that like in the embryo the status of focal clustering of AChRs influences the maintenance of the presynaptic nerve at the NMJ (Fig. 2).

Chronic blockade of transmitter release or denervation induced a complete loss of focal AChR clusters in DeSyn muscles in mice of up to approximately 2-3 months of age. However, this sensitivity to the absence of nerve-evoked activity decreased in older mice, and no disassembly could be detected in mice 6 months and older. Therefore, marked differences between NMJs of FaSyn and DeSyn muscles persist in young adult mice, where they can be revealed as differences in sensitivity to chronic transmitter release blockade or denervation (Figs. 2, 3).

It is well established that in partially denervated or paralysed muscle, and during reinnervation by regenerating nerves, tSCs sprout (Reynolds and Woolf, 1992), and ultraterminal nerve sprouts at the NMJ are consistently associated with processes of tSCs (Son and Thompson, 1995; Love and Thompson, 1999). In addition, processes from SC implants can cause ultraterminal sprouts to grow from NMJs in otherwise untreated muscle, and when terminal nerves sprout, there are usually more processes from tSCs than from nerve extending away from the synapse. On the other hand, at least at neuromuscular synapses forming during development, the presence of SCs is not a requirement for nerve sprouts to grow beyond synaptic contacts. Thus, in ErbB2-/- mice in which an early defect in heart development had been rescued, NMJs formed in the absence of SCs, but nerves defasciculated and sprouted distally from the synaptic contacts (Woldeyesus et al., 1999). Irrespective of whether tSC sprouting plays a permissive or instructive role in nerve sprouting at the NMJ, nerve sprouting at paralysed DeSyn, but not FaSyn NMJs may involve the induction of sprouting-inducing conditions for tSCs selectively at DeSyn muscles. We reasoned that if this was the case, such conditions may also exist in denervated muscles, i.e. in the absence of motor nerves. Indeed, a comparison of tSCs sprouting at denervated NMJs of FaSyn and DeSyn muscles in 6 weeks old mice revealed substantial differences in the two types of muscles. Thus, while strong tSC sprouting is detected at all NMJs in DeSyn muscles, sprouting is weak to absent in FaSyn muscles. These results are consistent with the notion that chronic absence of neuromuscular transmission leads to the growth of

tSC processes, which in turn promote sprouting of nerves in DeSyn, but not in FaSyn muscles.

4) Possible existence of a plasticity pathway induced by blockade of transmitter release in young adult DeSyn muscles.

Although treatment with BotA induces comparable paralysis and expression of denervation-related genes in DeSyn and FaSyn muscles (Santos and Caroni, unpublished), tSC sprouting, nerve sprouting and AChR cluster remodeling are restricted to DeSyn muscles. This may reflect a greater stability and independence from activity-dependent maintenance of NMJs on FaSyn muscles. According to this interpretation, NMJs on DeSyn muscles would further consolidate during the first postnatal months in mice, becoming resistant to chronic paralysis from approximately 6 months on. However, several lines of evidence argue against this possibility, instead supporting the opposite view that NMJs on DeSyn muscles of young adult mice exhibit considerable anatomical plasticity, whereas those on FaSyn muscles do not. First, sprouting of nerves at non-functional NMJs leads to the formation of ectopic synaptic contacts between MN and muscle. Although immature in their appearance, exhibiting comparatively weak AChR levels, and lacking terminal arborization and synapse-associated tSCs, these contacts sites exhibit synaptic vesicle accumulation and are functional (De Paiva et al., 1999). Second, when the toxin treatment is terminated, one of these sites develops into an NMJ of mature appearance (Santos and Caroni, unpublished; Fig. 4). Third, NMJs at non-sprouting muscles are lost early on in a mouse model of familial ALS, suggesting that plasticity and resilience to presynaptic terminal loss in disease may be related causally (see below).

The notion that NMJs on DeSyn muscles may exhibit anatomical plasticity absent in FaSyn muscles, is supported by recent studies in our laboratory, aimed at analyzing in more detail the cellular responses to BotA-induced paralysis in the two types of muscle (Santos and Caroni, unpublished). To visualize at high resolution the

plasma membrane of presynaptic motor nerves reliably, we used transgenic mice expressing a plasmamembrane-targeted version of green fluorescent protein (mGFP) under the control of a strong neuronal promoter cassette (mouse Thy1.2; Caroni, 1997a; DePaola et al., 2003; Livet et al., 2002). Some of these lines expressed the transgene in most spinal MNs, whereas other lines exhibited transgene expression in small subsets of MNs, allowing visualization of single MN projections within a muscle or muscle compartment. In further transgenic mouse lines, the GFP sequence was fused to the synaptic vesicle protein synaptophysin (spGFP), allowing visualization of presynaptic terminals in these mice (DePaola et al., 2003). We found that NMJs on DeSyn and FaSyn muscles both exhibited occasional short nerve sprouts in the absence of paralysis (less than 5 μm in length, and less than 5% of non-paralysed NMJs). Starting 4-6 days after the onset of BotA induced paralysis, there was a gradual increase in nerve sprouting at NMJs of DeSyn, but not FaSyn muscles (Santos and Caroni, unpublished). Ectopic AChR clusters appeared at 6-10 days of paralysis, and were consistently associated with nerve sprouts and local accumulations of synaptic vesicles. Starting at 12-15 days of paralysis, motor nerves on DeSyn muscles exhibited collateral sprouting, which coincided with the disassembly of the AChR cluster complex at the original NMJ.

The progressive sequence of responses in paralysed DeSyn muscles is consistent with the presence of a plasticity response in paralysed DeSyn muscles, leading to ectopic synaptogenesis, and restoration of neuromuscular transmission (Fig. 4). Sprouting and NMJ disassembly could be interrupted at any time after the onset of paralysis by experimental interventions enhancing signaling at the NMJ (Santos and Caroni, unpublished), further arguing for the existence of a progressive plasticity response in DeSyn muscles. The extent of the plasticity response was highest in 1-2 months mice, and it declined during the following 3-4 months. DeSyn muscles in mice older than 6 months exhibited some paralysis-induced ultraterminal sprouting, but no disassembly of the original synaptic complex, no collateral sprouting, and no massive muscle atrophy, despite an equally effective blockade of neuromuscular transmission (Santos and Caroni, unpublished). Anatomical plasticity was not lost at

the same rate in different regions of the same DeSyn muscle. Generally, plasticity was lost first in the most lateral sections of muscles and muscle compartments, whereas medial, and bone-facing regions remained plastic for 2-3 more months (Santos and Caroni, unpublished; Fig. 5). These regional differences were particularly prominent in large DeSyn muscles such as lateral gastrocnemius (LGC), where sprouting and synapse disassembly varied along compartmental gradients in mice aged 2 to 6 months (Frey et al., 2000a; Santos and Caroni, unpublished).

5) Selective early loss of non-plastic NMJs in a mouse model of familial motoneuron disease.

Transgenic mice overexpressing high levels of mutated human Cu,Zn superoxide dismutase SOD1(G93A) associated with familial amyotrophic lateral sclerosis (ALS) provide a mouse model of motoneuron disease (Gurney et al., 1994; Chiu et al., 1995). Due to the remarkable reproducibility of the phenotype among individuals of the same transgenic line, these mice provide excellent tools to investigate how disease progression affects peripheral innervation (Frey et al., 2000a). In a line of mice exhibiting particularly high transgene expression levels, clinical symptoms of muscle weakness develop at about postanatal day (P) 90, spinal MNs are lost after P100, and the mice die on average at P136 (Gurney et al., 1994; Chiu et al., 1995). Significantly, however, these mice already exhibit extensive local muscle denervation at P50 (Frey et al., 2000a). Systematic mapping of the innervation pattern in the triceps surae of SOD1(G93A) mice revealed a highly regionalized and topographic distribution of the denervation (Frey et al., 2000a). Topographic distributions of denervation were also detected in other muscles, such as gluteus and gracilis. Analysis of SOD1(G93A) mice at P80 revealed extensive atrophy and degeneration of peripheral muscle fibers in extensive sections of medial (MGC) and lateral gastrocnemius, consistent with persistent denervation. Comparable early losses of peripheral innervation were detected in the SMA (Frugier et al., 2002), pmn (Frey et al., 2000a), and Mnd (Frey et al., 2000a) models of motoneuron disease, suggesting that axonal „dying-back“ (Raff et al., 2002) may be a defining feature of early disease progression in many motoneuron

diseases. In fact, pioneering work by Pinter and his colleagues using a canine model of motoneuron disease revealed that progressive NMJ dysfunction is detected very early on in the disease process, suggesting that the disease process selectively leads to deficits in neuromuscular transmission, followed by the progressive loss of subgroups of NMJs, leading to paralysis and death (Pinter et al., 1995; Pinter et al., 1997; Rich et al., 2002a; Rich et al., 2002b). Accordingly, and in contrast to initial expectations, peripheral synapses and axons are affected selectively in these neurodegenerative diseases, and the actual loss of MNs does not seem to be a major factor in disease progression (Frugier et al., 2002; Sagot et al., 1995; Sagot et al., 1996; Sagot et al., 1998).

To determine whether the early and selective disconnection of defined neuromuscular synapses was due to early vulnerability of the corresponding MNs to the mutated SOD1, we analyzed the pathology of neuromuscular synapses in muscle regions that were prone or resistant to denervation. Ultrastructural analysis of NMJs in the MGC, LGC and soleus at P50 revealed vacuolation of presynaptic terminals, and shrinkage of postsynaptic sole plate cytoplasm at many NMJs in all three muscles (Frey et al., 2000a; Pun, Santos and Caroni, unpublished). Therefore, although subsets of NMJs on MGC and LGC were lost selectively, some pre- and postsynaptic pathology was detected at vulnerable and resistant NMJs in MGC, LGC and soleus. Mutated SOD1 thus induced comparable pathology in many MN and muscle subtypes, but only some of these exhibited early peripheral denervation.

To determine how selective denervation in the SOD1 mice evolved with time, we mapped triceps surae innervation patterns between P30, soon after motor units have acquired their adult properties, and P120 when these mice exhibit pronounced MN loss. Between P30 and P40, we detected progressive thinning of neurofilament-positive terminal branches, predominantly in the peripheral sections of MGC and of LGC compartments. Between P45 and P80, dramatic denervation developed, predominantly in lateral regions of MGC and LGC compartments, whereas medial regions and the soleus were spared. Beginning around P60, and extending into the clinical phase of the disease, ultraterminal nerve sprouting and local reinnervation by collateral and ul-

traterminal sprouting were detected in medial muscle regions. In the soleus, significant denervation was restricted to the very last phase of the disease (P120). Therefore, throughout the disease process, triceps surae synapses on lateral sections of muscle and muscle compartments are affected early on, whereas synapses in medial sections of these DeSyn muscles resist denervation for longer times, and can sprout to reinnervate nearby vacated synapses.

The pattern of early denervation in the SOD1 model was a close mirror image of the distribution of NMJs exhibiting paralysis-induced nerve sprouting (Frey et al., 2000a), suggesting that NMJs with low potential for anatomical plasticity were lost early on in the motoneuron disease model (Fig. 5). A good correlation between the distribution of FaSyn muscles and that of early denervation was also found in other muscles in the hindlimb. "Non-plastic" NMJs were lost through progressive thinning of the presynaptic nerve, with no evidence of sprouting, and no loss of the postsynaptic AChR cluster, which persisted apparently intact for many days after denervation (Pun, Santos and Caroni, unpublished). In contrast, "plastic" NMJs on triceps surae exhibited early evidence of ultraterminal sprouting, and broadening of the presynaptic nerve also found at paralysed NMJs (Pun, Santos and Caroni, unpublished). When ultraterminal sprouting was stimulated with BotA in SOD1(G93A) mice beween P50 and P80, sprouting was substantially weaker than in wild-type mice (Frey et al., 2000a), consistent with the notion that axonal weakening is an early target of the disease in these mice. Together with the findings by Pinter and colleagues (Pinter et al., 1995; Pinter et al., 1997; Rich et al., 2002a; Rich et al., 2002b), these combined observations suggest that early MN dysfunction may induce trophic signals for motor nerves in "plastic" muscles, whereas the absence of such restorative signals may lead to early loss of presynaptic nerves in "non-plastic" muscles.

6) Relative roles of muscle and motoneuron in NMJ assembly during development.

What cellular components and molecular mechanisms underlie the specific features of NMJ assembly, plasticity and loss in FaSyn and DeSyn muscles ? To dissect the rela-

tive roles of MNs and muscles in the differences between FaSyn and DeSyn NMJs, we analyzed NMJ assembly in mice lacking MNs or agrin (Pun et al., 2002). In MN-free embryos, AChRs accumulated and clustered in central bands of forming muscles in the complete absence of motor axons, in agreement with previous findings on diaphragm (Yang et al., 2001b; Lin et al., 2001). In addition, while the level of AChR labeling intensity at E16.5 was reduced in all hindlimb muscles in the absence of motor axons, FaSyn-muscles still accumulated compact focal clusters, and DeSyn-muscles still exhibited dispersed arrays of small clusters. These findings suggest that the distinct temporal patterns of neuromuscular synaptogenesis in FaSyn and DeSyn muscles reflect properties intrinsic to individual developing muscles (Fig. 6).

Although muscles lacking both motor-nerves and nerve-derived agrin, cluster AChRs in a muscle-type specific pattern, the presence of the nerve had a strong influence on the intensity of AChRs. We therefore extended our analysis to agrin mutant mice, to determine whether FaSyn and DeSyn muscles differ in their sensitivity to agrin. In agreement with published reports (Burgess et al., 1999; Yang et al., 2001b), muscle fibers in several muscles, including the diaphragm (a DeSyn muscle) were defective in AChR clustering in the absence of agrin from E14.5 on. In addition, however, we detected dramatic differences between FaSyn and DeSyn muscles (Fig. 6). In FaSyn-muscles of agrin-/- mice, a majority of the AChR clusters were normal in size, and AChR clusters were associated with nerves and tSCs at E14.5. At later developmental stages, AChR clusters failed to grow, and then dispersed in the absence of agrin. Thus, at least in FaSyn muscles, agrin does not appear to be essential for the initial formation of a synaptic complex of AChR cluster, nerve, and SC. Instead, agrin appears to have a critical role in augmenting focal AChR clustering, enhancing alignment of nerve and SC with the AChR cluster, and in promoting NMJ maintenance (Pun et al., 2002). The presence of an intrinsically efficient process of focal AChR clustering may initially be sufficient to protect nascent NMJs on FaSyn muscles from disassembly in response to the absence of agrin, whereas the higher sensitivity in DeSyn muscles may be due to the low intrinsic efficiency of the clustering process in these muscles. In agreement with previous reports, agrin may thus promote synapse maturation and

maintenance by strengthening and sustaining the pathway for AChR clustering, presumably through MuSK (Sanes and Lichtman, 2001).

The intrinsic mechanism enhancing focal AChR cluster assembly in FaSyn muscles has not been identified yet, but one possibility involves the clustering-enhancing activity of the dystroglycan complex. This complex is co-assembled with MuSK, AChR and rapsyn into a postsynaptic signalling scaffold, where it links extracellular matrix components such as laminin to the cytoskeleton at the NMJ, possibly functioning as a modulatory pathway to enhance AChR cluster assembly (Heathcote et al., 2000). Consistent with this notion, laminin can promote AChR clustering on cultured myotubes in the absence of agrin (Marangi et al., 2002), and mice lacking α-dystroglycan exhibit poorly organized and unstable focal AChR clusters (Jacobson et al., 2001). Accordingly, efficient focal clustering in FaSyn muscles may reflect enhanced recruitment of the dystroglycan complex at forming AChR clusters, e.g. due to the organization of extracellular matrix in these muscles. A recent study carried out in the sternomastoid muscle of young and adult mice (a DeSyn muscle), has provided evidence that blocking skeletal muscle TrkB receptor activity leads to a fragmentation of AChR clusters and to the disassembly of synapses (Gonzales et al., 1999). TrkB receptor activity may also be required to prevent the fragmentation of agrin-induced AChR clusters on cultured myotubes (Gonzales et al., 1999), raising the possibility that FaSyn and DeSyn muscles differ in their dependence on signal transduction events downstream of TrkB receptor activation.

A comparison of AChR clusters in the absence of MNs or agrin supports and extends the notion that the motor nerve can promote synaptogenesis in the absence of agrin (Lin et al., 2001; Yang et al., 2001b). Thus, not only did motor nerves promote AChR cluster growth in the absence of agrin in FaSyn muscles, but they also enhanced cluster dispersal at ectopic sites in DeSyn muscles, and at disassembling synapses in DeSyn and FaSyn muscles (Pun et al., 2002). These findings are similar to the effects of synaptic and extra-synaptic activity on AChR gene expression and AChR cluster formation and stability (Sanes and Lichtman, 1999; Sanes and Lichtman, 2001). They

are also reminiscent of the effects of agrin and electrical activity on the formation, growth, and stability of ectopic AChR clusters on living soleus muscle in adult rats (Skorpen et al., 1999). There are several parallels between the processes of NMJ disassembly for FaSyn and DeSyn muscles in the embryo and in the adult. By analogy to its role in the adult, it is thus possible that during NMJ development, activity promotes focal AChR clustering at synapses, and promotes AChR dispersal in the absence of agrin, and at extra-synaptic sites (Sanes and Lichtman, 2001). This interpretation is consistent with the finding that in the absence of acetylcholine release in ChAT-/- mice, muscle fibers exhibit an excess of NMJs, that are distributed over an abnormally broad territory of muscle (Misgeld et al., 2002; Brandon et al., 2003). In Munc-18-/- mice lacking any form of transmitter release initially normal NMJs disassembled after a few days (Verhage et al., 2000), but this may have involved severe neuronal degeneration in these mice.

Glial cells are specifically and closely associated with central and peripheral synapses, where they regulate several aspects of synaptic function, including synapse maturation and maintenance. In addition, glial cells can sense synaptic activity, and respond to bursts of transmitter release with intracellular calcium waves and alterations in gene expression, suggesting that these cells could regulate synapses in an activity-dependent manner. At the NMJ, 4-5 non-myelinating Schwann cells (tSCs) cap the terminal nerve, effectively shielding it from non-synaptic extracellular space (e.g. Herrera et al., 2000). When tSCs are induced to migrate away from NMJs of neonatal mice by local applications of excess soluble neuregulin into muscle, terminal nerves retract and the postsynaptic apparatus disassembles. Therefore, tSCs are essential for the maintenance of immature NMJs. An analysis of neuromuscular synaptogenesis in rescued ErbB2-/- mice, expressing transgenic ErbB2 in the heart, but lacking Schwann cells, revealed that Schwann cells are not required for neuromuscular synapse formation (Woldeyesus et al., 1999). However, in the absence of Schwann cells, intramuscular nerves were poorly fasciculated, and terminal nerves exhibited excessive sprouting during synaptogenesis. In addition, the innervation pattern of intercostal muscle, a FaSyn muscle, was abnormal, exhibiting evidence of denervation/ reinnervation at

many NMJs at E18.5. The association of tSCs with developing NMJs in FaSyn and DeSyn muscles coincided with the formation of focal clusters of AChRs (see above), and with the alignment of motor nerves with these clusters. Terminal-SCs may thus produce an enhancement of synaptic transmission at developing NMJs, leading to a local growth of the postsynaptic complex, and promoting the dispersal of ectopic AChR clusters (Yang et al., 2001b).

7) Role of muscles and the postsynaptic receptor complex in NMJ plasticity in the adult.

Nerve sprouting induced by BotA at the adult NMJ is largely restricted to DeSyn muscles, where there is a close correlation between the assembly state of post-synaptic AChR clusters and the extent of the sprouting reaction. These observations raise the possibility that, like during NMJ assembly in the embryo, muscles may also play a predominant role in controlling anatomical plasticity at NMJs in the adult. To examine more directly the relative roles of nerve and muscle in controlling BotA-induced sprouting, we recently carried out crossinervation experiments in the adult (Santos and Caroni, unpublished). The nerves to soleus (a muscle exhibiting robust BotA-induced sprouting) and extensor digitorum longus (EDL) (a muscle exhibiting no BotA-induced sprouting) were transsected close to their respective muscles, and one of the proximal stumps was connected to the distal stump on either soleus or EDL. Following a period of 2 months that allowed for muscle reinnervation and stabilization of the NMJs, muscles were paralyzed with BotA, and analyzed for nerve sprouting. These experiments revealed that soleus and EDL motoneurons sprout on paralysed soleus muscle, but not on EDL muscle, indicating that BotA-induced sprouting is controlled by the postsynaptic muscle (Santos and Caroni, unpublished).

What site in muscle may control plasticity at adult NMJs ? The close correspondence between the status of focal assembly of AChR clusters and the plasticity response suggested that plasticity may be controlled from the postsynaptic complex. To investigate

this possibility, we analyzed the relationship between agrin-mediated AChR cluster and synapse maintenance, and inactivity-mediated destabilization (Pun et al., 2002). We found that overexpression of z-agrin in Thy1-agrin mice protected AChR clusters and presynaptic nerves against destabilization induced by chronic blockade of nerve-evoked activity in the presence of BotA (Pun et al., 2002). Conversely, significant AChR disassembly and collateral nerve sprouting characteristic of synapse disassembly was detected in both DeSyn and FaSyn muscles one month after the onset of the chronic BotA treatment in z-agrin+/- mice. In addition, tSC sprouting was much more pronounced in z-agrin+/- mice, and denervation-induced tSC sprouting was reduced in adult Thy1-agrin mice. Taken together, these findings suggest that agrin and synaptic activity act in concert to maintain postsynaptic AChR clusters and NMJs in the adult. In DeSyn muscles of young adult mice, this maintenance is critical to suppress sprouting and synapse rearrangements, whereas in FaSyn muscles the postsynaptic apparatus appears to be unresponsive to all but the harshest conditions, such as chronic denervation.

8) Roles of the presynaptic nerve in anatomical plasticity at the adult NMJ.

Although anatomical plasticity at NMJs appears to be controlled primarily by postsynaptic muscles, possibly through the production of sprouting factors (e.g. Siegel et al., 2000), the motor nerve continues to play an important role in maintaining AChR clusters and in synapse integrity postnatally. One pathway through which the nerve promotes synaptic maintenance involves muscle activity (Tam et al., 2001). Thus, the chronic paralysis experiments provide experimental evidence that a minimal amount of nerve-induced synaptic activity is required in the adult to maintain neuromuscular synapses on DeSyn muscles. These findings are consistent with those of a study on the turnover of AChRs at blocked NMJs of the sternomastoideum (Akaaboune et al., 1999), a DeSyn muscle. A similar role of nerve-evoked activity for maintenance of postsynaptic dendritic spines has been described in hippocampal neurons in slice cultures (McKinney et al., 1999). In addition to activity, nerve-derived z-agrin also pro-

tected synapses on DeSyn muscles from disassembly in the adult, suggesting that a low level of nerve-evoked activity may act together with z-agrin to protect synapses from the activation of an AChR cluster and synapse disassembly pathway in young adult mice.

Although the ability of nerves to sprout and grow processes is generally higher during development, axonal sprouting competence can be expressed by many neurons in the adult, and regeneration of lesioned axons can be induced under favorable conditions in the adult. Axonal growth and sprouting is thought to involve the activation of intrinsic growth-promoting programs and the expression of growth-promoting components in neurons (Skene, 1989; Bisby and Tetzlaff, 1992; Goldberg et al., 2002a; Goldberg et al., 2002b). The growth-associated proteins GAP43 (Skene, 1989) and CAP23 (Widmer and Caroni, 1990) are intrinsic determinants of nerve sprouting in neurons (Aigner et al., 1995; Caroni, 1997b), and their combined expression is sufficient to produce substantial regeneration of lesioned sensory neuron axons in the adult spinal cord (Bomze et al., 2001). In spinal MNs GAP43 and CAP23 are expressed at high levels during axonal growth and target innervation, and are downregulated to undetectable (GAP43) or low (CAP23) levels between P8 and P15, when neuromuscular synapses initiate their final maturation (Caroni and Becker, 1992; Caroni et al., 1997). In CAP23-/- mice lacking CAP23, BotA-induced nerve sprouting in soleus muscle was greatly impaired (Frey et al., 2000b). The absence of nerve sprouting was particularly striking, when considering the pronounced hypertrophy and process extension by synapse-associated tSC's in these mice, which can promote nerve sprouting in wild-type mice (Son and Thompson, 1995). To determine whether it was the absence of CAP23 in the motor nerve that impaired nerve sprouting, we crossed Thy1CAP23 mice that overexpress CAP23 from P7-9 on specifically and constitutively in neurons (Caroni et al., 1997) into the CAP23-/- background. This restored BotA-induced sprouting in the soleus (Frey et al., 2000b). Similar results were obtained when CAP23-/- mice were crossed into a Thy1GAP43 (Aigner et al., 1995) background, indicating that intrinsic CAP23 or GAP43 are necessary for effective paralysis-induced ultraterminal sprouting at this synapse.

Transgenic mice overexpressing GAP43 or CAP23 in neurons in the adult exhibit greatly enhanced stimulus-induced sprouting at many synapses, including NMJs (Aigner et al., 1995; Caroni et al., 1997), and the combined expression of GAP43 and CAP23 in double-transgenic mice further enhances this sprouting (Caroni et al., 1997). Significantly, however, we recently found that sprouting in the transgenic mice was restricted to DeSyn muscles, and that NMJs on paralysed FaSyn muscles failed to exhibit significant BotA-induced sprouting even in the presence of both growth-promoting proteins in motoneurons (Santos and Caroni, unpublished; Fig. 7). These findings further support the notion that anatomical plasticity at the NMJ is primarily controlled by processes in the postsynaptic muscle. In addition, these observations provide encouraging evidence that interventions aimed at boosting the growth potential of neurons in the adult will likely not enhance anatomical rearrangements indiscriminately throughout the brain, but may instead produce enhanced plasticity restricted to the vicinity of deafferented target regions.

9) Distinct patterns of synapse assembly and plasticity in muscles: possible roles and outlook

What may be the roles for the differences in NMJ assembly and plasticity in DeSyn and FaSyn muscles ? One possibility is that they may influence the rate of maturation of neuronal circuits involved in motor control through retrograde signals. During development, presynaptic differentiation involves the stopping, alignment and thickening of the presynaptic nerve, and positioning of tSC bodies at the maturing synapse. The presynaptic nerve promotes synapse differentiation through activity, and by providing growth factors such as neuregulin (Sandrock et al., 1997). The tight association of tSCs with maturing presynaptic terminals may promote further synapse strengthening by enhancing the efficacy of synaptic transmission (Robitaille, 1998). A similar role for synaptic activity in promoting synapse maturation and maintenance has been suggested for developing retino-tectal synapses (e.g. O'Rourke et al., 1994; Antonini et al., 1999). Such heightened efficacy, in turn, may signal back from muscle to the

presynaptic nerve to promote further presynaptic differentiation, locally at the nerve terminal, and through retrograde signaling pathways to the terminal arbor, and on to the cell body (Fitzimonds and Poo, 1998). This process would parallel local regulation at the developing NMJ in Drosophila, where postsynaptic differentiation and synaptic efficacy generate retrograde signals that control presynaptic differentiation (Davis and Goodman, 1998; Davis, 2000). Through such retrograde signals, the assembly of the synaptic apparatus through processes intrinsic to particular postsynaptic muscles may affect the timing of presynaptic MN maturation.

In addition to affecting the timing of pre- and postsynaptic maturation, the differences in synaptogenesis and synapse maintenance in FaSyn and DeSyn muscles may confer distinct regulatory properties to forming and maturing synaptic connections in the two types of muscles. Thus, due to their relative instability in the embryo and in young mice, synapses on DeSyn muscles may be more sensitive to control through activity or trophic support than those on FaSyn muscles. Similar differences in maturation rate may also exist at central synapses, raising the possibility that intrinsically distinct susceptibilities to regulation may be a general mechanism affecting the plasticity of synaptic connections during development and the restriction of this plasticity in the adult.

There is increasing evidence for the existence of substantial activity-regulated synapse rearrangement processes in mature circuits in the brain (Zito and Svoboda, 2002). In addition to playing key roles in brain repair, it is expected that synaptic rearrangements mediate long-term aspects of experience-related learning and memory. While progress in this emerging area of neuroscience depends critically on understanding the mechanisms controlling the onset, extent and selectivity of synapse rearrangements, these questions are difficult to address in the CNS due to the inacessibility and overwhelming complexity of the synapses in brain neuropil. The discovery that entire muscles in the mouse differ substantially in the anatomical plasticity of their NMJs, that this plasticity appears to be controlled predominantly at the level of the postsynaptic muscle, i.e. outside the CNS, and that the plasticity declines between 2 and 6

months of age, establishes adult NMJs as a uniquely advantageous experimental system to investigate mechanisms controlling synaptic rearrangements at defined synapses in vivo.

Figures

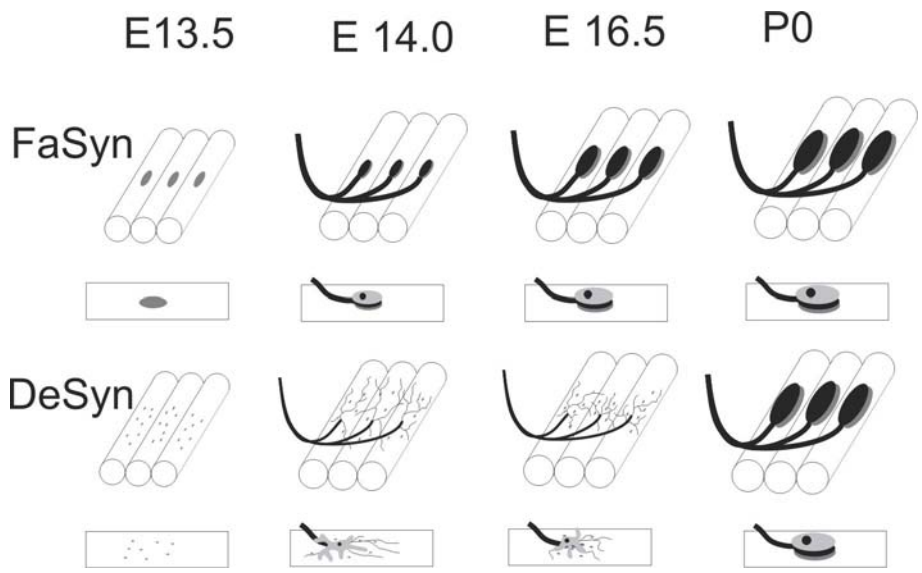

Figure 1 : Distinct patterns of synapse assembly in FaSyn and DeSyn Muscles
FaSyn muscles assemble focally organized clusters of AChRs in the absence of nerve, which rapidly become aligned to presynaptic nerve and Schwann cells. In contrast, DeSyn muscles exhibit dispersed microclusters of AChRs between E13.5 and E16.5. During this developmental time, nerves and Schwann cells fail to align with AChR microclusters, and extensive sprouting is detected. Nerves to individual muscle fibers are fasciculated (polyinnervation), whereas the sprouts appear thin, and are presumably defasciculated. Subsequently, AChR clusters, presynaptic nerve and Schwann cell become organized focally on DeSyn muscles, and NMJs on FaSyn and DeSyn muscles exhibit undistinguishable organizations at birth. The boxes below the sets of three muscle fibers represent schematics for single muscle fibers.

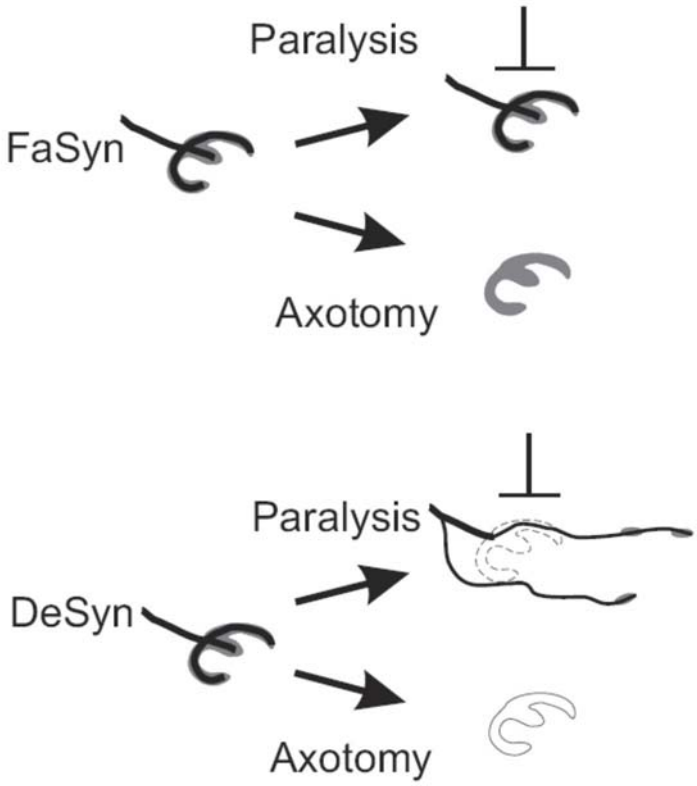

Figure 2 : Distinct responses of NMJs on FaSyn and DeSyn muscles to paralysis or denervation in the adult.

Postsynaptic AChR complexes on FaSyn muscles are resistant to chronic paralysis or denervation, and nerves fail to sprout upon paralysis. In contrast, the same experimental conditions induce AChR complex dispersal on DeSyn muscles, which exhibit pronounced nerve sprouting upon paralysis. The inverted T bars indicate blockade of neuromuscular transmission with BotA.

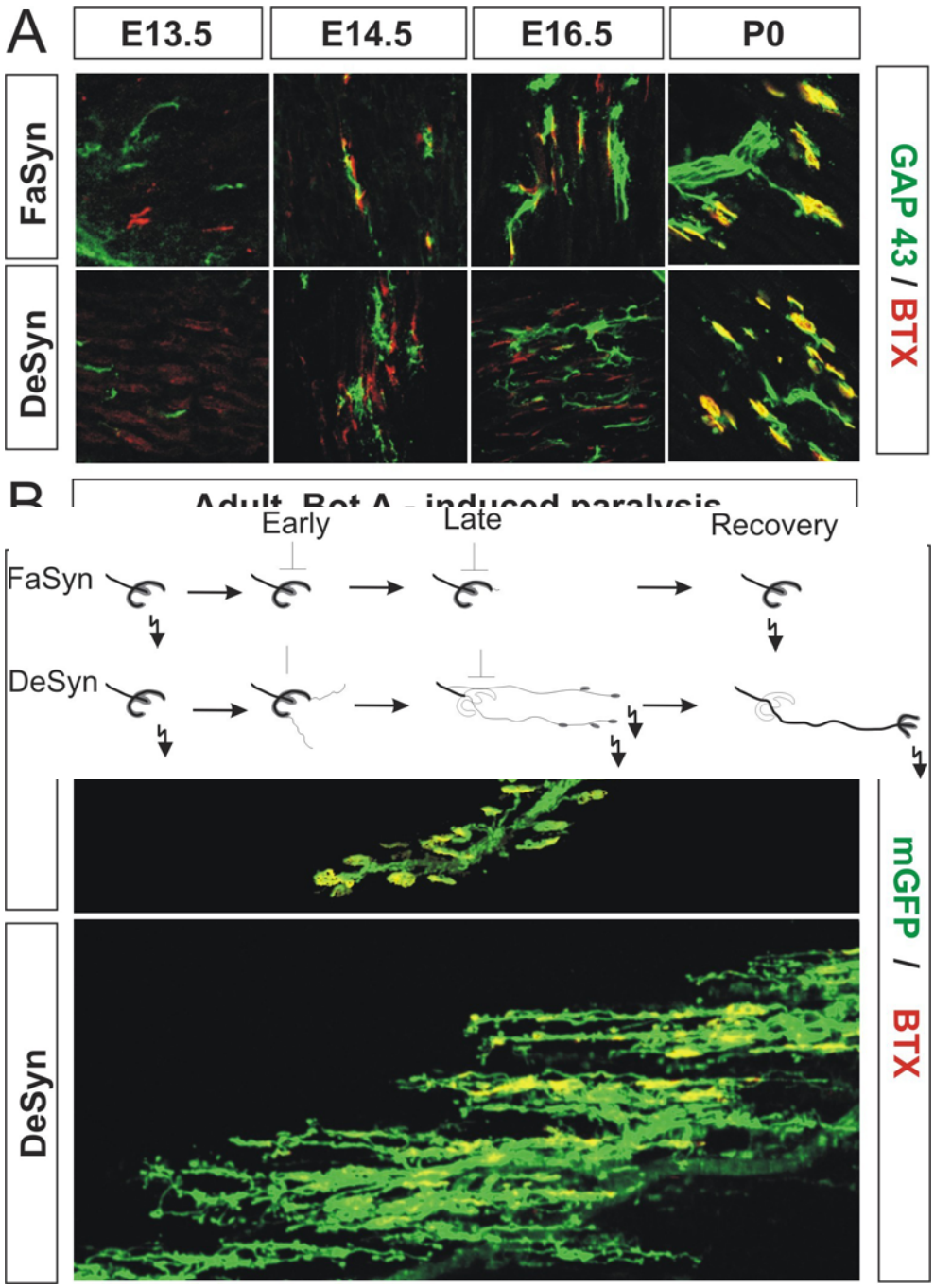

In DeSyn muscles, blockade of calcium-induced transmitter release with BotA (invert-

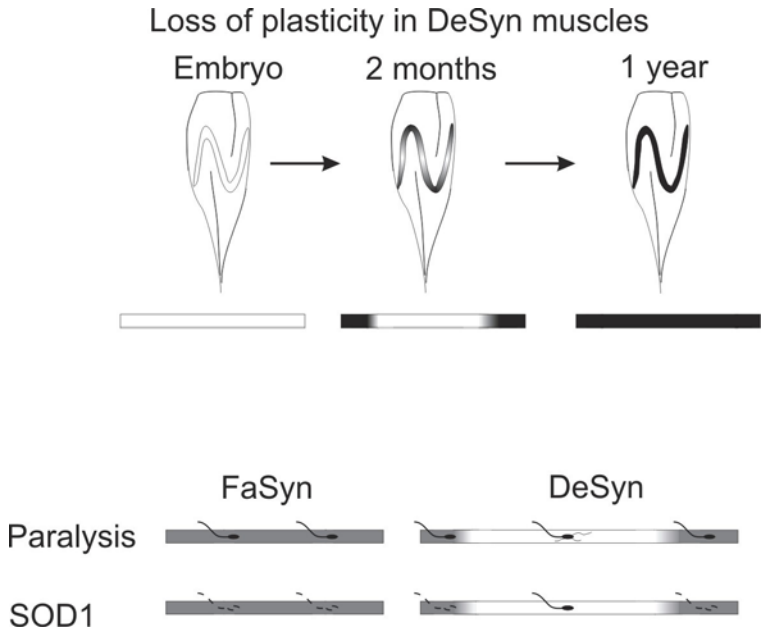

Figure 5: Selective vulnerability of non-plastic NMJs on FaSyn muscles in a mouse model of familial ALS.

In mouse DeSyn muscles and muscle compartments, the loss of plasticity that occurs between 2 and 6 months of age proceeds along a lateral-to-medial gradient.

Non-plastic NMJs on FaSyn muscles, and on lateral regions of many DeSyn muscles are lost selectively and early on in the SOD1 model of motoneuron disease.

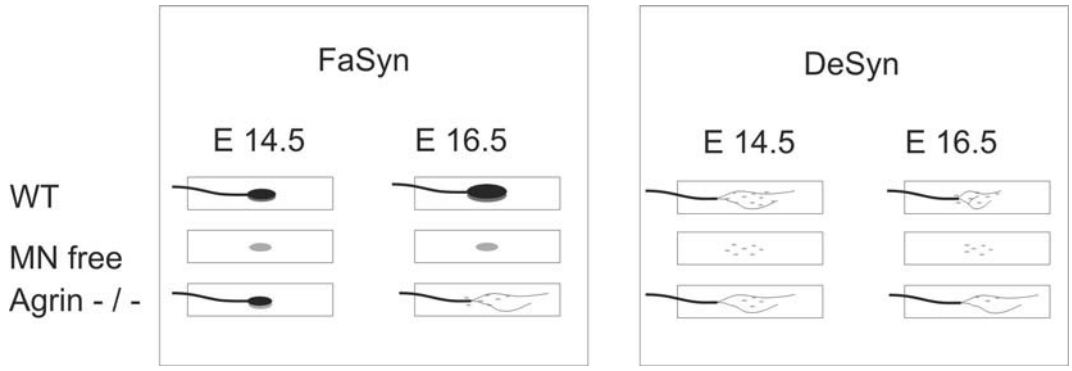

Figure 6 : Relative roles of muscles and agrin during the assembly of NMJs in the mouse.

AChR clusters assemble focally on FaSyn, but not DeSyn muscles in the complete absence of motor nerves, indicating that the characteristic AChR assembly patterns reflect properties intrinsic to FaSyn and DeSyn muscles. However, AChR labeling in-

tensities in the absence of nerve are substantially reduced, indicating that nerve-derived signals promote postsynaptic AChR accumulation. NMJs on FaSyn muscles initially assemble normally in the absence of agrin, but subsequently disassemble between E15 and E17, leading to a loss of AChR clusters and sprouting of nerves. agrin thus plays an essential role to augment and maintain postsynaptic AChR clusters. MN free: mice with a specific deletion of MNs well before their axons would reach the periphery; agrin-/- : mice lacking all forms of agrin.

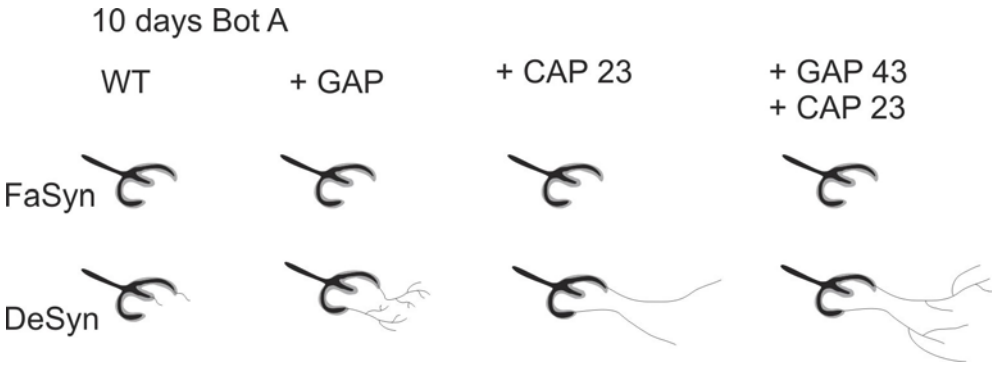

Figure 7 : Growth-associated proteins in motoneurons specifically enhance nerve sprouting in paralyzed plastic DeSyn muscles, but not in non-plastic FaSyn muscles. Overexpression of the growth-associated proteins GAP43 or CAP23 as transgenes specifically in neurons postnatally greatly enhances BotA-induced sprouting in DeSyn muscles, but fails to affect sprouting in non-plastic FaSyn muscles. Each individual transgene augments sprouting in its own characteristic pattern, and the two growth-associated proteins synergize in enhancing nerve sprouting at plastic NMJs of DeSyn muscles.

Appendix 3 NMJ plasticity and ECM remodeling

Plasticity at NMJs depends on remodeling of synaptic ECM, which (under permissive conditions) is directed by presynaptic nerve.

A: Upper two rows: dispersal of agrin from synaptic ECM of chronically paralyzed LGCDeSyn. Lower two rows: Accumulation of WFA binding sites at synaptic ECM of mature, non-remodeling NMJs. The concentration of WFA binding was lost selectively at remodeling AChR clusters of chronically paralyzed LGCDeSyn; also note how the loss of WFA is a late process (+10d panel).

B: Left and center: blockade of BotA-induced plasticity in LGCDeSyn by tPA-STOP, and reduced efficiency of the tPA inhibitor in blocking sprouting in myd/myd mice. tPA-STOP was added daily, from day +8 on. Right: application of tPA (daily, from day +8 on) is not sufficient to induce sprouting in BotA-treated RFFaSyn. All BotA treatments were started at 1 month. Combined silver-esterase reactions.

C: Presynaptic nerve directs remodeling of synaptic ECM at the NMJ under permissive conditions. Combined silver-esterase reactions. All LGCDeSyn panels are from the same lateral compartment region. Note absence of AChE redistribution from non-permissive RFFaSyn NMJs and from denervated LGCDeSyn NMJs (focal labeling coinciding with dark sole plate nuclei background); also note dramatic redistribution of AChE at permissive BotA-treated LGCDeSyn NMJs. Sprouts in Thy-nagrin or Thy-GAP43 transgenic mice were more effective in inducing stable ectopic AChR/AChE clusters under permissive conditions.

Bars: 20 (A) and 100 (B, C) μm.

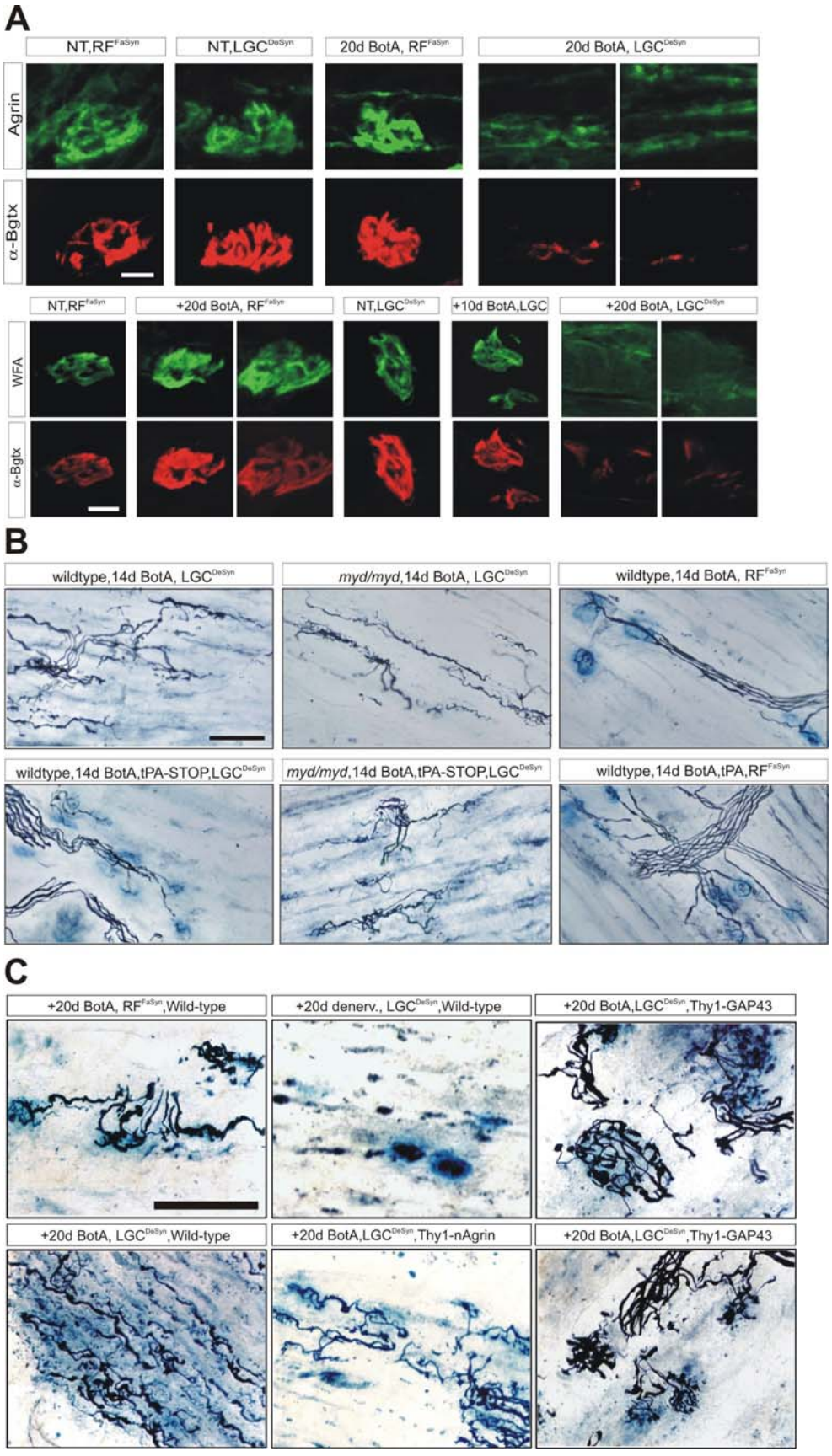
A
NT,RF FaSyn
NT,LGC DeSyn
20d BotA, RF FaSyn
20d BotA, LGC DeSyn
Agrin
α-Bgtx
NT,RF FaSyn
+20d BotA, RF FaSyn
NT,LGC DeSyn
+10d BotA,LGC
+20d BotA, LGC DeSyn
WFA
α-Bgtx
B
wildtype,14d BotA, LGC DeSyn
myd/myd,14d BotA, LGC DeSyn
wildtype,14d BotA, RF FaSyn
wildtype,14d BotA,tPA-STOP,LGC DeSyn
myd/myd,14d BotA,tPA-STOP,LGC DeSyn
wildtype,14d BotA,tPA,RF FaSyn
C
+20d BotA, RF FaSyn,Wild-type
+20d denerv., LGC DeSyn,Wild-type
+20d BotA,LGC DeSyn,Thy1-GAP43
+20d BotA, LGC DeSyn,Wild-type
+20d BotA,LGC DeSyn,Thy1-nAgrin
+20d BotA,LGC DeSyn,Thy1-GAP43